TECHNISCHE UNIVERSITÄT WIEN

VIENNA UNIVERSITY OF TECHNOLOGY

Diplomarbeit

A Sensitivity Analysis of Muscle Forces and Body Mass Accelerations during Gait to Changes of Muscle Parameters

ausgeführt zum Zwecke der Erlangung des akademischen Grades eines
Diplom-Ingenieurs unter der Leitung von

Ao.Univ.Prof. Dipl.-Ing. Dr.techn. Margit Gföhler
E307
Institut für Konstruktionswissenschaften und Technische Logistik

eingereicht an der
Technischen Universität Wien
Fakultät für Maschinenwesen und Betriebswissenschaften

von

Gisela Höflinger
0125588/E740
Rochusgasse 15a/1
A-1030 Wien

Wien, am 30. Oktober 2008

_____
Unterschrift

Danksagung

Zu allererst möchte ich meinen Eltern und Familie danken für die es selbstverständlich war, dass ich ein Studium absolviere und mir den finanziellen Rückhalt gaben, dieses auch zu genießen ohne mich groß um den Lebenserhalt sorgen zu müssen. Ich weiß es zu schätzen diese Zeit in meinem Leben gehabt zu haben.

Meine Studienzeit war geprägt von einer Reihe sehr positiver menschlicher Erfahrungen; Professoren und Assistenten waren immer entgegenkommend und bemüht Probleme zu lösen und meine Studienkollegen hilfsbereit und haben für viele schöne Stunden innerhalb und außerhalb der Uni gesorgt.

Mein besonderer Dank geht an Prof. Dr. Margit Gföhler und Prof. Dr. Marcus Pandy für die angenehme Zusammenarbeit und gute Betreuung. Aber vor allem, dass sie einen Aufenthalt an der Universität von Melbourne im Rahmen meiner Diplomarbeit ermöglicht haben. Dies hat nicht nur den Werdegang dieser Arbeit sehr beeinflusst sondern auch mein ganzes weiteres Leben.

Für die vielen ermunternden und anspornenden Worte und das mühevolle Korrekturlesen danke ich Christopher Ackland.

Gisela Höflinger

Contents

1. Abstract

Models are used to simulate and calculate individual muscle forces and body mass acceleration because their direct measurement is impractical. Among other parameters, the parameters which describe and define the characteristic of the elements of the muscle-tendon model are important input variables. Since they are difficult to obtain and cannot be measured *in vivo*, they are estimated values. The purpose of this work is to conduct a sensitivity analysis to those parameters on the output of an inverse-dynamic gait model.

It was desired to show how muscle parameters contribute to the body mass acceleration. Body mass acceleration can be broken down to all accelerations delivered by the individual muscles. Hence, muscle parameters are varied and a new sets of muscle forces are calculated. Those new muscle forces are input to a perturbation analysis which calculates the contribution of muscle induced acceleration to the body mass acceleration. The comparison of the nominal values and the values due to the variation give a conclusion about sensitivity of accelerations to muscle parameters.

The analysis of this study includes the variation of pennation angle, optimal muscle force, resting fiber length and tendon slack length (specific values for each muscle) as well as maximal shortening velocity, activation and deactivation time (constants for all muscles). The model of walking includes 54 muscles (each leg 24, upper body 6), of which 13 have been included in this study. The analysis was examined over the stance phase of the gait cycle for normal walking.

Muscles were most sensitive to a variation of tendon slack length. The combined muscles plantar flexors were found to be the most sensitive muscle group and, additionally, variation of their parameters had a considerable influence on other muscles. The results clearly show dependencies between the several muscles contributing to locomotion. The variation of a parameter for a muscle can have a similar or even larger impact on the other muscles than on the muscle which was changed. The findings of this work emphasize the importance of accurate parameter setting and consideration of interactivity of muscles and muscle groups.

2. Zusammenfassung

Modelle werden verwendet um einzelne Muskelkräfte und die Beschleunigung des Körperschwerpunkts zu berechnen, da deren direkte Messung nicht möglich ist. Unter vielen anderen Parametern sind diejenigen, welche die Eigenschaften der Elemente des Muskel-Sehnen Modells beschreiben, wichtige Eingangsgrößen. Da diese sehr schwierig zu bestimmen sind und *in vivo* nicht gemessen werden können, sind sie geschätzte Größen. In dieser Arbeit wurde eine Sensitivitätsanalyse bezüglich dieser Parameter an einen invers-dynamischen Gangmodell durchgeführt.

Es sollte gezeigt werden wie Muskelparameter die Beschleunigung des Körperschwerpunktes beeinflussen. Diese Körperschwerpunktsbeschleunigung kann aus den Beschleunigungen, die von den einzelnen Muskeln beigesteuert werden, zusammengesetzt werden. Es werden die Muskelparameter variiert und Sets von Muskelkräften berechnet. Diese neuen Muskelkräfte sind die Eingangsdaten für eine Perturbationsanalyse, welche den Beitrag eines jeden einzelnen Muskels zu der Beschleunigung des Körperschwerpunktes ermittelt. Der Vergleich von nominalen mit variierten Werten gibt Rückschlüsse über die Sensitivität von Beschleunigungen zu Parametern.

Die Analyse umfasst die Variation von Fiederungswinkel, optimaler Muskelkraft, optimaler Muskelfaserlänge und Sehnenruhelänge (für jeden Muskel spezifische Werte) wie auch maximale Verkürzungsgeschwindigkeit, Aktivierungs- und Deaktivierungszeit (konstant für alle Muskeln). Das Gangmodel beinhaltet 54 Muskeln (jedes Bein 24, Oberkörper 6) von denen 13 untersucht wurden. Durchgeführt wurde die Analyse über die Standphase eines Gang-Zyklus bei normalem Gehen.

Muskeln zeigten größte Sensitivität zu einer Variation der Sehnenruhelänge. Als sensitivste Muskel Gruppe stellten sich die zusammengefassten Muskeln der plantar flexoren heraus. Außerdem hatte eine Variation ihrer Parameter einen beträchtlichen Einfluss auf die anderen Muskeln. Die Resultate zeigen deutlich Abhängigkeiten zwischen den verschiedenen Muskeln, die zur Fortbewegung beitragen. Die Ergebnisse dieser Arbeit unterstreichen die Wichtigkeit Parameterwerte richtig zu setzen und veranschaulichen die wechselseitige Beeinflussung von Muskeln und Muskelgruppen.

3. Introduction

Individual muscle forces produced by humans in every-day tasks and athletic activities are important quantities. The knowledge about that has numerous applications in human biology, orthopedics, and motor control. Methods of mathematical modeling are used to estimate individual muscle forces in the human body because their direct measurements are difficult to make. [28]

The accuracy of any modeling approach is determined, in part, by the values of the parameters assumed in the model. Muscle models are defined by numerous parameters, which cannot be measured directly due to the invasiveness of determining some muscle parameters. A model of movement can incorporate various elements, including a model of the skeleton, a model of the muscle paths, a model of muscle actuation, and a model of excitation-contraction coupling. Many studies have examined the sensitivity of model calculations to variations in body anthropometry but few have quantified the sensitivity of muscle force estimates to changes in muscle properties. The latter is important in view of the wide variation in muscle properties reported in the literature, even for the same muscles in humans, as well as the fact that muscle properties can change as a function of both age and activity level. [29]

The influence of different parameter values on musculoskeletal models is not well understood [31]. Some authors report that predicted muscle forces correlate reasonable well with muscle activations of the selected task, whereas others report that these or similar criteria do not predict magnitudes and patterns satisfactorily. Possible reasons for these contradictions are that calculated muscle forces are very sensitive to model parameters and different authors use different sets of model parameters [28].

Musculoskeletal simulations of human movement commonly use Hill muscle models to predict muscle forces, but their sensitivity to model parameter values is not clear. Scovil and Ronsky [31] say that the sensitivities of their running and walking simulations were reduced compared to the sensitivity of the muscle model alone. Results demonstrate the importance of evaluating sensitivity of a musculoskeletal simulation in a controlled manner and provide an indication of which parameters must be selected most carefully based on the sensitivity of a given movement. Further Raikova and Prilutsky [28] say that the sensitivity of the optimal solution to model parameters should be investigated for the model of interest and, preferably, analytical relationships between predicted muscle forces and model parameters should be obtained so that the effect of model parameters can be clearly seen.

Hence, not just a reliable model is necessary to receive useful data (in matters of describing the reality well enough) but the setting of the model describing parameters is also crucial. That is why sensitivity analyses have to be executed on a model. It must be understood how a model reacts to its input parameters to receive reliable data. Especially when the input parameters can be set in a wide range and there is not yet

a consensus found of which are the most important parameters and how values have to be set. There is not yet a consensus found of which are the most important parameters and how values have to be set.

The purpose of this work is to improve the understanding of how far and to which amount the muscle describing parameters are able to affect the model output. Each parameter can not just affect the force and so accelerations of its own muscle but also forces produced by all the other muscles. Calculating those sensitivities will give knowledge about dependencies of muscles and muscle groups and which parameters and so muscle characteristics have to be treated more carefully. It might help to find more consistent parameter ranges and so improve the simulation of movement.

3.1. Biomechanical modeling and simulation

Muscles control body movement by developing forces and exerting torques about the joints. Direct measurement of muscle force *in vivo* is currently not practical, and so mathematical models of the musculoskeletal system are often used to estimate muscle forces non-invasively. Muscle forces cannot be determined uniquely, however, as the muscles form a mechanically redundant system (i.e. the number of muscles crossing a joint is usually greater than the number of degrees of freedom prescribing joint motion) as well as the activation strategy of the central-nerve-system is unknown. One method used to resolve this redundancy involves the application of optimization theory, in which physiological cost function is minimized subject to the constraints imposed by the musculoskeletal system and the motor task being modelled. [29]

Creating a muscle-driven simulation of a motor task requires two basic steps: (1) the formulation of a dynamical model of the musculoskeletal system and its interaction with the environment (e.g. the ground in walking); and (2) a method to find the muscle excitations to be applied as inputs to the model. A simulation is evaluated by how well the simulated kinematics, kinetics, and muscle excitation pattern agree with the measured kinematics, kinetics, and EMGs in the context of the intended use of the simulation. [35] The kinematic information are the dynamical joint angles during the whole gait cycle. In three dimensional measurements there are three orthogonal rotational components to be considered. The kinetic data is joint moment and joint power. The joint moment is a vector with three orthogonal components, corresponding to the kinematic data. [22]

3.1.1. Gait Analysis

Gait analysis is important for several clinical applications like orthopedics, physical medicine and rehabilitation. The systematic analysis of locomotion helps in pretreatment assessment, surgical decision making and postoperative follow-up. It has played a key role in advancement of surgical treatment of children with cerebral palsy. From

isolated treatment and procedures the current comprehensive multi-level approach corrections could be emerged. Gait analysis is also a useful tool for study of neuromuscular disorders, the evaluation of prosthetic joint replacement and the study of athletic injuries, amputees, orthotics and assisting devices.

There are three main clinical applications. Simulation of gait can be used as a part of clinical assessment. Gait analysis can support to follow the progress of a disease as a monitoring tool and is used as a quantitative measurement for research. [22]
Those topics were subjects or inspiration for numerous papers and research-projects (e.g. [7], [5], [12], [9], [20]). Premise for such surveys are working and reliable models for simulation of locomotion.

3.1.2. Different methods to calculate muscle forces

In biomechanics, the general distribution or force-sharing problem is aimed at predicting the forces of individual musculoskeletal structures from known resultant joint forces and moments. The problem is the determination of individual muscle forces during movement. The difficulty in determining individual muscle forces arises from the inherent redundancy of musculoskeletal systems; that is, movements can typically be produced by an infinite number of muscle force patterns. [21] Therefore, different methods were developed to compute those muscle forces.

Inverse dynamics (IVD): Inverse dynamics use link-segment models to represent the mechanical behavior of the body. From observation of movement inverse dynamics analysis compute the associated moments which lead to that movement. It has been used extensively to estimate *in vivo* muscle forces during gait. By static optimization those computed joint torques can be decomposed into individual muscle forces. Static optimization is based on the idea that movements are controlled in a way to optimize some physiological criterion. For example that muscular fatigue is minimized in cyclic, low effort movement tasks [21] or the level of muscle activation or muscle stress is minimized. Such models are computationally efficient (obtained realtively quickly on single-processor computers), allow full three-dimensional motion and can incorporate large numbers of muscles. Although this approach is computationally efficient, it has several shortcomings, beginning with the inaccuracies of IVD. This makes it highly influenced by the accuracy of collected and processed body segmental kinematics (this is experimental data). Static methods perform a separate optimization at each instant during the task, and therefore cannot take into account physiological cost functions, such as total muscular effort or metabolic energy consumption, which are evaluated over time. Also due to the time-independent nature of static optimization, it is relatively difficult to incorporate the objected motor task properly. [3], [4], [6]

Dynamic optimization (DO): Dynamic optimization is potentially more powerful than static optimization. It is inherently a forward-dynamics method, and so the problem may be formulated independent of experimental data. It executes a forward

8

simulation to evaluate performance over the entire motor task period, a time-dependent criterion can be posed. For example, the optimization problem could be to calculate the muscle excitation histories, muscle force and limb motions by the cost function of minimizing the metabolic energy expenditure per unit distance traveled. Muscle metabolic energy can be calculated by summing five terms: the basal or resting heat, activation heat, maintenance heat, shortening heat and the mechanical work done by all the muscles in the model [4]. These attributes allow the motor patterns and kinematics of movement to be *predicted* and is more likely to provide realisticly estimated muscle forces. The main disadvantage is that it is computationally very expensive, this requiring that dynamic models are greatly simplified. The Number of muscles included are significantly less than those used in analogous static optimization work. The question occurs whether this is computational expense is justified. [4], [3] Generally speaking, dynamic optimization is impractical for common use due to the calculating time issue caused by the numerical methods used to solve these problems. [6]

Neuromusculoskeletal tracking (NMT): The method estimates muscle forces from observed motion data. The NMT method combines skeletal motion tracking and optimal neuromuscular tracking to produce forward simulations of human movement quickly and accurately. The skeletal motion tracker calculates the joint torques needed to actuate a skeletal model and track observed segment angles and ground forces in a forward simulation of the motor task. The optimal neuromuscular tracker resolves the muscle redundancy problem dynamically and finds the muscle excitations (and muscle forces) needed to produce the joint torques calculated by the skeletal motion tracker. The NMT method requires 3 orders-of-magnitude less CPU time than DO done by parameter optimization. NMT method is an alternative to the conventional approach of combining inverse dynamics and static optimization to compute muscle forces in human movement. [6]

Anderson and Pandy [3] aimed to asses whether or not dynamic optimization provides more realistic estimates of muscle forces than static optimization (for normal gait). They address two questions, first if the large computational cost of dynamic optimization is justified and second if it is important to account activation dynamics and force-length-velocity properties to describe muscle physiology truthfully.

They found similarity between the static and dynamic solution which suggests that this computational expenditure does not significantly improve predictions of muscle or joint contact forces. Further it appears that a time-independent performance criterion is adequate and that both activation dynamics and the force-length-velocity properties can be neglected. The striking similarity between the solutions of the methods also suggest that the different optimization criteria, minimizing muscle fatigue at each time step (static optimization) and minimizing metabolic energy expended per unit distance traveled (dynamic optimization), are roughly the same. To conclude, if one can accurately solve the inverse dynamics problem for normal gait and if one seeks only to

estimate muscle and joint contact forces, the use of dynamic optimization is currently not justified. But dynamic optimization may be preferred or even necessary when accurate experimental data are not available, activation dynamics plays an important role, an appropriate time-independent performance criterion is not available or prediction of novel movement is desired. [3]

3.1.3. Hill-type muscle model

The mechanical behavior of muscle is described as a traditional three- component Hill muscle model which consists of a contractile element (CE), that models active muscle force, the series elastic element (SEE), that models stretch soft tissue and the parallel elastic element (PEE), that models passive muscle force (see Figures 1 and 2).

The muscle-tendon unit is the muscle fiber in series with tendon. The pennation angle α is the angle between the lines of action of the tendons and the muscle fiber. l_o^m is the optimal length of the muscle, l_s^t is the length of the tendon, and l^{mt} is the muscle-tendon length. The width w of the muscle remains constant as muscle length changes. (Figure 1) The contractile element produces the active force as a function of fiber length (Figure 2)and fiber velocity (Figure 3). The elastic component gives passive force (Figure 2).
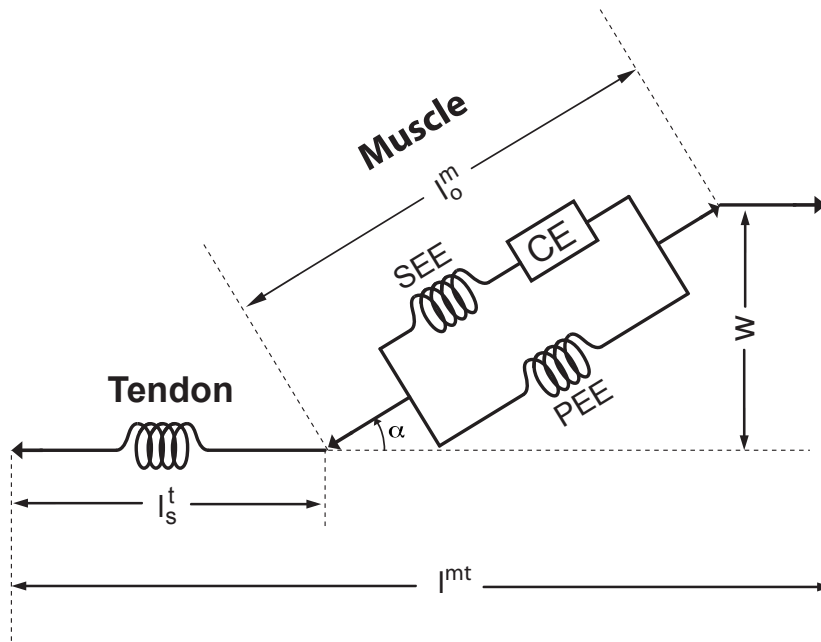
Figure 1: Schematic of the musculotendon model. Muscle is described by a three element Hill-type model.
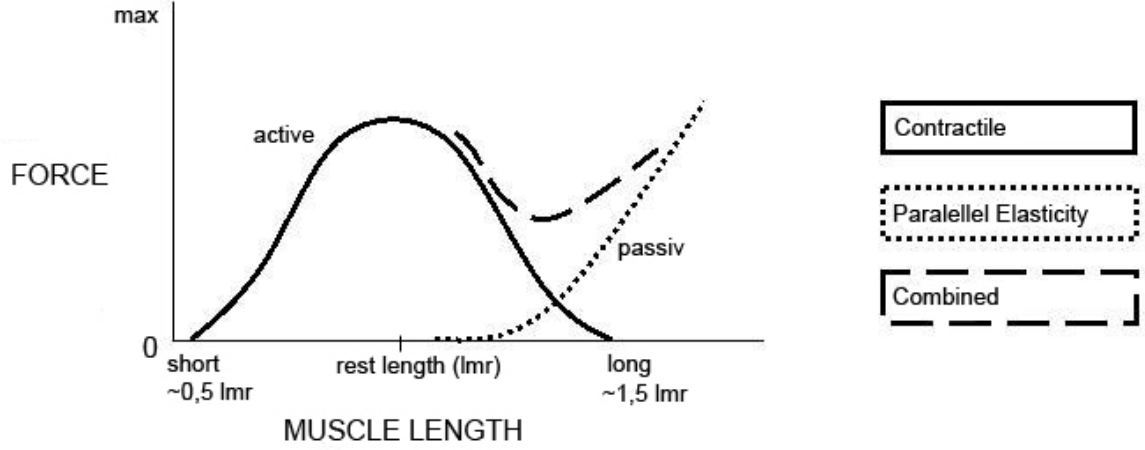
Figure 2: The force development of a muscle due to the contractile and parallel-elastic element according to its length. *Source: http://www.elitefts.com/ documents/power_and_strength.htm, 1.09.08*

The force producing characteristics of an actuator depend on the maximum isometric strength of the muscle and its corresponding fiber length and pennation angle, the maximum shortening velocity and the rest length of the tendon. A nonlinear differential equation defines the relationship between the time rate of change of musculotendon force ($\dot{F}^{MT}$) and musculotendon length (l^{MT}), musculotendon velocity (v^{MT}) and muscle activation (a) [2] :

$$\dot{F}^{MT} = f(F^{MT}, l^{MT}, v^{MT}, a); \qquad 0.01 \leq a \leq 1 \qquad (1)$$

Given the instantaneous values of F^{MT}, l^{MT}, v^{MT} and a the force developed by the actuator at the next time instant is found by numerically integrating equation (1).

Muscle cannot be activated or relaxed instantaneously. This behavior is explained by the time course of muscle activation. A first-order differential equation relates the time rate of change of the muscle activation ($\dot{a}$) to muscle excitation (u) [2]:

$$\dot{a} = \frac{1}{\tau_{rise}}(u^2 - ua) + \frac{1}{\tau_{fall}}(u - a) \qquad u = u(t); a = a(t) \qquad (2)$$

The constants τ_{rise} and τ_{fall} are the rise and decay times of the muscle activation. τ_{rise} is the time which the muscle requires to reach 70% of the maximum force. τ_{fall} is the time which it takes until the muscle produces just 30% of the maximum force anymore.
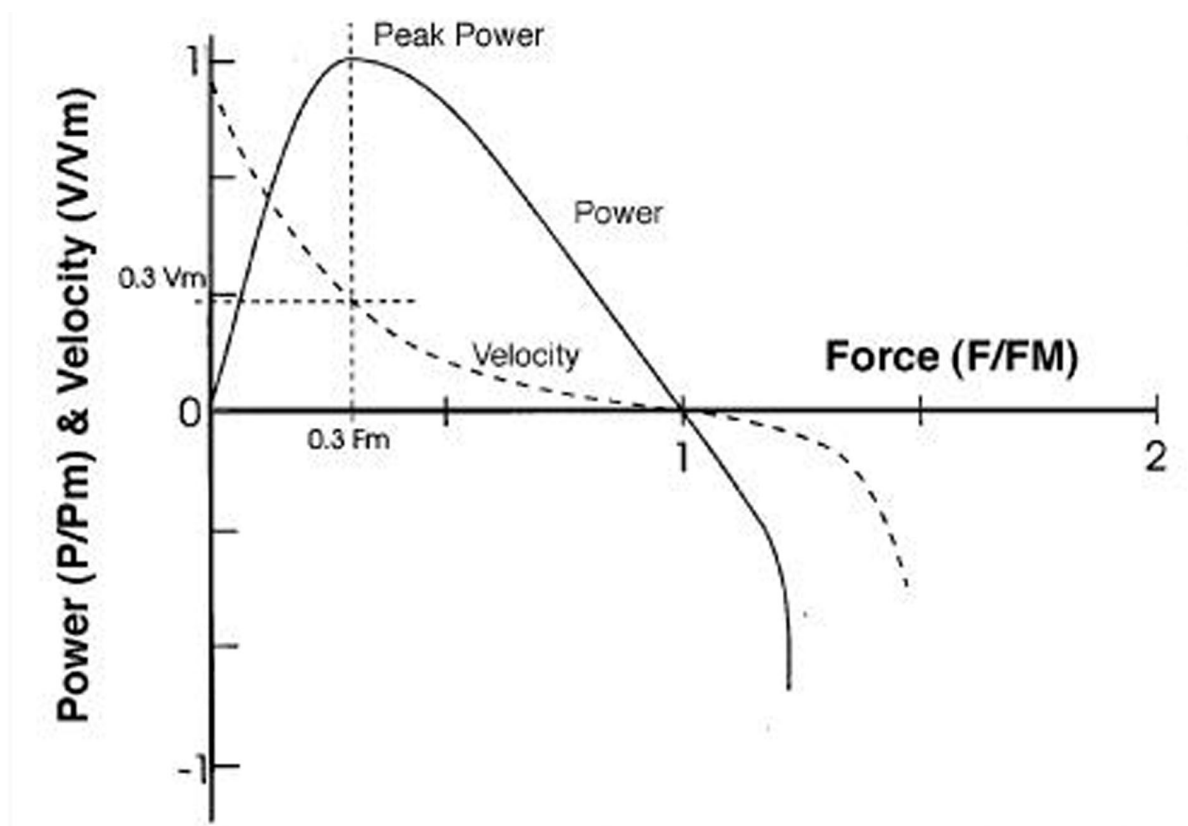
Figure 3: The Force velocity power relationship for skeletal muscle. Vm, Pm and Fm are maximum movement velocity, maximum power output and maximum isometric force output respectively. The mechanical power output is maximized at approximately 30% of maximum shortening velocity and a load of 30% of maximum isometric strength. *Source: http://www.fittech.com. au/products/kms.asp?loc=training, 1.09.08*

3.1.4. Muscles function in human gait

A muscle can perform many mechanical functions. It can develop force and power, and over time produce work output. Or it can dissipate mechanical energy if its active fibers are stretched. When its tendon and other in series elastic elements are stretched, energy is stored. The force-length-velocity property of muscle can stabilize movement.

Muscles coordinate multi-joint motion by generating forces that cause reaction forces throughout the body. Thus, a muscle can redistribute existing segmental energy by accelerating some segments and decelerating others. In the process, a muscle may also produce or absorb energy, in which case its summed energetic effect on the segments is positive or negative, respectively. If the segments are not at rest, segmental energy increases in the accelerated segments and decreases in the decelerated ones. The function of a muscle to cause energy to be exchanged among segments, whether the muscle is isometric (muscle is activated but holding its constant length), eccentric (muscles are lengthened while they are active), or concentric (the muscle shortens, the force which is generated is always less then the muscle's maximum), can be more important to task execution than its role in producing energy and delivering that energy to the segments. [35]

When any muscle in the human musculoskeletal system is damaged, other muscles and ligaments tend to compensate for the role of the damaged muscle by exerting extra effort. Deactivation of one muscle can often lead to increment/decrement of force developed by muscles with completely different primary functions. For example, deactivation of the iliopsoas leads to a large reduction in force by the soleus. [23]

3.2. Literature review

The first task for this thesis was to investigate two methods which could be suitable to conduct a sensitivity analysis of muscle forces. These methods being the Monte-Carlo simulation and the perturbation analysis. Following, the findings of the research are shortly presented, as well as investigated through different aspects to get an overview of how they work and which problems they can be applied to solve. A whole subsection is dedicated to summarize Liu et al's paper [24] ("Muscles that support the body also modulate forward progression during walking", section 3.2.3) because the perturbation analysis presented there is used in this work and was foundation to develop several ideas (see section 4.2). In the last section of this chapter the findings about sensitivity analysis in recent publications are briefly presented (section 3.2.4).

3.2.1. Monte-Carlo Simulation

The Monte Carlo Simulation, also known as stochastic simulation, is a technique which uses random numbers to solve a modeled problem. The parameters of the model are varied by a probability distribution. Using these variations several simulations are executed. The goal is to determine how random variation, lack of knowledge or measurement errors can affect the sensitivity, performance or reliability of the system that is being modeled.[1] The result is an amount of solutions which are statistically evaluated in the next step. [11]

According to Halton [17] the Monte Carlo Method can be described as followed: "Within the Monte Carlo Method, the solution to a problem is represented as parameters of a hypothetical totality. By using randomly chosen numbers a potential sample is constructed and the value of the parameters of interest are estimated by statistical methods."

To simplify, the method can be characterized and implemented by five steps:

1. Creating a parametric model : $y = f(x_1, x_2, \ldots, x_q)$

2. Generating a random set of inputs: $x_{i1}, x_{i2}, \ldots, x_{iq}$

3. Calculating the model and storing the result as y_i

4. Repeating step 2 and 3 for $i = 1 \ldots n$

5. Analyzing the results by histograms, summary statistics, confidence intervals etc.

The key to the MC-Method is the use of random numbers. One way to generate these numbers is to identify statistical properties for the parameters. Such properties are sometimes given directly by the description of the model (e. g. the parameters describe

---

[1]http://www.vertex42.co,/ExcelArticles/mc/MonteCarloSimulation.html, 10.06.2007

the durability of a working piece). Another possible way is to conduct a series of measurements on the real system to receive different values for the parameters. For those numbers several statistical tests are carried out to identify a certain distribution of the values. Based on that, one is able to find a known distribution (e.g. normal distribution, exponential distribution,...) that is close to the actual surveyed distribution of the parameters. The parameter is determined by an interval, so can therefore be simulated by a continuous equal distribution or by dividing the interval by the number of test runs. [11]

Ermakov [14] sums it up like this: "The Monte Carlo Method can be defined as a method for modeling random variables, whereas the objective is to calculate specific characteristics of the distribution."

To generate random numbers is not as easy as one would think. Random numbers (i.e. independent realization of a random variable) can only be obtained by a random process, which means carrying out a random experiment. There are existing charts of random numbers but often a big quantity of numbers is required to get the sufficient results. Due to that limitation, pseudo random numbers are often used instead, which are much easier to generate. These are "random numbers" which are built by a mathematical law. That means they are deterministic (using the same initial value, the same numbers can be calculated again), and really anything but random. Despite the obvious contradiction, these pseudo random numbers are very suitable for practical use. They just need to pass certain given tests like the real random numbers are able to.[18]

Historical Background   Since the method relies on random numbers which could be produced by a roulette game, the name Monte Carlo Simulation derives from the place Monte-Carlo, which is famous for its gambling.

Already in the 1940's, when the first computers were developed, Monte Carlo Methods had been used for solving numerical problems. Particularly for the construction of the atomic bomb was the simulation of random processes already used on a grand scale. Here they wanted to forecast theoretically the interaction between neutrons and matter.[2] Since the 1950's the application of the method has broadened.

Applications   In principle, the Monte Carlo Method is suitable for any kind of process which is influenced by random factors. It allows a simulation of the studied process, but also deterministic problems which are not random at all. For example, the calculation of a surface area or an integral, can be solved. Therefore, a stochastic model equivalent to the mathematical system can be built. The solution of the problem results from a parameter of the model (e.g. as the expectation value of a distribution). Hence, insolvable analytical problems can be solved numerically. The justification for using that kind of method is the law of large numbers (typically a simulation that can include over 10 000 runs). So generally, any method which uses random numbers to solve either

---

[2]http://www.exp.univie.ac.at/sc/sim.html, 10.06.07

deterministic or stochastic problems is a Monte Carlo Method[18]. It is also a common method to treat problems which are in fact numerically solvable but the exact solution cannot be received for some reason (e. g. matter of time)

An easy example is the calculation of the mean value of a function within a certain interval. Points are randomly chosen out of the interval for which the function is calculated. Afterwards the mean value of those function values is worked out. The more function values are calculated, the more precise becomes the solution. [33]

First of all, the method is very suitable for problems which can be described using probability. But also for strict deterministic problems it can be very helpful to create a stochastic model. Therefore the problem is randomized and the MC-Method can be applied. Characteristics and input parameters often have a certain measurement error. For that reason it is very important to know how those parameters and their possible deviation influence the model. Sometimes even small changes can have a great impact on the result of the simulation. Information about the character of such parameters gives a sensitivity analysis of the system of equations. In most of the cases the deviations of the parameters which have to be analyzed can be simulated by a distribution. [11]

Some examples for which the MC-Method can be applied:

- Analytically unsolvable problems of mere mathematical background (e. g. approximation of pi, integrals of higher dimensions [3])

- Physical/nature constants

- Distribution character of random numbers with unknown type of distribution [4]

- Simulation of complex processes which cannot be simulated straight forward (e. g. processes of production to avoid shortages, weather and climate [5])

- For the simulation of uncertainties and statistical characteristics (e. g. path of a water drop) [6]

- Cross Impact Analysis

- Electrical circuits [33]

- Biology and Economy: Simulation of external influences on an ecosystem (e. g. predator-prey System [33], queueing theory)

---

[3]http://de.wikipedia.org/wiki/Monte Carlo Simulation, 10.06.07
[4]http://de.wikipedia.org/wiki/Monte Carlo Simulation, 10.06.07
[5]http://de.wikipedia.org/wiki/Monte Carlo Simulation, 10.06.07
[6]http://de.wikipedia.org/wiki/Monte Carlo Simulation, 10.06.07

Monte Carlo Method as an optimization method The main principle is: Numbers are produced by a random generator and assigned to the parameters which should be optimized. With those parameters the simulation is executed and the results are compared with the previous best solution. If the new given solution is the best one it is stored as the new best solution. This procedure is repeated until the desired accuracy of the result is reached. The advantage of this linear searching is that less simulations are required to get the same result. This is especially an effective method for systems with a high number of parameters. [16]

Sensitivity analysis by the Monte Carlo Method The principle structure is shown by a system of ordinary differential equations.

$$\vec{y} = \vec{g}(t; y_0, y_1, \ldots, y_{n-1}) \qquad \text{whereas} \qquad \vec{y}(t_0) = \vec{x}$$

One parameter of the initial value problem is not known whereas the disturbed parameter is either the initial value $\vec{x}$ or any other parameter of the ordinary differential equation. The disturbed parameter is seen as a stochastic value. Due to previous knowledge or experiences is a n-dimensional distribution defined (e.g. Normal distribution $N(\vec{x}^{(0)}, \sigma^2)$). A certain number a of random vectors $\vec{x}^{(j)}$ is picked out of the distribution. Thus, a disturbed initial value problems are received. To compare the varied solutions with the original solutions certain moments t_i are chosen for which the comparison shall be done. For every moment t_i the mean value is built $\vec{y}^1(t_i), \vec{y}^2(t_i), \ldots, \vec{y}^a(t_i) \implies y^m(t_i)$. Hence, at every moment t_i one is interested in the comparison between $\vec{y}^0(t_i)$ and $\vec{y}^m(t_i)$ can be done. [18]

To actually calculate this sensitivity analysis the simulation system MOSIS (MOdular SImulation System), which was developed at the TU Vienna, could be used.

3.2.2. Perturbation analysis

It is the nature of data material never being disposal in an absolute exact form. To cite from a more philosophical viewpoint from Avrachenkov [8]: "As long as we have to work with data, we have to deal with its perturbations". Therefore, it is very important to analyze the influence of perturbations (i.e. the deviation of the nominal value of the data material). Sometimes even small perturbations cause a dramatic change in the problem properties. Such sensitivity analysis can be efficiently done by the technique developed for singular analytic perturbations. Usually data material is stored and worked with in matrix form. This general idea of perturbation can be written mathematically in the following additive form:

$$\tilde{A} = A + D$$

Where $\tilde{A}$ is the matrix of the perturbed data, A the matrix of nominal data and D is the matrix of the perturbation itself, and additionally the rank of $\tilde{A}$ is different from the rank of A, the perturbation is said to be singular. If they have the same rank the perturbation is regular. Since the additive form is very inconvenient for singular problems, a perturbation parameter ϵ is introduced [8]:

$$A(\epsilon) = A + \epsilon B$$

ϵ reflects the value of the deviation of the perturbed data from the nominal set and B represents the likely direction of the data deviation. This model is called linear perturbation.

The Perturbation Analysis is likely to be used for the numerical calculation of sensitivities. To calculate the influence of a single parameter on the output, each parameter of the perturbed model answer has to be calculated. In the case where there are large matrices involved, the calculation can become computationally intensive. In some cases the differential quotients can be that small that they are numerical distorted due to small rounding errors. [25]

The literature review on perturbation analysis has shown that the key word "Perturbation Analysis" gives many and diversified results. For every single problem the applications are very specific and often difficult to comprehend. Because on the one hand one needs a good mathematical know-how, and on the other hand specialist knowledge in the field is required for the understanding. Now, there are just a few examples given where Perturbation analysis is used:

- Economics: "Optimization of a single-component maintenance system: A smoothed perturbation analysis approach" [19]

- Physics: "Acoustical Klein-Gordon equations: A Time-Independent Perturbation Analysis" [15], preparative fluid chromatographic, fracture mechanics: to solve fast forward expanding cracks analytically

- Mathematics: often mentioned in connection with Markov Chains [8]

As an example for an application of a perturbation analysis on a bio-mechanical problem, look at section 3.2.3

Variation-Perturbation   Usually the terms perturbation and variation are used equally. But when talking about perturbation analysis and variation of a parameter those two terms can have a specific and different meaning which should be defined (see also Figure 4).

Variation: Is the change of an input value at the beginning of the simulation. It is observed how an initial disturbance develops over time until the end of simulation. It is a normal simulation proceeded with a different input value.

Perturbation: Is a small deviation applied on an input value and then simulated forward in time. The duration of the perturbation is defined by Δt. At each time step t_i the function is evaluated. In comparison to the variation the perturbation just runs for this interval Δt and it is observed how the values of the function change. New starting point for the next perturbation simulated forward in time is the original (unperturbed) value of the function at t_i. (compare to perturbation analysis in section 3.2.3)
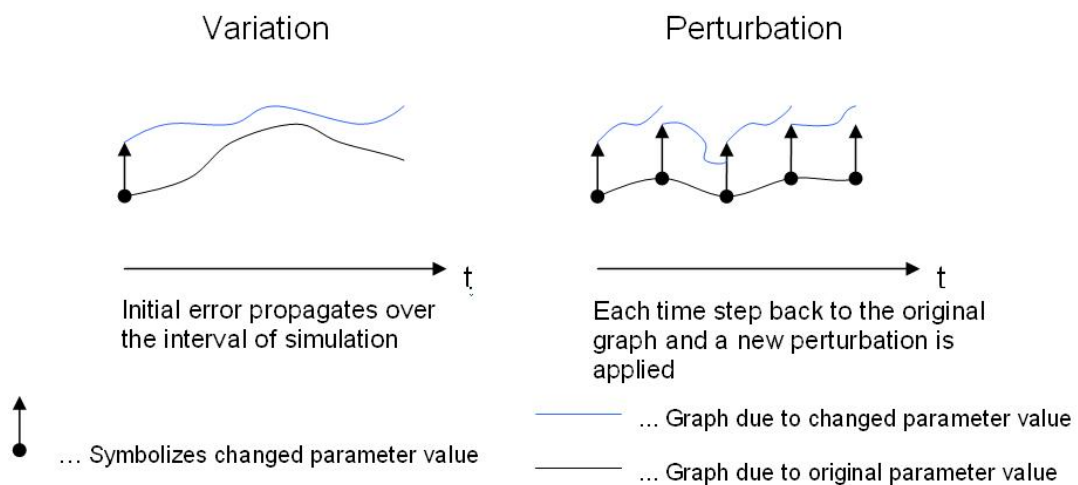
Figure 4: The difference between variation and perturbation.

3.2.3. Application of the perturbation analysis on a bio-mechanical problem, Liu at al. [24]

The purpose of the study was to characterize the contribution of individual muscles to the forward progression and the vertical support during walking. Therefore, forces of the 54 muscles of the 3-dimensional gait-model were systematically perturbed. Afterwards, the changes in the for-aft and vertical acceleration of the body mass center due to the altered muscle forces during the stance phase were computed. The simulation of walking was obtained by solving a dynamic optimization problem that minimizes the metabolic energy expenditure per distance. A suitable formula for the perturbation analysis to estimate the acceleration caused by a specific muscle is:

$$\ddot{x}_m(t_i) \approx 2 \frac{x(F_m + \Delta F_m, t_i + \Delta t) - x(F_m, t_i + \Delta t)}{\Delta t^2 \Delta F_m} F_m \tag{3}$$

t_i ... current time in the simulation
$\ddot{x}_m(t_i)$ ... contribution of muscle m to fore-aft acceleration of body mass center
F_m ... force generated due to muscle m
ΔF_m ... small perturbation of F_m
Δt ... duration of the perturbation, a short interval over that the simulation is run

Derivation of the equation:

$$\ddot{x}_m(t_i) = \frac{\partial \ddot{x}}{\partial F_m} F_m = \frac{\ddot{x}(F_m + \Delta F_m, t_i) - \ddot{x}(F_m, t_i)}{\Delta F_m} F_m \tag{4}$$

$\ddot{x}$ ... fore-aft acceleration of body mass center

Since the accelerations can be assumed as being constant over the short interval Δt, the observed changes in position can be related to the acceleration using the following relations (according to the Taylor-Theorem, a linearization at F_m within a small interval Δt) :

$$x(F_m, t_i + \Delta t) \approx x(F_m, t_i) + \dot{x}(F_m, t_i)\Delta t + \frac{1}{2}\ddot{x}(F_m, t_i)\Delta t^2 \tag{5}$$

and

$$x(F_m + \Delta F_m, t_i + \Delta t) \approx x(F_m + \Delta F_m, t_i) + \dot{x}(F_m + \Delta F_m, t_i)\Delta t + \frac{1}{2}\ddot{x}(F_m + \Delta F_m, t_i)\Delta t^2 \tag{6}$$

where $x(F_m, t_i + \Delta t)$ and $x(F_m + \Delta F_m, t_i + \Delta t)$ are the unperturbed and perturbed for-aft positions, respectively, of the mass center at $t_i + \Delta t$. One should notice that $x(F_m + \Delta F_m, t_i)$ is equal to $x(F_m, t_i)$ and $\dot{x}(F_m + \Delta F_m, t_i)$ is equal to $\dot{x}(F_m, t_i)$ because positions and velocities cannot change instantaneously in response to a force perturbation. Subtracting equation (5) from equation (6) and substituting the result into (4) provides the formula for estimating the acceleration of a muscle (3).

Those transformations are an elegant way to turn the continuous problem into a discrete one. For this a computer program can be written easily, the velocity and the acceleration have been eliminated of the formula for the perturbation analysis as well as it was achieved that the perturbation ΔF_m is part of the formula.

ΔF_m was set as $1N$, the perturbation has to be small because the system is very sensitive to force changes. If the variation of force is to big, kinematics and spring reactions start to behave very different and results become wrong. The acceleration due to each muscle was evaluated every $0.02s$ during the simulation.

The accelerations were calculated during the stance phase, accelerations from muscles during the swing phase were very small. Since left and right side muscle forces are symmetric, only data for the right-side muscles is presented. The stance phase was divided into halves, the first half from initial contact to midstance ($0 - 32\%$ of the gait cycle), and the second half from midstance to toe-off ($32 - 65\%$ of the gait cycle). Exactly the stance phase was considered to be 67.5% of the gait cycle which equates 0.754 seconds.

Several muscles were found to contribute most to the body mass acceleration in the three orthogonal directions (1, 2 and 3 respectively forward, vertical and lateral). The five greatest peaks for individual muscle for-aft accelerations in each half of stance were due to just four muscle groups. The combined accelerations from vasti, gluteus maximus, gluteus medius, dorsifelxors, soleus and gastrocnemius accounted for almost all of the net fore-aft acceleration. The combined accelerations from from vasti, gluteus maximus, gluteus medius, dorsiflexors, soleus, gastrocnemius and other plantarflexors accounted for most of the net vertical acceleration.

21

3.2.4. A short literature study for sensitivity analysis

Sensitivity illustrates how a certain change of input data effects the output data. It is a measure for how a system reacts to a variation of its parameters or any kind of value which is input for producing the systems outcome. The higher the sensitivity, the stronger a system responses to even small disturbances.

While muscle models are commonly used, limited evaluation of muscle model sensitivity to input parameters has been reported [31]. Musculoskeletal models have been found to be sensitive to tendon slack length, optimal muscle fiber length and muscle moment arm (as well as the muscle activation time constant). Other parameters were found to have a low sensitivity in a musculoskeletal model, including the parallel elastic element parameters, pennation angle and muscle deactivation time constant. Several studies have reported differing sensitivities to muscle parameters. Model insensitivity to series elastic compliance has been reported, while other models were found to be sensitive to compliance. Two cycling simulations were insensitive to maximal force after re-optimization of the muscle activation timings, while other models were sensitive to that parameter. The variation in reported sensitivities may be due to differences in models or types of motion simulated, but comparison between studies is confounded by the use of different sensitivity analysis techniques. [31]

But literature has also shown that different authors used methods for processing their data which are quite similar, if looked at them closer. All of the considered ones were dealing with muscle outputs. One concept, slightly modified, stands behind the several applications.

In Liu at al. [24], as introduced above in section 3.2.3, the following expression can be found; a partial derivative of the muscle acceleration multiplied by the muscle force:

$$\ddot{x}_m(t_i) = \frac{\partial \ddot{x}}{\partial F_m} F_m \tag{7}$$

Scovil and Ronsky [31] evaluate muscle model sensitivity to perturbations in 14 Hill-type muscle model parameters in forward-dynamic simulations of running and walking. They refer to a standardized method to calculate sensitivity which has been employed in several studies. This method divides the normalized change in a model output by the normalized change in a model parameter.

$$S_{ij} = \frac{\frac{M_{iP} - M_{i0}}{M_{i0}}}{\frac{P_{jP} - P_{j0}}{P_{j0}}} \tag{8}$$

where

S_{ij} ...   sensitivity for a model with i outputs and j defining parameters
M_{iP} ...   model output
M_{i0} ...   model output original
P_{jP} ...   model parameter
P_{j0} ...   unperturbed parameter value

As a more general method, also discussed in Scovil and Ronsky [31], they describe the calculation of the partial derivative of the muscle equations with respect to each model parameter. The following partial derivative, gives the instantaneous rate of change in the muscle output (MUS_{OUT}) as a function of the change in a parameter (X).

$$\frac{\partial MUS_{OUT}}{\partial X} \tag{9}$$

In their work Redl et al.[29] introduce the *instantaneous sensitivity ratio* (which is presented into more detail in section 4.6):

$$\epsilon_{ij} = \frac{\frac{F^m_{new,ij} - F^m_{nom,ij}}{F^m_{nom,ij}}}{\frac{p_{new,j} - p_{nom,j}}{p_{nom,j}}} \tag{10}$$

where

ϵ_{ij} ...   instantaneous sensitivity ratio for muscle j (j=1..27) at
                     time step i (i=1..135)
$F^m_{nom,ij}$ ...   nominal value of muscle force
$F^m_{new,ij}$ ...   perturbed value of muscle force
$p_{nom,j}$ ...   nominal value of given parameter
$p_{new,j}$ ...   perturbed value of given parameter

Obviously, sensitivity in (8) and instantaneous sensitivity ratio in (10) are equivalent. The partial derivative in (9) provides a continuous equation for the sensitivity of model outputs to each input parameter value, which can be evaluated over time and the range of model inputs. That is how they describe by the continuous equation the models sensitivity. Liu at al. use the partial derivative to calculate the contribution of a particular muscle to the body mass acceleration. For that the rate of change of the body mass acceleration due to the force muscle m produces, is multiplied by the muscles force. Thus, turning the ratio into a real value and so representing the magnitude of F_m. Again acceleration is given, a value with physical relevance. For a *continuous* sensitivity Redl et al. integrate the values of the instantaneous sensitivity ratio over the entire gait cycle.

Additionally the partial derivative and the sensitivity ratio can be connected easily. At a certain time step, the partial derivative can be written as the differential quotient

(e. g. according to formula (4)). The values of the function at the time-steps $t + \Delta t$ and t can be thought of as the varied and original output, respectively, and ΔF_m as the change of the parameter value. The formula is transfered into the formulas for the sensitivity seen above. Dividing by the original values provides a normalized ratio which is free from units.

The following gives a short summary of what parameters have been investigated and some of the major findings which have been found in literature. It is also summarized which muscles have been matter of interest.

Redl/Gföhler/Pandy [29]: They calculated the sensitivity of muscle forces by changing the parameters from 2.5% to 10% of the nominal value in incrediments of 2.5 . Parameters are:

- optimal muscle fiber length
- tendon rest length
- muscle physiological cross-sectional area (PCSA $= \frac{v^M}{l^M}$, where v^M is muscle volume and l^M is muscle fiber length)

Redl [30]: He compared the nominal parameter values of the model with those found in the literature and picked a certain percentage of reduction or increase of the parameter and described the effects on the force-graphs. The parameters in the study are:

- optimal muscle fiber length
- tendon rest length
- PCSA which is proportional to PCSA optimal muscle force
- joint torques

Scovil/Ronsky [31]: They investigated the influence of 14 parameters on the muscle model. They looked at the general sensitivity according to the parameter class and not muscles in specific. Three evaluations of the muscle model were performed based on:

- calculating sensitivity of muscle model only
- determining the continuous partial derivatives of the muscle equations with respect to each parameter
- evaluating the effects on the running and walking simulation

Input states are the optimal muscle length , the properties of the CE and the muscle activation level. Output states are muscle force and velocity of the CE. Model evaluations were found to be very sensitive to parameters defining:

- elastic components (tendon)
- force-length curve of the contractile element
- maximum isometric force

Raikova/Prilutsky [28]: The optimal muscle force for the joint moments was calculated changing one parameter *ceteris paribus*:

- muscle moment arms (d_{oi}), nominal values were were calculated from the joint angles and changed from 0 to $2.0d_{oi}$ in increments of $0.02d_{oi}$

- PCSA (A_{oi}), each PCSA was changed from 0.05 to $2A_{oi}$ in increments of $0.01A_{oi}$

They found that, generally, the non-zero optimal force of each muscle depends in a very complex non-linear way on moments at all joints and moment arms and PCSA of all muscles. Deviation of the model parameters within the feasible range affected not only the magnitude of the forces predicted, but also the number and combination of muscles with non-zero forces. Muscle force magnitudes could change several times as the model parameters changed, whereas patterns of muscle forces were typically not as sensitive.

Chumanov/Heiderscheit/Thelen [12]: The purpose of this study was to characterize the effect of speed and the influence of individual muscles on hamstrings stretch, loading and work during the swing phase of sprinting. Perturbations of the double float simulations were used to asses the influence of individual muscles on biceps femoris long head muscolotendon stretch. For each muscle the nominal force trajectory was perturbed by a fixed ratio (0.1%), while excitation for all other muscles was held constant $\rightarrow$ a set of perturbed joint musculotendon kinematic trajectories was produced. The influence of an individual muscle was defined as the change of peak stretch of biceps femoris longhead (BF), scaled by the inverse of the force perturbation magnitude. Perturbations with a fixed force magnitude ($1N$) were also performed to asses the potential of muscles to influence BF stretch per unit force.

Thelen et al. [32]: They investigated the effects of tendon compliance on the excursion and power development of the muscle and tendinous components of the biceps femoris, respectively peak muscle stretch and negative muscle work. They investigated:

- $\pm 0.5\%$ and $\pm 1\%$ perturbation of the tendon compliance

- effects of larger variations, because of a large range of estimates in literature

A sensitivity ratio was computed by normalizing the percent change in the output to the percent change in the model parameter. The sensitivity ratios were conformed to be highly linear for these small perturbations.

Liu/Anderson/Pandy [24]: They did not investigate any muscle parameters but perform a perturbation analysis to determine the contribution of each muscle to the body mass acceleration.

The following are the muscles and muscle groups summarized which have been investigated in the above papers. This should give an idea which muscles are likely to be subject of an investigation. The papers [12] and [32] investigated just one muscle (biceps femoris long head) or muscle group (hamstrings, one part is the biceps femoris long head). The hamstrings were found in two other papers ([30] and [31]). [30] and [28] investigated the biceps femoris short head. Just two muscles have been subject in all papers (except those which just looked at one muscle), namely soleus and vasti, although in [31] as quadriceps muscles which is vasti combined with rectus femoris. The single rectus femoris was treated by two other ones ([30]and [31]). Gluteus maximus and gastrocnemius have been considered in all works except in [29]. In this paper they just surveyed four muscles but as the only ones sartorius, because of its long moment arm, and gluteus minimus, as a part of gluteus medius. In one paper [24] gluteus medius was divided into its anterior and posterior part and just one paper [28] did not put it into the study. The same paper also did not take the combined hamstring muscles but the short and long head compartment of bicep femoris. The last muscle which was mentioned more than once is tibialis anterior, once in combination with extensor hallucis longum. Paper [24] investigated the combined plantar flexors and and the dorsi flexors.

4. Method

Following shortly summarizes the method to receive data to perform a sensitivity analysis on: One parameter at time is varied *ceteris paribus* by different percentages (p) in the different muscles and resultant muscle forces are calculated by static optimization. The result is a set of new muscle forces $F_m = F_m^{new}$. Those new muscle forces F_m^{new} are input for the perturbation analysis according to Liu et al. [24]. It is calculated how each muscles' induced acceleration contributes to the body mass acceleration. The output shows how specific muscles are contributing to the body mass acceleration and how this contribution changes due to the different input forces. The comparison of the varied result ($\ddot{x}_m^{new}$) to the nominal result ($\ddot{x}_m$) indicates the impact of this variation on the varied muscle as well as on all the other muscles contributing to the body mass acceleration, since this was the only variable which was changed. For example:

$$p = 5\% \quad \Rightarrow F_m^{new} \Rightarrow \ddot{x}_m^{new} \quad \overset{compared\,to}{\longleftrightarrow} \quad \ddot{x}_m \dots \text{ acceleration of muscle m}$$

4.1. The muscle-skeleton model

For calculating muscle forces which are produced during the task of walking, a 3D musculoskeletal model of the body, which is described in detail by Anderson and Pandy [2], was used for this work.

Briefly, the body was represented as a 10-segment, 23 degree-of-freedom (dof) mechanical linkage, actuated by 54 muscle-tendon units (each leg actuated by 24 muscles and the upper body by 6, see Figure 6). The pelvis was modeled as a rigid segment that could translate and rotate in three dimensions relative to the ground. Each hip was modeled as a ball-and-socket joint, each knee as a hinge joint, each ankle-subtalar joint as a universal joint, and each metatarsal joint as a hinge joint. The head, arms, and torso (HAT) were represented as a single rigid segment that articulated with the pelvis via a ball-and-socket joint located at approximately the 3rd lumbar vertebra. Contact between each foot and the ground was characterized by five stiff spring-damper units distributed under the sole of the foot. Therefore this model can be used to simulate a wide range of activities. Ligaments were modeled as passive torques that prevent hyperextension or extreme flexion.

Each of the 54 muscle-tendon units was represented as a three-element, Hill-type muscle (see section 3.1.3) in series with tendon. The muscle parameters, as well as the origin and insertion sites of each actuator, were based on data reported by Delp [13] (parameters and values see section 4.4 and Table 2).
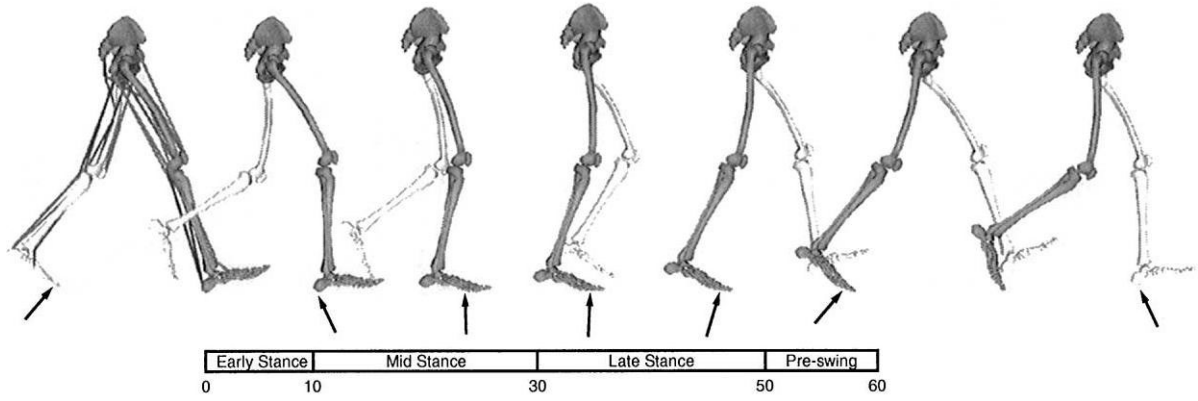
Figure 5: Gait pattern of the two-legged musculoskeletal walking simulation. The simulation starts and ends with right heel-strike. Regions of the stance phase are indicated in percent of the gait cycle. Heel-strike and toe-off occur at 0% and 60% of the gait cycle, respectively. Early stance and pre-swing correspond to approximately double-leg stance [26].

The gait cycle was assumed to be bilateral symmetric, meaning that stance phase and swing phase of the left and the right leg being congruent (Figure 5). Therefore just half of the gait cycle has to be simulated, which saves computing time. The optimization problem was solved using a gradient-based sequential quadratic programming algorithm. [4]

The following diagram shows the muscles included in the walking model (Figure 6). In the table of the abbreviations for the muscles, there are also some listed which are not shown in the diagram but still included in the model (Table 1).
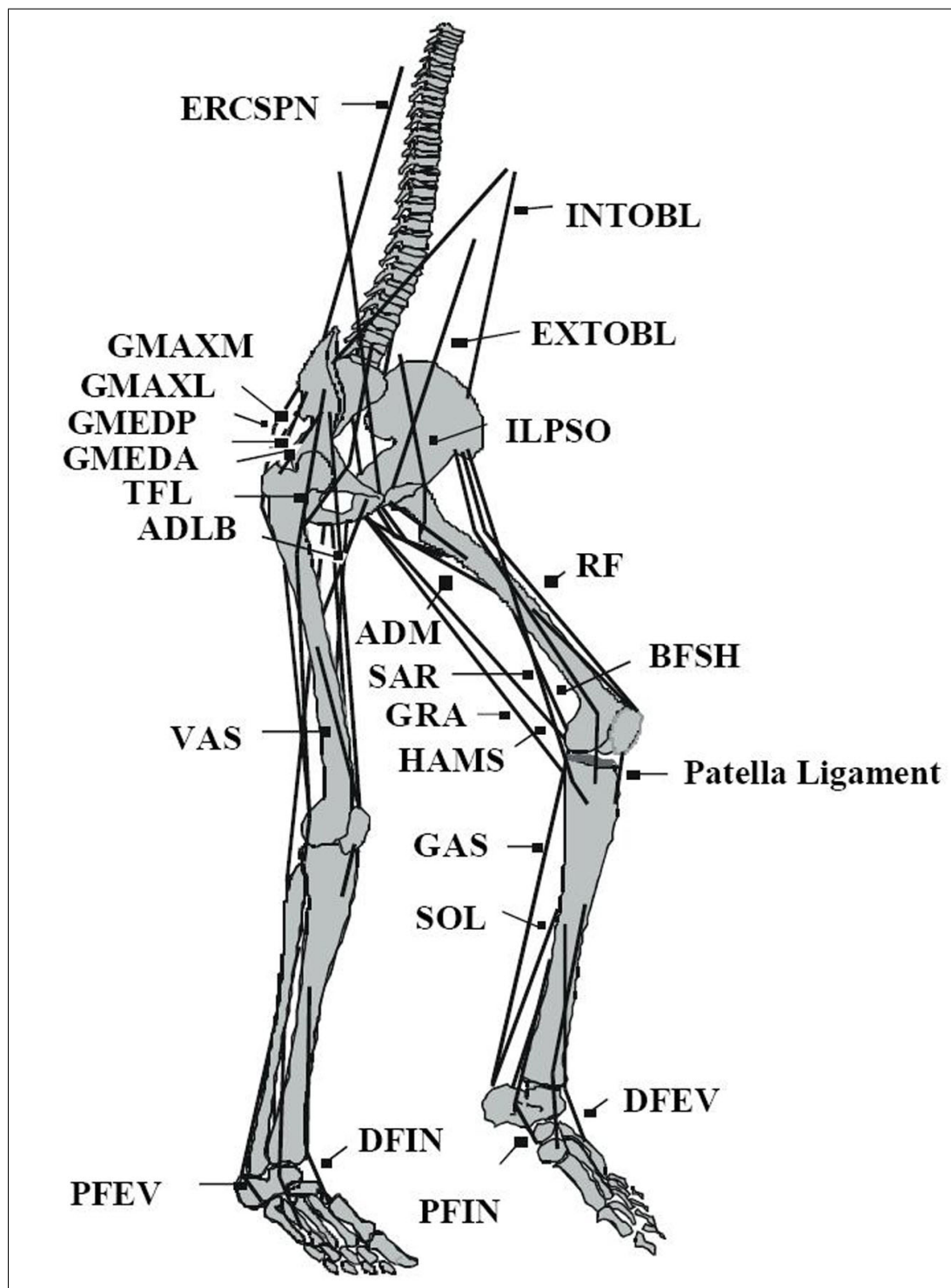
Figure 6: Muscles used in the model [2]

ERCSPN	erector spinae
EXTOBL	external abdominal obliques
INTOBL	internal abdominal obliques
ILPSO	iliopsoas (musculus psoas and illiacus)
ADLB	adductor longus brevis
ADM	adductor magnus
GMEDA	anterior gluteus medius
GMEDP	posterior gluteus medius and posterior gluteus minimus
GMAXM	medial gluteus maximus
GMAXL	lateral gluteus maximus
TFL	tensor fasciae latae
SAR	sartorius
GRA	gracilis
HAMS	hamstrings (semimembranosus, semitendinosus and biceps femoris longhead)
RF	rectus femoris
VAS	vastus medialis, vastus intermedius and vastus lateralis
BFSH	biceps femoris short head
GAS	gastrocnemius
SOL	soleus
DFEV	peroneus tertius and extensor hallucis longus
DFIN	tibialis anterior and flexor hallucis longus
PFEV	peroneus brevis and peroneus longus
PFIN	tibialis posterior, flexor digitorum longus and flexor hallucis longus
PIRI	piriformis
PECT	pectinius
FDH	flexor digitorum longus/brevis and flexor hallucis longus/brevis
EDH	extensor digitorum longus/brevis and extensor hallucis longus/brevis

Table 1: Abbreviations of muscles included in the model which are illustrated in Figure 6

4.2. Drawing a relationship between parameters and body mass acceleration

In developing a method to survey sensitivity of muscle parameters and studying the paper of Liu at al [24] (see section 3.2.3), several ideas were precipitated which should be discussed. Liu et al. present their results in graphs which show how a single muscle contributes to the body mass acceleration. Notably, it could be useful if the contribution of a parameter to the acceleration could be shown in a similar way.

This could be done by adapting the formula of the partial derivative in equation (4) to something similar to $\frac{\partial \ddot{x}}{\partial p_{mi}}$, the instantaneous rate of change of the body mass acceleration as function of the parameters of the individual muscles; hence the sensitivity of the body mass acceleration to the parameters describing the muscles. Another conceivable partial derivative could be $\frac{\partial \ddot{x}_m}{\partial p_i}$, the instantaneous rate of change of the acceleration due to muscle m as a function of parameter i, hence the sensitivity of muscle acceleration to muscle parameters.

So far the theoretical consideration but it must not be forgotten that this is not a pure mathematical problem but has real physical relevance. Hence, for further development of the formulas the assumptions and conditions which were made for the original problem have to be investigated. To express the partial derivative *exactly* as the differential quotient as shown in equation (4), a linear dependency between $\ddot{x}$ and F_m must exist. Further simplifications are applied because velocity and position cannot change instantaneously in response to a force perturbation (compare to section 3.2.3). The question is whether those restrictions are crucial or not. Since all models are simplifications of the reality, sufficient accuracy has to be achieved. So even nonlinear dependencies as well as the other simplifications could provide sufficiently accurate results. Even though in the case parameters are set instead of forces, which might have no physical relevance.

The fact is that acceleration and forces are linear dependent ($\sum F = m * a$) but parameters and forces are not. Further, parameters are not all of the same type and so each of them differently (indirect by the forces) connected to the accelerations. To close the circle and go back to the desire to show graphically how parameters contribute to the body mass acceleration, one can easily see the difference. The sum of accelerations contributed by the force of a muscle gives the body mass acceleration, this analogy cannot be drawn as easily to parameters. Therefore acceleration cannot be simply split up into the contribution of the several parameters by its partial derivative.

However, it might be possible to achieve such a connection between accelerations and parameters and illustrate it clearly but this would go beyond the scope of this work. The final solution of receiving data for a sensitivity analysis was to calculate sets of muscle forces with varied input parameters. Using those varied muscle forces to calculate their contribution to the body mass acceleration (according to the method presented in section 3.2.3), and performing a sensitivity analysis.

4.3. The simulation: Basic formulas and the program

On this point an overview about the simulation program and how it is applied on this work and the kind of output it produces is given. The code was written in MATLAB and using Frank Andersons [2] modified hard-constrained method in an upgraded version by Hyung Joo Kim.

Input data, this being joint angular displacements, joint angular velocities and muscular joint moments, is required for the static optimization. Here it is received from a dynamic optimization. Formula 11 is used to solve the optimization problem, giving many possible combinations to satisfy this equation:

$$F_{54}^m R = T_{17} \tag{11}$$

The Vector F_{54}^m contains the muscle forces produced by the 54 involved muscles, R is the matrix of moment arms and T_{17} the vector of the 17 torques acting about the joint axes. [3]

The vector of the muscle forces is constrained by the muscles force-length-velocity properties:

$$F_{54}^m = a_m f(F_o^m, l_m, v_m) \tag{12}$$

The function $f(F_o^m, l_m, v_m)$ is the force-velocity-length surface of a muscle assumed in the musculoskeletal model, F_o^m is the maximum isometric force, l_m is the length and v_m the shortening velocity of muscle m and a_m is the activation level of each muscle. Obviously the system is highly redundant. The condition for optimization (J_i) is to minimize the squared activations, summed across all muscles. Note that $i = 172$, half of the gait cycle is simulated because of its symmetry. [3]

$$J_i = \sum_{m=1}^{54} a_m(t_i)^2 \qquad i = 1, \dots, 172 \tag{13}$$

Muscle forces are calculated by running an MATLAB m-file called *pso* (physiological muscle model static optimization) which calculates a set of 54 muscle forces at each of the 346 time steps of the gait cycle. The time for one cycle is 1.12 seconds.

The muscle forces are dependent on many different parameters which can be manipulated in the muscle model (mm). Thus giving the opportunity to calculate sets of new muscle forces, where the input parameters were varied. The m-file *plotkimm33* plots all the by static optimization calculated forces, including also the ground reaction forces (not shown in following graphics). Also data from a neuro-muscular tracking is available. That data and the data from a dynamic optimization can be compared in a plot (see Figures 7, 8 and 9). All right side muscles (left and right are considered to be symmetric) which are included in the model are presented in the three plots. The force development over a full cycle of gait for each muscle is shown.

RunMia (muscle induced acceleration) performs the above (section 3.2.3) described perturbation analysis. It calculates the contribution of each muscle to the body mass acceleration at each of the 135 time steps during the stance phase of the gait cycle (67.5% or 0.754 seconds). Just the stance phase is considered because accelerations from muscles during the swing phase are very small. 27 muscles are considered in the simulation, since left and right foot are assumed to be equivalent. Accelerations of all three directions are calculated. The x direction is the direction of locomotion (fore-aft acceleration) and the y direction describes the vertical acceleration. Lateral acceleration is the third or z direction. Those acclerations of the orthogonal directions over the stance phase are shown in Figure 10, 11 and 12. The muscles which are considered to contribute the most to the body mass acceleration are chosen to be presented in the graphs.

The following abbreviations are used in Figure 7 to Figure 12. Compare also to the graphic of gait pattern (Figure 5).

rHS   ...   right heel strike
lTO   ...   left toe off
lHS   ...   left heel strike
rTO   ...   right toe off
lHS   ...   left heel strike
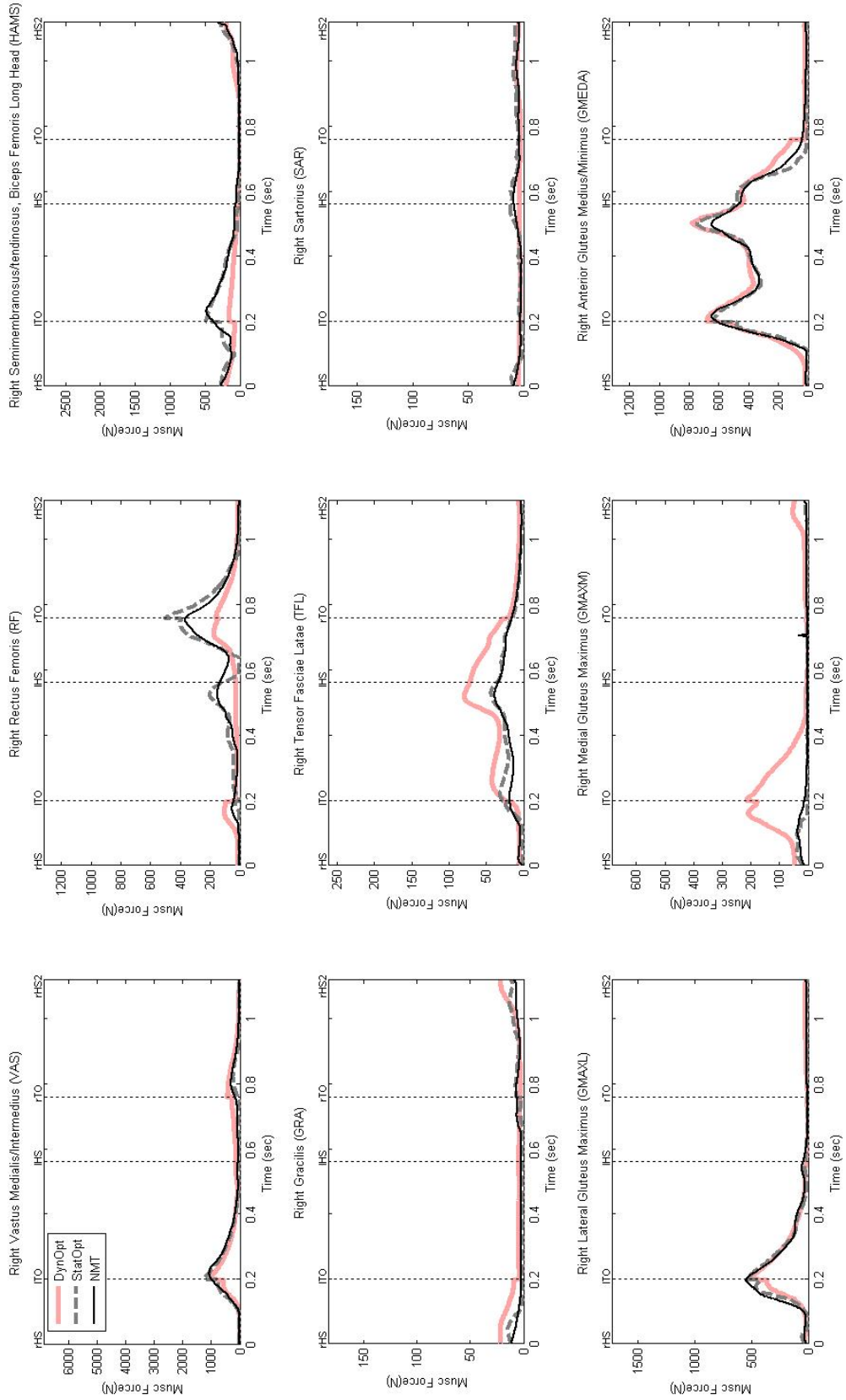
Figure 7: Muscle forces calculated with dynamic optimization, static optimization and neuro-muscular tracking over a full cycle of gait.
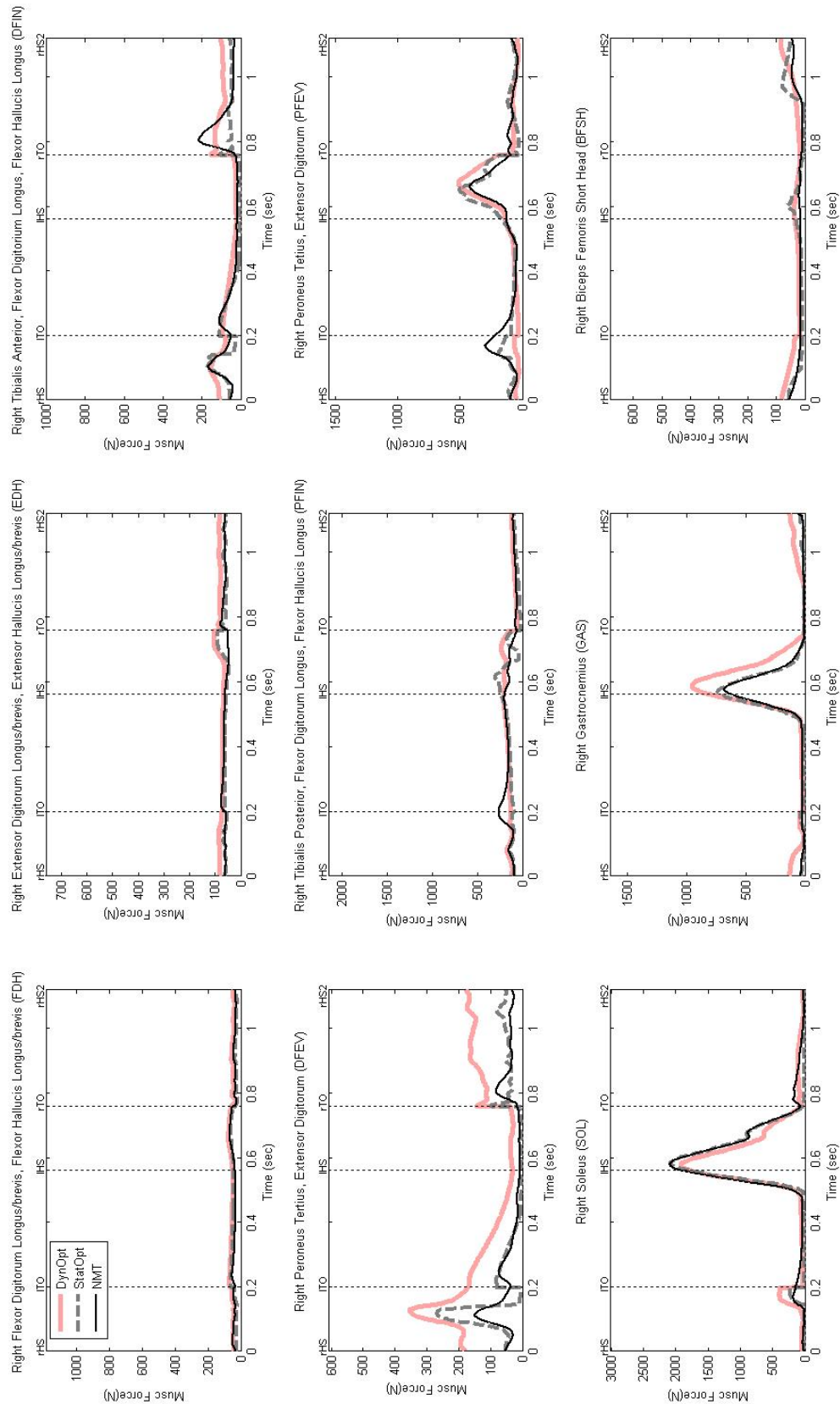
Figure 8: Muscle forces calculated with dynamic optimization, static optimization and neuro-muscular tracking over a full cycle of gait
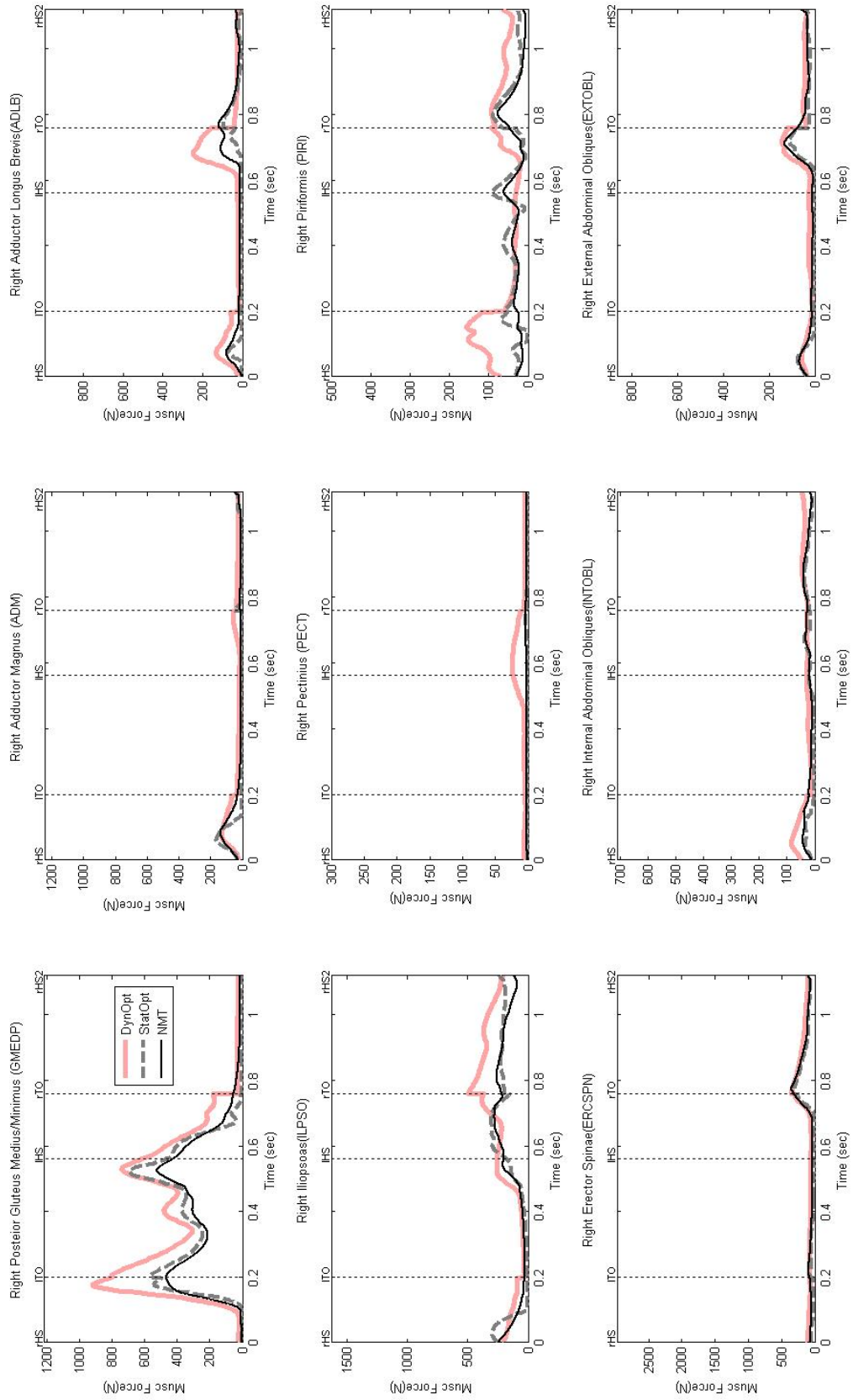
Figure 9: Muscle forces calculated with dynamic optimization, static optimization and neuro-muscular tracking over a full cycle of gait
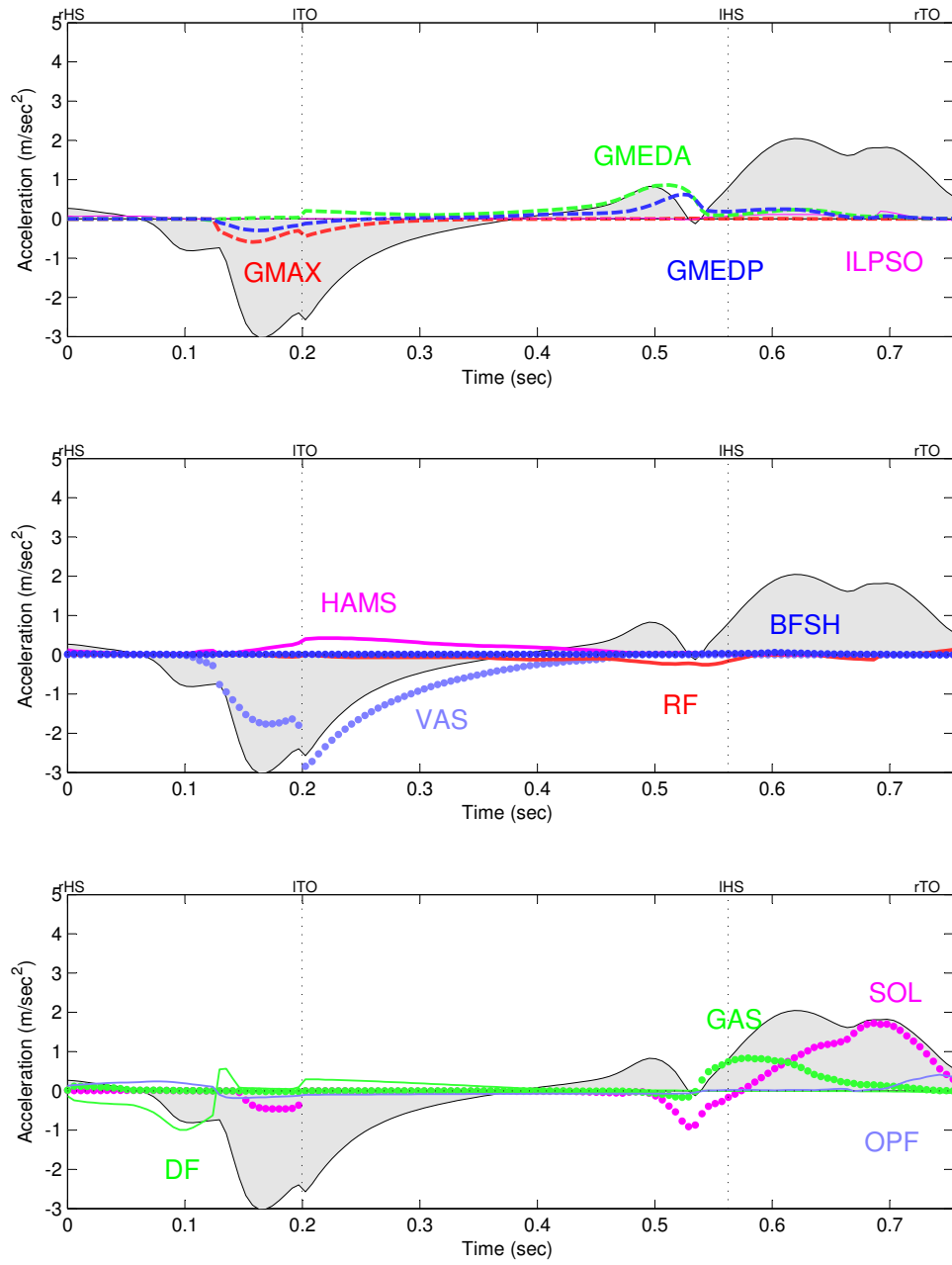
Figure 10: For-aft body mass acceleration and the contribution of the for gait most important muscles over the stance phase. Top panel: GMAX, GMEDP, GMEDA, ILPSO, middle panel: HAM, VAS, RF, BFSH, bottom panel: DF; OPF, SOL, GAS
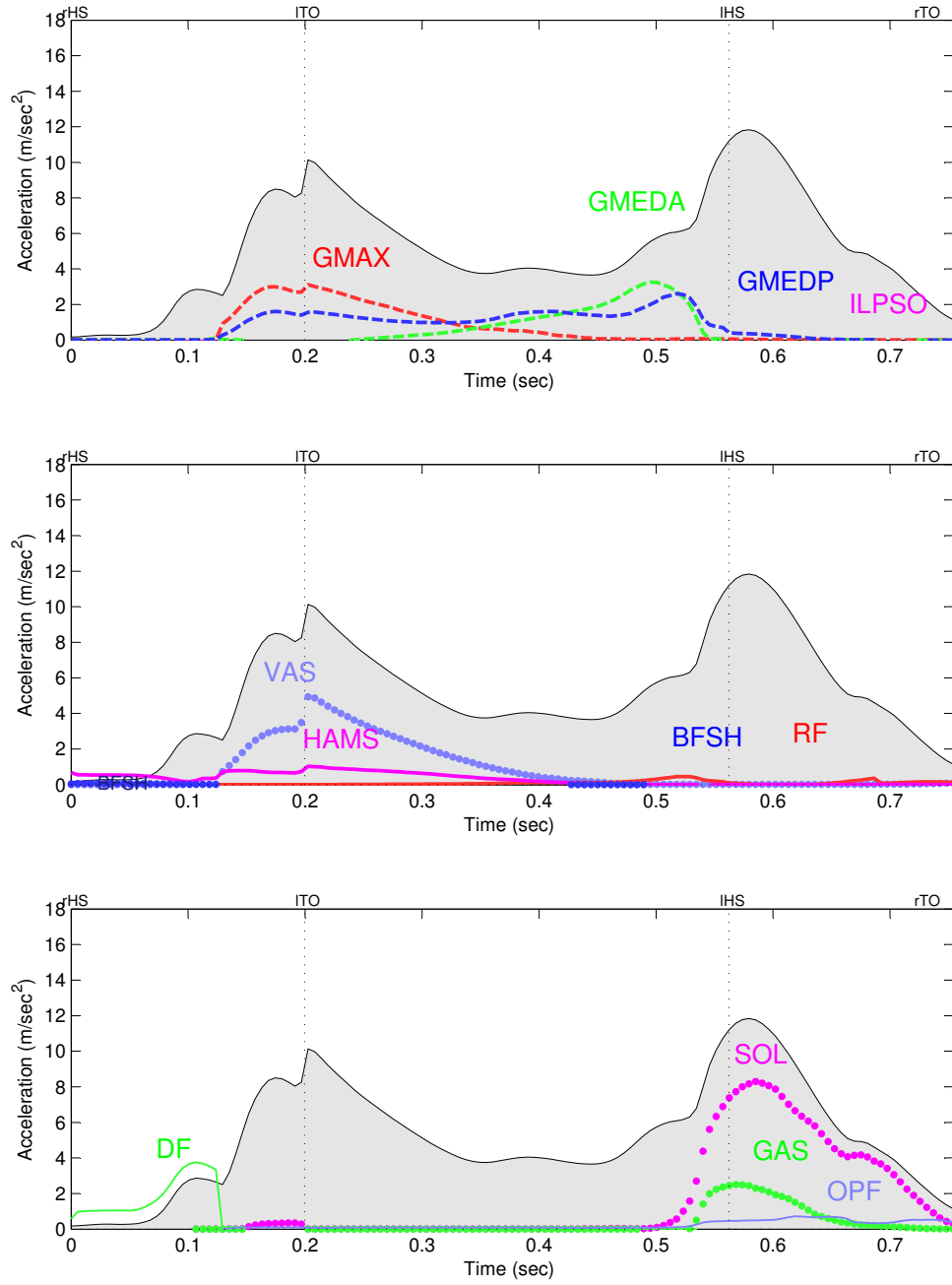
Figure 11: Vertical body mass acceleration and the contribution of the for gait most important muscles over the stance phase. Top panel: GMAX, GMEDP, GMEDA, ILPSO, middle panel: HAM, VAS, RF, BFSH, bottom panel: DF; OPF, SOL, GAS
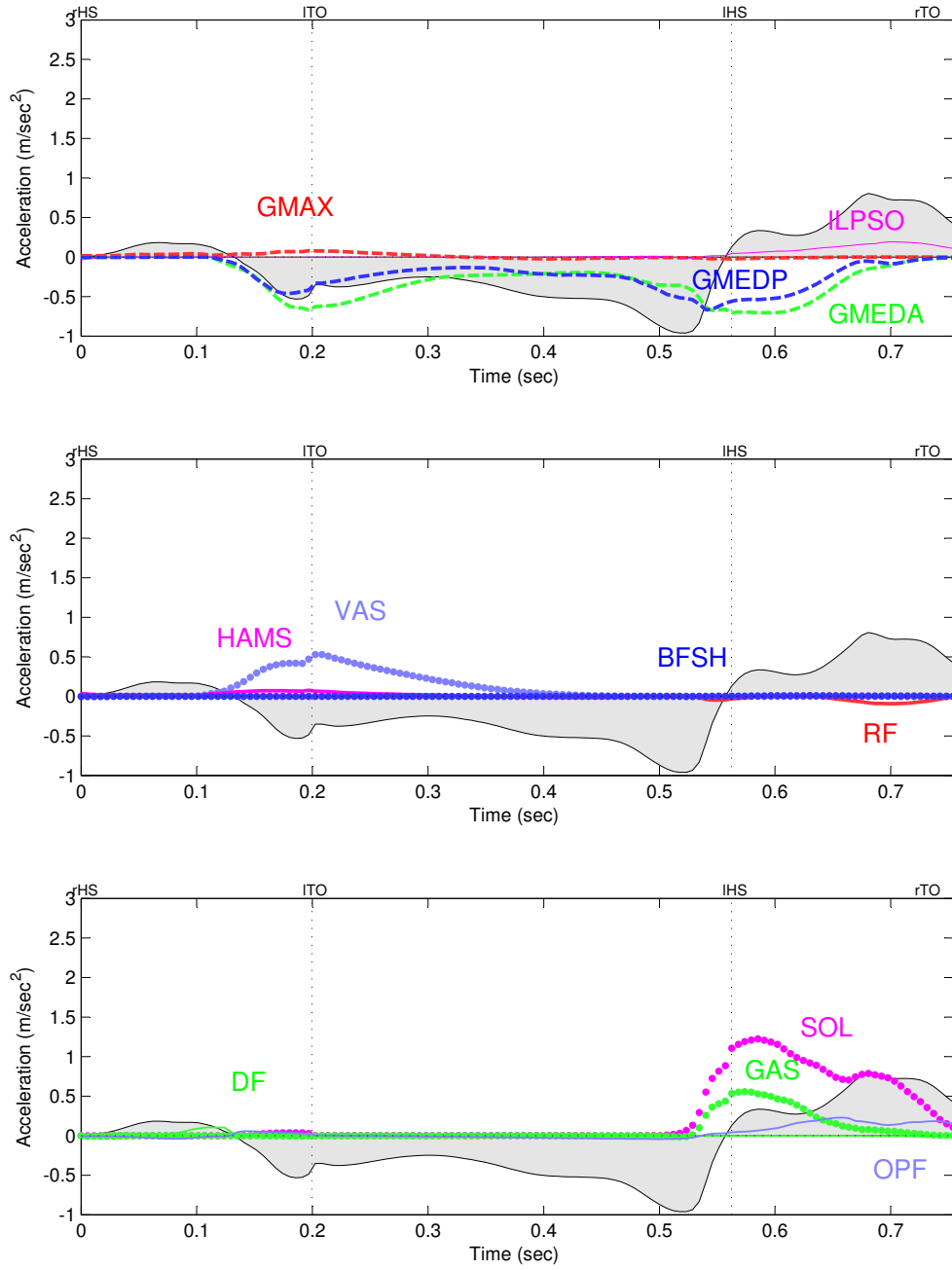
Figure 12: Lateral body mass acceleration and the contribution of the for gait most important muscles over the stance phase. Top panel: GMAX, GMEDP, GMEDA, ILPSO, middle panel: HAM, VAS, RF, BFSH, bottom panel: DF; OPF, SOL, GAS

4.4. The muscle parameters and their range of variation

Compared to the number of considered parameters in other studies, relatively many are surveyed in this work. This shall enable a more rounded down view on the sensitivity of the muscle model. Out of the same reason, also parameters which have been found to be less sensitive in other studies are chosen for the investigation.

These are the parameters which describe the muscle model which have been considered in this work. All muscle parameters were taken from Anderson and Pandy (1999) [2]. The values for l_o^m, l_s^t, F_o^m and α are found in Table 2.

l_o^m ...   resting (optimal) fiber length
l_s^t ...   tendon slack length
F_o^m ...   optimal muscle force
α ...   pennation angle
τ_A ...   activation time is constant $= 0.011$
τ_D ...   deactivation time is constant $= 0.068$
v_{max}^m ...   shortening velocity , changed indirectly via τ_c
$\qquad\qquad v_{vmax}^m = \frac{l_o^m}{\tau_c}$, τ_c is constant $= 0.1$

Note that changing the parameters F_o^m and PCSA has the same effect since those variables are linked by a scalar. The formula for the ideal force generator is:

$$F_o^m = \sigma_m * PCSA \qquad (14)$$

F_o^m ...   optimal muscle force
$PCSA$ ...   physiological cross-sectional area
σ_m ...   muscle stress

Perturbations were made in increments of 2.5% of the nominal value of the parameter for the first four parameters (l_o^m, l_s^t, α, F_o^m), and ranged from 2.5% to 10%. Since τ_A, τ_D and v_{max}^m showed little response to those variations the range was extended to 50% and the increments increased to 10%.

Some other parameters which describe the muscle model but are not considered in this work are for instance a muscle damping coefficient, a normalized tendon strain modulus and the proportion of the slow twitch fibers.

Actuator	F_o^m [N]	l_o^m [m]	l_s^t [m]	α [deg]
FDH	1184	0.04	0.03	8
EDH	760	0.11	0.32	7
DFIN	1003	0.105	0.026	5
DFEV	609	0.1	0.3	9
PFIN	2149	0.04	0.37	10
PFEV	1556	0.05	0.3	7
SOL	3016	0.05	0.254	25
GAS	1651	0.06	0.395	17
BFSH	681	0.173	0.005	23
VAS	6865	0.087	0.14	3
RF	1320	0.114	0.32	5
HAMS	2814	0.109	0.34	8
GRA	183	0.352	0.135	3
TFL	262	0.095	0.425	3
SAR	176	0.579	0.04	0
GMAXL	1730	0.145	0.106	2
GMAXM	686	0.154	0.12	5
GMEDA	1319	0.0653	0.0551	4
GMEDP	1215	0.065	0.0484	7
ADM	1245	0.121	0.12	4
ADLB	994	0.128	0.042	6
ILPSO	1627	0.0104	0.135	8
PECT	301	0.133	0.001	0
PIRI	502	0.03	0.102	10
ERCSPN	2974	0.12	0.03	0
INTOBL	712	0.125	0.165	0
EXTOBL	864	0.125	0.211	0

Table 2: Values of the optimal muscle force F_o^m, resting fiber length l_o^m, tendon slack lenght l_s^t and muscle pennation angle α assumed in the model. Left and right actuators of the body are assumed to have the same parameter values [2].

4.5. The muscles which have been investigated

54 muscles have been implemented in the gait simulation, 24 for each leg and 6 for the upper body (see Figure 6). For the sensitivity analysis 13 muscles, respectively combined muscles, which are considered to be important for the walking task, have been chosen (for the abbreviations look at table 1):

- The exteriors rotator and hip extenders GMAXL and GMAXM, both have been varied but they are combined to GMAX

- The hip joint abductors GMEDP and GMEDA

- The strongest flexor of the hip joint ILOPS, also exterior rotator of the thigh

- The extensors of the knee joint, the VAS group

- The biarticular knee extensor and hip flexor RF

- The biarticular knee joint flexor and hip joint extensor HAM

- The knee flexor BFSH, biceps femoris is the only muscle with the ability to perform an exterior rotation of the knee

- SAR, exterior rotation and abduction of the thigh and interior rotation of the shank as well as flexion of hip and knee joint. SAR is chosen because its potential to contribute to hip and knee joint acceleration is relatively large [7]

- The plantar flexors GAS (biarticular) and SOL, together with the musculus plantaris they are called musculus triceps surae and merge to the Achilles tendon

- The combined dorsi flexors DF (DFIN and DFEV), just DFIN was varied

- The combined plantar flexors OPF (OPFIN and OPFEV), just OPFIN was varied

4.6. Metrics

The perturbation analysis delivers accelerations for three orthogonal directions. For the further analysis, the resultant vector combining the accelerations of the fore-aft direction and the vertical direction is calculated. The lateral direction is neglected since it does not deliver significant values. To not loose information about the direction of the resultant vector, the angle between the resultant vector and the horizontal is calculated.

Instantaneous sensitivity ratio: As the first step to prepare the data for the analysis the *instantaneous sensitivity ratio* was calculated, as introduced by Redl et al. [29] in a slightly modified form (input forces became input accelerations).

$$\epsilon_{ij} = \frac{\frac{a^m_{new,ij} - a^m_{nom,ij}}{a^m_{nom,ij}}}{\frac{p_{new,j} - p_{nom,j}}{p_{nom,j}}} \tag{15}$$

ϵ_{ij} . . .   instantaneous sensitivity ratio for muscle j (j=1..27) at time step i (i=1..135)

$a^m_{nom,ij}$ . . .   nominal value of muscle induced acceleration

$a^m_{new,ij}$ . . .   perturbed value of muscle induced acceleration

$p_{nom,j}$ . . .   nominal value of given parameter

$p_{new,j}$ . . .   perturbed value of given parameter

In theory, the absolute value of ϵ_{ij} can range from zero to infinity. $\epsilon_{ij} = 0$ implies that any change in the tendon rest length of SOL, for example, will have no effect on the acceleration developed by SOL; whereas large values of ϵ_{ij} imply that even small changes in SOL's tendon rest length will have a significant effect on the acceleration developed by SOL. $\epsilon_{ij} = 1$ means that a 5% change in the tendon rest length of SOL will produce a 5% change in the acceleration developed by SOL. ϵ_{ij} could also be negative, implying that an increase in the value of a given parameter will cause a decrease in the acceleration produced by the muscle, and vice versa.

The idea to this metric was driven by the in economic well known price elasticity. It is calculated how a change of prices effects the quantity of demand. The computed ϵ value can be interpreted as following:

ϵ =   0   no changes, the system does not react to any input change

-1 $< \epsilon <$ 1   inelastic, under proportional change

$\epsilon < -1$ v $\epsilon > 1$ elastic, over proportional change

Integrated sensitivity ratio: Second metric introduced by Redl et al. [29] is the *integrated sensitivity ratio*, it is the *instantaneous sensitivity ratio* integrated over time:

$$\epsilon_j = \int_0^{t_f} |\epsilon_{ij}| dt \tag{16}$$

ϵ_j ...   integrated sensitivity ratio for muscle j

t_f ...   final time of stance phase

Smoothening grade: Looking at the formula above (15) one will notice that there is divided by the nominal acceleration. To prevent the sensitivity ratio of being large just due to small values of the nominal acceleration a *smoothening grade* was applied (peaks in the graph of the instantaneous sensitivity ratio due to small values in the denominator are smoothened). If the original acceleration is lower than this value, it is set equal to this value. A high sensitivity during a phase where the muscle is not contributing significantly to the overall body mass acceleration is not of much relevance. This condition was implemented to avoid this bias and make the result more meaningful. It was decided to set the *smoothening grade* to 0.01

Relevance of sensitivity: Also to improve the significance of a muscles sensitivity a *relevance of sensitivity* was introduced. The idea was to make use of the information given by how much each muscle contributes to the body mass acceleration. This in comparison to previous analysis where just the magnitudes of the forces of the several muscles are calculated, thus not giving exact information about how much they really influence the forward progression. Dividing the muscle induced accelerations by the overall acceleration at that instant of time gives the relevance of this muscle for the body mass acceleration. At each time step the *instantaneous sensitivity ratio* of a muscle is multiplied by its relevance. Those values are input for the calculation of the *integrated sensitivity ratio* and so the muscle's ability to influence locomotion is considered.

$$\epsilon_{ij}^{rel} = \frac{a_{nom,ij}^m}{a_{nom,i}} * \epsilon_{ij} \tag{17}$$

ϵ_{ij}^{rel} ...   instantaneous sensitivity of relevance for muscle j (j=1..27) at time step i (i=1..135)

ϵ_{ij} ...   instantaneous sensitivity ratio for muscle j at time step i

$a_{nom,ij}^m$ ...   nominal induced acceleration by muscle j at time step i

$a_{nom,i}$ ...   nominal body mass acceleration at time step i

Sensitivity over the interval of variation: The *sensitivity over the interval of varia-tion* is the sum of the integrated sensitivity ratios of a muscle calculated by the variation of a parameter from -10% till $+10\%$ in incrediments of 2.5%. Those integrated sensitivity ratios according to the change in percent of the parameter are shown in a graphic. To illustrate that the change of one parameter of a certain muscle influences also the performance of the other muscles, the integrated sensitivity ratios of the other muscles are found in the same graphic (see charts in section 5 and appendix A).

$$\epsilon_{jvar} = \sum_{v=1}^{8} \epsilon_{jv} \tag{18}$$

ϵ_{jvar} . . .   sensitivity over the interval of variation for muscle j
ϵ_{jv} . . .   integrated sensitivity ratio for muscle j at each
                  variation v $(-10\% \ldots +10\%)$ of the interval of variation

Significance of sensitivity: A significance of the sensitivity was calculated by dividing the *sensitivity over the interval of variation* by the *sensitivity of relevance over the interval of variation* and multiplying by 100. The higher this percentage is the more actively the muscle has contributed to the body mass acceleration when its sensitivity was measured. It can happen that this percentage is greater than 100% because sometimes a single muscles acceleration exceeds the resulting accumulated muscle accelerations, as seen in figures 10, 11 and 12 (e.g. DF in early stance).

$$s_j = \frac{\epsilon_{jvar}^{rel}}{\epsilon_{jvar}} * 100 \tag{19}$$

s_j . . .   significance of muscle j
ϵ_{jvar} . . .   integrated sensitivity ratio for muscle j over the
                  interval of variation
ϵ_{jvar}^{rel} . . .   integrated sensitivity ratio of relevance for muscle j
                  over the interval of variation

Summed-cross-sensitivity Also introduced by Redl et al. [29] was the *summed-cross-sensitivity*, which is computed in this work as well. Here it is the sum of the values of the *sensitivities over the interval of variation* except of the one which was varied. This metric quantifies the effects of changes on the muscle coordination of walking. In other words, the higher this value is, the more a deviation of this specific muscles affects the other muscles.

$$\sigma = \sum_{j=1}^{26} \epsilon_{jvar} \tag{20}$$

σ ...   summed cross sensitivity

ϵ_{jvar} ...   integrated sensitivity ratio for muscle j over the interval of variation

5. Results

After the variation of a muscle parameter and running the simulation with the disturbed input values, a set of muscle induced accelerations was delivered. At each time step the instantaneous sensitivity was calculated. The panels in Figure 13 show those instantaneous sensitivities over the percentage of the stance phase of the gait cycle for a -10% variation of tendon slack length of SOL. Sensitivity for all muscles considered in this study are included. The last graph on the right side bottom (see Figure 13), accS, is the sensitivity of the body mass acceleration. This sensitivity is, as expected, always very small since it is a criteria for the model to produce given joint moments. The human body tries to keep the total acceleration constant even though the contribution to the acceleration of the several muscles has changed.
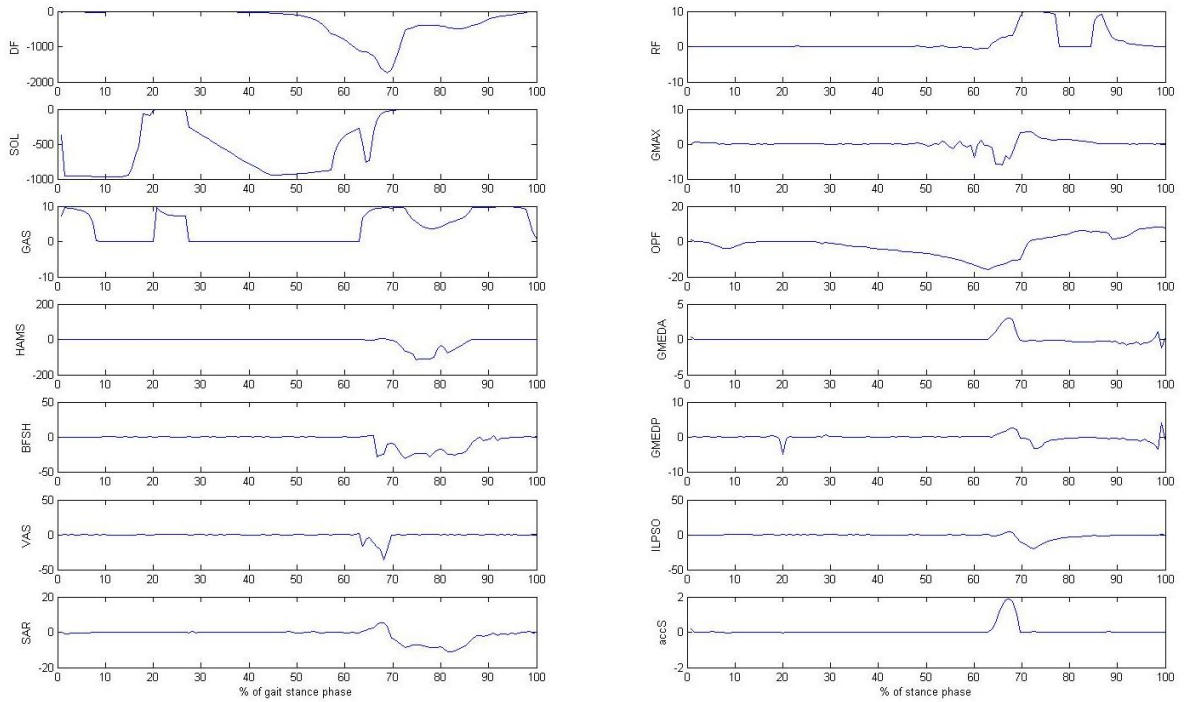
Figure 13: Instantaneous sensitivity for the variation of -10% of tendon slack length of soleus. It is shown how sensitive the several muscles react to SOL's variation of l_s^t over the stance phase

Those graphs of the instantaneous sensitivities clearly show that not only the muscle whose parameter was changed is affected but also other muscles react sensitive; sometimes even more then the varied muscle. In this case, for instance, the dorsi flexors peak down to a sensitivity of about 1800 at 68 % of the stance phase. The other plantar flexors (OPF) also peak at this part of the gait cycle. GAS shows a notable sensitivity in the beginning of gait cycle and also over a longer period in late stance, as well as RF and BFSH. It cannot been established from these graphs, if those sensitive reactions happen when the muscle is actually contributing significantly to the body mass acceleration. Therefore, a relevance measurement is applied like described in section 4.6.

Note that the muscles GMAXL and GMAXM are individually varied but in the results presented as the combined GMAX. This means a sensitive reaction of GMAX is always a combination of the effects on GMAXM and GMAXM but it is distinguished between a variation of those two.

The following tables (3 to 17) summarize the integrated sensitivity ratios over the interval of variation during the stance phase (as introduced in section 4.6). Each variation per muscle and per parameter delivers 8 values of integrated sensitivity; for the varied muscle and for each of the other muscles. Those values are accumulated over the interval of variation and presented in the tables. The summed-cross-sensitivity and the significance of sensitivity, as described in section 4.6, can also be found. Those matrices give an overview of the findings of this work and the dependencies of the muscles.

alpha   . . .   pennation angle
Fom   . . .   optimal muscle force
Lo   . . .   resting fiber length
Lst   . . .   tendon slack length

Table 3: Results for variation of BFSH. The matrix includes integrated sensitivity ratio, sensitivity of relevance, summed-crossed-sensitivity and significance over the interval of variation.

Integrated sensitivity ratio for BFSH

	BFSH	DF	GAS	GMAX	GMEDA	GMEDP	HAM	ILPSO	OPF	RF	SAR	SOL	VAS	Summed-cross-Sensitivity
alpha	806	6	47	16	8	12	30	13	2	9	20	31	65	259
Fom	1349	16	113	20	15	24	145	46	7	48	61	32	53	580
Lo	6825	15	88	39	22	37	127	77	4	81	87	48	241	866
Lst	1848	7	53	10	10	16	34	20	2	25	27	37	84	325

Sensitivity of relevance for BFSH

	BFSH	DF	GAS	GMAX	GMEDA	GMEDP	HAM	ILPSO	OPF	RF	SAR	SOL	VAS	Summed-cross-Sensitivity
alpha	6	4	3	0,3	1	2	4	1	0,4	0,4	0,09	0,7	3	19,89
Fom	37	37	34	0,4	0,4	1	34	10	2	1	0,5	2	2	124,3
Lo	50	21	20	0,8	0,9	2	26	9	1	2	0,5	2	22	107,2
Lst	13	5	4	0,2	0,3	0,8	6	2	0,4	0,8	0,1	0,9	6	26,5

Significance = (Sensitivity relevance/Sensitivity)*100

	BFSH	DF	GAS	GMAX	GMEDA	GMEDP	HAM	ILPSO	OPF	RF	SAR	SOL	VAS
alpha	0,7%	66,7%	6,4%	1,9%	12,5%	16,7%	13,3%	7,7%	20,0%	4,4%	0,5%	2,3%	4,6%
Fom	2,7%	231,3%	30,1%	2,0%	2,7%	4,2%	23,4%	21,7%	28,6%	2,1%	0,8%	6,3%	3,8%
Lo	0,7%	140,0%	22,7%	2,1%	4,1%	5,4%	20,5%	11,7%	25,0%	2,5%	0,6%	4,2%	9,1%
Lst	0,7%	71,4%	7,5%	2,0%	3,0%	5,0%	17,6%	10,0%	20,0%	3,2%	0,4%	2,4%	7,1%

Highest sensitivity to this parameter
Second highest sensitivity to this parameter
Third highest sensitivity to this parameter
Higher sensitivity than the varied muscle's one

Table 4: Results for variation of DF. The matrix includes integrated sensitivity ratio, sensitivity of relevance, summed-crossed-sensitivity and significance over the interval of variation.

Integrated sensitivity ratio for DF

	BFSH	DF	GAS	GMAX	GMEDA	GMEDP	HAM	ILPSO	OPF	RF	SAR	SOL	VAS	Summed-cross-Sensitivity
alpha	2	29	9	3	4	9	3	2	3	2	3	9	8	57
Fom	13	512	240	11	3	80	21	13	192	4	15	54	34	680
Lo	39	4418	609	33	12	340	64	32	256	12	28	509	30	1964
Lst	130	16463	3169	95	16	374	217	105	1244	39	112	4759	88	10348

Sensitivity of relevance for DF

	BFSH	DF	GAS	GMAX	GMEDA	GMEDP	HAM	ILPSO	OPF	RF	SAR	SOL	VAS	Summed-cross-Sensitivity
alpha	0,05	1	0,6	0,08	0,07	0,7	0,3	0,2	0,4	0,04	0,01	0,2	0,1	2,75
Fom	2	191	116	0,5	0,2	13	19	5	59	0,1	0,3	2	0,4	217,5
Lo	2	276	160	1	1	53	26	7	78	0,5	0,3	21	2	351,8
Lst	11	1368	818	5	1	57	133	35	377	1	2	79	5	1524

Significance = (Sensitivity relevance/Sensitivity)*100

	BFSH	DF	GAS	GMAX	GMEDA	GMEDP	HAM	ILPSO	OPF	RF	SAR	SOL	VAS
alpha	2,5%	3,4%	6,7%	2,7%	1,8%	7,8%	10,0%	10,0%	13,3%	2,0%	0,3%	2,2%	1,3%
Fom	15,4%	37,3%	48,3%	4,5%	6,7%	16,3%	90,5%	38,5%	30,7%	2,5%	2,0%	3,7%	1,2%
Lo	5,1%	6,2%	26,3%	3,0%	8,3%	15,6%	40,6%	21,9%	30,5%	4,2%	1,1%	4,1%	6,7%
Lst	8,5%	8,3%	25,8%	5,3%	6,3%	15,2%	61,3%	33,3%	30,3%	2,6%	1,8%	1,7%	5,7%

Highest sensitivity to this parameter
Second highest sensitivity to this parameter
Third highest sensitivity to this parameter
Higher sensitivity than the varied muscle's one

Table 5: Results for variation of GAS. The matrix includes integrated sensitivity ratio, sensitivity of relevance, summed-crossed-sensitivity and significance over the interval of variation.

Integrated sensitivity ratio for GAS

	BFSH	DF	GAS	GMAX	GMEDA	GMEDP	HAM	ILPSO	OPF	RF	SAR	SOL	VAS	Summed-cross-Sensitivity
alpha	37	34	393	15	9	17	34	20	10	38	26	56	36	332
Fom	409	55	809	60	20	57	823	224	90	904	190	154	35	3021
Lo	199	269	2163	61	15	42	313	106	58	237	115	348	151	1914
Lst	4526	60649	138387	1148	307	569	9177	2139	12179	2487	2332	96793	97793	290099

Sensitivity of relevance for GAS

	BFSH	DF	GAS	GMAX	GMEDA	GMEDP	HAM	ILPSO	OPF	RF	SAR	SOL	VAS	Summed-cross-Sensitivity
alpha	0,3	5	9	0,2	0,2	1	1	1	1	1	0,03	5	1	16,73
Fom	2	18	54	0,5	1	4	4	4	7	10	0,4	45	2	101,9
Lo	2	52	63	0,7	1	3	8	8	5	5	0,3	26	8	118
Lst	65	7596	6673	21	30	59	603	212	396	86	12	463	406	9949

Significance = (Sensitivity_relevance/Sensitivity)*100

	BFSH	DF	GAS	GMAX	GMEDA	GMEDP	HAM	ILPSO	OPF	RF	SAR	SOL	VAS
alpha	0,8%	14,7%	2,3%	1,3%	2,2%	5,9%	2,9%	5,0%	10,0%	2,6%	0,1%	8,9%	2,8%
Fom	0,5%	32,7%	6,7%	0,8%	5,0%	7,0%	0,5%	3,1%	8,9%	1,1%	0,2%	29,2%	5,7%
Lo	1,0%	19,3%	2,9%	1,1%	6,7%	7,1%	2,6%	4,7%	12,1%	2,1%	0,3%	7,5%	5,3%
Lst	1,4%	12,5%	4,8%	1,8%	9,8%	10,4%	6,6%	9,9%	3,3%	3,5%	0,5%	0,5%	0,4%

Highest sensitivity to this parameter
Second highest sensitivity to this parameter
Third highest sensitivity to this parameter
Higher sensitivity than the varied muscle's one

Table 6: Results for variation of GMAXL. The matrix includes integrated sensitivity ratio, sensitivity of relevance, summed-crossed-sensitivity and significance over the interval of variation.

Integrated sensitivity ratio for GMAXL

	BFSH	DF	GAS	GMAX	GMEDA	GMEDP	HAM	ILPSO	OPF	RF	SAR	SOL	VAS	Summed-cross-Sensitivity
alpha	4	3	27	27	4	12	9	4	1	4	8	16	29	121
Fom	11	10	43	1087	131	2384	361	36	3	241	432	27	186	3865
Lo	67	29	91	5407	312	4237	1154	226	5	429	775	70	669	8064
Lst	90	46	159	8129	423	5377	1637	339	8	605	1087	120	923	10814

Sensitivity of relevance for GMAXL

	BFSH	DF	GAS	GMAX	GMEDA	GMEDP	HAM	ILPSO	OPF	RF	SAR	SOL	VAS	Summed-cross-Sensitivity
alpha	0,1	0,6	0,7	1	0,2	1,5	0,7	0,4	0,3	0,1	0,02	0,3	0,5	5,42
Fom	0,4	5	4	111	9	396	33	3	0,4	3	1	0,7	37	492,5
Lo	0,7	7	8	288	38	729	77	8	0,6	7	2	3	97	977,3
Lst	1	9	10	401	54	931	107	12	0,8	9	3	4	134	1274,8

Significance = (Sensitivity_relevance/Sensitivity)*100

	BFSH	DF	GAS	GMAX	GMEDA	GMEDP	HAM	ILPSO	OPF	RF	SAR	SOL	VAS
alpha	2,5%	20,0%	2,6%	3,7%	5,0%	12,5%	7,8%	10,0%	30,0%	2,5%	0,3%	1,9%	1,7%
Fom	3,6%	50,0%	9,3%	10,2%	6,9%	16,6%	9,1%	8,3%	13,3%	1,2%	0,2%	2,6%	19,9%
Lo	1,0%	24,1%	8,8%	5,3%	12,2%	17,2%	6,7%	3,5%	12,0%	1,6%	0,3%	4,3%	14,5%
Lst	1,1%	19,6%	6,3%	4,9%	12,8%	17,3%	6,5%	3,5%	10,0%	1,5%	0,3%	3,3%	14,5%

Legend:
- Highest sensitivity to this parameter
- Second highest sensitivity to this parameter
- Third highest sensitivity to this parameter
- Higher sensitivity than the varied muscle's one

Table 7: Results for variation of GMAXM. The matrix includes integrated sensitivity ratio, sensitivity of relevance, summed-crossed-sensitivity and significance over the interval of variation.

Integrated sensitivity ratio for GMAXM

	BFSH	DF	GAS	GMAX	GMEDA	GMEDP	HAM	ILPSO	OPF	RF	SAR	SOL	VAS	Summed-cross-Sensitivity
alpha	5	3	30	**7**	4	8	7	3	1	3	6	19	28	117
Fom	13	4	41	**145**	29	81	21	20	1	4	12	21	47	294
Lo	13	4	27	**117**	19	65	24	18	1	11	15	14	25	236
Lst	11	2	15	**118**	18	68	16	16	1	12	13	3	17	192

Sensitivity of relevance for GMAXM

	BFSH	DF	GAS	GMAX	GMEDA	GMEDP	HAM	ILPSO	OPF	RF	SAR	SOL	VAS	Summed-cross-Sensitivity
alpha	0,1	0,6	0,6	**0,1**	0,3	0,8	0,5	0,4	0,3	0,1	0,01	0,4	0,2	4,31
Fom	0,4	4	3	**4**	0,5	12	3	2	0,3	0,1	0,1	0,4	2	27,8
Lo	0,4	3	3	**3**	1	10	2	2	0,4	0,2	0,09	0,4	1	23,49
Lst	0,5	3	3	**3**	0,6	10	3	2	0,4	0,1	0,09	0,2	2	24,89

Significance = (Sensitivity_relevance/Sensitivity)*100

	BFSH	DF	GAS	GMAX	GMEDA	GMEDP	HAM	ILPSO	OPF	RF	SAR	SOL	VAS
alpha	2,0%	20,0%	2,0%	**1,4%**	7,5%	10,0%	7,1%	13,3%	30,0%	3,3%	0,2%	2,1%	0,7%
Fom	3,1%	100,0%	7,3%	**2,8%**	1,7%	14,8%	14,3%	10,0%	30,0%	2,5%	0,8%	1,9%	4,3%
Lo	3,1%	75,0%	11,1%	**2,6%**	5,3%	15,4%	8,3%	11,1%	40,0%	1,8%	0,6%	2,9%	4,0%
Lst	4,5%	150,0%	20,0%	**2,5%**	3,3%	14,7%	18,8%	12,5%	40,0%	0,8%	0,7%	6,7%	11,8%

Legend:
- Highest sensitivity to this parameter
- Second highest sensitivity to this parameter
- Third highest sensitivity to this parameter
- Higher sensitivity than the varied muscle's one
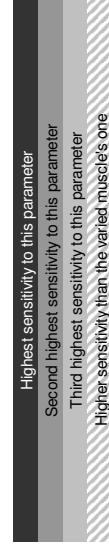
Table 8: Results for variation of GMEDA. The matrix includes integrated sensitivity ratio, sensitivity of relevance, summed-crossed-sensitivity and significance over the interval of variation.

Integrated sensitivity ratio for GMEDA

	BFSH	DF	GAS	GMAX	GMEDA	GMEDP	HAM	ILPSO	OPF	RF	SAR	SOL	VAS	Summed-cross-Sensitivity
alpha	5	3	31	7	9	11	7	4	1	4	7	23	31	134
Fom	76	24	64	645	313	1599	511	51	4	297	280	53	79	3683
Lo	46	19	112	323	860	877	194	52	3	161	166	46	82	2081
Lst	67	21	113	401	939	961	301	63	3	176	186	45	96	2433

Sensitivity of relevance for GMEDA

	BFSH	DF	GAS	GMAX	GMEDA	GMEDP	HAM	ILPSO	OPF	RF	SAR	SOL	VAS	Summed-cross-Sensitivity
alpha	0,1	0,6	0,7	0,2	0,3	1	0,5	0,3	0,3	0,1	0,02	0,4	0,3	4,52
Fom	0,7	4	6	37	32	263	15	3	0,5	8	0,6	4	10	351,8
Lo	2	32	28	23	23	146	18	11	1	3	0,8	1	7	272,8
Lst	2	33	30	23	27	155	19	12	1	4	1	2	6	288

Significance = (Sensitivity relevance/Sensitivity)*100

	BFSH	DF	GAS	GMAX	GMEDA	GMEDP	HAM	ILPSO	OPF	RF	SAR	SOL	VAS
alpha	2,0%	20,0%	2,3%	2,9%	3,3%	9,1%	7,1%	7,5%	30,0%	2,5%	0,3%	1,7%	1,0%
Fom	0,9%	16,7%	9,4%	5,7%	10,2%	16,4%	2,9%	5,9%	12,5%	2,7%	0,2%	7,5%	12,7%
Lo	4,3%	168,4%	25,0%	7,1%	2,7%	16,6%	9,3%	21,2%	33,3%	1,9%	0,5%	2,2%	8,5%
Lst	3,0%	157,1%	26,5%	5,7%	2,9%	16,1%	6,3%	19,0%	33,3%	2,3%	0,5%	4,4%	6,3%

Legend:
- Highest sensitivity to this parameter
- Second highest sensitivity to this parameter
- Third highest sensitivity to this parameter
- Higher sensitivity than the varied muscle's one

Table 9: Results for variation of GMEDP. The matrix includes integrated sensitivity ratio, sensitivity of relevance, summed-crossed-sensitivity and significance over the interval of variation.

Integrated sensitivity ratio for GMEDP

	BFSH	DF	GAS	GMAX	GMEDA	GMEDP	HAM	ILPSO	OPF	RF	SAR	SOL	VAS	Summed-cross-Sensitivity
alpha	3	1	5	16	6	54	7	3	1	14	12	2	7	77
Fom	122	30	101	1388	284	4491	517	95	6	1715	1358	79	146	5841
Lo	66	17	85	646	135	2906	278	62	37	678	530	45	79	2658
Lst	77	18	75	724	145	2491	301	67	4	717	632	39	106	2905

Sensitivity of relevance for GMEDP

	BFSH	DF	GAS	GMAX	GMEDA	GMEDP	HAM	ILPSO	OPF	RF	SAR	SOL	VAS	Summed-cross-Sensitivity
alpha	0,07	0,5	0,4	0,8	0,4	7	0,4	0,3	0,2	0,2	0,03	0,1	0,3	3,7
Fom	0,8	2	5	97	39	722	14	4	0,5	24	3	6	29	224,3
Lo	1	15	15	39	20	404	11	7	0,9	10	1	3	11	133,9
Lst	1	12	12	44	21	344	12	6	0,7	12	2	3	13	138,7

Significance = (Sensitivity_relevance/Sensitivity)*100

	BFSH	DF	GAS	GMAX	GMEDA	GMEDP	HAM	ILPSO	OPF	RF	SAR	SOL	VAS
alpha	2,3%	50,0%	8,0%	5,0%	6,7%	13,0%	5,7%	10,0%	20,0%	1,4%	0,3%	5,0%	4,3%
Fom	0,7%	6,7%	5,0%	7,0%	13,7%	16,1%	2,7%	4,2%	8,3%	1,4%	0,2%	7,6%	19,9%
Lo	1,5%	88,2%	17,6%	6,0%	14,8%	13,9%	4,0%	11,3%	2,4%	1,5%	0,2%	6,7%	13,9%
Lst	1,3%	66,7%	16,0%	6,1%	14,5%	13,8%	4,0%	9,0%	17,5%	1,7%	0,3%	7,7%	12,3%

Legend:
- Highest sensitivity to this parameter
- Second highest sensitivity to this parameter
- Third highest sensitivity to this parameter
- Higher sensitivity than the varied muscle's one

Table 10: Results for variation of HAM. The matrix includes integrated sensitivity ratio, sensitivity of relevance, summed-crossed-sensitivity and significance over the interval of variation.

Integrated sensitivity Ratio for HAM

	BFSH	DF	GAS	GMAX	GMEDA	GMEDP	HAM	ILPSO	OPF	RF	SAR	SOL	VAS	Summed-cross-Sensitivity
alpha	12	3	29	11	5	7	65	9	2	22	13	18	29	160
Fom	74	31	178	190	114	284	646	46	5	2043	718	31	159	3873
Lo	114	23	157	149	45	106	1120	94	10	944	367	43	142	2194
Lst	457	114	839	1797	590	1038	5583	370	34	6323	3249	116	1017	15944

Sensitivity of relevance for HAM

	BFSH	DF	GAS	GMAX	GMEDA	GMEDP	HAM	ILPSO	OPF	RF	SAR	SOL	VAS	Summed-cross-Sensitivity
alpha	0,2	1	1	0,3	0,7	0,9	1	0,5	0,3	0,6	0,03	0,4	0,4	6,33
Fom	5	68	61	32	4	44	60	7	4	23	2	1	16	267
Lo	4	47	44	14	4	18	36	6	3	21	0,9	2	9	172,9
Lst	22	289	263	282	38	167	312	33	15	116	9	8	145	1387

Significance = (Sensitivity_relevance/Sensitivity)*100

	BFSH	DF	GAS	GMAX	GMEDA	GMEDP	HAM	ILPSO	OPF	RF	SAR	SOL	VAS
alpha	1,7%	33,3%	3,4%	2,7%	14,0%	12,9%	1,5%	5,6%	15,0%	2,7%	0,2%	2,2%	1,4%
Fom	6,8%	219,4%	34,3%	16,8%	3,5%	15,5%	9,3%	15,2%	80,0%	1,1%	0,3%	3,2%	10,1%
Lo	3,5%	204,3%	28,0%	9,4%	8,9%	17,0%	3,2%	6,4%	30,0%	2,2%	0,2%	4,7%	6,3%
Lst	4,8%	253,5%	31,3%	15,7%	6,4%	16,1%	5,6%	8,9%	44,1%	1,8%	0,3%	6,9%	14,3%

Highest sensitivity to this parameter
Second highest sensitivity to this parameter
Third highest sensitivity to this parameter
Higher sensitivity than the varied muscle's one

Table 11: Results for variation of ILPSO. The matrix includes integrated sensitivity ratio, sensitivity of relevance, summed-crossed-sensitivity and significance over the interval of variation.

Integrated sensitivity ratio for ILPSO

	BFSH	DF	GAS	GMAX	GMEDA	GMEDP	HAM	ILPSO	OPF	RF	SAR	SOL	VAS	Summed-cross-Sensitivity
alpha	12	4	35	11	6	10	20	98	1	10	15	26	42	192
Fom	650	75	504	262	225	198	480	746	13	114	561	69	122	3273
Lo	816	86	560	698	212	261	2079	6138	28	687	968	468	5460	12323
Lst	889	103	673	776	225	285	2300	8096	31	815	1100	500	5903	13600

Sensitivity of relevance for ILPSO

	BFSH	DF	GAS	GMAX	GMEDA	GMEDP	HAM	ILPSO	OPF	RF	SAR	SOL	VAS	Summed-cross-Sensitivity
alpha	0,3	3	3	0,3	0,4	0,9	1	2	0,3	0,3	0,07	0,5	1	11,07
Fom	19	206	188	5	3	5	69	57	10	4	5	7	5	526
Lo	13	114	112	13	4	17	67	119	8	22	5	18	68	461
Lst	16	151	146	17	5	21	85	147	10	25	6	20	83	585

Significance = (Sensitivity_relevance/Sensitivity)*100

	BFSH	DF	GAS	GMAX	GMEDA	GMEDP	HAM	ILPSO	OPF	RF	SAR	SOL	VAS
alpha	2,5%	75,0%	8,6%	2,7%	6,7%	9,0%	5,0%	2,0%	30,0%	3,0%	0,5%	1,9%	2,4%
Fom	2,9%	274,7%	37,3%	1,9%	1,3%	2,5%	14,4%	7,6%	76,9%	3,5%	0,9%	10,1%	4,1%
Lo	1,6%	132,6%	20,0%	1,9%	1,9%	6,5%	3,2%	1,9%	28,6%	3,2%	0,5%	3,8%	1,2%
Lst	1,8%	146,6%	21,7%	2,2%	2,2%	7,4%	3,7%	1,8%	32,3%	3,1%	0,5%	4,0%	1,4%

Highest sensitivity to this parameter
Second highest sensitivity to this parameter
Third highest sensitivity to this parameter
Higher sensitivity than the varied muscle's one

Table 12: Results for variation of OPF. The matrix includes integrated sensitivity ratio, sensitivity of relevance, summed-crossed-sensitivity and significance over the interval of variation.

Integrated sensitivity ratio for OPF

	BFSH	DF	GAS	GMAX	GMEDA	GMEDP	HAM	ILPSO	OPF	RF	SAR	SOL	VAS	Summed-cross-Sensitivity
alpha	10	117	95	15	4	15	17	8	175	5	10	79	38	413
Fom	98	517	326	38	8	165	203	38	1027	20	51	358	20	1842
Lo	255	7792	2374	177	19	316	390	174	9370	92	172	2663	51	14475
Lst	13965	187991	17575	4154	8354	15847	3389	1323	96356	8009	3335	14970	91519	370431

Sensitivity of relevance for OPF

	BFSH	DF	GAS	GMAX	GMEDA	GMEDP	HAM	ILPSO	OPF	RF	SAR	SOL	VAS	Summed-cross-Sensitivity
alpha	0,4	22	25	0,2	0,7	2	4	1	51	0,2	0,06	2	0,3	57,86
Fom	2	108	117	0,9	1	26	19	6	257	0,6	0,3	19	0,5	300,3
Lo	12	1622	882	7	3	52	144	38	2677	4	2	71	4	2841
Lst	120	19539	1990	287	258	1203	523	278	29018	70	13	1094	824	26199

Significance = (Sensitivity relevance/Sensitivity)*100

	BFSH	DF	GAS	GMAX	GMEDA	GMEDP	HAM	ILPSO	OPF	RF	SAR	SOL	VAS
alpha	4,0%	18,8%	26,3%	1,3%	17,5%	13,3%	23,5%	12,5%	29,1%	4,0%	0,6%	2,5%	0,8%
Fom	2,0%	20,9%	35,9%	2,4%	12,5%	15,8%	9,4%	15,8%	25,0%	3,0%	0,6%	5,3%	2,5%
Lo	4,7%	20,8%	37,2%	4,0%	15,8%	16,5%	36,9%	21,8%	28,6%	4,3%	1,2%	2,7%	7,8%
Lst	0,9%	10,4%	11,3%	6,9%	3,1%	7,6%	15,4%	21,0%	30,1%	0,9%	0,4%	7,3%	0,9%

Legend:
- Highest sensitivity to this parameter
- Second highest sensitivity to this parameter
- Third highest sensitivity to this parameter
- Higher sensitivity than the varied muscle's one

Table 13: Results for variation of RF. The matrix includes integrated sensitivity ratio, sensitivity of relevance, summed-crossed-sensitivity and significance over the interval of variation.

Integrated sensitivity ratio for RF

	BFSH	DF	GAS	GMAX	GMEDA	GMEDP	HAM	ILPSO	OPF	RF	SAR	SOL	VAS	Summed-cross-Sensitivity
alpha	7	2	19	5	4	7	9	3	1	12	5	16	20	98
Fom	354	25	116	27	19	93	506	44	5	724	168	102	123	1582
Lo	232	23	80	20	17	69	473	34	9	1095	128	74	91	1250
Lst	904	46	321	83	71	342	1945	145	32	5925	641	392	1215	6137

Sensitivity of relevance for RF

	BFSH	DF	GAS	GMAX	GMEDA	GMEDP	HAM	ILPSO	OPF	RF	SAR	SOL	VAS	Summed-cross-Sensitivity
alpha	0,1	0,4	0,4	0,1	0,2	0,6	0,4	0,2	0,2	0,2	0,02	0,3	0,3	3,22
Fom	3	0,3	4	0,7	2	10	11	3	0,4	19	0,7	7	9	51,1
Lo	2	0,6	4	0,6	2	9	9	2	0,7	14	0,5	5	6	41,4
Lst	7	4	16	3	7	45	48	10	3	68	2	21	39	205

Significance = (Sensitivity_relevance/Sensitivity)*100

	BFSH	DF	GAS	GMAX	GMEDA	GMEDP	HAM	ILPSO	OPF	RF	SAR	SOL	VAS
alpha	1,4%	20,0%	2,1%	2,0%	5,0%	8,6%	4,4%	6,7%	20,0%	1,7%	0,4%	1,9%	1,5%
Fom	0,8%	1,2%	3,4%	2,6%	10,5%	10,8%	2,2%	6,8%	8,0%	2,6%	0,4%	6,9%	7,3%
Lo	0,9%	2,6%	5,0%	3,0%	11,8%	13,0%	1,9%	5,9%	7,8%	1,3%	0,4%	6,8%	6,6%
Lst	0,8%	8,7%	5,0%	3,6%	9,9%	13,2%	2,5%	6,9%	9,4%	1,1%	0,3%	5,4%	3,2%

Highest sensitivity to this parameter
Second highest sensitivity to this parameter
Third highest sensitivity to this parameter
Higher sensitivity than the varied muscle's one

Table 14: Results for variation of SAR. The matrix includes integrated sensitivity ratio, sensitivity of relevance, summed-crossed-sensitivity and significance over the interval of variation.

Integrated sensitivity ratio for SAR

	BFSH	DF	GAS	GMAX	GMEDA	GMEDP	HAM	ILPSO	OPF	RF	SAR	SOL	VAS	Summed-cross-Sensitivity
alpha						no pennation angle for Sartorius								0
Fom	55	11	59	27	21	44	45	44	3	48	**1685**	17	44	418
Lo	37	8	53	23	14	41	39	32	2	49	**1476**	27	49	374
Lst	6	2	10	4	4	9	6	5	1	5	**124**	12	10	74

Sensitivity of relevance for SAR

	BFSH	DF	GAS	GMAX	GMEDA	GMEDP	HAM	ILPSO	OPF	RF	SAR	SOL	VAS	Summed-cross-Sensitivity
alpha						no pennation angle for Sartorius								0
Fom	2	23	21	0,9	0,8	3	3	8	1	0,8	**9**	1	3	67,5
Lo	1,2	15	14	0,7	0,7	4	2	5	0,7	0,7	**7**	0,9	4	48,9
Lst	0,1	1	1	0,1	0,2	0,9	0,4	0,6	0,2	0,1	**0,6**	0,2	0,4	5,2

Significance = (Sensitivity_relevance/Sensitivity)*100

	BFSH	DF	GAS	GMAX	GMEDA	GMEDP	HAM	ILPSO	OPF	RF	SAR	SOL	VAS
alpha													
Fom	3,6%	209,1%	35,6%	3,3%	3,8%	6,8%	6,7%	18,2%	33,3%	1,7%	**0,5%**	5,9%	6,8%
Lo	3,2%	187,5%	26,4%	3,0%	5,0%	9,8%	5,1%	15,6%	35,0%	1,4%	**0,5%**	3,3%	8,2%
Lst	1,7%	50,0%	10,0%	2,5%	5,0%	10,0%	6,7%	12,0%	20,0%	2,0%	**0,5%**	1,7%	4,0%

Highest sensitivity to this parameter
Second highest sensitivity to this parameter
Third highest sensitivity to this parameter
Higher sensitivity than the varied muscle's one
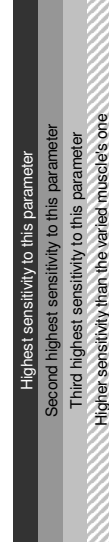
Table 15: Results for variation of SOL. The matrix includes integrated sensitivity ratio, sensitivity of relevance, summed-crossed-sensitivity and significance over the interval of variation.

Integrated sensitivity ratio for SOL

	BFSH	DF	GAS	GMAX	GMEDA	GMEDP	HAM	ILPSO	OPF	RF	SAR	SOL	VAS	Summed-cross-Sensitivity
alpha	70	85	96	41	6	16	137	35	56	47	40	**895**	14	643
Fom	551	76	592	54	21	58	1147	186	470	1673	261	**675**	37	5126
Lo	294	329	526	76	20	69	613	114	263	824	149	**2997**	38	3315
Lst	1986	52789	6006	314	117	385	2909	1103	3571	16156	966	**102607**	5379	91681

Sensitivity of relevance for SOL

	BFSH	DF	GAS	GMAX	GMEDA	GMEDP	HAM	ILPSO	OPF	RF	SAR	SOL	VAS	Summed-cross-Sensitivity
alpha	0,5	11	13	0,4	0,6	2	2	1	10	1	0,1	**34**	0,3	41,9
Fom	3	6	46	0,4	0,7	3	2	6	51	7	0,6	**113**	2	127,7
Lo	2	33	45	0,6	1	5	5	4	42	4	0,4	**125**	2	144
Lst	14	2082	528	5	13	32	55	44	386	47	3	**2896**	31	3240

Significance = (Sensitivity relevance/Sensitivity)*100

	BFSH	DF	GAS	GMAX	GMEDA	GMEDP	HAM	ILPSO	OPF	RF	SAR	SOL	VAS
alpha	0,7%	12,9%	13,5%	1,0%	10,0%	12,5%	1,5%	2,9%	17,9%	2,1%	0,3%	**3,8%**	2,1%
Fom	0,5%	7,9%	7,8%	0,7%	3,3%	5,2%	0,2%	3,2%	10,9%	0,4%	0,2%	**16,7%**	5,4%
Lo	0,7%	10,0%	8,6%	0,8%	5,0%	7,2%	0,8%	3,5%	16,0%	0,5%	0,3%	**4,2%**	5,3%
Lst	0,7%	3,9%	8,8%	1,6%	11,1%	8,3%	1,9%	4,0%	10,8%	0,3%	0,3%	**2,8%**	0,6%

Highest sensitivity to this parameter
Second highest sensitivity to this parameter
Third highest sensitivity to this parameter
Higher sensitivity than the varied muscle's one

Table 16: Results for variation of VAS. The matrix includes integrated sensitivity ratio, sensitivity of relevance, summed-crossed-sensitivity and significance over the interval of variation.

Integrated sensitivity ratio for VAS

	BFSH	DF	GAS	GMAX	GMEDA	GMEDP	HAM	ILPSO	OPF	RF	SAR	SOL	VAS	Summed-cross-Sensitivity
alpha	7	3	27	8	5	10	9	5	1	7	13	16	**34**	111
Fom	29	5	101	42	33	109	40	8	2	254	461	41	**283**	1125
Lo	242	8	217	182	313	486	191	45	4	788	1359	66	**1824**	3901
Lst	502	28	618	1058	1020	2052	849	102	14	10020	3586	154	**5204**	20003

Sensitivity of relevance for VAS

	BFSH	DF	GAS	GMAX	GMEDA	GMEDP	HAM	ILPSO	OPF	RF	SAR	SOL	VAS	Summed-cross-Sensitivity
alpha	0,1	0,5	0,6	0,2	0,05	1	0,5	0,4	0,2	0,03	0,04	0,3	**0,5**	3,92
Fom	0,4	1	1	7	0,6	15	4	1	0,3	4	1	1	**10**	36,3
Lo	3	2	4	23	3	50	19	10	0,5	19	5	4	**50**	142,5
Lst	6	8	12	180	18	273	83	21	1	107	11	9	**257**	729

Significance = (Sensitivity relevance/Sensitivity)*100

	BFSH	DF	GAS	GMAX	GMEDA	GMEDP	HAM	ILPSO	OPF	RF	SAR	SOL	VAS
alpha	1,4%	16,7%	2,2%	2,5%	1,0%	10,0%	5,6%	8,0%	20,0%	0,4%	0,3%	1,9%	**1,5%**
Fom	1,4%	20,0%	1,0%	16,7%	1,8%	13,8%	10,0%	12,5%	15,0%	1,6%	0,2%	2,4%	**3,5%**
Lo	1,2%	25,0%	1,8%	12,6%	1,0%	10,3%	9,9%	22,2%	12,5%	2,4%	0,4%	6,1%	**2,7%**
Lst	1,2%	28,6%	1,9%	17,0%	1,8%	13,3%	9,8%	20,6%	7,1%	1,1%	0,3%	5,8%	**4,9%**

Legend:
- Highest sensitivity to this parameter
- Second highest sensitivity to this parameter
- Third highest sensitivity to this parameter
- Higher sensitivity than the varied muscle's one

Table 17: Results for variation of activation time, deactivation time and maximal shortening velocity. The matrix includes integrated sensitivity ratio, sensitivity of relevance, summed-crossed-sensitivity and significance over the interval of variation.

Sensitivity over the itnerval of variation

	BFSH	DF	GAS	GMAX	GMEDA	GMEDP	HAM	ILPSO	OPF	RF	SAR	SOL	VAS
TauA	1,2	1,1	11	1,7	1,3	1,5	2	0,9	0,4	0,9	1,7	6,9	11
TauD	0,8	0,7	7,3	1,1	0,8	0,9	1,3	0,6	0,3	0,6	1,1	4,5	7
Vmax	1,6	14	2	1,6	1,9	2,6	1,2	0,5	0,5	1,2	2,1	8,8	14

Sensitivity relevance

	BFSH	DF	GAS	GMAX	GMEDA	GMEDP	HAM	ILPSO	OPF	RF	SAR	SOL	VAS
TauA	0,05	0,2	0,2	0,04	0,03	0,07	0,2	0,1	0,09	0,03	0,004	0,1	0,1
TauD	0,03	0,15	0,15	0,02	0,02	0,05	0,1	0,08	0,06	0,02	0,002	0,07	0,06
Vmax	0,06	0,3	0,3	0,05	0,03	0,09	0,2	0,15	0,1	0,04	0,005	0,1	0,1

Significance = (Sensitivity_relevance/Sensitivity)*100

	BFSH	DF	GAS	GMAX	GMEDA	GMEDP	HAM	ILPSO	OPF	RF	SAR	SOL	VAS
TauA	4,2%	18,2%	1,8%	2,4%	2,3%	4,7%	10,0%	11,1%	22,5%	3,3%	0,2%	1,4%	0,9%
TauD	3,8%	21,4%	2,1%	1,8%	2,5%	5,6%	7,7%	13,3%	20,0%	3,3%	0,2%	1,6%	0,9%
Vmax	3,8%	2,1%	15,0%	3,1%	1,6%	3,5%	16,7%	30,0%	20,0%	3,3%	0,2%	1,1%	0,7%

5.1. Sensitivity to pennation angle

The sensitivities for the pennation angle (α) are by far the smallest. The highest value of the integrated sensitivity ratio over the interval of variation is 895, reached by SOL (see Table 15 and Figure 75). Highest sensitivities show SOL, BFSH and GAS which are also the muscles with the greatest pennation angles (Figures 75, 53 and 57) The sensitivity curves of those muscles are far above the curves of the other muscles, indicating their variation has not much effect on the other muscles. The smaller the integrated sensitivity ratios, the more spiky and inconsistent the graphs (e.g. Figure 67) and 68) become, where curves are spread over the entire panel. This is due to their small values. Curves of the more sensitive muscles are flat or going up slightly to +10%. Often, those muscles which have a small pennation angle affect other ones much more than they react themselves. GMAXL/M and GMEDA show this behaviour (e.g. Figure 61. Muscles which are most likely to be affected are GAS and SOL with high pennation but also VAS which has a pennation of only 3 degrees. Interestingly, BFSH with the second highest pennation of 23 degrees is not affected by other muscles. The DFs which have a small sensitivity to α react to variations of the other muscles, especially when the relevance is considered.
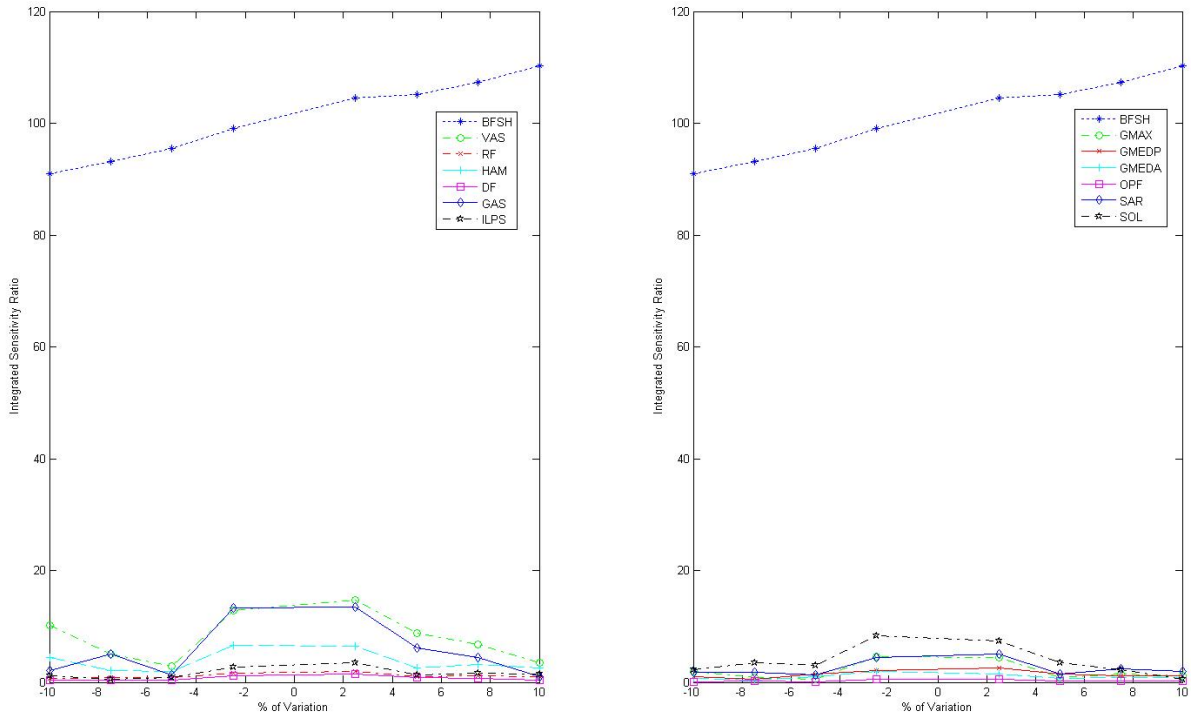
Figure 14: Integrated sensitivity ratios of the variation for BFSH to the parameter alpha.
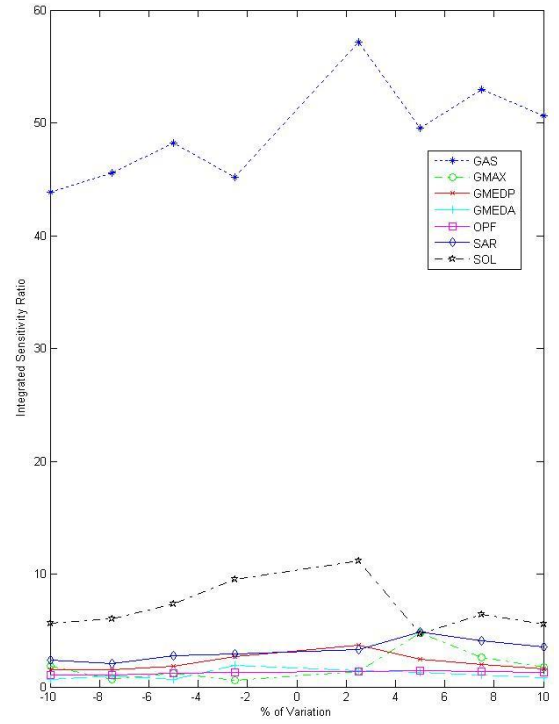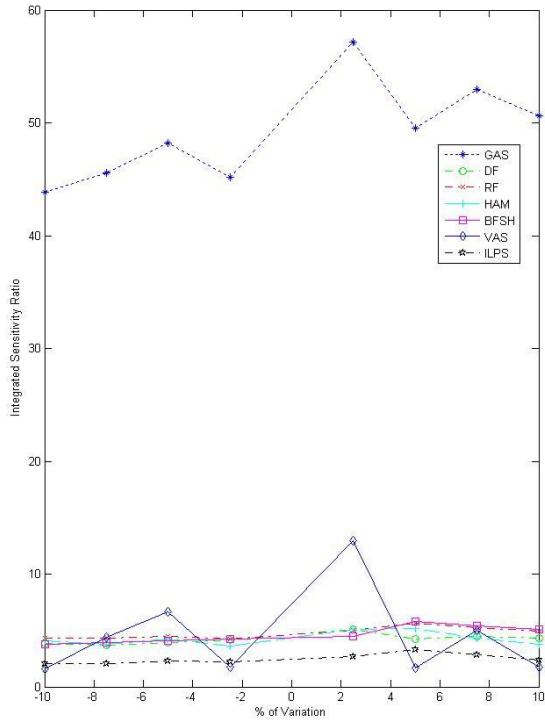
Figure 15: Integrated sensitivity ratios of the variation for GAS to the parameter alpha.
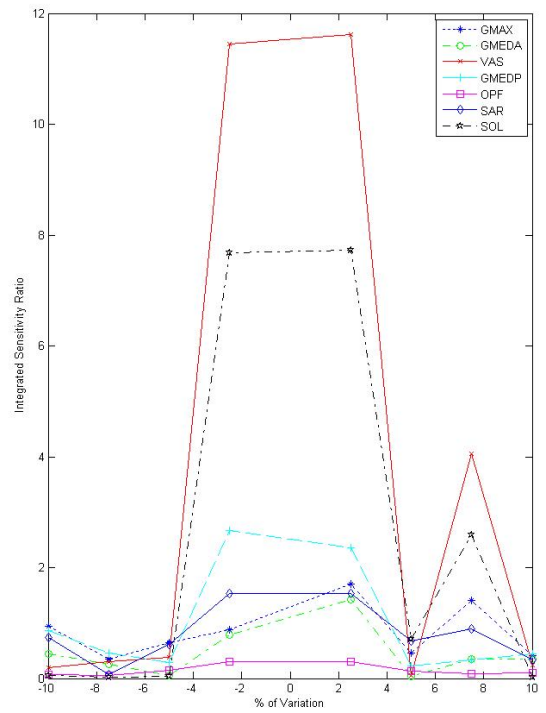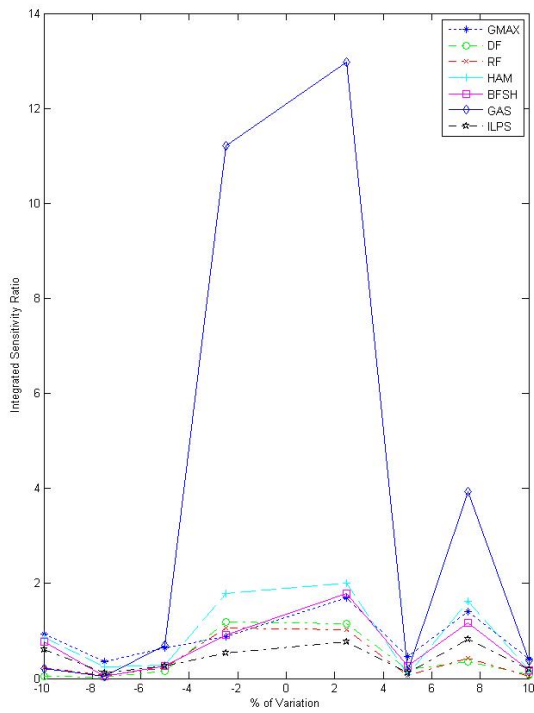
Figure 16: Integrated sensitivity ratios of the variation for GMAXM to the parameter alpha.
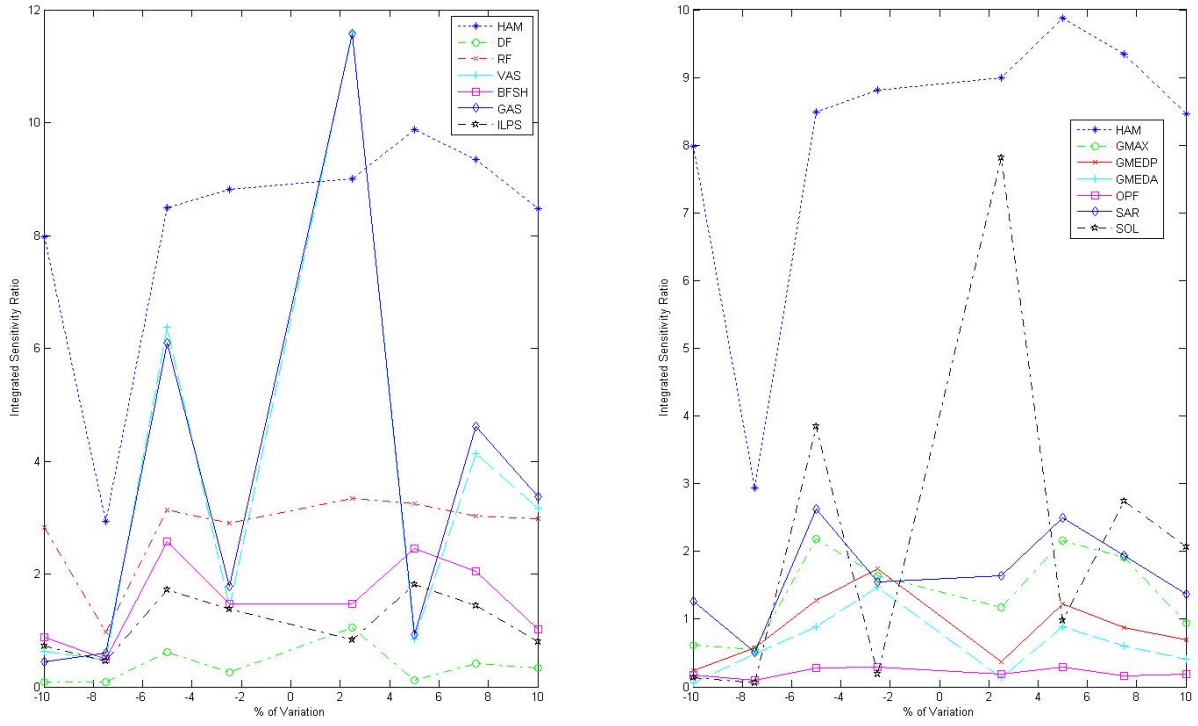
Figure 17: Integrated sensitivity ratios of the variation for GMAXM to the parameter alpha.
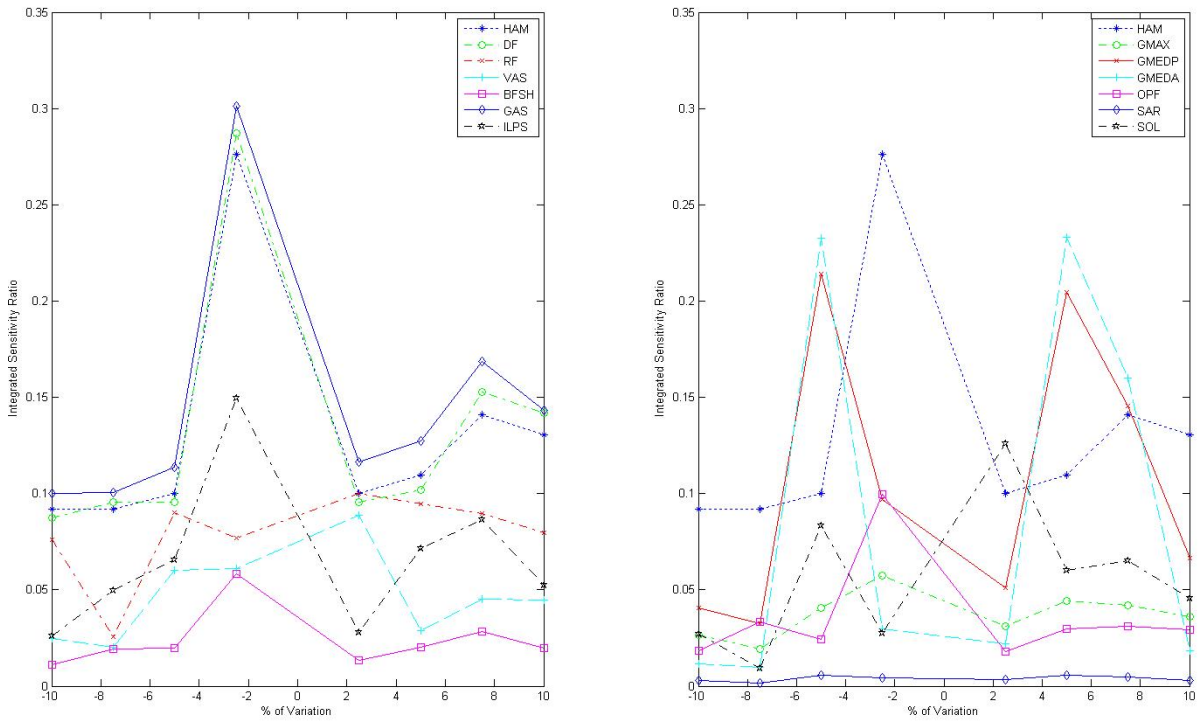
Figure 18: Integrated sensitivity ratios of the variation for GMAXM to the parameter alpha when relevance is considered.
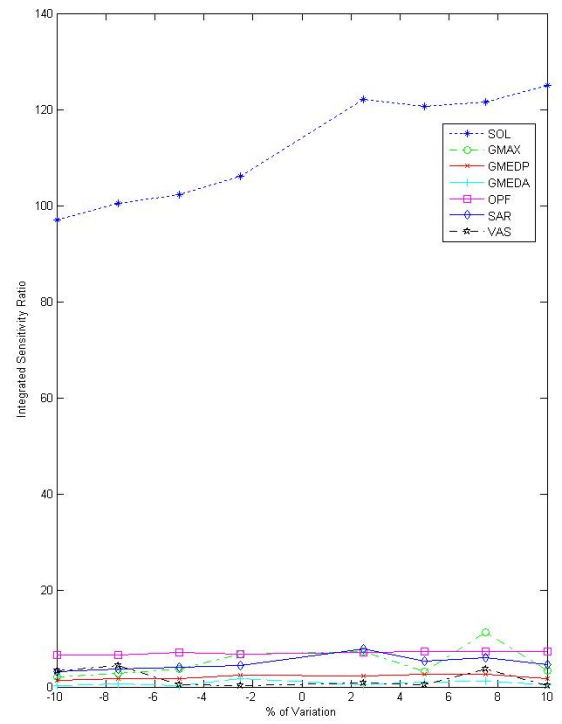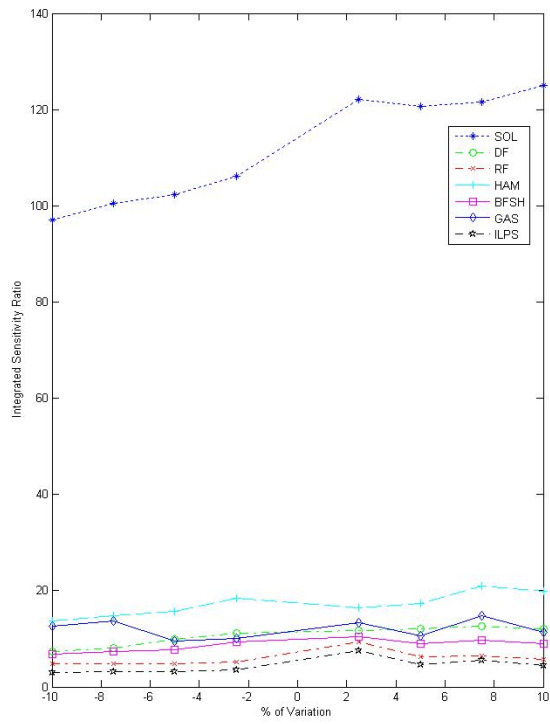
Figure 19: Integrated sensitivity ratios of the variation for SOL to the parameter alpha. Graphs for all muscles and parameters can be found in section A.

5.2. Sensitivity to optimal muscle force

Three muscles were found to be most sensitive out of all parameters to optimal muscle force (F_o^m); GMEDP, SAR and GMAXM (Tables 9, 14 and 7). Considering the relevance of sensitivity a fourth one, GMEDA shows the same behavior (Table 8) . The highest value reached for GMEDP was 4491 (Table 9) which is the sum of the integrated sensitivity ratios over the interval of variation (Figures 91 and 92). The smallest value was 145 (Table 9) for GMAXM; a muscle which shows very little sensitivity for all parameters. Generally, muscles are much more sensitive to F_o^m than to α. But sensitivity to muscle force in general is less than to resting fiber length (l_o^m) and even smaller to tendon slack length (l_s^t). The curves of integrated sensitivities are much more flat (constant sensitivity) than they are for l_s^t and l_o^m.

RF is likely to be strongly affected but does not affect other muscles much. When GAS, HAM and SOL are varied, the sensitivity curve of RF is far above the curves of those muscles (Figures 83, 93 and 103). The panel for the variation of SOL shows that sensitivity of RF goes up at a variation of -10% and HAM is in an almost glock shaped curve also above SOL's sensitivity (Figure 103). In comparison ILPSO is a muscle which is not affected by other muscles at all but has influence on several muscles (e.g. BFSH, SAR, GAS, HAM, Figure 95). If the relevance is considered GAS and DF are much more sensitive than ILPSO itself (Figure 96). SAR is a muscle which has little potential to affect muscles but very often reacts to the variation of others. In the cases of variation of VAS and HAM, its sensitivity graph is much above the graphs of the changed muscles (Figures 93 and 105). Most often influenced by other actuators is GAS. Also when relevance is considered, this muscle is very likely to be still one of the affected muscles. GAS itself mostly influences RF and HAM (Figure 83). The graph of relevance is more offset relative to other graphs. It is also notable that SOL comes close (Figure 84).

Within the gluteus group, GMEDP is the one which reacts greatly to changes of other muscles. Additionally, it is the most sensitive muscle to this parameter. When GMAXL and GMEDA are varied, GMEDP is much more sensitive than those muscles (Figures 85 and 89). In the panels of the sensitivity of relevance for GMAXL and VAS, the sensitivity curve of GMEDP is also above the curves of GMAX and VAS (Figures 86 and 106). GMEDP mostly affects RF, GMAX and SAR. The variation of GMEDA (Figure 89) has on three muscles (GMAX, GMEDP and HAM) a greater effect than on GMEDA, and two have approximately the same sensitivity (RF and SAR).

Another observation of HAM is that this muscle group, in different intensities, is very often affected by other muscles. It remains and sometimes strengthens its significance in the relevance of sensitivity. According to the relevance of sensitivity, the DFs have the characteristic to increase and overtake the respectively perturbed muscle (e.g. BFSH, GMAXM, HAM (Figure 94) , ILPS (Figure 96), SAR; Figures for all muscles can be found in the Appendix A).
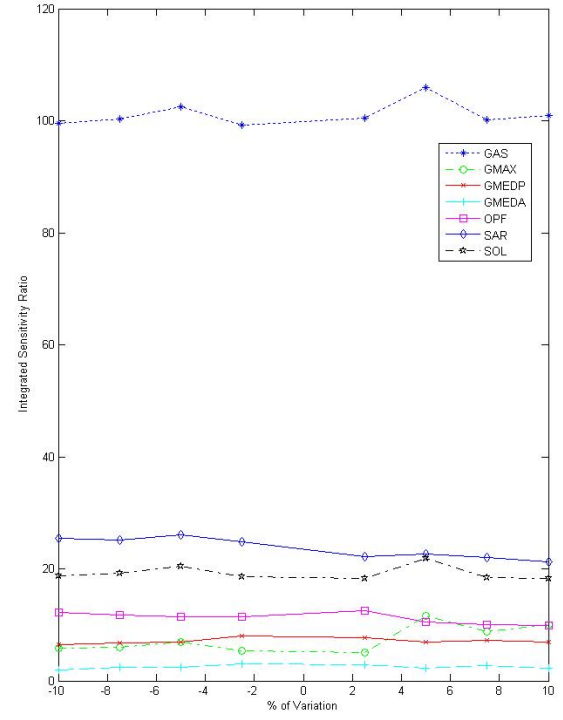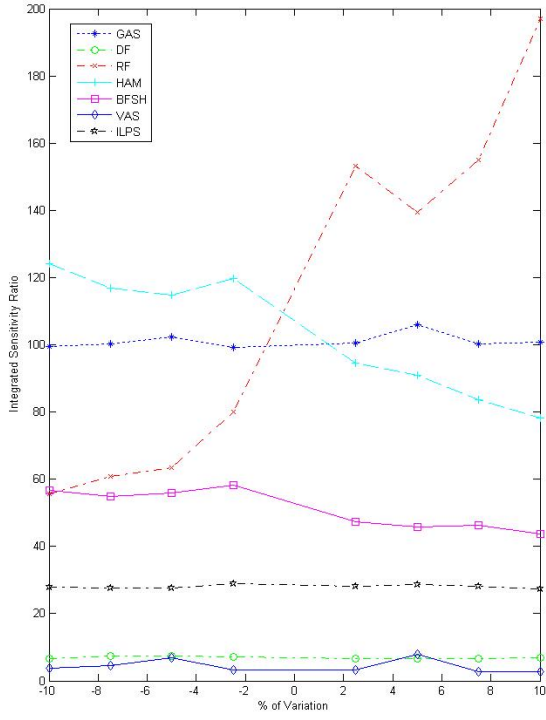
Figure 20: Integrated sensitivity ratios of the variation for GAS to the parameter optimal muscle force.
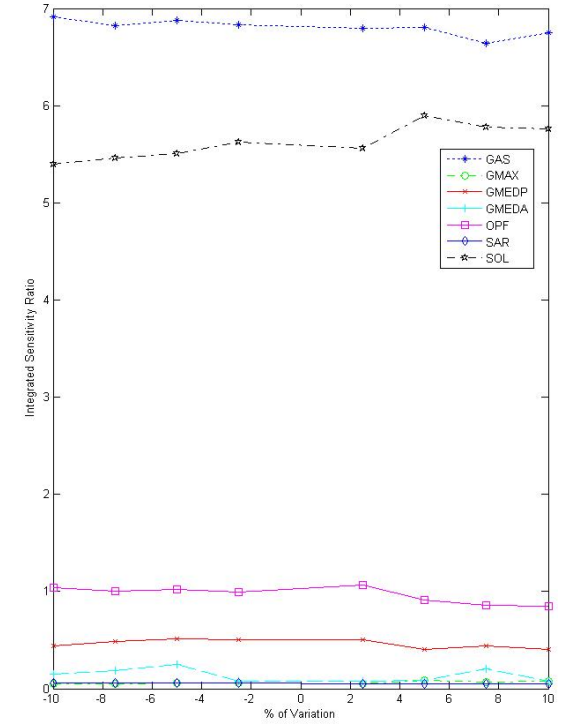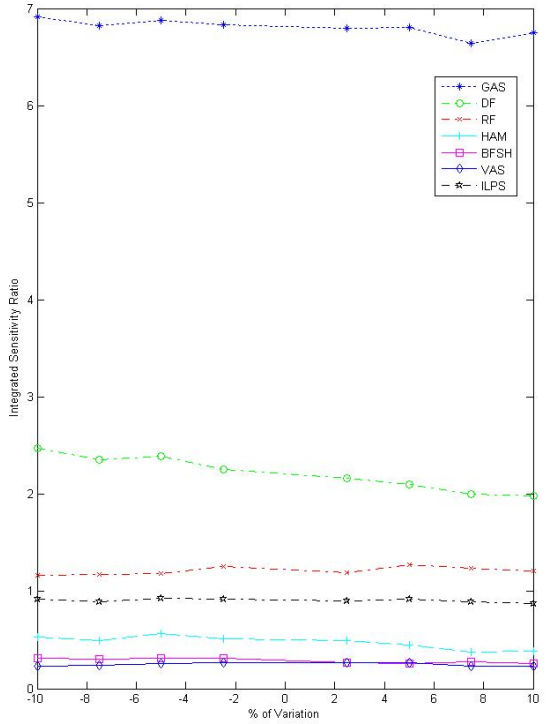
Figure 21: Integrated sensitivity ratios of the variation for SOL to the parameter optimal muscle force when relevance is considered.
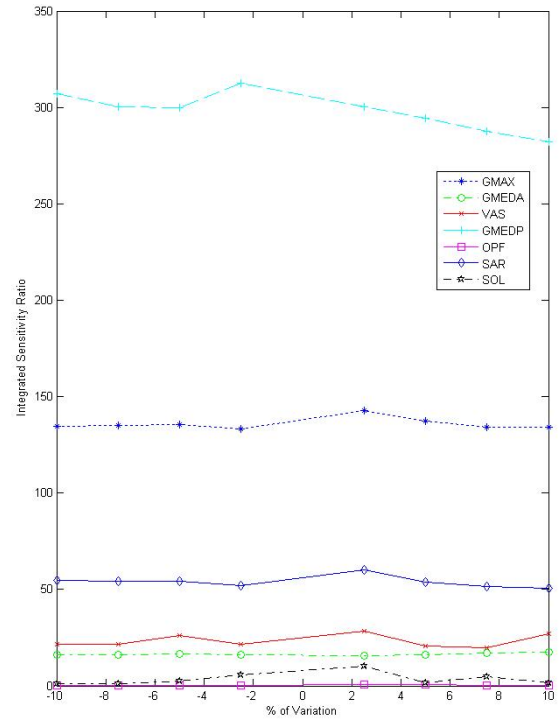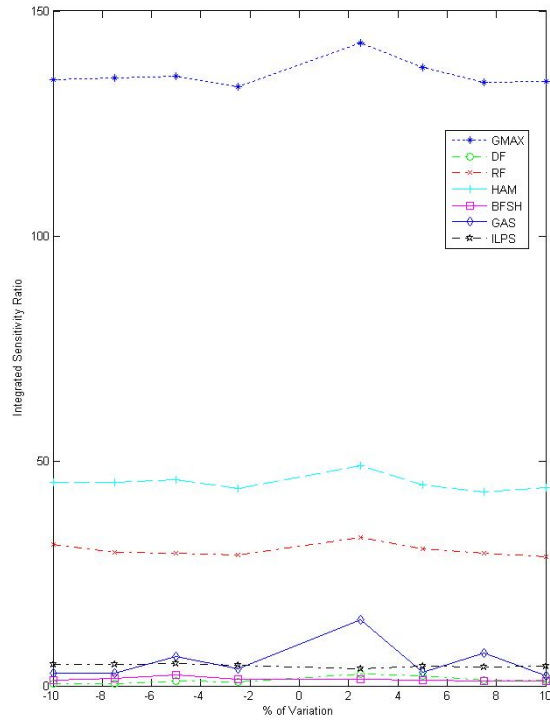
Figure 22: Integrated sensitivity ratios of the variation for GMAXL to the parameter optimal muscle force.
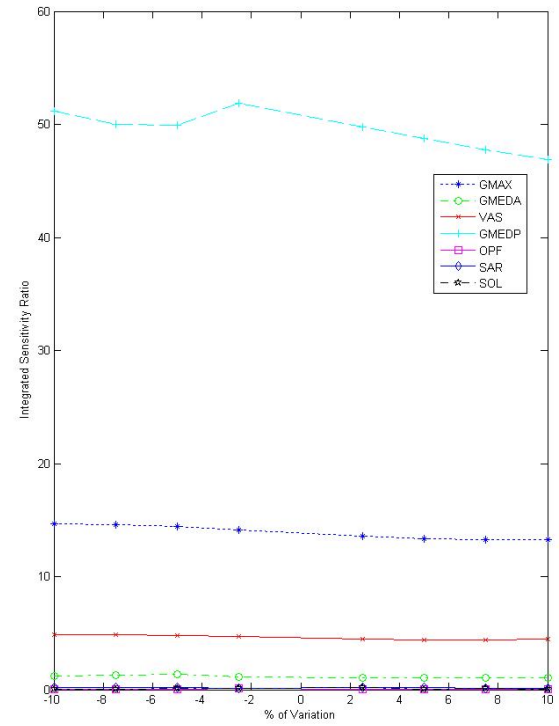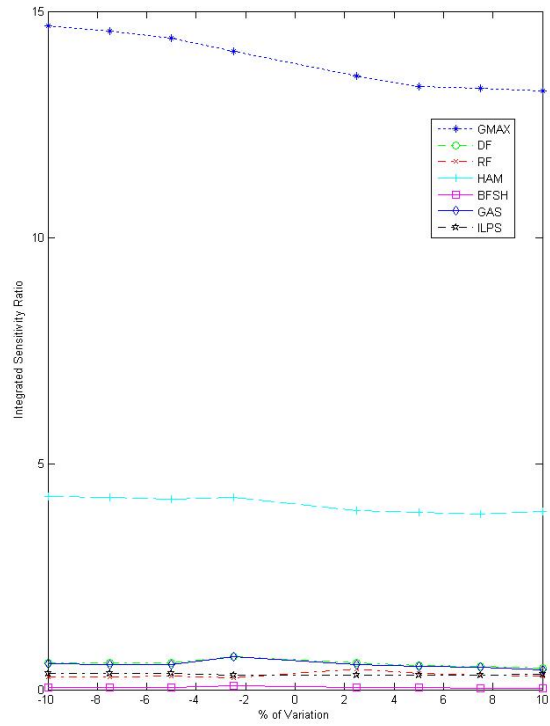
Figure 23: Integrated sensitivity ratios of the variation for GMAXL to the parameter optimal muscle force when relevance is considered..
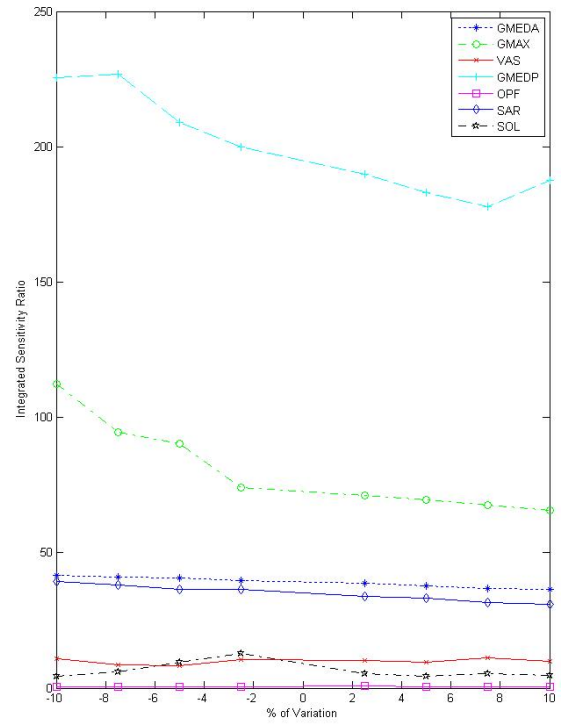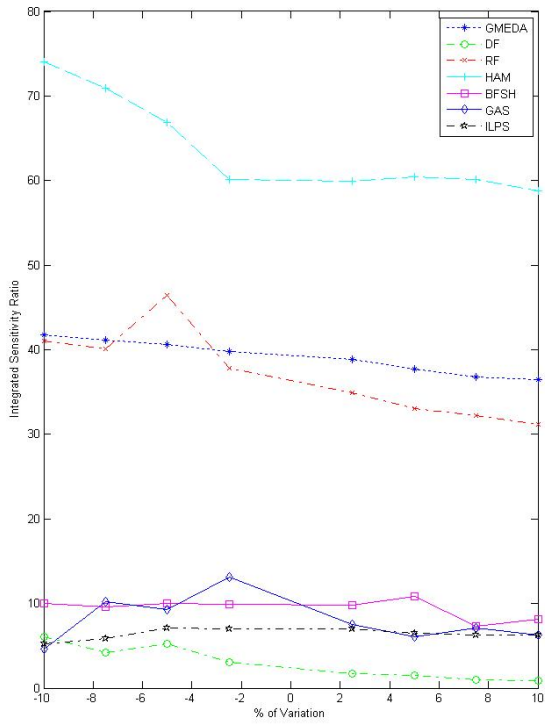
Figure 24: Integrated sensitivity ratios of the variation for GMEDA to the parameter optimal muscle force.
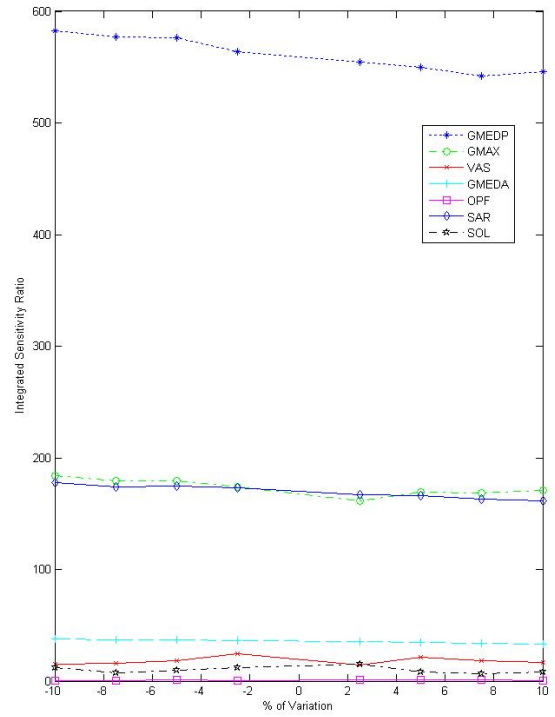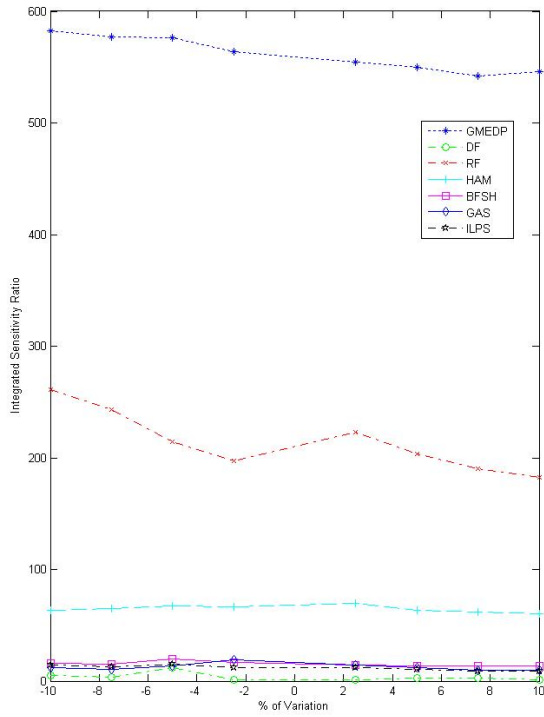
Figure 25: Integrated sensitivity ratios of the variation for GMEDP to the parameter optimal muscle force.
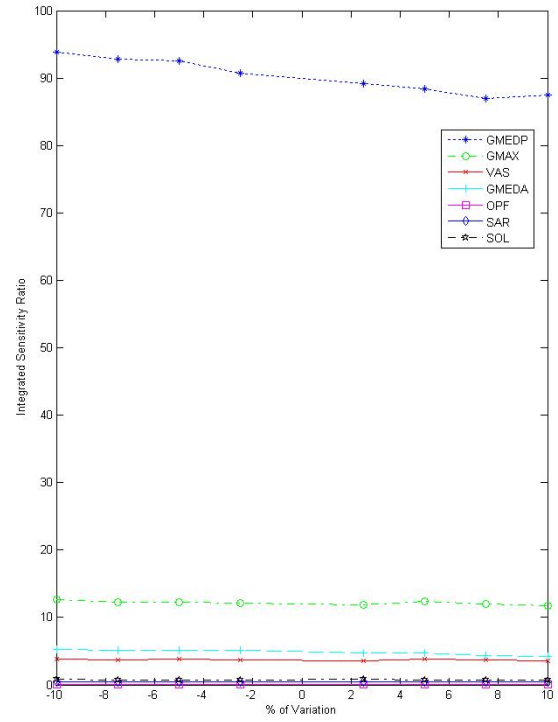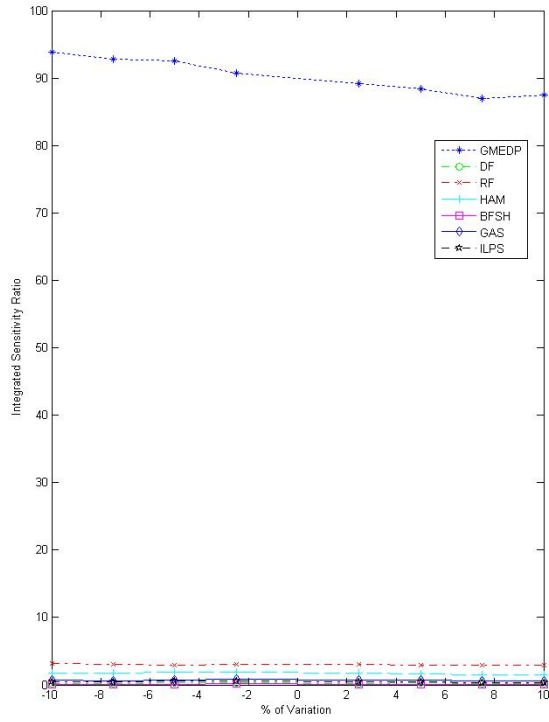
Figure 26: SIntegrated sensitivity ratios of the variation for GMEDP to the parameter optimal muscle force when relevance is considered.
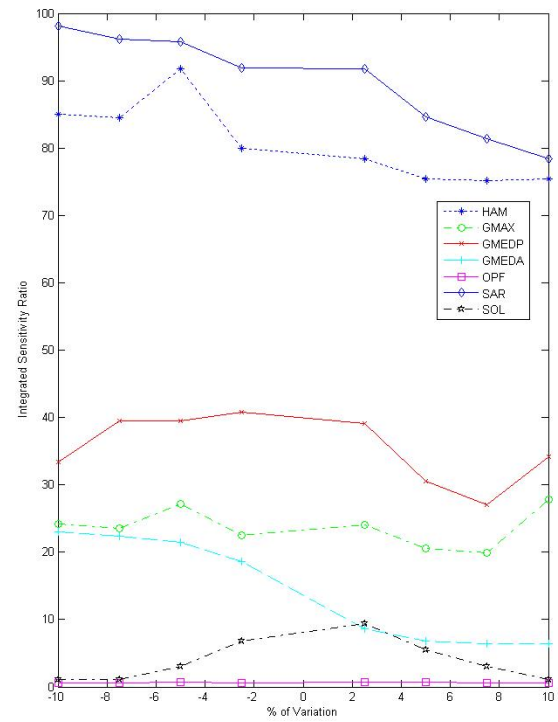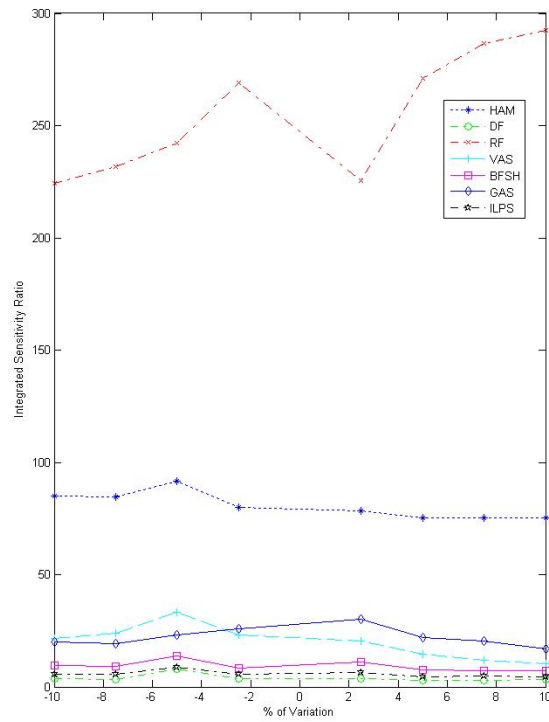
Figure 27: Integrated sensitivity ratios of the variation for HAM to the parameter optimal muscle force.
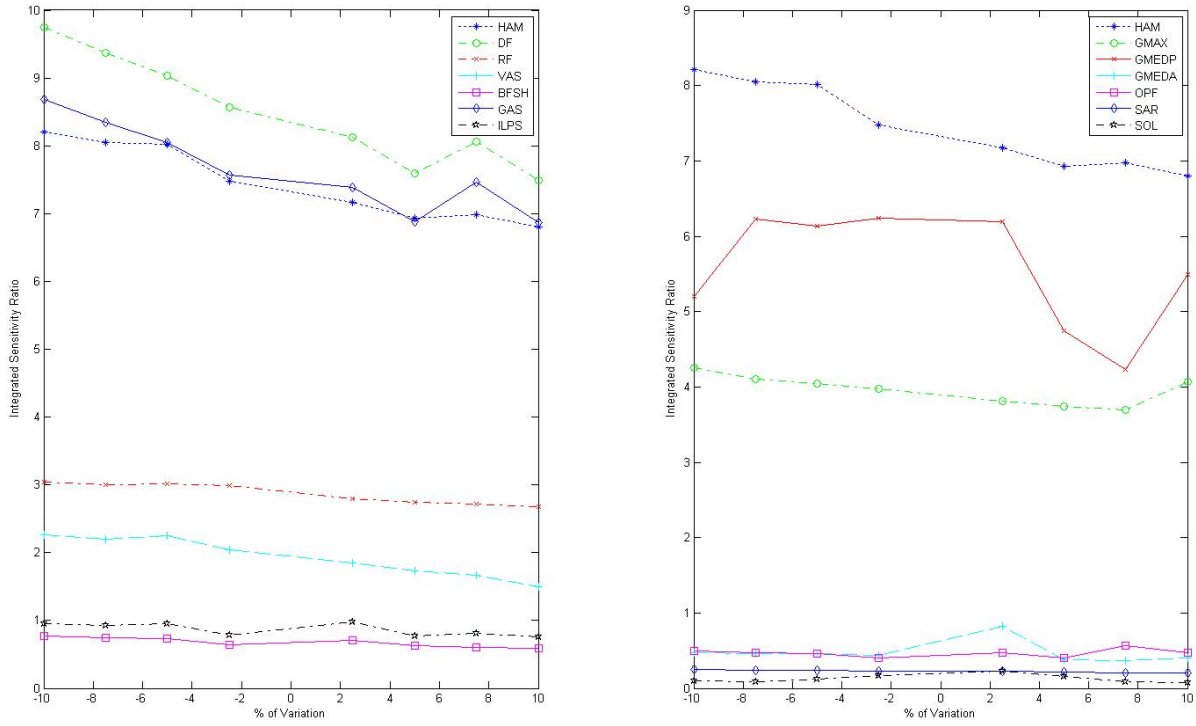
Figure 28: Integrated sensitivity ratios of the variation for HAM to the parameter optimal muscle force when relevance is considered.
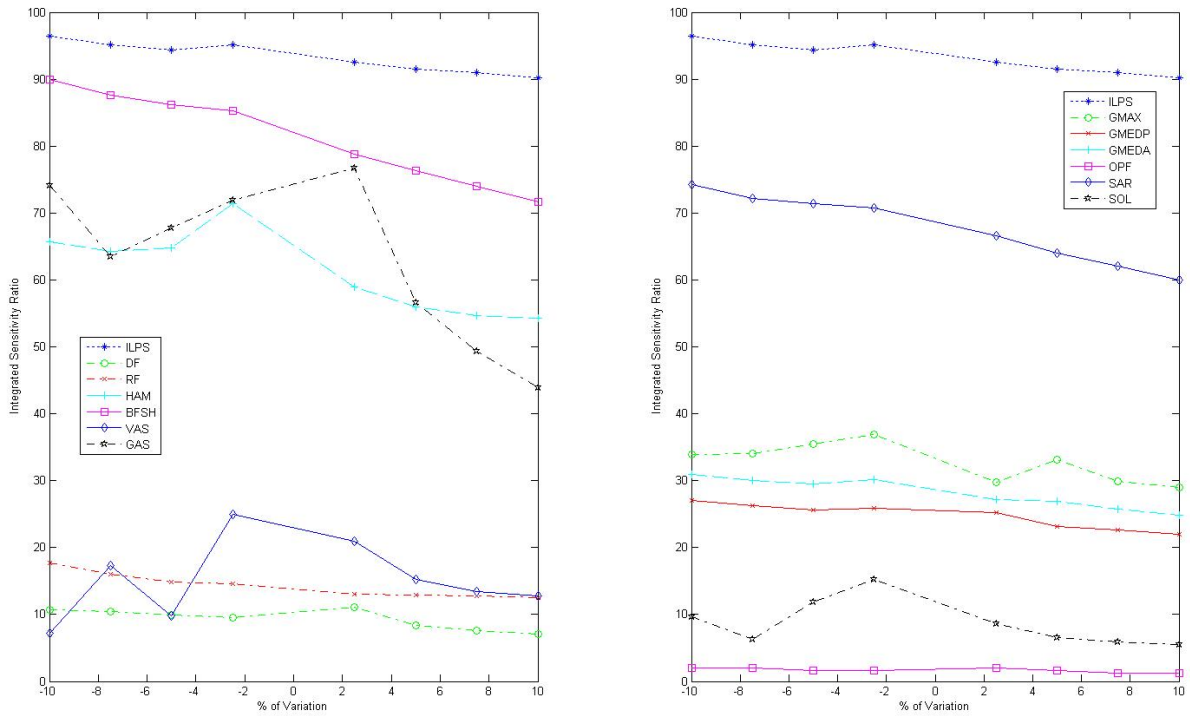
Figure 29: Integrated sensitivity ratios of the variation for ILPSO to the parameter optimal muscle force.
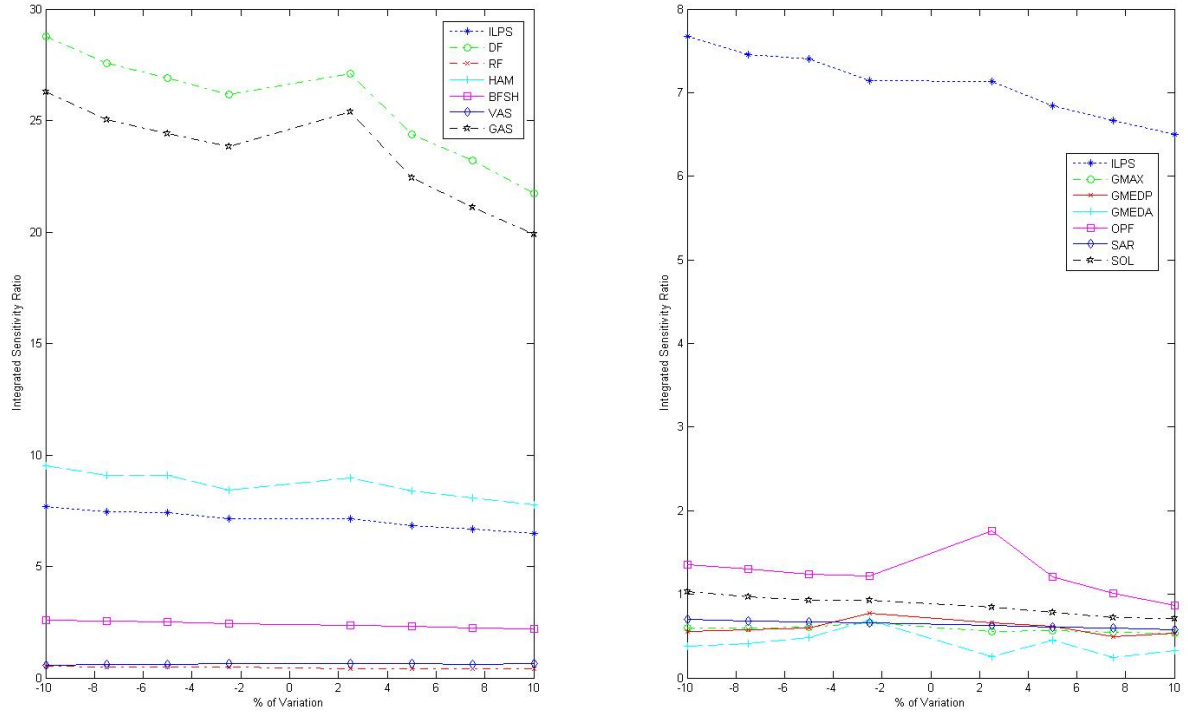
Figure 30: Integrated sensitivity ratios of the variation for ILPSO to the parameter optimal muscle force when relevance is considered.
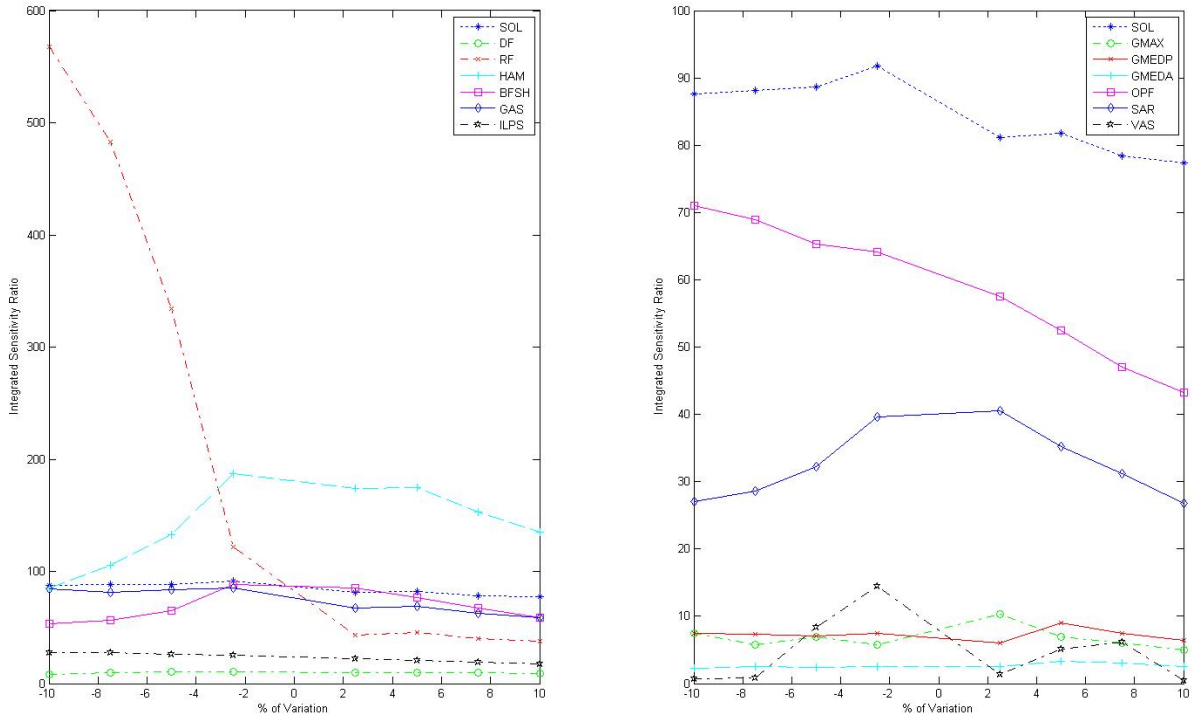
Figure 31: Integrated sensitivity ratios of the variation for SOL to the parameter optimal muscle force.

74
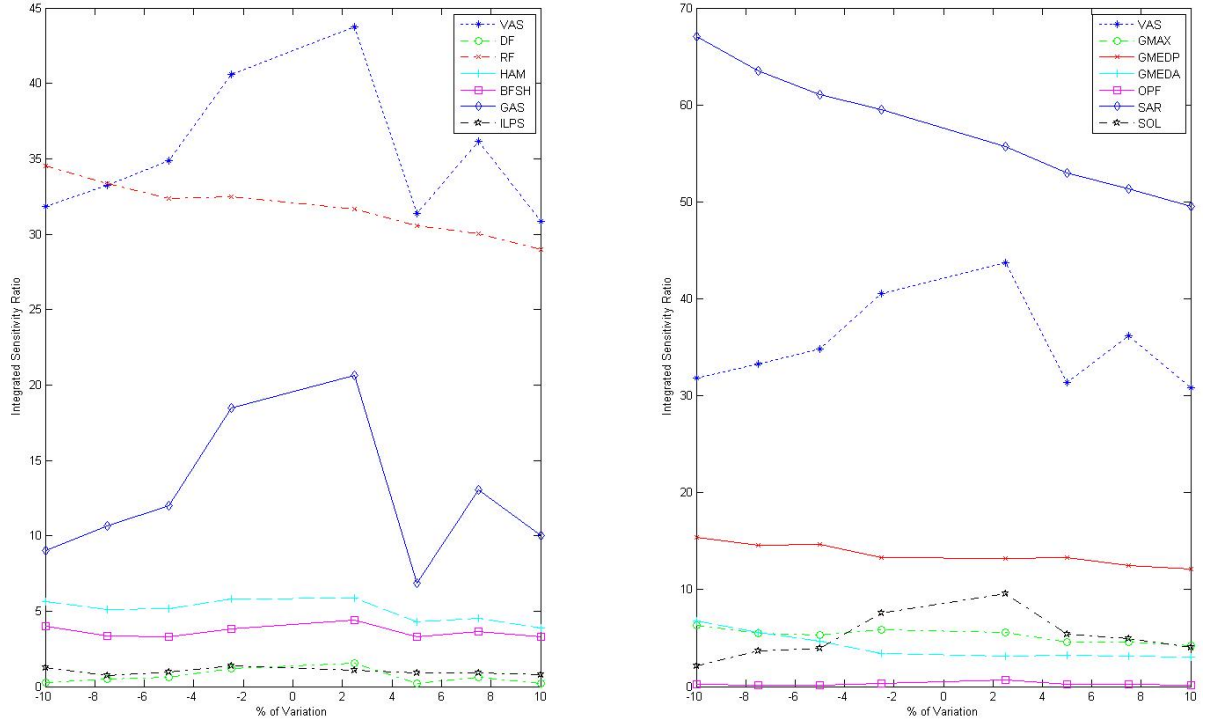
Figure 32: Integrated sensitivity ratios of the variation for VAS to the parameter optimal muscle force.
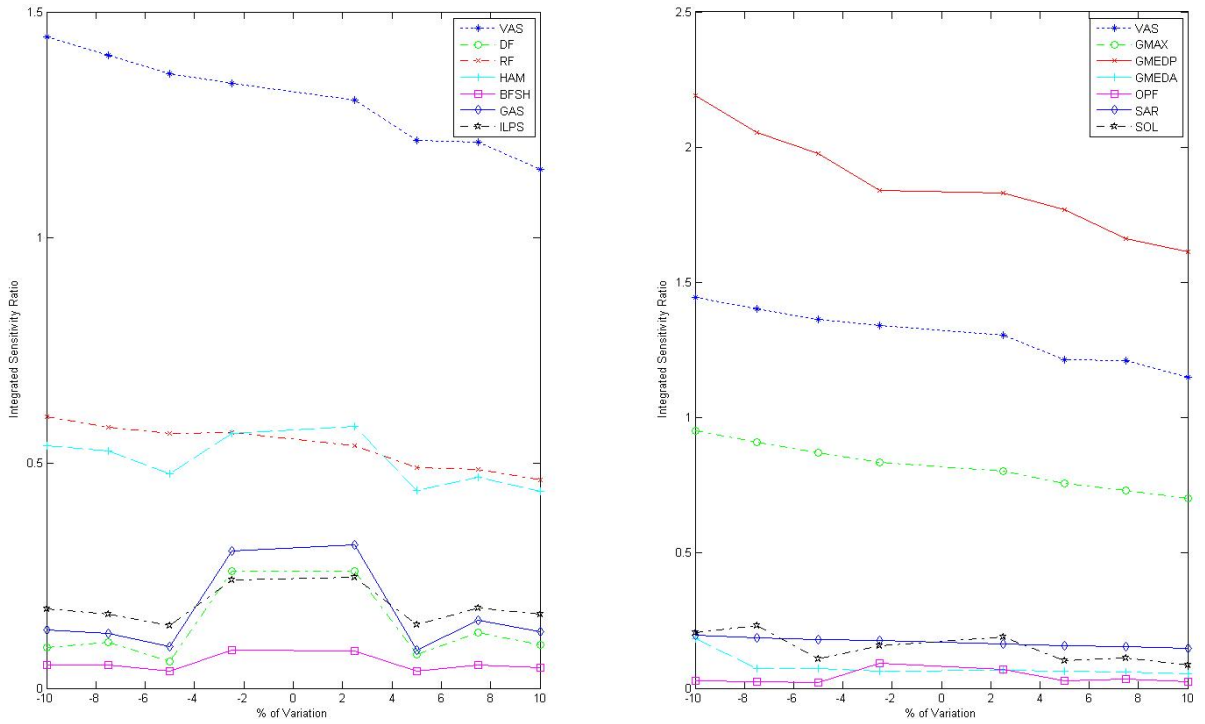
Figure 33: Integrated sensitivity ratios of the variation for VAS to the parameter optimal muscle force when relevance is considered.

5.3. Sensitivity to resting fiber length

The curves showing the sensitivity to resting fiber length (l_o^m) have a tendency to be more sensitive when the length is reduced; 10 out of 14 go up to a variation of -10%. Interestingly, the slopes for the muscles GMAXL and VAS are the opposite for the relevance of sensitivity. In this case they are more sensitive to an extension of the resting fiber length. Integrated sensitivity rations over the interval of variation range between 117 for GMAXM (Table 7) and 9370 for OPF (Table 7).

GMEDP has not much influence on other muscles' sensitivity when its fiber length is changed. But this muscle responds to the variation of others. For the sensitivities of relevance even more; in the cases of GMAXL/M, GMEDA and VAS it is by far more sensitive than the varied muscle (e.g. Figures 114 and 134) . The DF's sensitivity graphs, similar to as it is described in section 5.2, characteristically move upwards when the relevance is calculated (e.g. GAS, ILPSO; figures in Appendix A) or even overtake the varied muscles graph (e.g. GMEDA, HAM, SAR; figures in Appendix A). The OPFs have a great influence on DF in both graphs (Figures 125 and 126). When the VAS muscles are varied, RF and SAR react very sensitive; the more the longer the VAS fibers are (Figure 134). The HAM group is also mostly influencing RF and secondly (but much less) SAR (Figure 121). The RF impact on other muscles is, vice versa, also the most causing a sensitivity for HAM (Figure 127). When decreasing ILPSO's resting fiber length by 10%, the integrated sensitivity ratio over the interval of variation of VAS increases to 4000 which is more than two and a half times higher then the value for ILPSO (Table 11). Also, other muscles had a tendency to increase sensitivity (GAS followed by SAR, GMAX, RF, BFSH) to the variation of ILPSO (Figure 123). The most sensitive muscle to l_o^m, OPF, also affects three other muscles greatly. These muscles are DF, GAS and SOL (Figure 125). The pattern remains noticeable similar when relevance is applied, only SOL disappears (Figure 126).
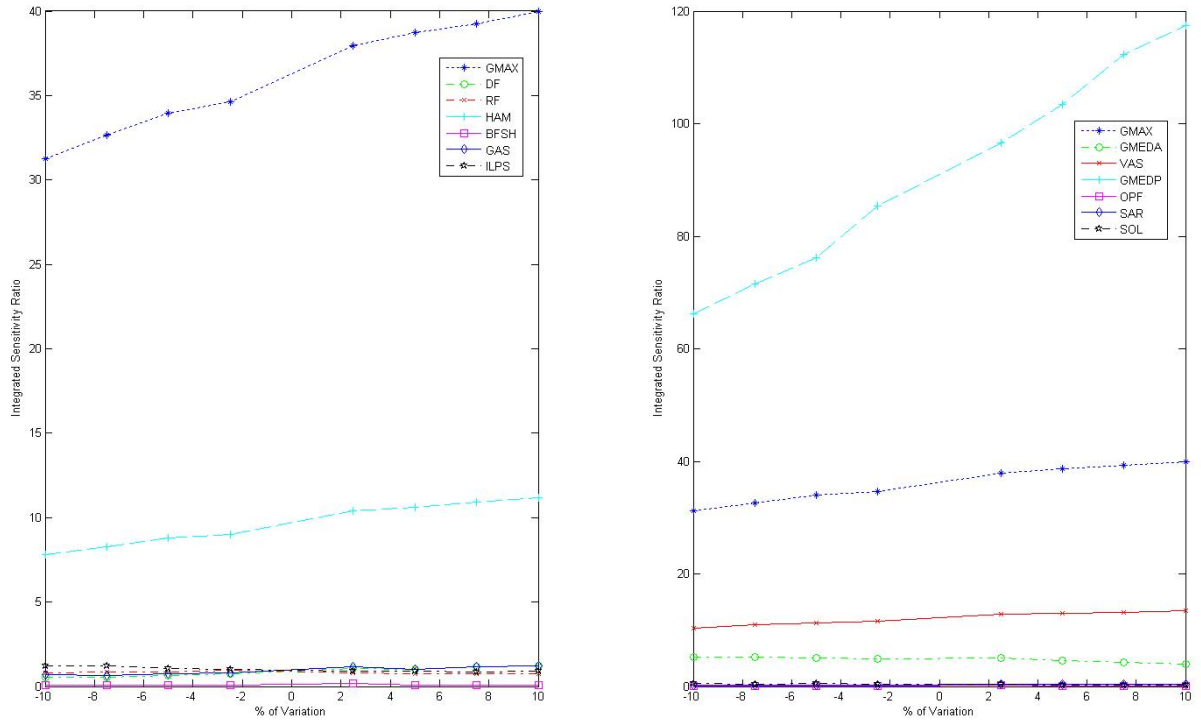
Figure 34: Integrated sensitivity ratios of the variation for GMAXL to the parameter resting fiber length when relevance is considered.
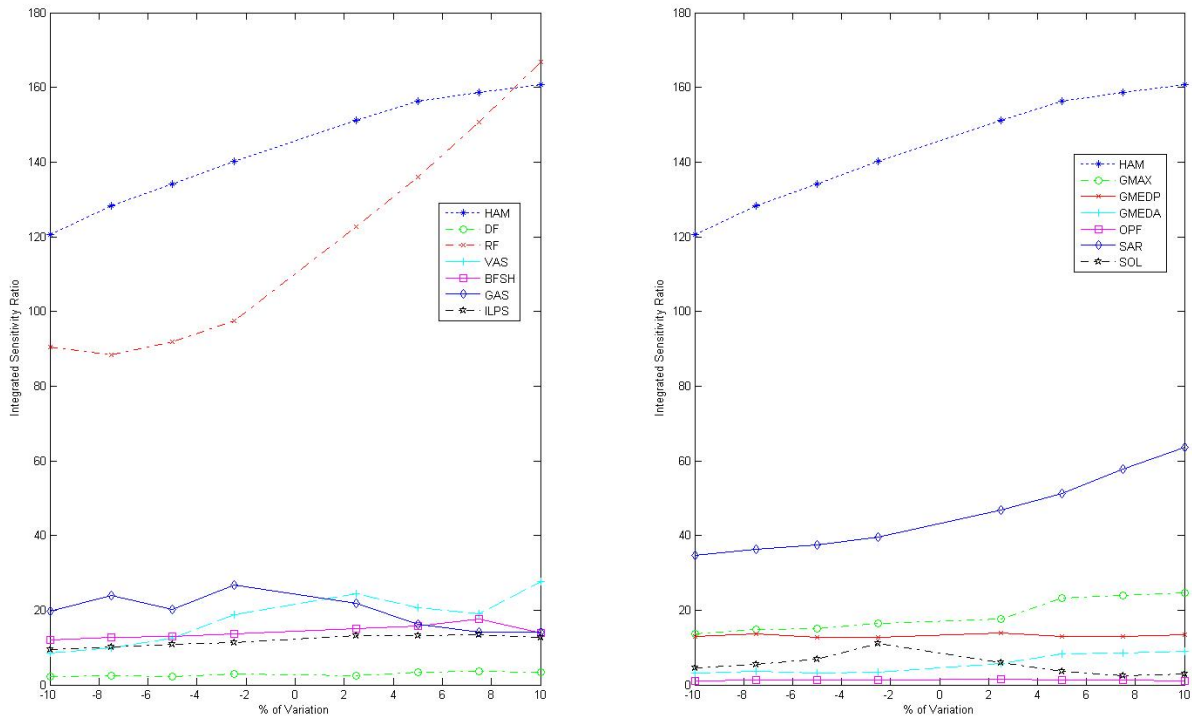
Figure 35: Integrated sensitivity ratios of the variation for HAM to the parameter resting fiber length.
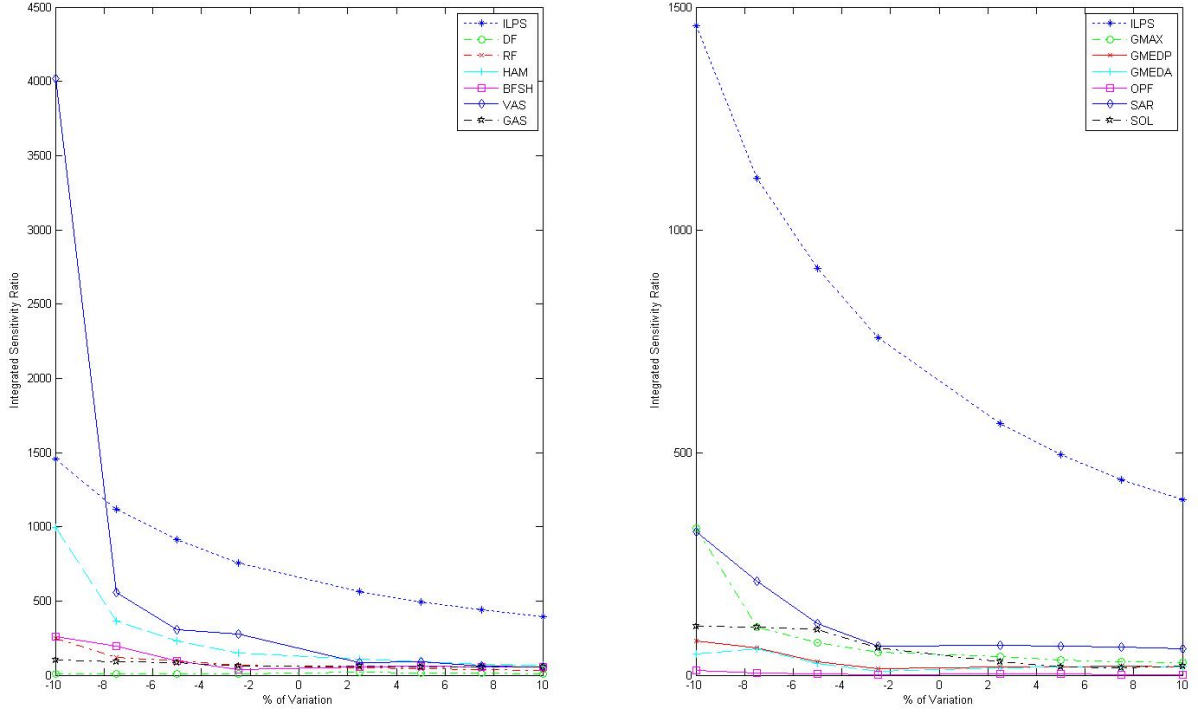
Figure 36: Integrated sensitivity ratios of the variation for ILPSO to the parameter resting fiber length.
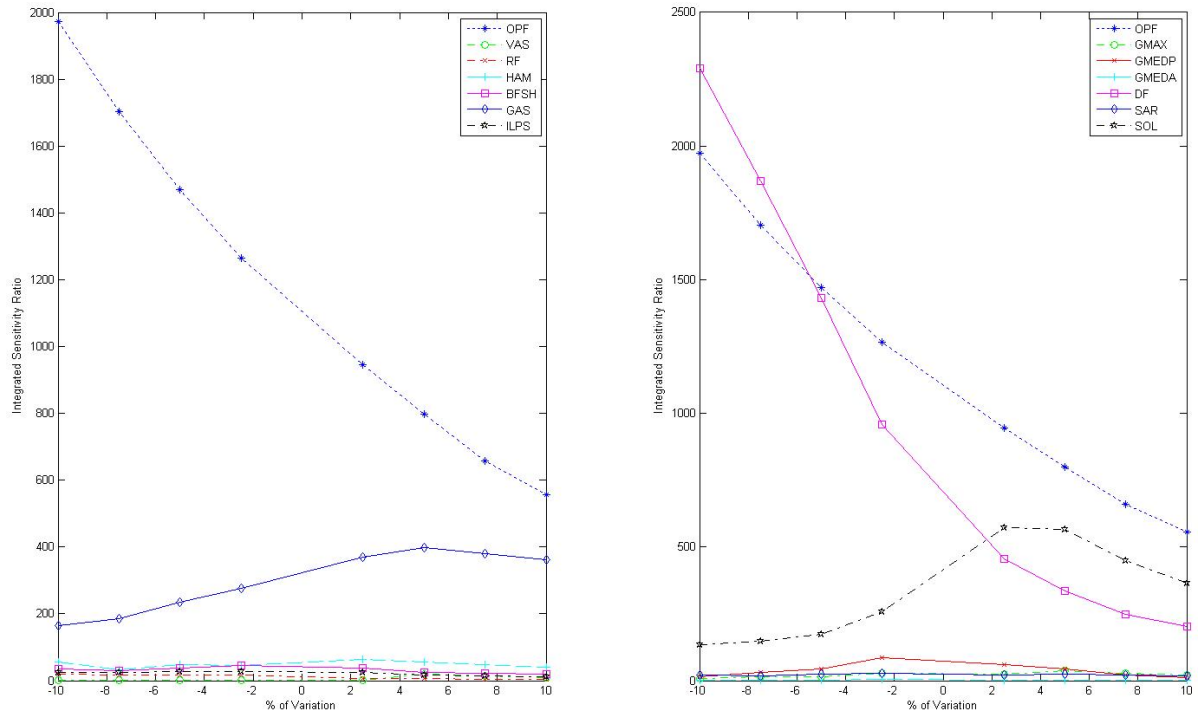
Figure 37: Integrated sensitivity ratios of the variation for OPF to the parameter resting fiber length.
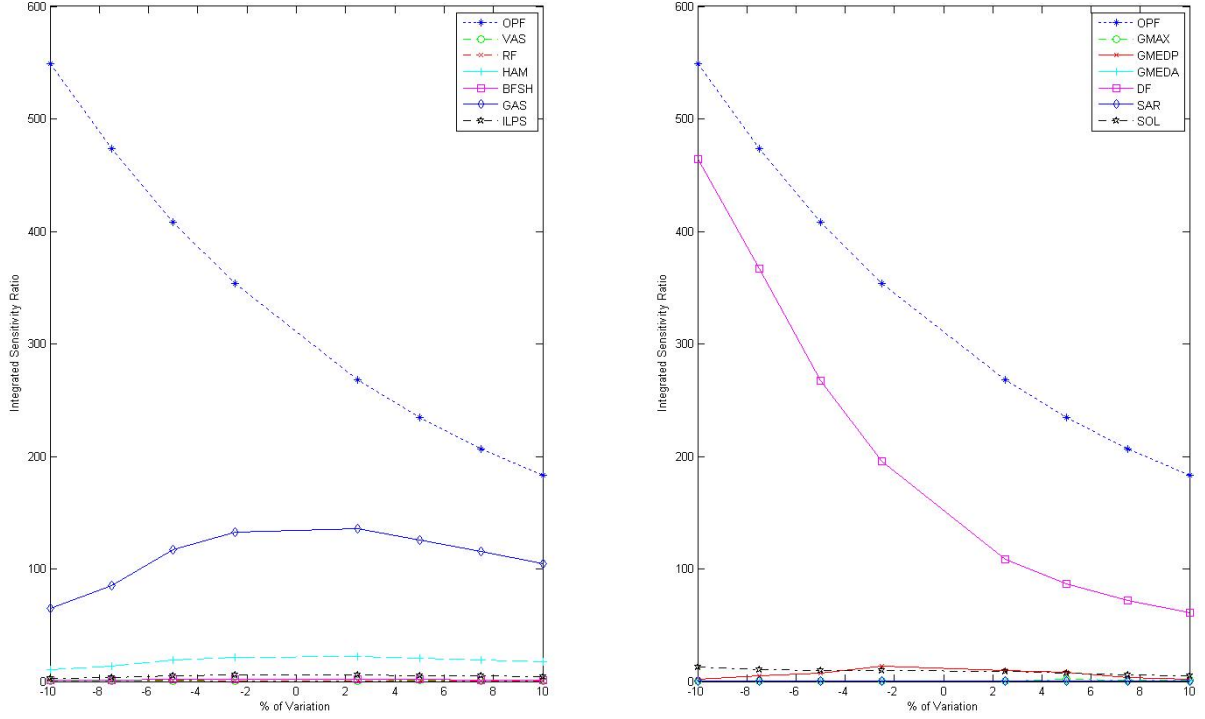
Figure 38: Integrated sensitivity ratios of the variation for OPF to the parameter resting fiber length when relevance is considered.
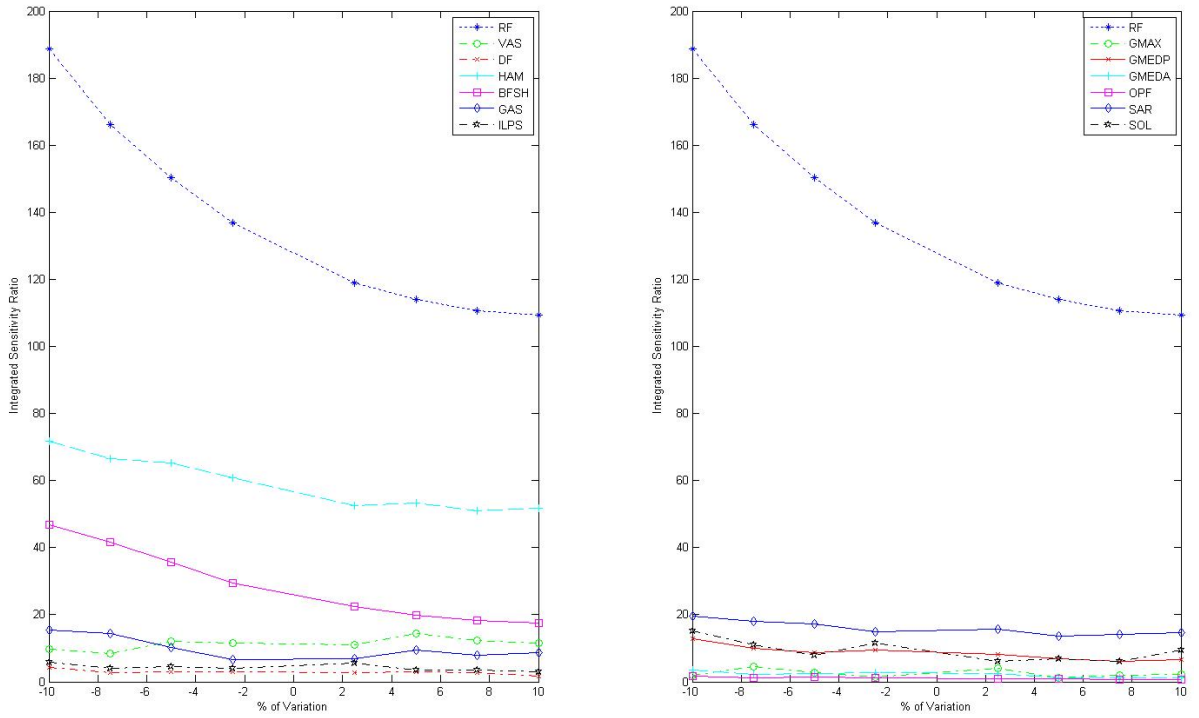
Figure 39: Integrated sensitivity ratios of the variation for RF to the parameter resting fiber length.
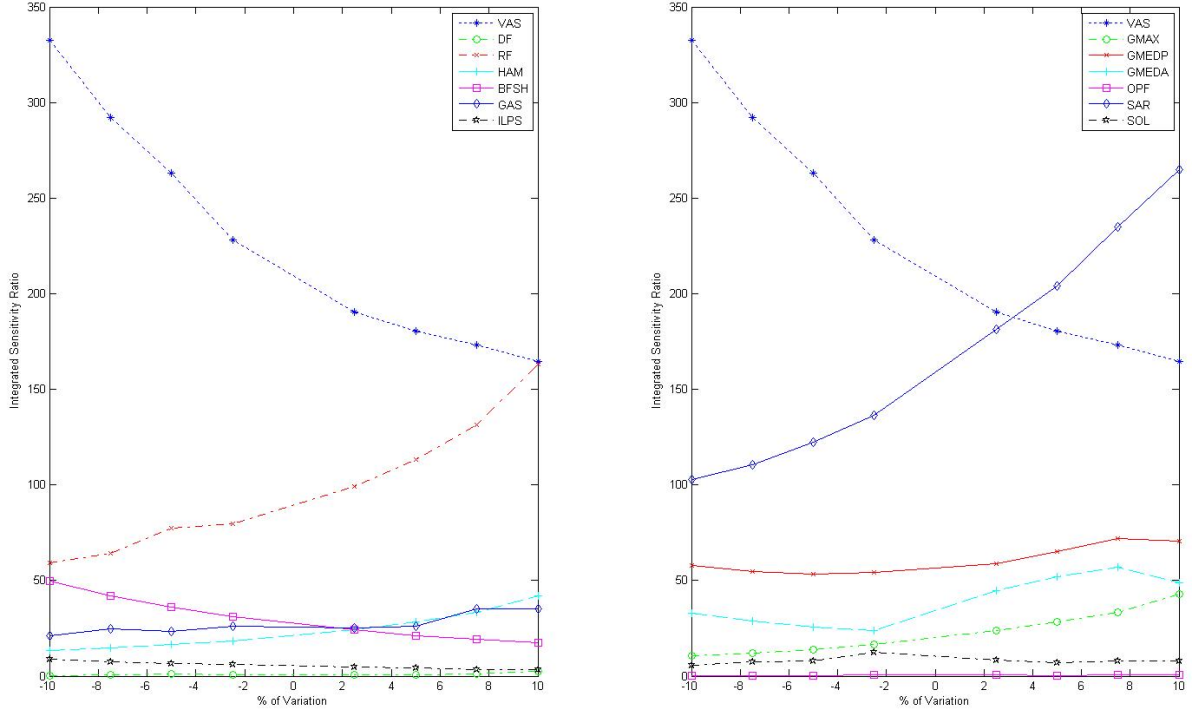
Figure 40: Integrated sensitivity ratios of the variation for VAS to the parameter resting fiber length.
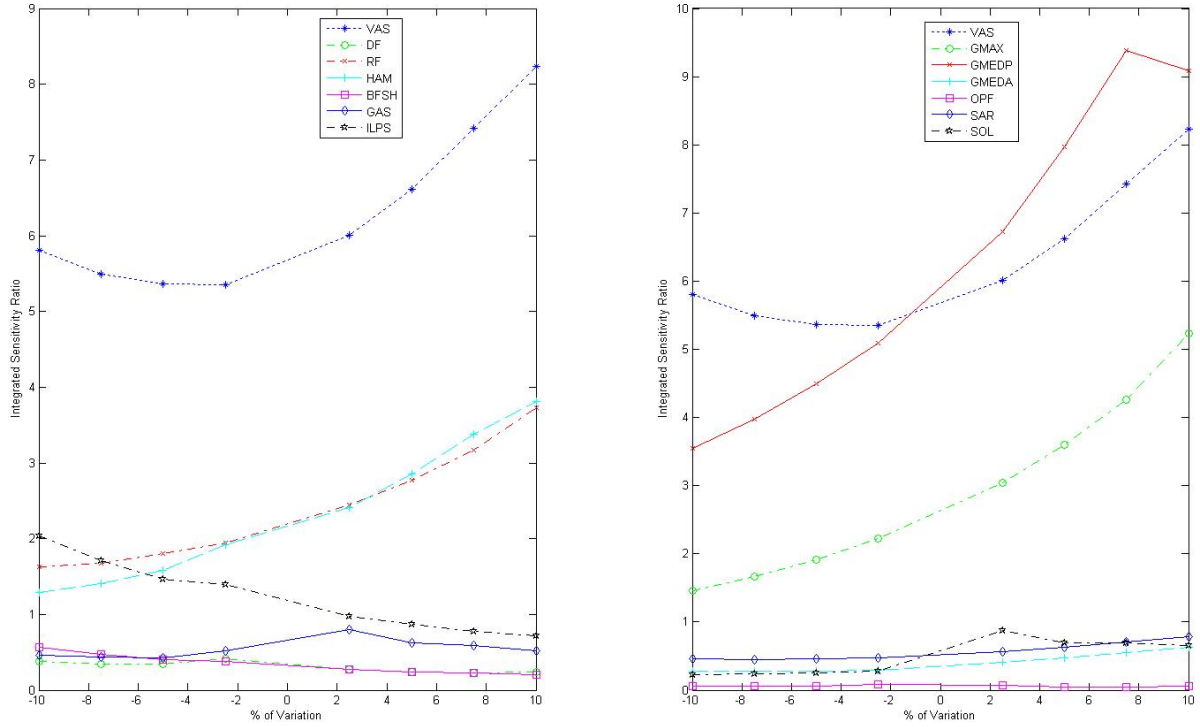
Figure 41: Integrated sensitivity ratios of the variation for VAS to the parameter resting fiber length when relevance is considered.

5.4. Sensitivity to tendon slack length

In general, the sensitivity graphs of tendon slack length l_s^t and resting fiber length l_o^m look similar. Often just the values are different but the pattern remains. Especially similar sensitivities and patterns are shown for muscles GMAXL, GMEDP and ILOPS (figures can be found in the Appendix A). Notably, muscles are most sensitive to tendon slack length. Highest integrated sensitivity ratio over the interval of variation reached by GAS was 138 387, followed by SOL with 102 907 and OPF with 96 356 (Tabels 5, 15 and 12). Once again least sensitive is GMAXM with 118.

When tendon length of GAS is reduced the sensitivity shoots up immensely, but not just for GAS itself; VAS has almost the same sensitivity. Thereafter, but still with large sensitivity values are DF and RF (Figure 139). When the relevance is considered, the distribution changes and DF becomes the most sensitive muscle (Figure 140). Sensitivity due to a variation of HAM looks different to most other panels. A peak is reached at +2.5% and RF is more affected by the disturbance of HAM than HAM itself (Figure 149). In the graph of sensitivity with relevance, muscles are most sensitive at +10% and DF and GAS reach the highest values (Figure 154). The tendon length of OPF cannot be decreased more than 7.5%, as no results are delivered by the simulation. DF and VAS are even more sensitive to this certain variation than OPF (Figure 149). However, this is not the case when relevance is considered and the DFs now reach their maximal sensitivity at 5% (Figure 154). Sensitivity of RF is small compared to the average values of this parameter and even more so when the relevance is considered. Interestingly, RF is first most sensitive to a shorting then changes to being most sensitive to a lengthening of tendon in the sensitivity of relevance (Figures 155 and 156). Due to its anatomy (i.e. very long muscle, very short tendon) SAR does not show reaction to a variation. SOL's sensitivity increases in a steep slope with shortening l_s^t and is mostly influencing DF which is similar shaped as SOL. VAS and RF become more sensitive when SOL's tendon is lengthened (Figure 154). The behavior of VAS to a variation of l_s^t is similar to the behavior when l_o^m is perturbed (Figures 161 and 133). Just the absolute values are much higher and RF highly affected (at +10% ten times greater then VAS's sensitivity).
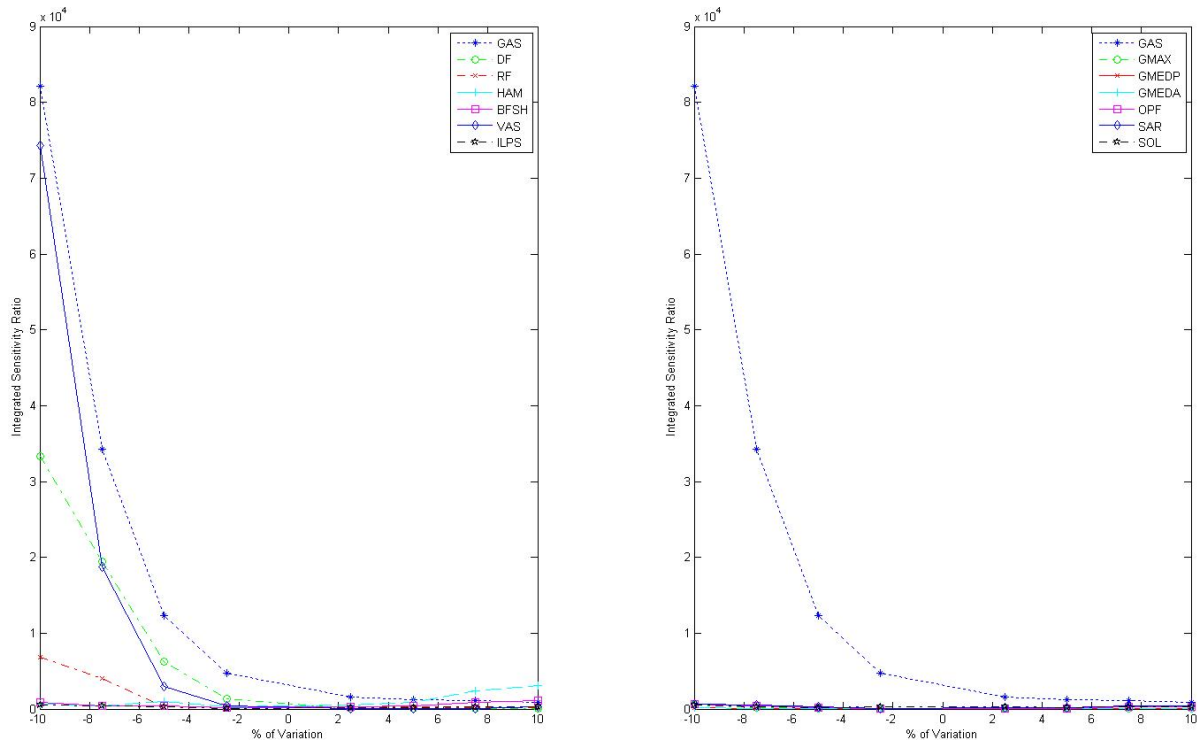
Figure 42: Integrated sensitivity ratios of the variation for GAS to the parameter tendon slack length.
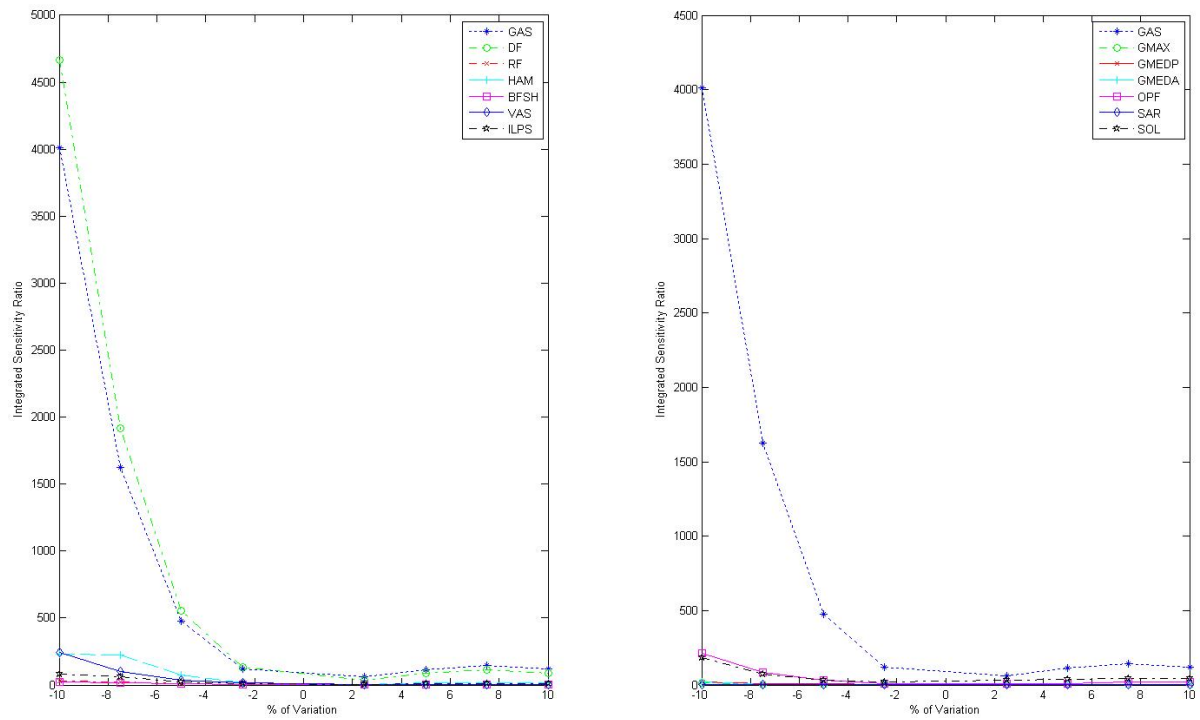
Figure 43: Integrated sensitivity ratios of the variation for GAS to the parameter tendon slack length when relevance is considered.
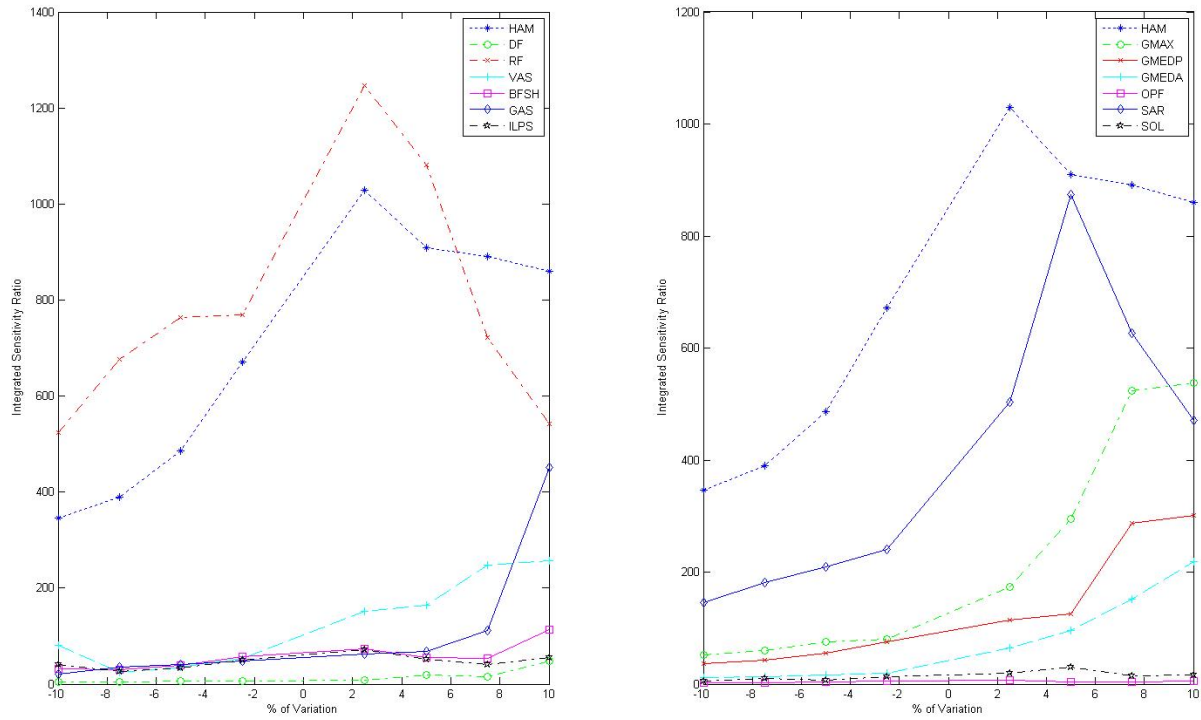
Figure 44: Integrated sensitivity ratios of the variation for HAM to the parameter tendon slack length.
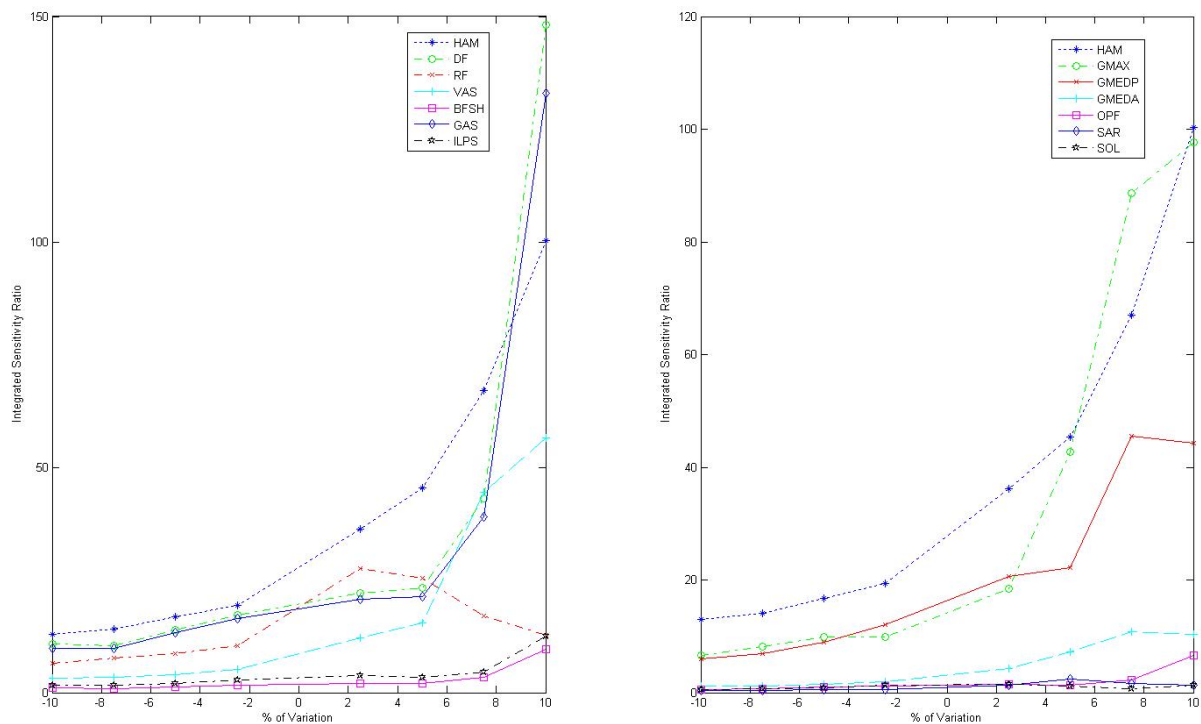
Figure 45: Integrated sensitivity ratios of the variation for HAM to the parameter tendon slack length when relevance is considered.

83
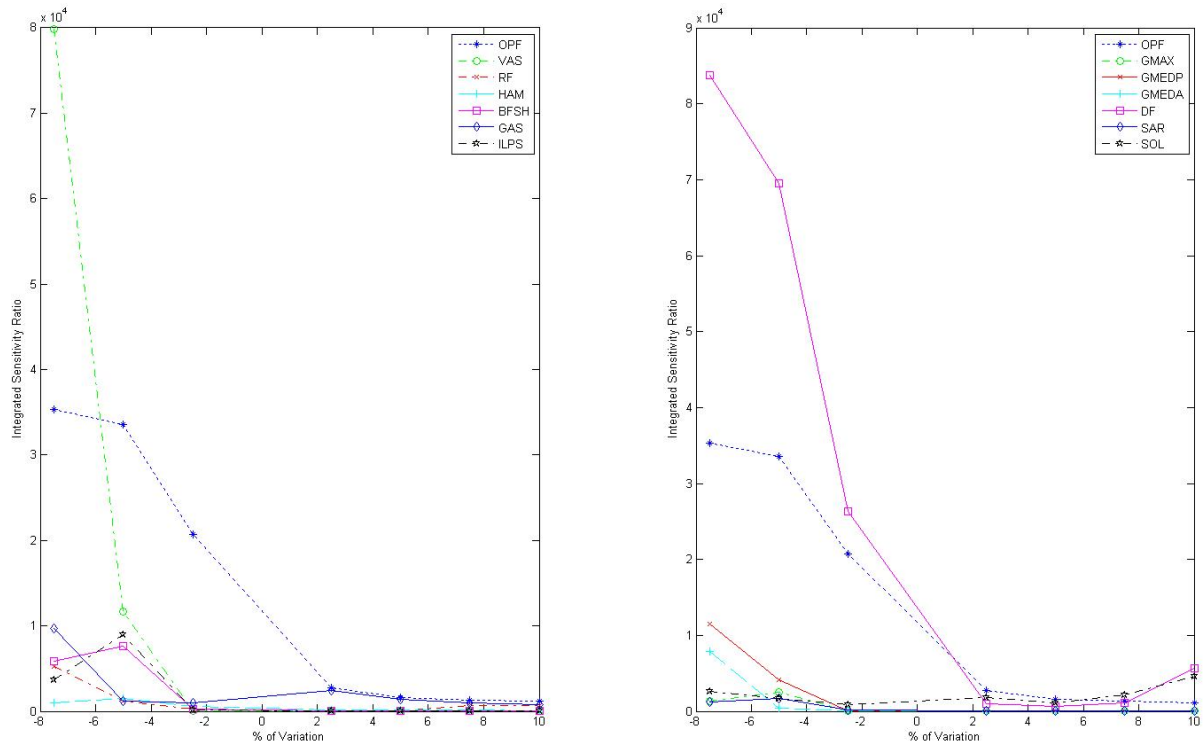
Figure 46: Integrated sensitivity ratios of the variation for OPF to the parameter tendon slack length.
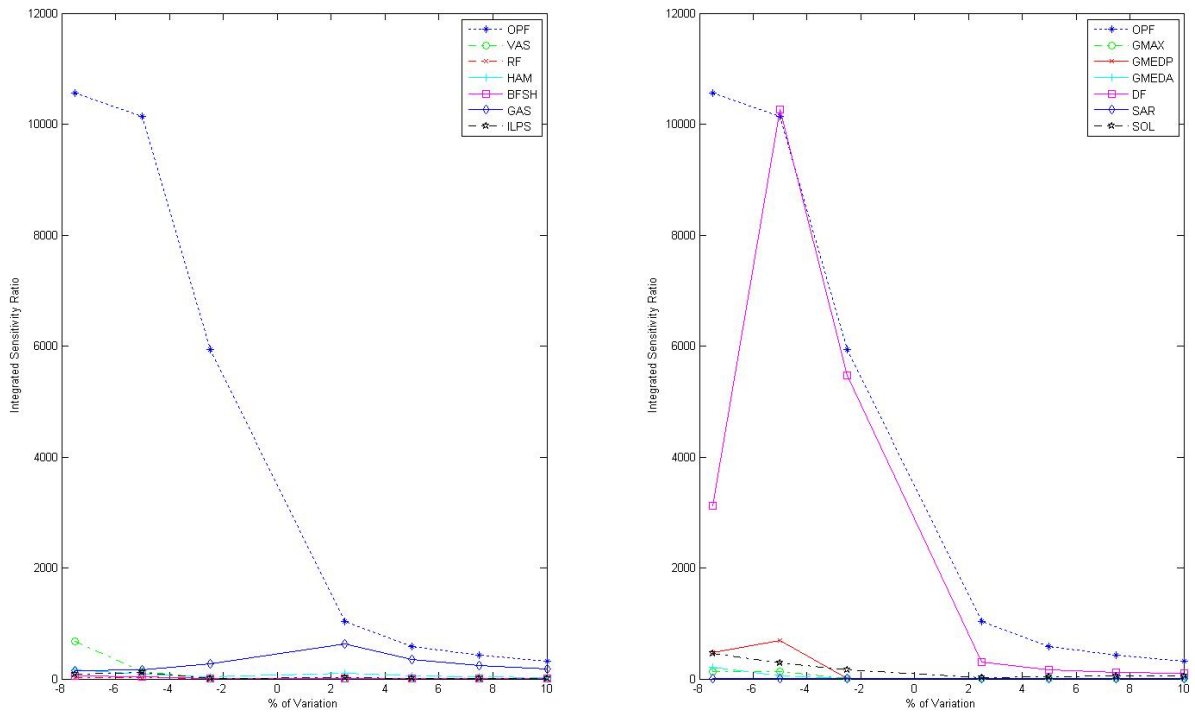
Figure 47: Sensitivity over the interval of variation for OPF to the parameter tendon slack length when relevance is considered.

84
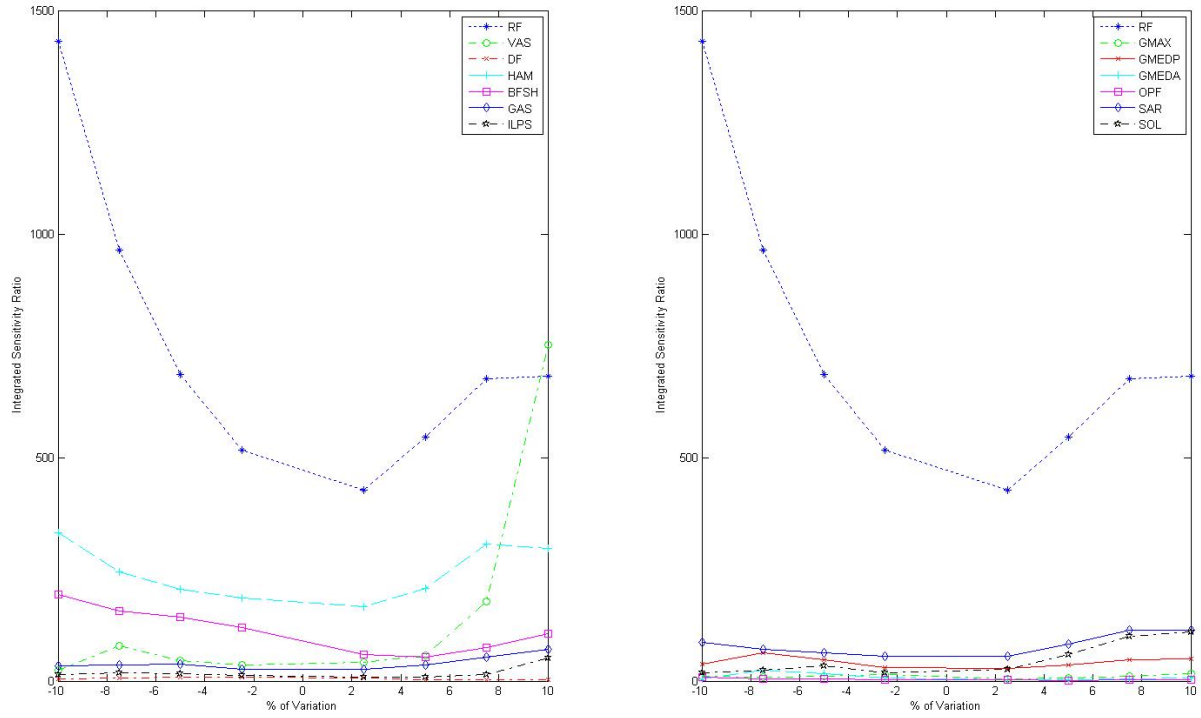
Figure 48: Integrated sensitivity ratios of the variation for RF to the parameter tendon slack length.
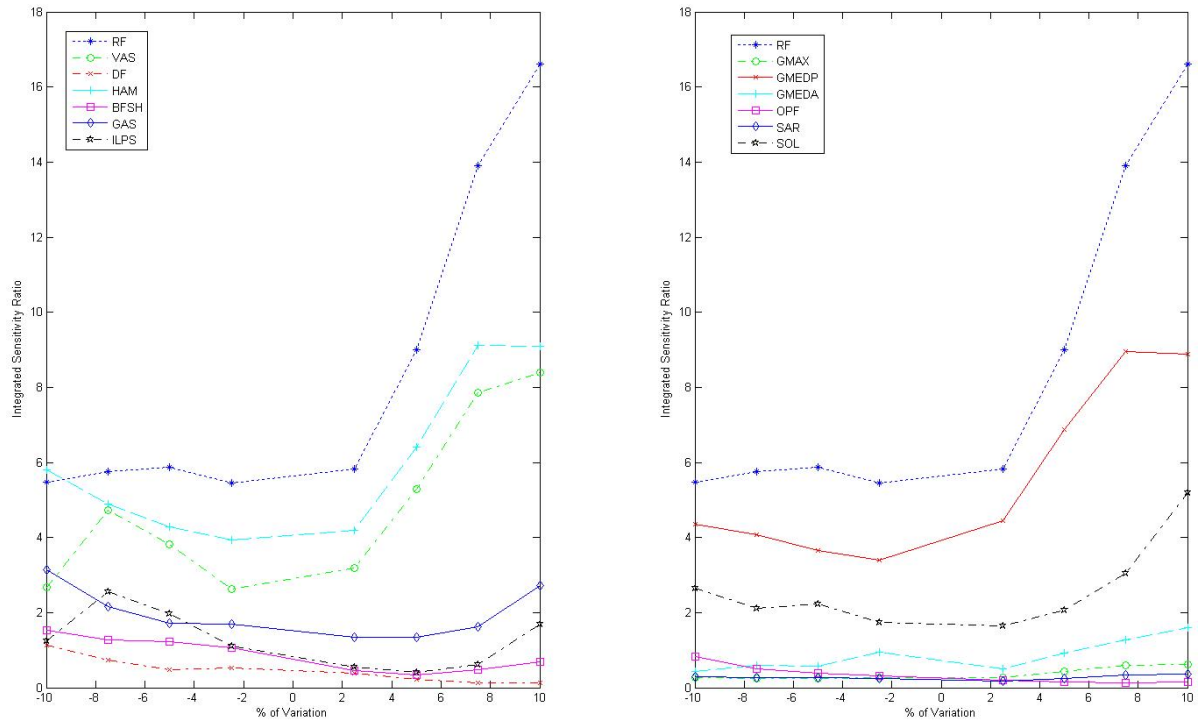
Figure 49: Integrated sensitivity ratios of the variation for RF to the parameter tendon slack length when relevance is considered.
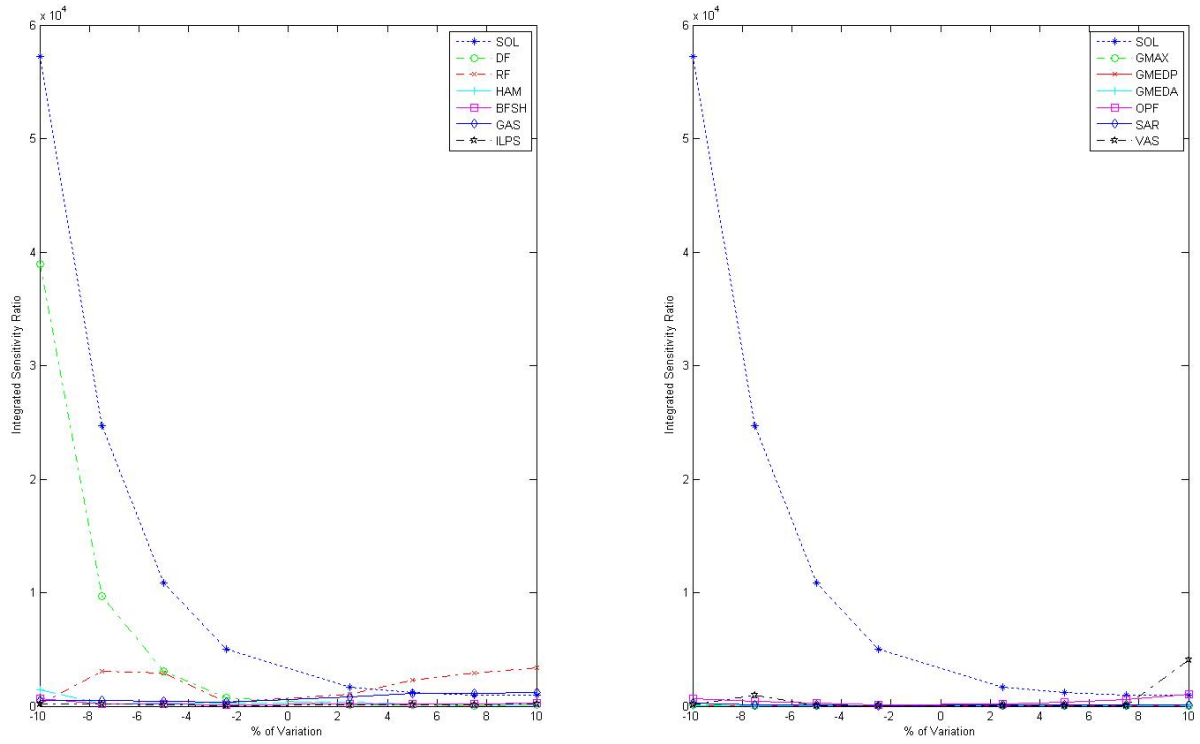
Figure 50: Integrated sensitivity ratios of the variation for SOL to the parameter tendon slack length.
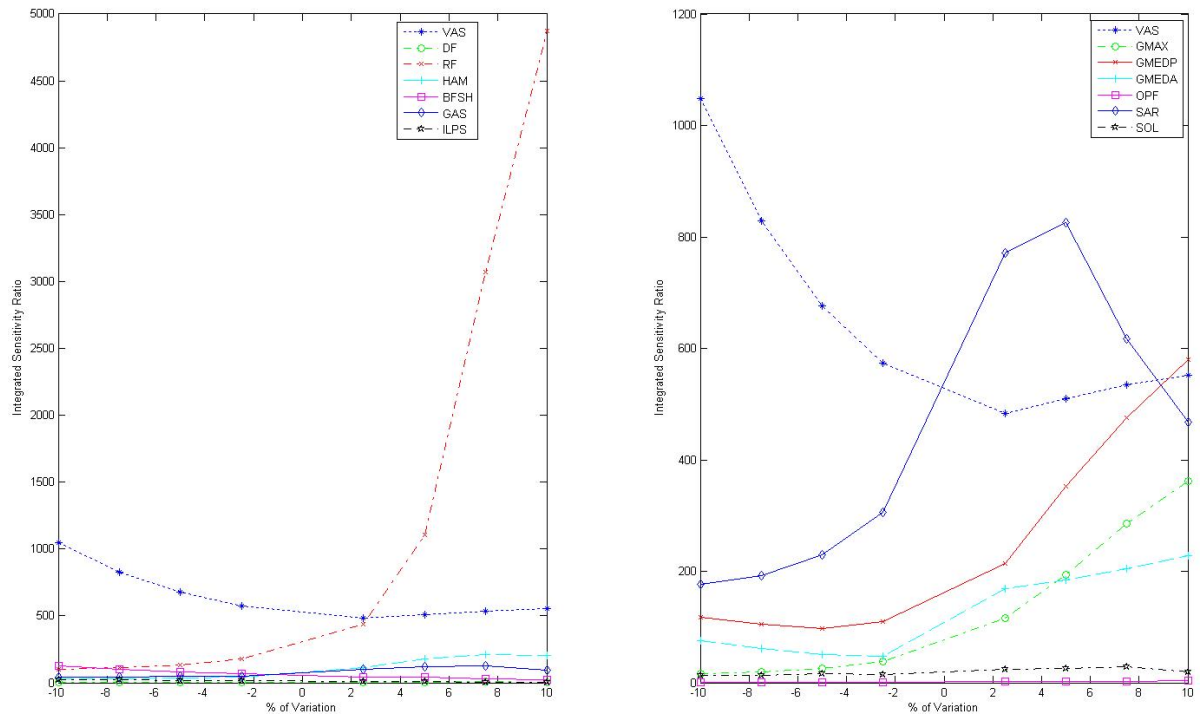
Figure 51: Integrated sensitivity ratios of the variation for VAS to the parameter tendon slack length.

5.5. Sensitivity to activation time, deactivation time and maximal shortening velocity

Although those parameters were varied by up to 50%, muscles do not show any significant sensitivity to them. The maximum value is 14 for VAS to the shortening velocity (Table 17. The graphs to the shortening velocity are bell-shaped for all muscles. They are most sensitive to a small variation, meaning the greater the change the less the relative impact on the output (Figure 167).
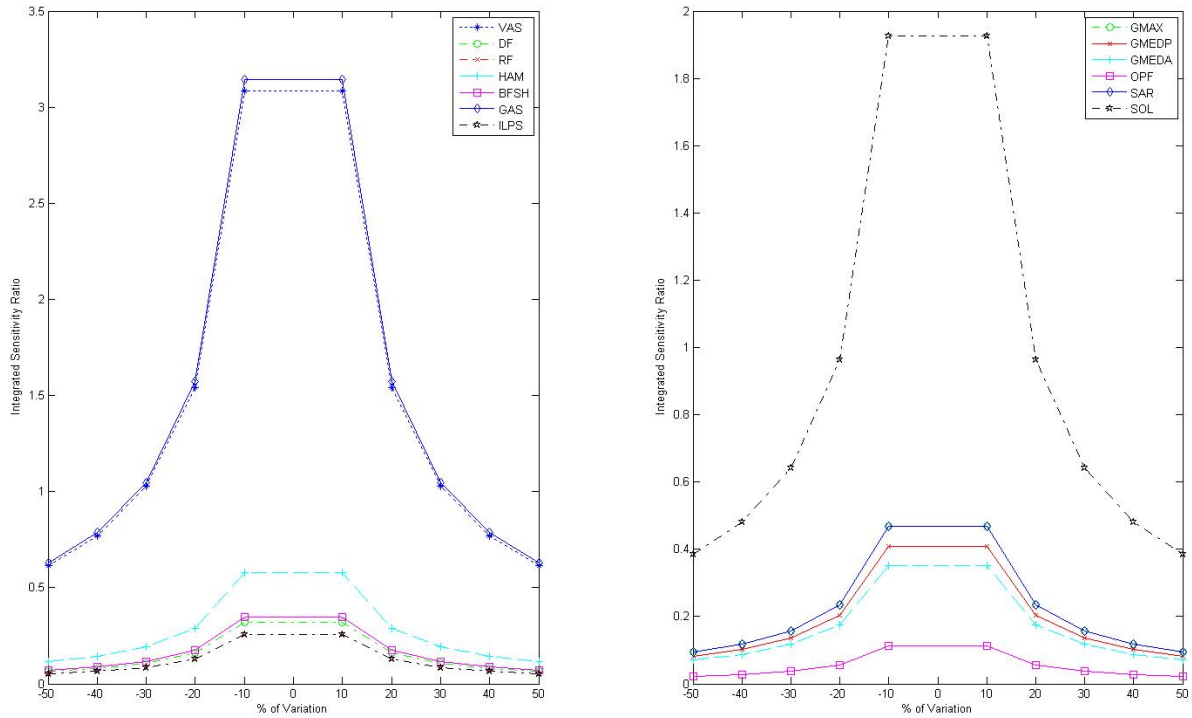
Figure 52: Integrated sensitivity ratios of the variation for maximal shortening velocity.

5.6. Summary of results

Muscles were found to be most sensitive to variation of their tendon slack length l_s^t, with the maximum value (integrated sensitivity ratio over the interval of variation) being almost 15 times greater than the maximum value reached for the resting fiber length l_o^m. The maximal sensitivity for resting fiber length was 2 times greater than for optimal muscle force F_o^m and 10.5 times greater then for the variation of the pennation angle (α).

The absolutely highest integrated sensitivity ratio over the interval of variation is reached for DF (187 991) when OPF's l_s^t is varied (Table 12). The OPF muscles are the most sensitive ones. They are most sensitive for l_o^m and third for l_s^t. When relevance is considered they are the most sensitive muscles to the parameters α, l_o^m and l_s^t, and second for F_o^m. Additionally, they are mostly influencing other muscles in the categories l_o^m and l_s^t, both with and without relevance, and α just for relevance (Summed-cross-sensitivity in Table 12). For α and F_o^m, with calculated relevance, they are third in ability to affect other muscles. Also, their significance is high, which indicates that they are actually contributing much to induce body mass acceleration when sensitivity is measured. Thus, and because the plantarflexors are the key muscle group for generating both support and progression during late stance [24], it is particularly important to set their parameters right.

The significance was generally very high for DS, mostly when the respective sensitivity values were little. Nevertheless, this muscle group should be considered since relatively small sensitivities can have a great impact because they are very active at early stance (see Figures 10 and 11). BFSH is one of the most sensitive muscles to α, F_o^m and l_o^m but only when it does not contribute much to gait which is indicated by low values of significance and sensitivity of relevance (Table 3). GAS and SOL are the other muscles being somewhat sensitive to α. Keeping in mind muscles are not very sensitive to pennation angle at all. GAS and SOL are extremely sensitive to l_s^t and also have affection on the other muscles in those parameter classes showed by a large summed-cross-sensitivity (Tables 5 and 15).

Variations of GMAXL have a general impact on other muscles, all ahead GMEDP. Values of GMEDP for the sensitivity of relevance and significance in three parameters $(F_o^m, l_o^m$ and $l_s^t)$ are considerable (Table 6). GMEDP is also the most sensitive muscle to F_o^m for integrated sensitivity ratio and summed-cross sensitivity, and this with high significance. Additionally, F_o^m is the parameter which GMEDP is absolutely (out of all parameter categories) most sensitive to.

Results emphasize that changing the parameter of one muscle can greatly influence the performance of another one. Specifically, some muscles show sensitivities which are higher than the result of the variation of their own parameter. For instance when l_s^t of GAS is varied DF (3.7 times), VAS (18.8 times), HAM (1.6 times), SAR (18.8 times) and BFSH (2.5 times) reach greater values for the sensitivity over the interval of variation than when their own parameter is changed. And SOL has almost the same, very high sensitivity value as if it was changed itself. Conversely, changing tendon slack length of SOL does not generate a high sensitivity for GAS, it has much less influence on VAS but much more on RF.

Also the variation of a parameter can cause higher sensitivity for other muscles than for the muscle which was varied; or even lead to sensitivities which are almost as high as the maximum values of sensitivity over the interval of variation in this parameter-category. Examples are the variation of F_o^m for GMEDP (Table 9) and SOL (Table 15). According to GMEDP, the sensitivity of RF would be second highest and sensitivities of GMAX and SAR third highest in this parameter-class. When SOL is investigated concerning optimal force, HAM is 1.7 and RF 2.5 as sensitive (and second in this parameter-category) as SOL. This ability to influence other muscles is reflected in the relatively high summed-cross-sensitivity.

6. Discussion

Beside the graphs of the integrated sensitivity ratios, four different types of metrics are summarizing the results of this work. The sensitivity over the interval of variation of a muscle to a parameter, which is simply the sum of the integrated sensitivity ratios of each of the eight variations. The relevance of sensitivity, meaning that this value incorporates information about the degree of activity when the instantaneous sensitivity was measured. These two metrics give similar information, but also contrast in aspects of what is focused on. The other two are significance of sensitivity and summed-cross-sensitivity.

The integrated sensitivity ratio can be seen as a qualitative approach. It gives information on a muscle's ability to react sensitively to a disturbed parameter and also on the impact this variation has on the rest of the involved muscles. Thus providing a general understanding of how muscles are connected and depend on each others performance. A high integrated sensitivity ratio reflects the muscles potential to respond to this specific parameter. The limitation of this sensitivity is that it does not provide any information about, when this sensitivity was measured. The muscle could have been very active or producing negligible forces.

If one is interested in how relevant the measured sensitivity is for the muscles' contribution to locomotion, the second sensitivity metric (sensitivity of relevance) is of more use. It is a rather quantitative approach in aspects of the actual effect of a sensitive behavior. If the muscles generate little acceleration when relatively high sensitivity is given, this value of sensitivity shrinks although the muscle is actually reacting sensitively. But anyway, a sensitivity which has no impact on the output is in practice not of much interest. The drawback of only looking at those sensitivities of relevance is that smaller, little force producing muscles tend to decrease disproportionately. This is because compared to the stronger muscle their delivered acceleration is just a little percentage of the accumulated body mass acceleration. So the information about an isolated muscle's sensitivity gets blurred in the context of the combined generation of acceleration. An example of this is the sartorius muscle. It shows relatively high sensitivity, for instance, to optimal muscle force and also is often affected by others muscles. But when focus is placed on the sensitivity of relevance none of these characteristics can be seen.

The significance of sensitivity, being the percentage of the the sensitivity of relevance to the integrated sensitivity ratio, should be used with care and just in combination with the two other metrics, as described above. It mainly reflects how much sensitivity is left when the relevance is considered, and thus how much effect this certain sensitivity has on the overall output (gait). A high significance does not necessarily mean that the associated muscle and parameter are of substantial sensitivity. Often high significance occurs when the respective sensitivities are negligible. But it gives an indication that those muscles should be considered because their impact on the body mass acceleration is greater the higher the significance. Therefore, even actuators with mediocre sensitivities can have an noticeable influence.

The presented adjustments of the data *smoothening grade* and *relevance of sensitivity*, which is output of the parameter variation and perturbation analysis, are an approach to improve limitations which were mentioned in previous studies. For instance Redl/Gföhler/Pandy [29] say that sometimes the largest instantaneous sensitivity ratios occurred during periods of the gait cycle when the respective muscle force was negligible. So, even though the integrated sensitivity ratio was high, the resultant effect on muscle force was relatively minor, as the muscle remained inactive at these times. This shall be improved by taking the *relevance of sensitivity* into account. Secondly, they take into consideration that the instantaneous sensitivity ratio was high when the muscle was inactive because this quantity was found by dividing by the value of the nominal muscle force. That problem the *smoothening grade* is meant to solve.

Komura and Nagano [23] investigated what influence the deactivation of one muscle has on the other muscles which maintain the gait motion. Their findings about muscle dependencies can be related to and agreed with the results of this work. Here it is stated that sensitivities which are induced for the other muscles when one muscles' parameter was varied, hold information about how muscles are connected and affect each other. Muscles which cross same joints and so can be expect to influence each other since they have similar functions or being antagonists confirm this (e.g. GAS and SOL or GAS, SOL, OPF and DF; see graphics in Appendix (A)). Therefore, those interdependencies shown by the sensitivity graphs should correlate to Komura and Naganos findings. For example they say when GMAX was deactivated, the hip extension moment was produced by GMED and HAM. Looking at the panels for GMAX, it clearly can be seen that HAM and GMEDP are sensitive to a perturbation of each of the parameters of GMAX. GMEDP is actually more sensitive than GMAX itself. The matrix of dependence of muscles, which can be found in the mentioned paper, suggests high influence of VAS on RF when deactivated. Also here the sensitivity graphs for VAS show high values for RF. Additionally other correlations can be found, like ILOPS having a great influence on several other muscles. However, their results as well as the findings in this work emphasize that some muscles affect performance of other actuators with quite different functions. Specifically, biarticular muscles such as HAM, GAS, RF tend to have strong influence on all muscles and joints of the leg.
Previous work (Raikova and Prilutsky [28]) has also shown that variation in one model parameter (in this case moment arm and PCSA) profoundly changes not only force magnitude of this and other muscles but also the number of active muscles in the set of muscles with active/silent states.

Evaluation of the sensitivity of muscle model to parameter perturbations indicates that the muscle output (i.e. acceleration) is extremely sensitive to l_s^t, and sensitive to l_o^m and F_o^m. Those findings are very similar to Scovil and Ronsky [31] although they evaluated a muscle models output and not sensitivities of single muscles. And also in contrast, the present analysis quantifies the sensitivity over the whole stance phase of walking and not just the impact of a perturbed input value on an output value. Same

findings about muscles' general sensitivity to those parameters are reported by Redl et al. [29]. For instance they found SOL being the most sensitive muscle to l_s^t and the integrated sensitivity ratios 11-38 times greater for changes to l_s^t than to l_o^m. Those results are confirmed in this survey. SOL is the second most sensitive actuator, only GAS exceeds but Redl et al. did not consider this muscle. The integrated sensitivity ratios over the interval of variation of l_s^t are 15 times greater than the ones for l_o^m, which is perfectly consistent with their results. However, GAS and SOL produce the majority of the forward acceleration during the second half of stance; and the second peak of vertical acceleration was large due to those two muscles [24]. Additionally, across all muscles, SOL (followed by GAS) store and recover the largest amount of elastic energy [27]. Therefore it is suggested to choose parameters for those muscles with special care, since they play an important roll in several aspects of walking.

Only Redl et al's [29] findings about VAS differ significantly; here it turned out to be much less sensitive than they report. This is interesting since the VASs are the strongest muscle group and are responsible for significant parts of acceleration and deceleration during stance [24]. But in the present work VAS was found to be affected much by other muscles (e.g. variationm of l_s^t of GAS and OPF, variation l_o^m of ILOPS).

As third parameter, Redl et al. [29] investigated the PCSA (physiological cross section area) which is the equivalent to the optimal muscle force. In contrast to this analysis it was found that the parameter had relatively small effect on the integrated sensitivity ratio. Raikova and Prilutsky [28] on the other hand say that although sensitivity of the optimal force to changes in PCSAs was smaller than to moment arms, the effects were also rather large for some muscles.

The activation and deactivation times τ_A and τ_D did not cause any reaction, even though they were changed by 50%. This insensitivity was also reported by Scovil and Ronsky [31], which was similar to several other studies.

In Redl et al. [29] the authors state that they chose to include SAR even though it does not develop much force during normal walking, because of the virtue of its geometry. Similar applies for HAM and ILOPS. In Arnold et al. [7] this high potential of SAR is shown. When hip and knee acceleration per unit force are calculated, SAR reaches the highest values. That high potential to significantly contribute to locomotion is also reflected in the findings of this work. SAR is sensitive to optimal muscle force. Because of its relatively large moment arm, small changes of the muscle force cause a notable change of the joint accelerations.

In the figure of the instantaneous sensitivity ratios (Figure 13), there is also a panel of the body mass acceleration which does not show any remarkable response to the variation of a muscle. This is because the movement simulations are able to compensate for changes in muscle parameters better than the muscle model alone. The combined system can react by internal or damping effects, by reduction of muscle forces and velocity

changes due to interactions and by evaluation of movement over time [31]. Therefore, those sensitivities to the global muscle-model output were not further considered.

Redl et al. [29] who investigated the sensitivity of four muscles (SOL, VAS, GMEDP, SAR) found an interesting feature. The sensitivity of muscle force to changes in tendon rest length (l_s^t) and resting fiber length (l_o^m) was governed by the ratio of these parameters. When the ratio of l_s^t to l_o^m was greater than 1, muscle force estimates were most sensitive to changes in tendon lengths. Conversely, when this ratio was less than one, the calculated values of muscle force were most sensitive to fiber length.

This result is understandable when one considers the difference between the force response of a compliant actuator ($l_s^t/l_o^m > 1$) and that of a stiff one ($l_s^t/l_o^m < 1$). Because compliant actuators have longer tendons than muscle fibers, their force response is governed by the force-length curve of tendon; conversely, stiff actuators with shorter tendons than muscle fibers have a force response that is governed by the force-length curve of muscle.

Actuator	l_s^t/l_o^m	Sensitivity l_s^t/l_o^m	Sensitivity with relevance l_s^t/l_o^m
BFSH	0.29	0.27	0.26
DF	2.73	3.7	4.9
GAS	6.58	64.0	105.9
GMAXL	0.73	1.5	1.4
GMAXM	0.78	1.01	1.0
GMEDA	0.84	1.09	1.18
GMEDP	0.75	0.86	0.85
HAM	3.12	5.0	8.67
ILPSO	1.3	1.3	1.24
OPF	7.44	10.3	10.8
RF	2.8	5.4	4.86
SAR	0.069	0.08	0.086
SOL	5.08	34.2	23.2
VAS	1.61	2.85	5.4

Table 18: Ratios of tendon slack length and resting fiber length compared to the ratios of the integrated sensitivity over the interval of variation of l_s^t and l_o^m, respectively sensitivity with applied relevance. Illustrating that if $l_s^t/l_o^m < 1$ muscle is more sensitive to a variation of resting fiber length and if $l_s^t/l_o^m > 1$ sensitivity to tendon slack length is greater.

The findings in this work reinforce this relation. Table 18 includes ratios of the resting fiber length and tendon slack length as well as the ratios of the integrated sensitivity summed over the interval of variation of l_s^t and l_o^m. The higher the ratio of l_s^t/l_o^m, the more (nonlinear) the sensitivity to tendon length differs from the sensitivity of fiber length (i.e., GAS, OPF and SOL). Just one muscle (GMAXL) does not fulfill this theory. This one should be more sensitive to the fiber length but in fact is slightly more sensitive to tendon length. GMAXM and GEMDA show equal sensitivity to the two parameters although their fiber length is slightly longer than their tendon length. This is an indication that this rule of governed sensitivity might become less strong for ratios being close to 1.

Limitation of this study is that it only covers normal gait, which has to be kept in mind when results are applied. Muscle function is strongly task-dependent, as the pattern of force development changes and so results of sensitivity analysis are likely to change. Scovil and Ronsky [31] found different results for parameter sensitivity of forward simulations of running and walking. Neptune et al. [27] investigated and identified the functional and energetic adaptations in individual muscles in response to different walking speeds. They found that some muscles change more than others to increasing speed (SOL and GMAX in stance and tibialis anterior, ILPS and HAM in swing).

Even though many of the most relevant muscles for gait have been considered in this sensitivity analysis, there are more incorporated in the used model and even more in reality. The range of variation was just $\pm 10\%$ and in only one case the simulation could not deliver a result. It might give more information and a better understanding of muscle's sensitive characteristic and interdependencies when the interval of variation is exceeded and maximal variation which still can be realized in the simulation is reached.

7. Conclusion

The main purpose of this diploma thesis was to conduct a sensitivity analysis to muscle describing parameters in an inverse simulation of human gait. Resultant body mass accelerations were calculated and it was investigated how much they changed compared to when nominal parameter values were used. This analysis is time dependent; at discrete time steps of the stance phase of the gait cycle, sensitivity was evaluated.

Compared to other studies, a relatively large number of leg-muscles was considered in this sensitivity analysis. In the study not only the effect on the perturbed muscles is illustrated but also the sensitive reaction of all the other muscles which were taken into account in the analysis. For those who want to use the results of this investigation, panels of graphs and tables of data are provided (Tables 3 to 17 and figures in sections 5 and A). Those panels present graphically the value of the integrated sensitivity at a percentage of variation. They hold information about how much sensitivity changes to decreasing and increasing parameters. There is a graphic for each muscle which was varied and each parameter incorporating both the graphs for the muscle whose parameter was disturbed and the 12 other muscles (Figures in section A). There is a table for each muscle including the metrics sensitivity over the interval of variation (sum of the integrated sensitivity ratios from all variations), sensitivity of relevance (a time-dependent contribution to body mass acceleration is considered compared), significance of sensitivity (percentage of sensitivity of relevance to sensitivity) and summed-cross sensitivity (summed sensitivity of all muscles but the varied one), which are all to find in section 5.

The findings reinforce that accurate parameter setting is crucial for reliable musculoskeletal models. In particular, this is most important for tendon slack length but also for resting fiber length and optimal muscle force. Unfortunately, *in vivo* measurements of the parameters are difficult to carry out and dissection of cadaver specimens provide unsatisfactory results. It is difficult to distinguish the aponeurotic part of tendon from muscle belly and tissue might be stretched when measured post-mortem. Also, settings of parameters might change for different groups of people (e.g. state of health and training, age etc.). When better methods to estimate parameters are developed , the simulation of gait can be improved substantially and more accurate predictions of force and acceleration values as well as patterns can be done.

References

[1] Anderson F.C. 1999: *A dynamic optimization solution for an complete cycle of normal gait* Ph.D. Thesis, The University of Taxas, Austin.

[2] Anderson F.C., Pandy M.G. 1999: *A dynamic solution for vertical jumping in three dimensions* Computer Methods in Biomechanics and Biomedical Engineering, 2, 201-203.

[3] Anderson F.C., Pandy M.G. 2001: *Static and dynamic optimization solutions for gait are practically equivalent* Journal of Biomechanics 34, 153-161.

[4] Anderson F.C., Pandy M.G. 2001: *Dynamic Optimization of Human Walking* Journal of Biomechanical Engineering, 123, 381-390.

[5] Anderson F.C., Goldberg S.R., Pandy M.G., Delp S.L. 2004: *Contribution of muscle force and toe-off kinematics to peak knee flexion during the swing phase of normal gait: an induced position analysis* Journal of biomechanics 37, 731-737.

[6] Ajay S., Pandy M.G., 2007: *A neuromusculoskeletal tracking method for estimating individual muscle forces in human movement* Journal of Biomechanics 40, 356-366.

[7] Arnold A.S., Anderson F.C., Pandy M.G., Delp S.L. 2005: *Muscular contributions to hip and knee extension during the single limb stance of normal gait: a framework for investigating the causes of crouch gait* Journal of Biomechanics 38, 2181-2189.

[8] Avrachenkov K.E. 1999: *Analytic Perturbation Theory and its Applications* Thesis Faculty of Information Technology, University of South Australia

[9] Bae T.S., Choi K., Hong D., Mun M. 2007: *Dynamic analysis of above-knee amputee gait* Journal of Biomechanics 22, 557-566.

[10] Bassett D. N., Gardinier J.D., Manal K.T., Buchanan T. S. 2006: *Estimation of Muscle Forces About the Ankle During Gait in Healthy and Neurologically Impaired Subjects* Chapter 12, Master Thesis, University of Delaware, 317-340.

[11] Brenner R. 1995: *Methoden zur Monte Carlo Simulation und deren Implementierung* Diplomarbeit TU-Wien, 15-17.

[12] Chumanov E., Heiderscheit B., Thelen D. 2007: *The effect of speed and influence of individual muscle on hamstring mechanics during the swing phase of sprinting* Journal of biomechanics.

[13] Delp S.L., Loan J.P., Hoy M.G., Zajac F.E., Topp E.L, Rosen J.M. 1990: *An interactive graphics-based model of the lower extremity to study orthopaedic surgical procedures* IEEE Transactions on Biomedical Engineering, 37, 757-767.

[14] Ermakov S. M. 1975: *Die Monte-Carlo-Methode und verwandte Fragen* Oldenburg Verlag München Wien, 15.

[15] Forbes B.J. 2004: *Acoustical Klein-Gordon equations: A Time-Indipendent Perturbation Analysis* Physical Review Letters, Vol 93, Num 5.

[16] Gradl R. 1997: *Optimierung in diskreter Simulation inklusive linearem Suchen, Monte-Carlo Methode und genetischen Algorithmen bei GPSS/H, Micro Saint und Simple* Diplomarbeit TU-Wien, 35.

[17] Halton J. H. 1970: Siam.Rev., Vol 12, 1.

[18] Haeusle T. 1994: *Parallelisierung von Verfahren zur Analyse der Sensitivität von Differentialgleichungen bezüglich eines Parameters sowie deren Implementierung im Simulationssystem MOSIS* Diplomarbeit TU-Wien, 3-36.

[19] Heidergott B. 1998: *Optimisation of a single-component maintenance system: A smoothed perturbation analysis approach* European Journal of operational research.

[20] Hicks J.L., Schwartz M.H., Arnold A.S., Delp S.L. 2008: *Crouched postures reduce the capacity of muscles to extend the hip and knee during the single-limb stance phase of gait* Journal of Biomechanics, 970-967.

[21] Jinha A., Ait-Haddou R., Binding P., Herzog W. 2006: *Antagonistic activity of one-joint muscles in three-dimensions using non-linear optimisation* Mathematical Biosciences 202, 57-70.

[22] Kollmitzer L. 1996: *Quantitative Gait Analysis* Dissertation, TU-Wien, 3-8.

[23] Komura T., Nagano A. 2004: *Evaluation of the influence of muscle deactivation on other muscles and joints during gait motion* Journal of Biomechanics 37, 425-436.

[24] Liu M., Anderson F.C., Pandy M. G., Delp S.L. 2006: *Muscles that support the body also modulate forward progression during walking* Journal of Biomechanics 39, 2623-2630.

[25] Martin R. at al. 2003: *Sensitivitätsberechnungen mit adjungierten Green'schen Funktionen für eine mehrdimensionale TEM-Inversion auf Linux-Clustern* 20. Kolloquium Elektromagnetische Tiefenforschung, Königsstein, 261.

[26] Neptune R.R., Kautza S.A., Zajac F.E. 2001: *Contributions of the individual ankle plantar flexors to support forward progression and swing initiation during walking* Journal of Biomechanics 34, 1387-1398.

[27] Neptune R.R., et al. 2007: *The effect of walking speed on muscle function and mechanical energetics*, GaitPosture, doi:10.1016/j.gaitpost.2007.11.004.

[28] Raikova R., Prilutsky B. 2001: *Sensitivity of predicted muscle forces to parameters of the optimization-based human leg model revealed by analytical and numerical analyses* Journal of Biomechanics 34, 1243-1255.

[29] Redl C., Gföhler M., Pandy M. 2007: *Sensitivity of muscle force estimates to variations in muscle tendon properties* Human Movement Science 26, 306-319.

[30] Redl C. 2005: *Eine Sensitivitätsanalyse von Muskelkräften in einem inversen Gangmodell* Diplomarbeit TU-Wien.

[31] Scovil C. Y., Ronsky J. L. 2006: *Sensitivity of a Hill-based muscle model to perturbations in model parameters* Journal of Biomechanics, 39, 2055-2063.

[32] Thelen D., Chumanov E., Best T., Swanson S., Heiderscheit B. 2005: *Simulation of Biceps Femoris Musculotendon Mechanics during the Swing Phase of Sprinting* Med. Sci. Sports Exerc., Vol. 37, No. 11, 1931-1938.

[33] Udvary L. 1996: *Monte Carlo Methode in der Elektronenstrahlmikroanalyse* Diplomarbeit TU-Wien, 2.

[34] Zajac, F.E. 1989: *Muscle and tendon: properties, models, scaling, and application to biomechanics and motor control* CRC Critical Reviews in Biomedical Engng, 17, 359-411.

[35] Zajac, F.E. 2002: *Understanding muscle coordination of the human leg with dynamical simulations* Journal of Biomechanics 35, 1011-1018.

List of Figures

List of Tables

A. Appendix

- Graphs of sensitivity to pennation angle

- Graphs of sensitivity to optimal muscle force

- Graphs of sensitivity to resting fiber length

- Graphs of sensitivity to tendon slack length

- Graphs of sensitivity to activation time, deactivation time and shortening velocity

Figure 53: Sensitivity for BFSH to pennation angle.

Figure 54: Sensitivity of relevance for BFSH to pennation angle.

Figure 55: Sensitivity for DF to pennation angle.
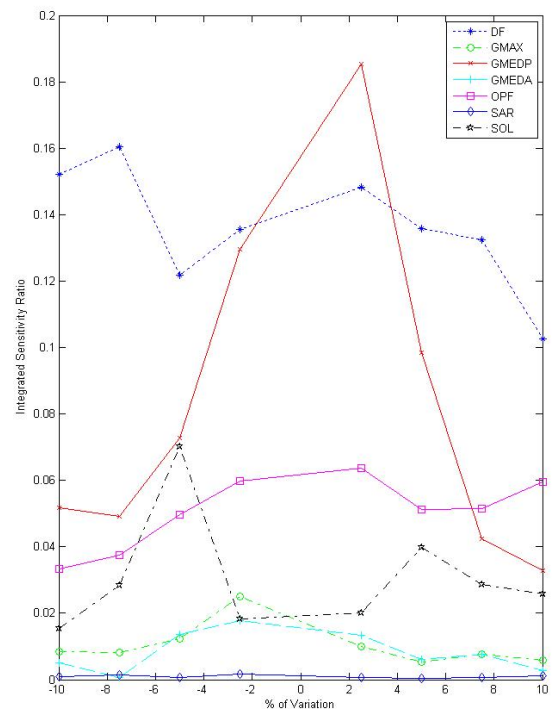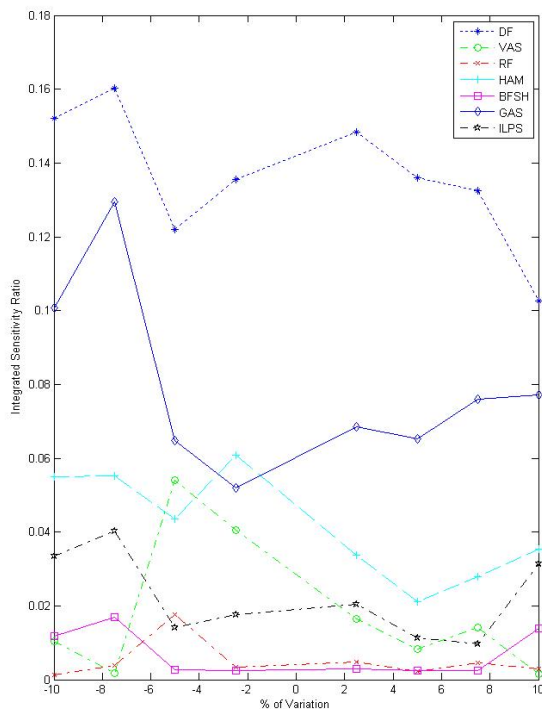
Figure 56: Sensitivity of relevance for DF to pennation angle.

108
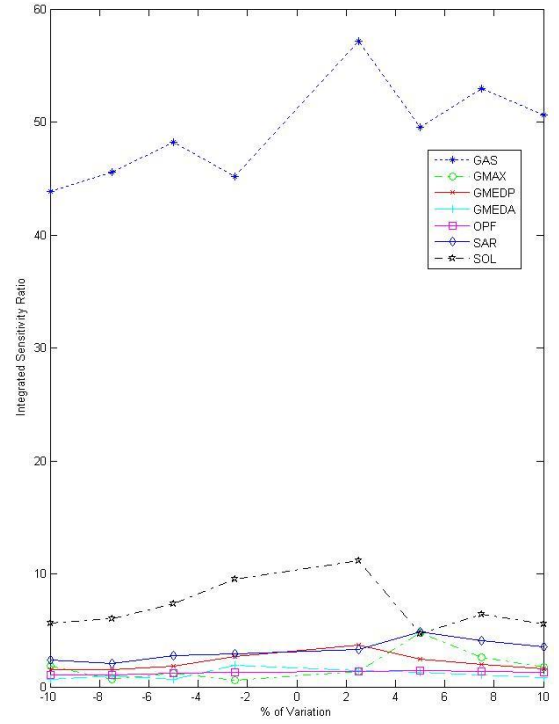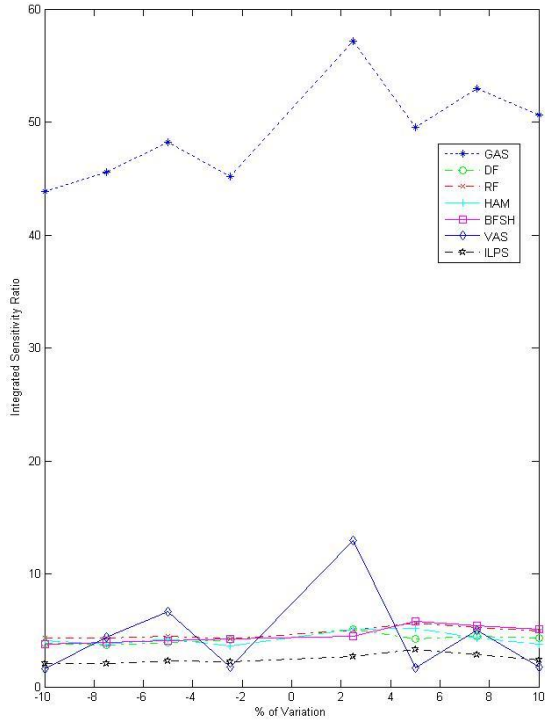
Figure 57: Sensitivity for GAS to pennation angle.
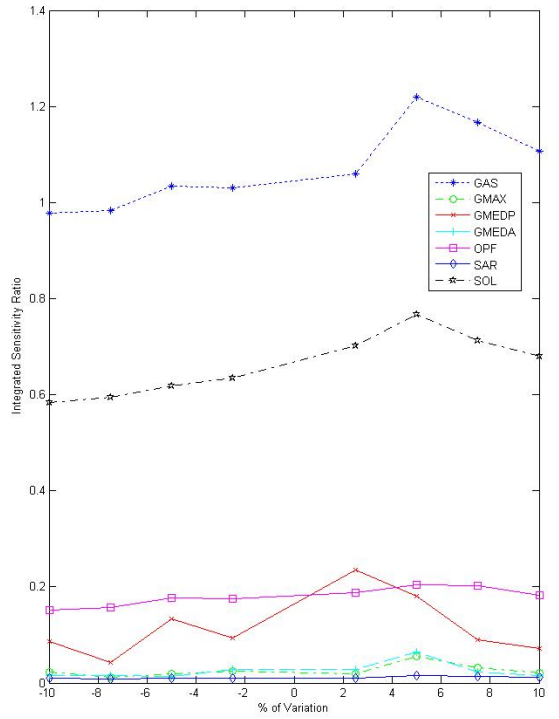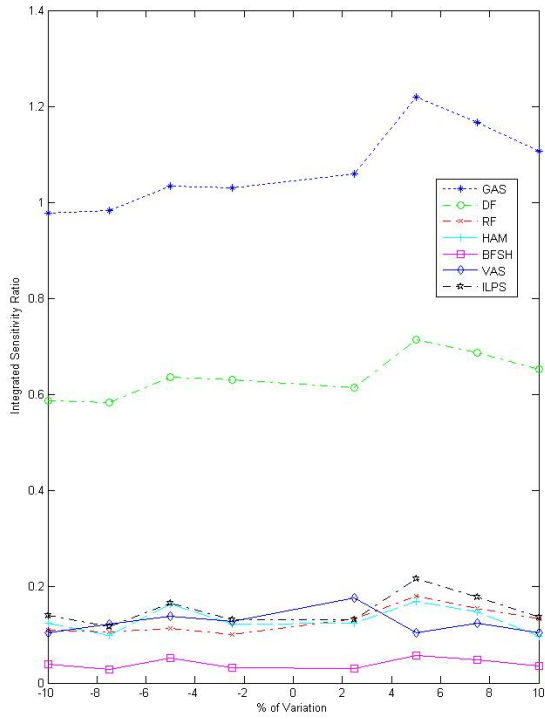
Figure 58: Sensitivity of relevance for GAS to pennation angle.
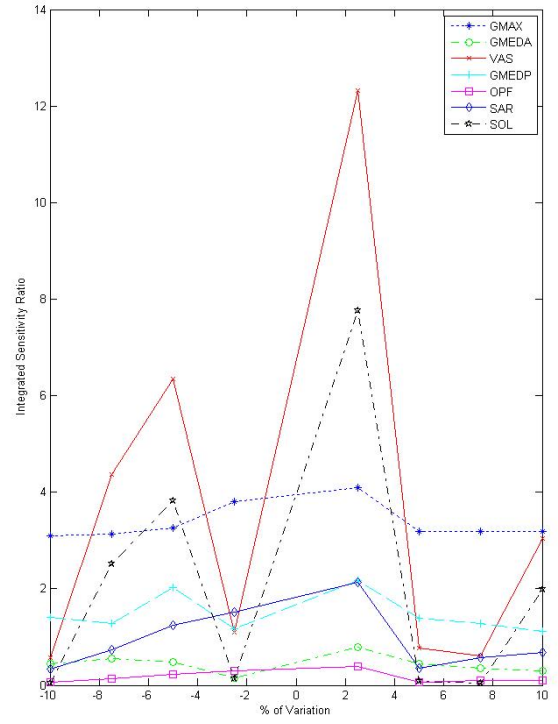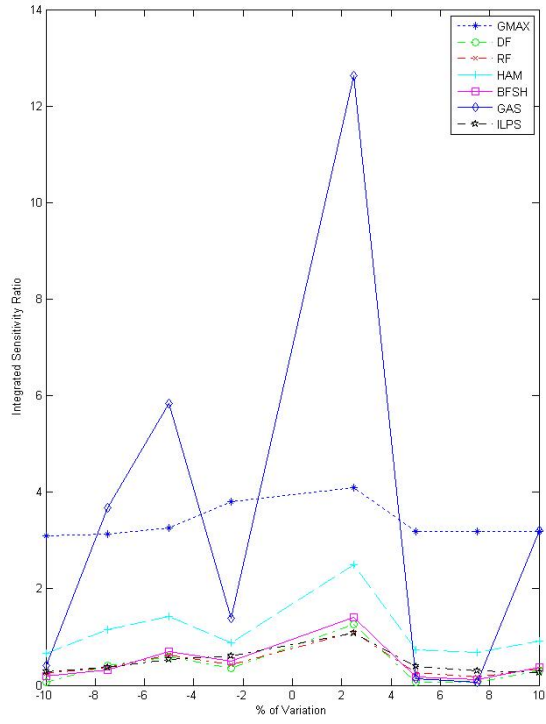
Figure 59: Sensitivity for GMAXL to pennation angle.
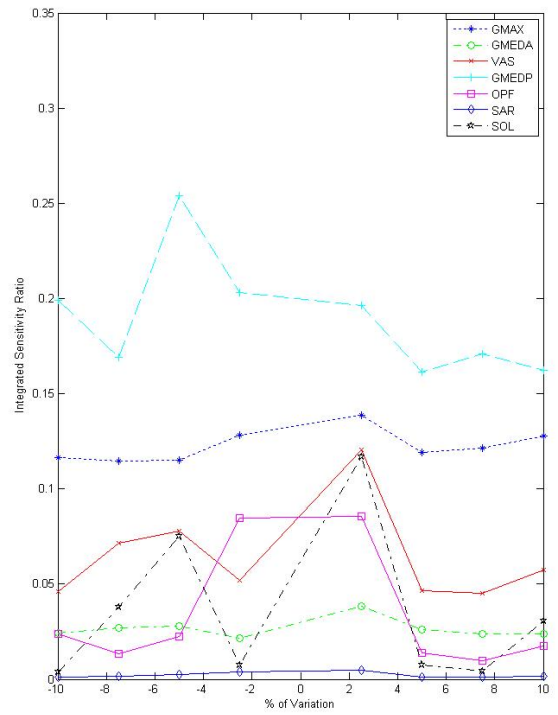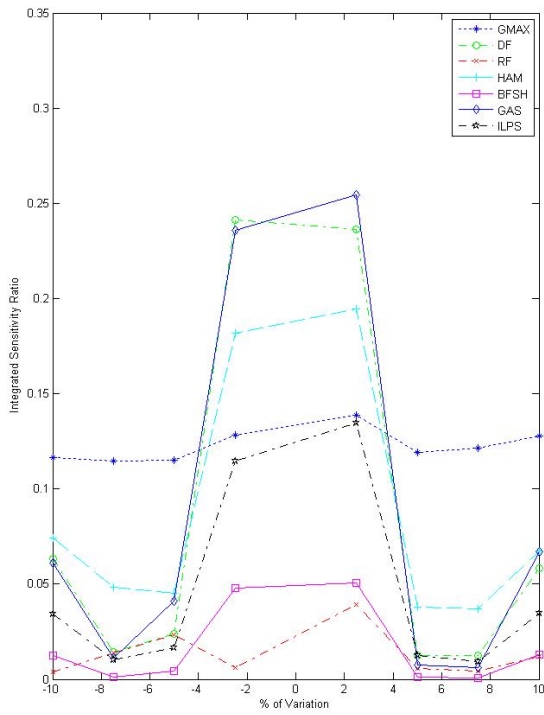
Figure 60: Sensitivity of relevance for GMAXL to pennation angle.
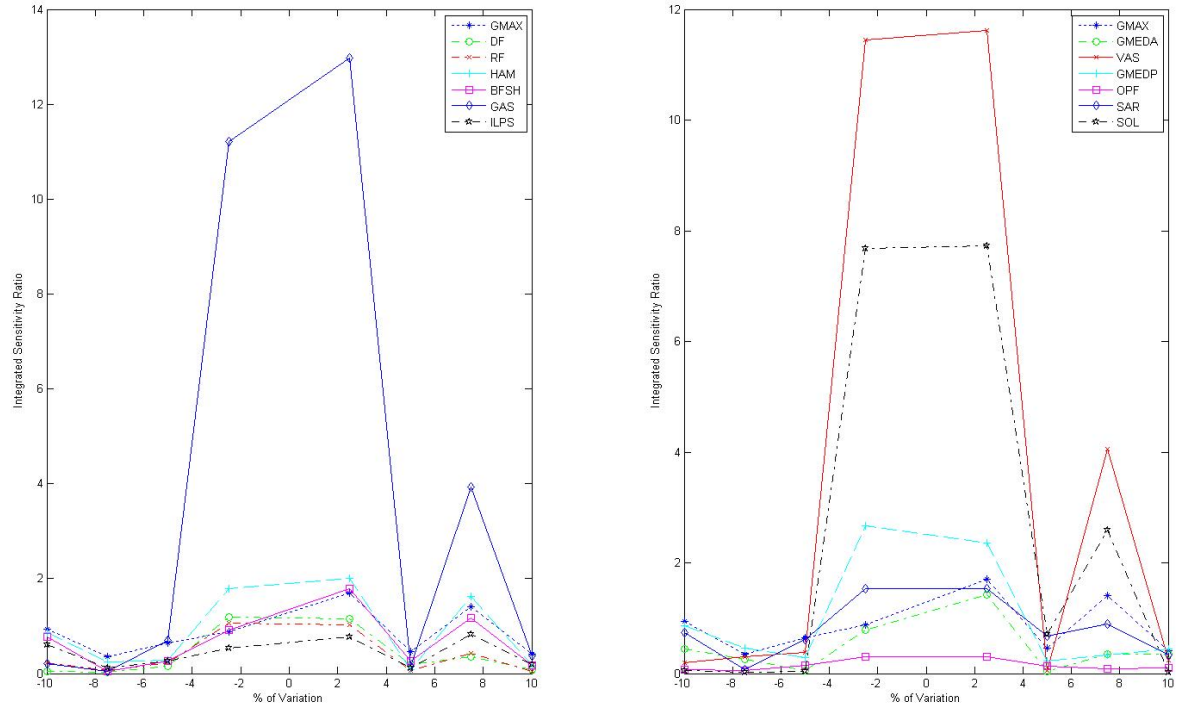
Figure 61: Sensitivity for GMAXM to the parameter alpha.
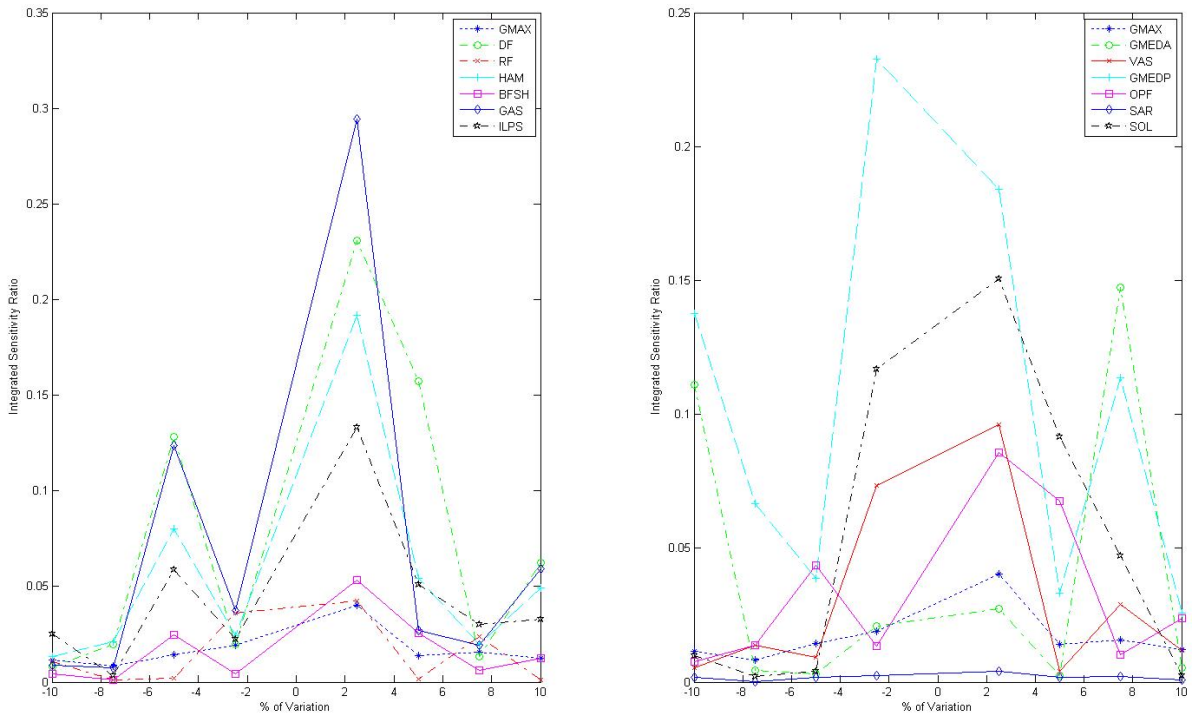
Figure 62: Sensitivity of relevance for GMAXM to pennation angle.
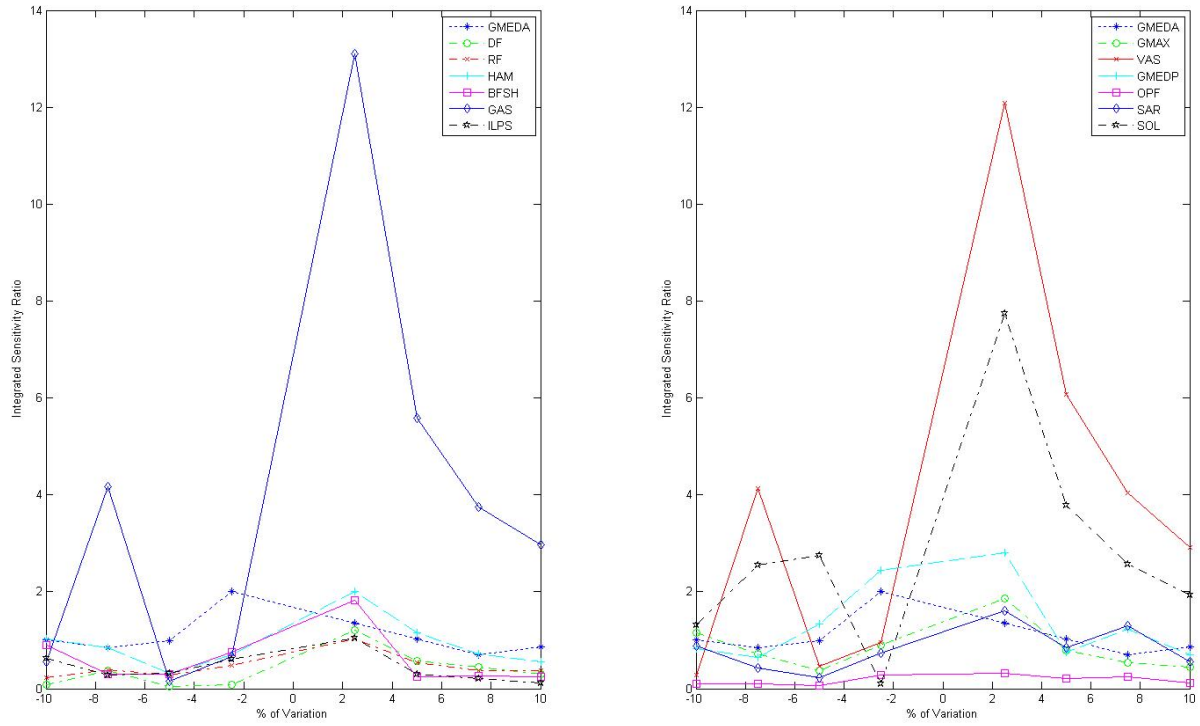
Figure 63: Sensitivity for GMEDA to pennation angle.
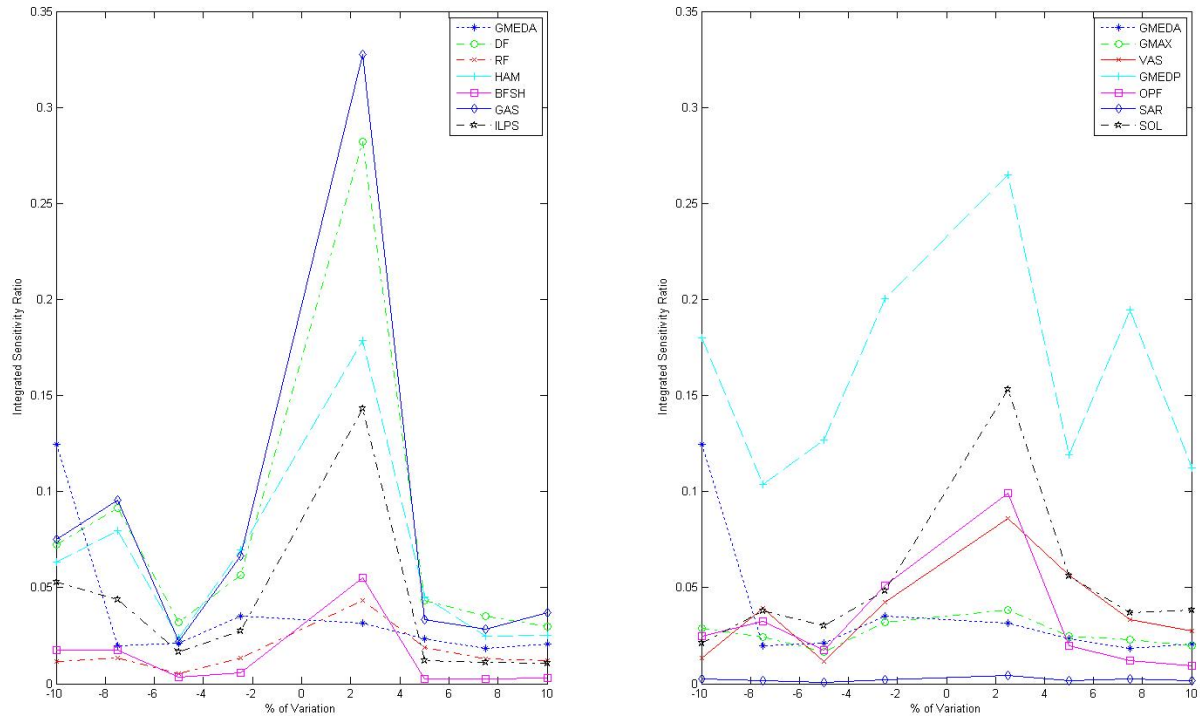
Figure 64: Sensitivity of relevance for GMEDA to pennation angle.
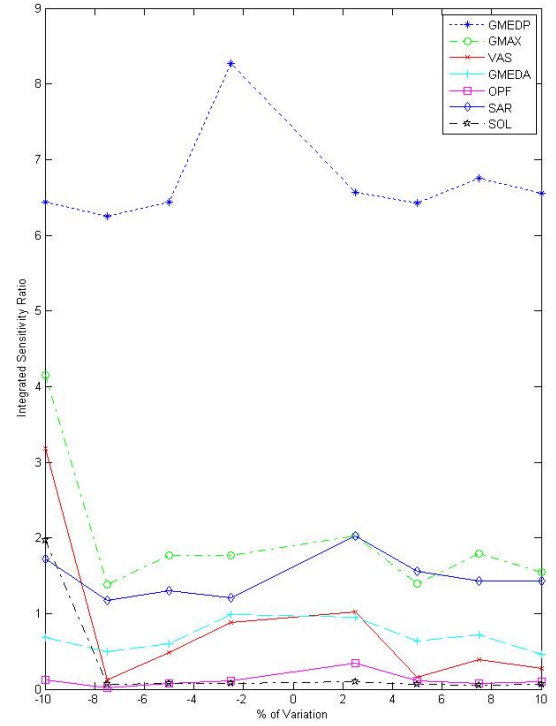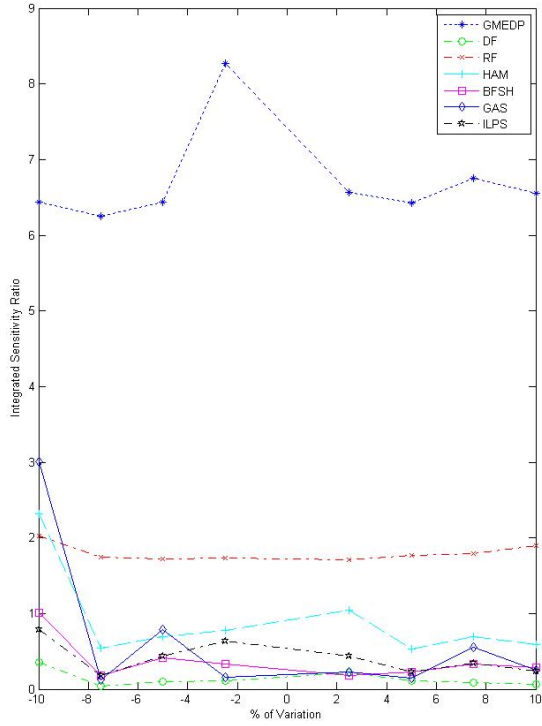
Figure 65: Sensitivity for GMEDP to pennation angle.
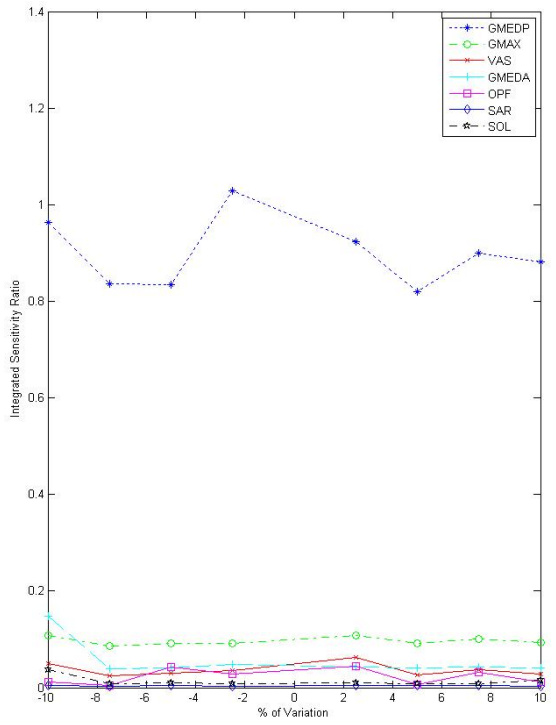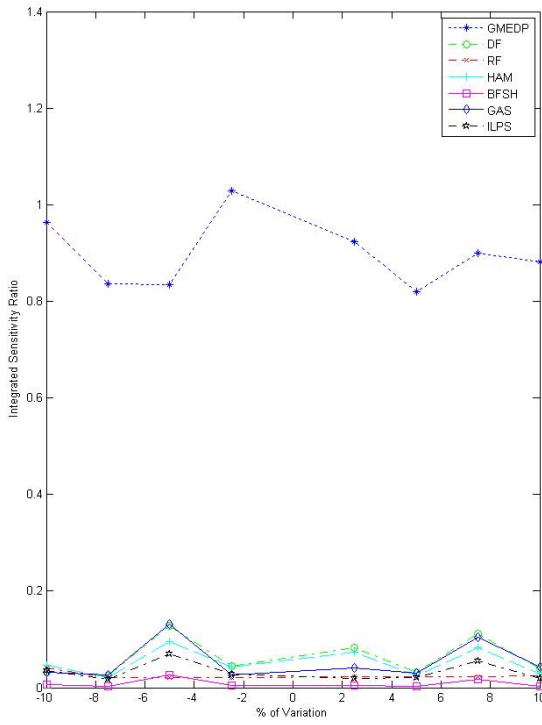
Figure 66: Sensitivity of relevance for GMEDP to pennation angle.

113
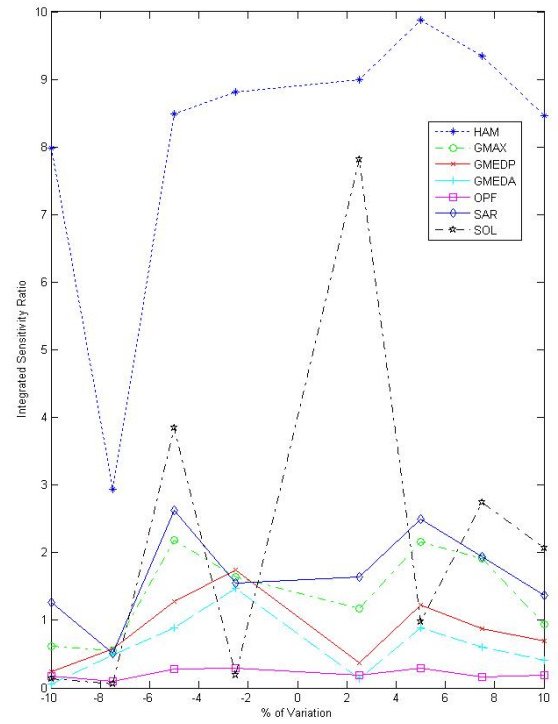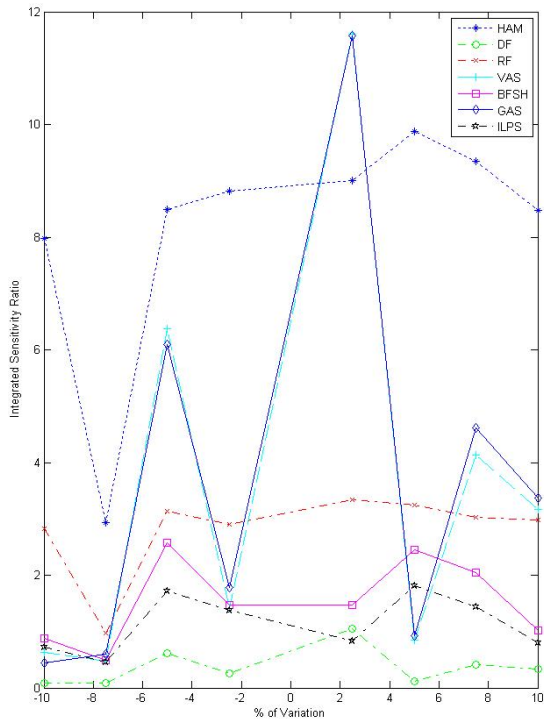
Figure 67: Sensitivity for HAM to pennation angle.
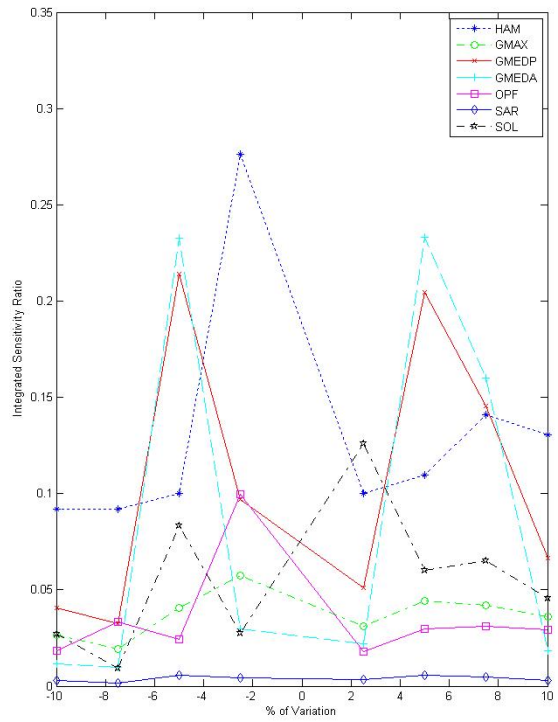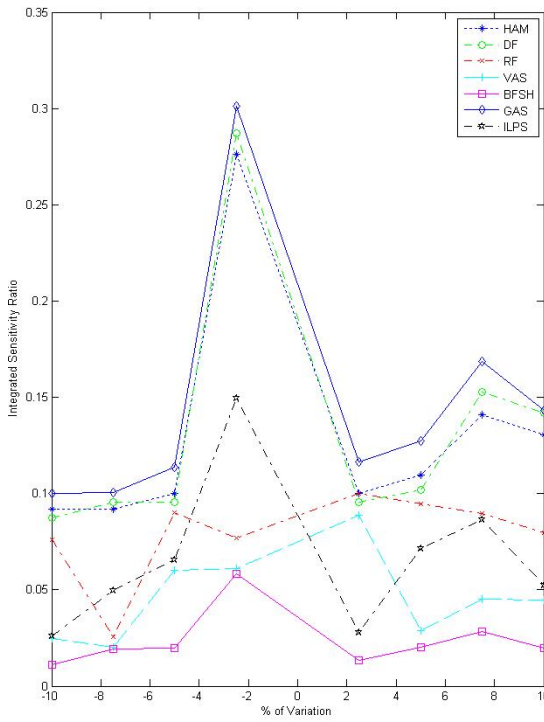
Figure 68: Sensitivity of relevance for HAM to pennation angle.
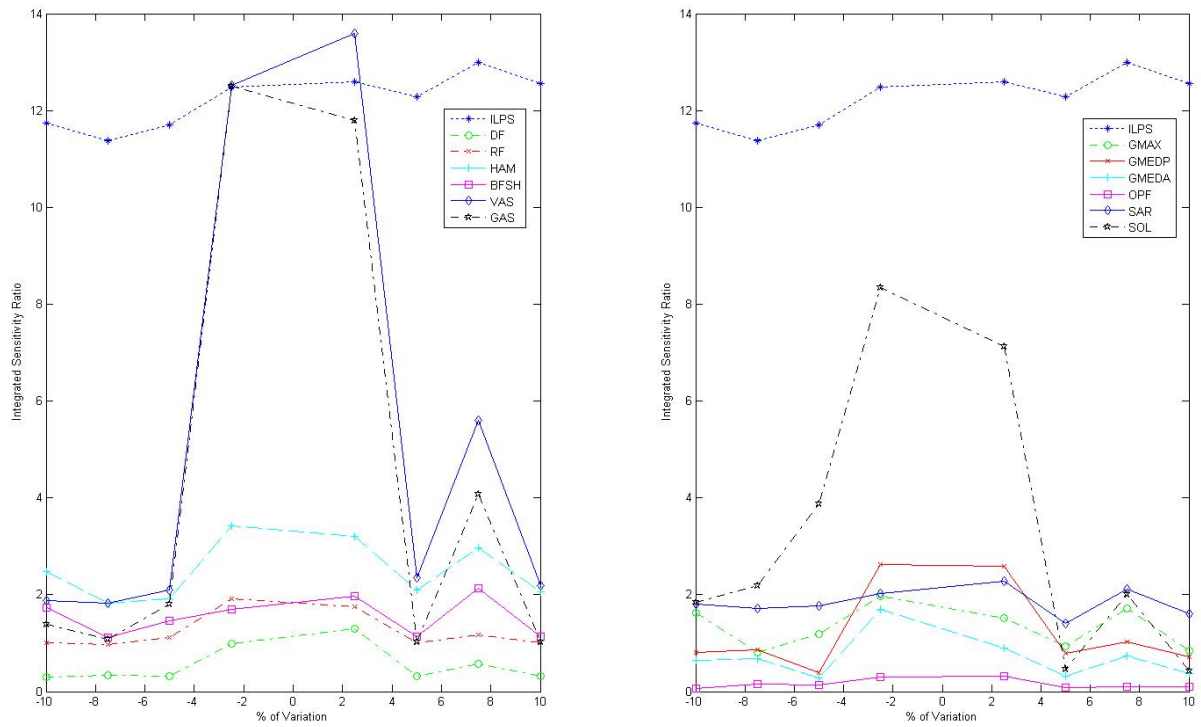
Figure 69: Sensitivity for ILPSO to pennation angle.
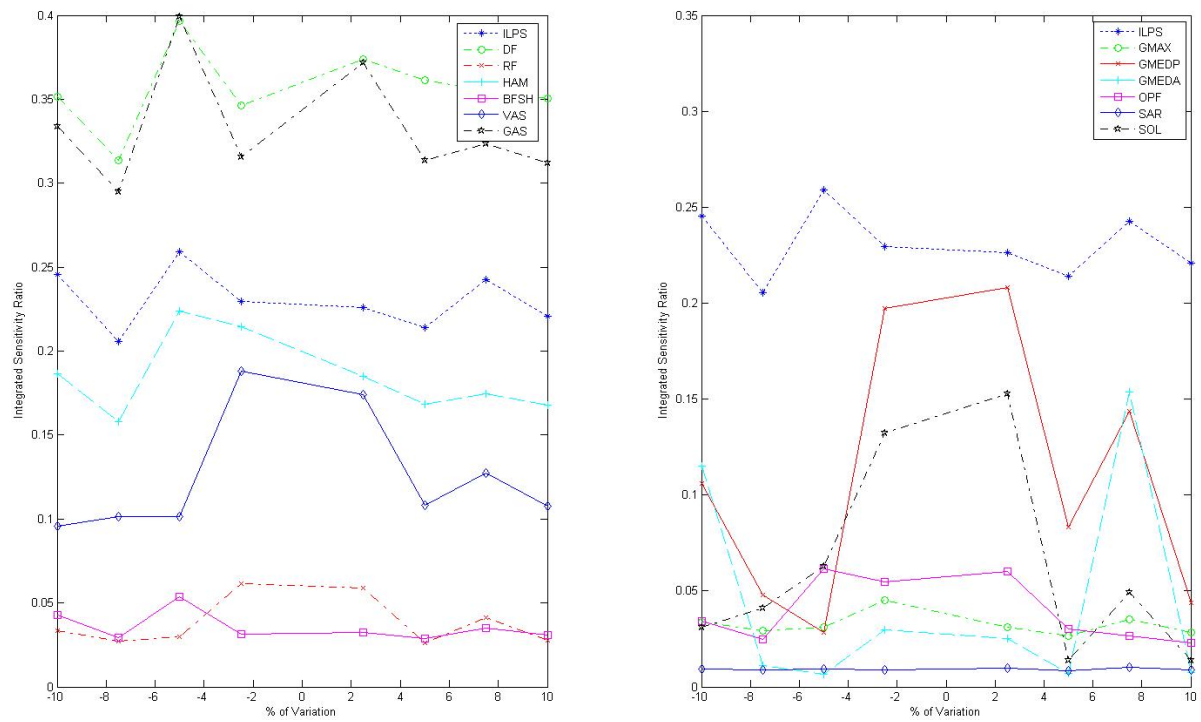
Figure 70: Sensitivity of relevance for ILPSO to pennation angle.
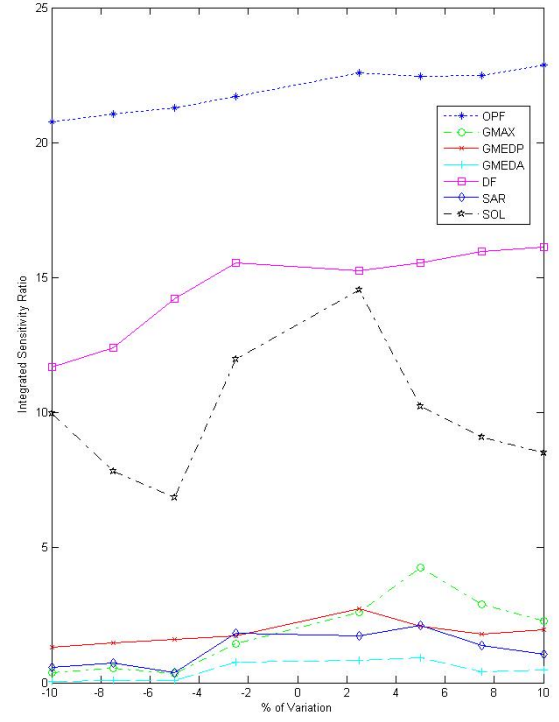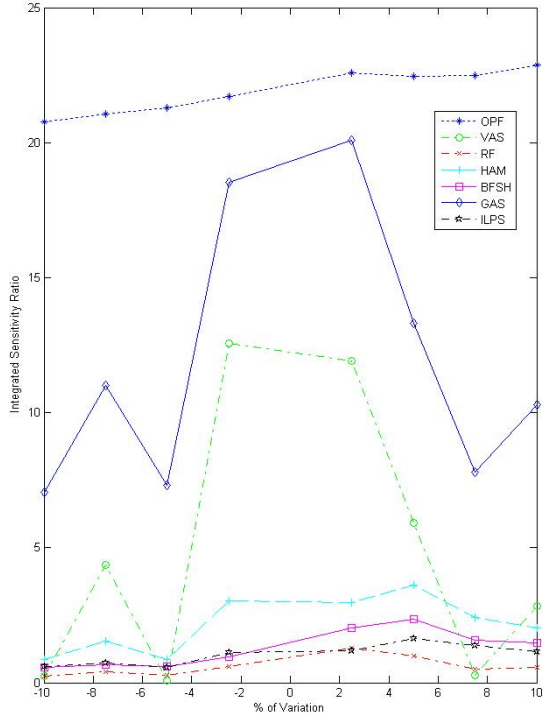
Figure 71: Sensitivity for OPF to pennation angle.
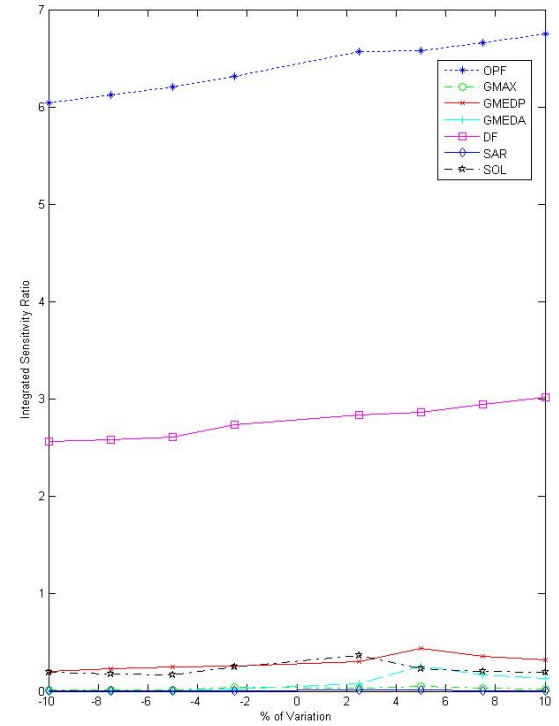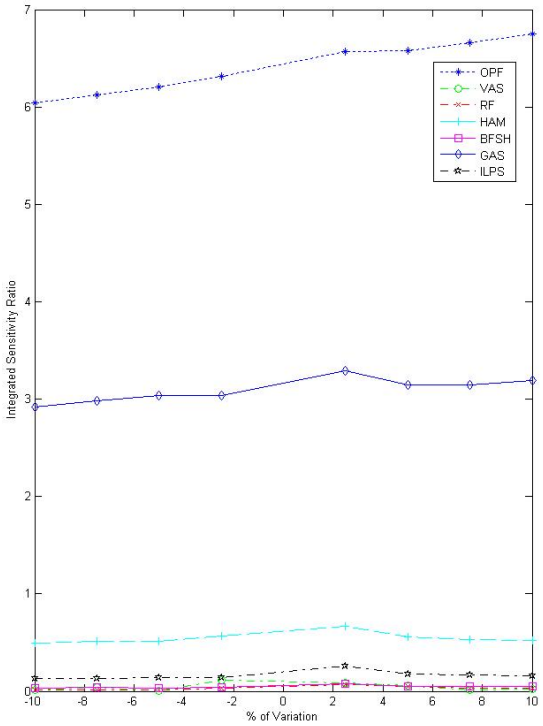
Figure 72: Sensitivity of relevance for OPF to pennation angle.

116
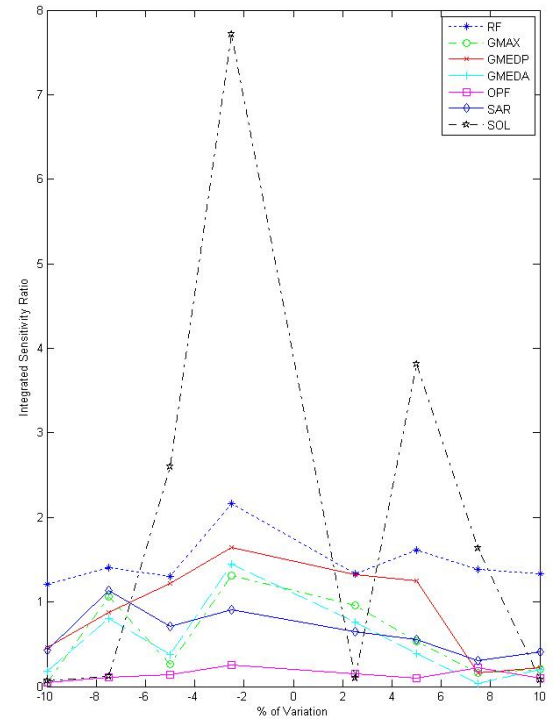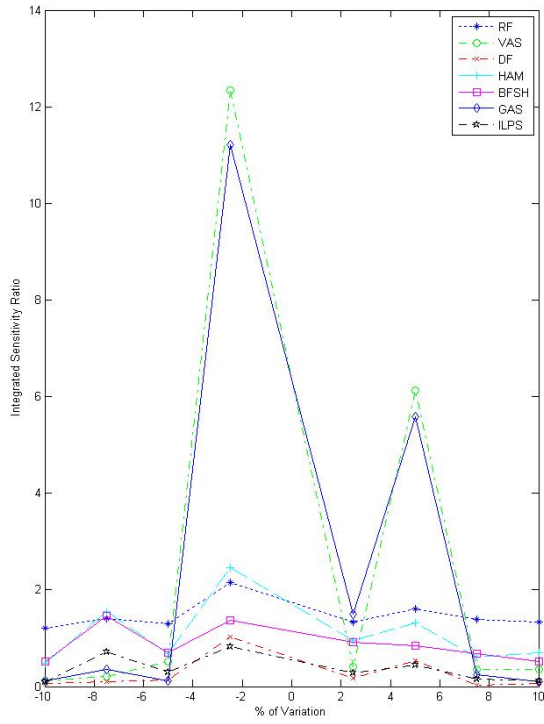
Figure 73: Sensitivity for RF to pennation angle.
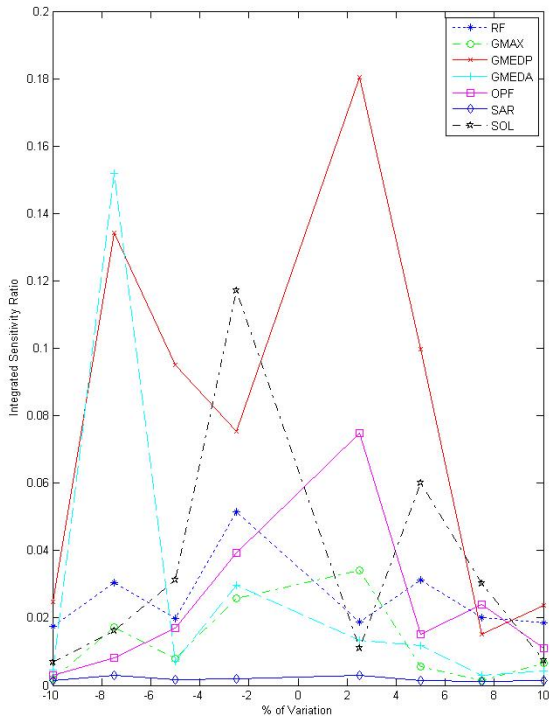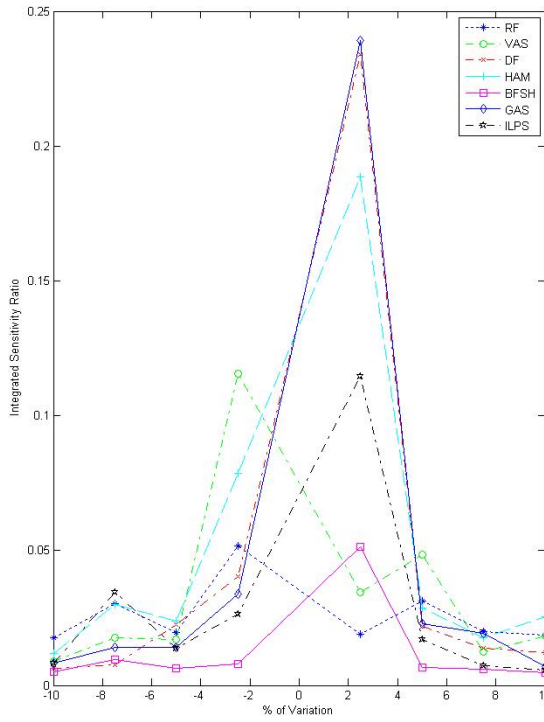
Figure 74: Sensitivity of relevance for RF to pennation angle.
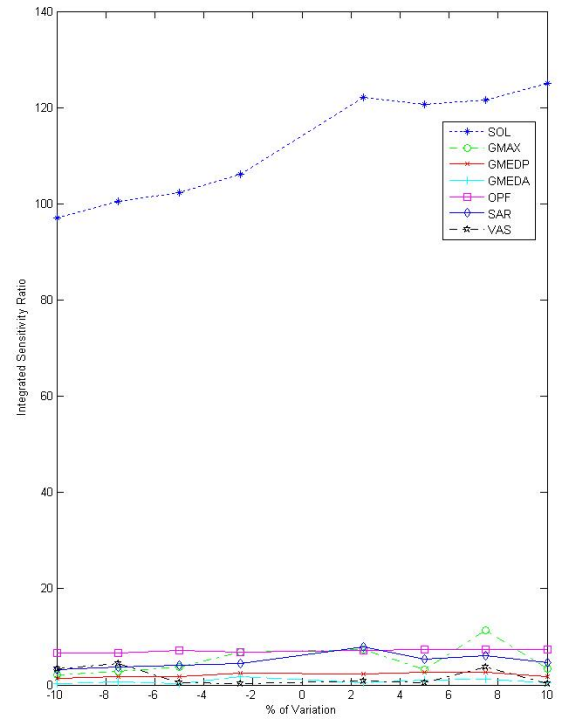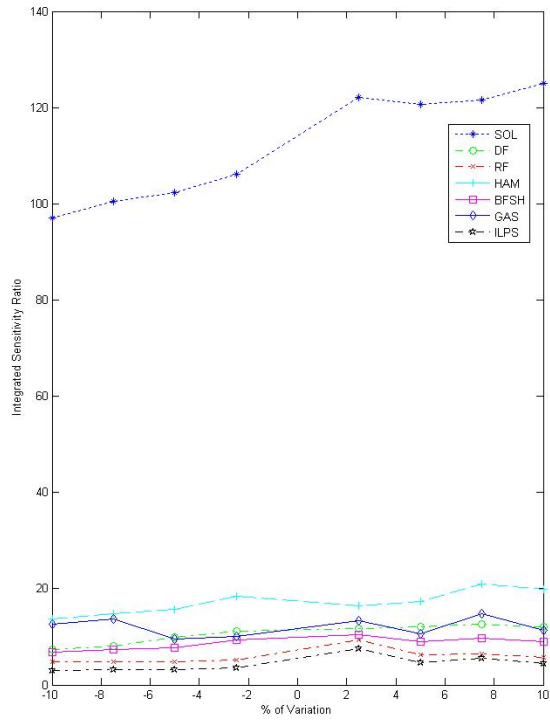
Figure 75: Sensitivity for SOL to pennation angle.
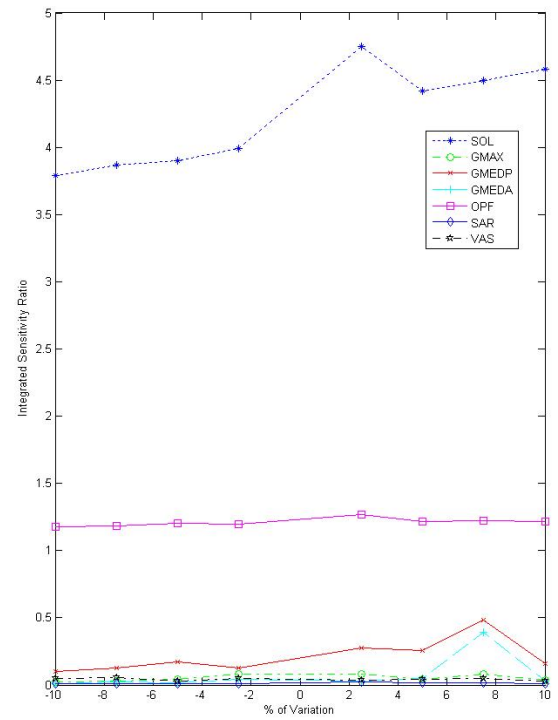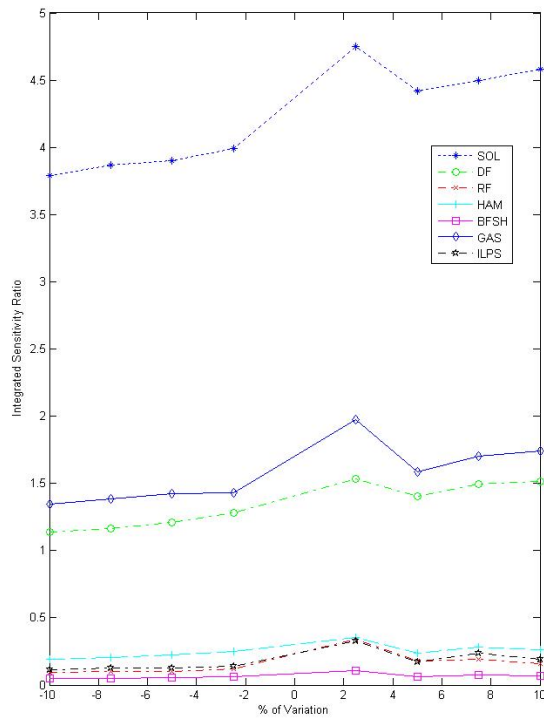
Figure 76: Sensitivity of relevance for SOL to pennation angle.

118
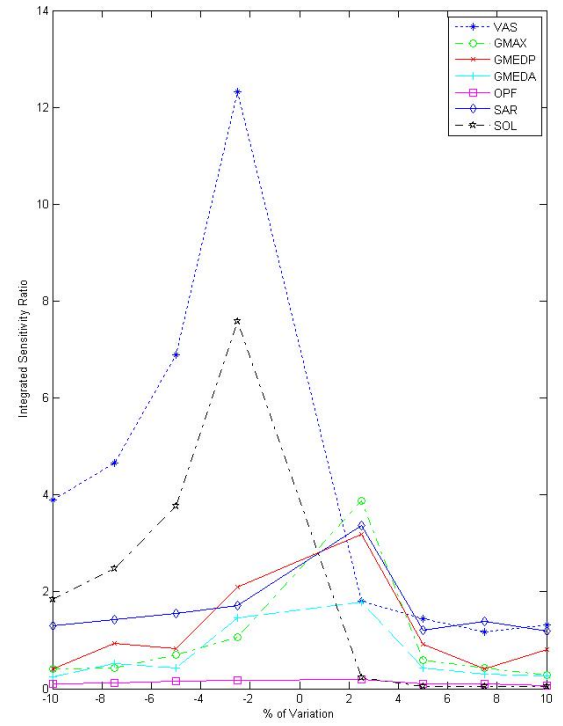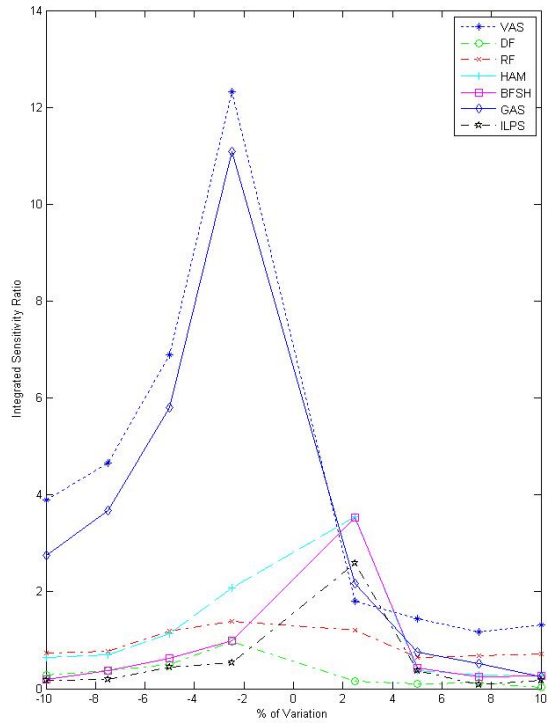
Figure 77: Sensitivity for VAS to pennation angle.
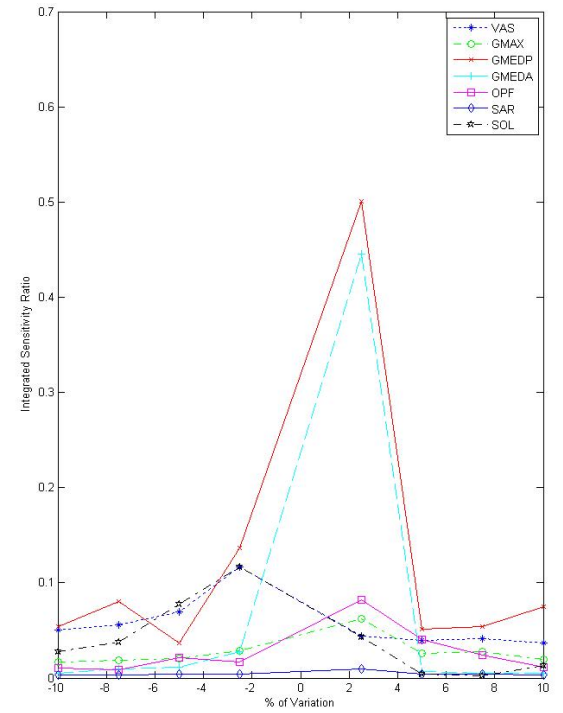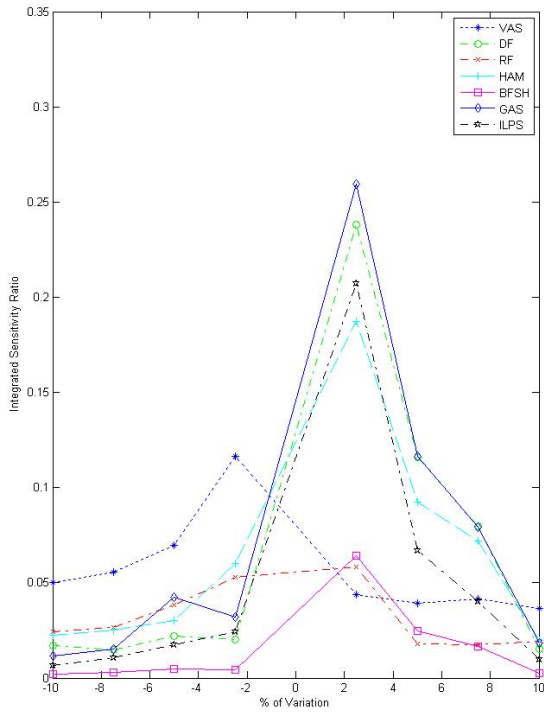
Figure 78: Sensitivity of relevance for VAS to pennation angle.
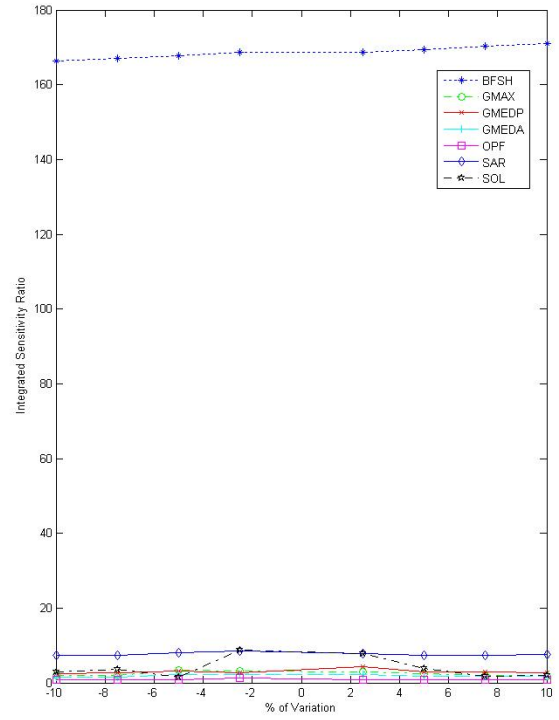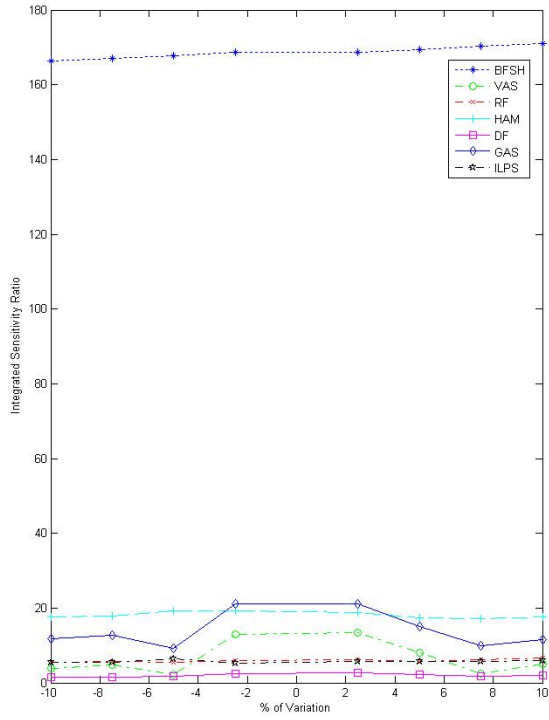
Figure 79: Sensitivity for BFSH to optimal muscle force.
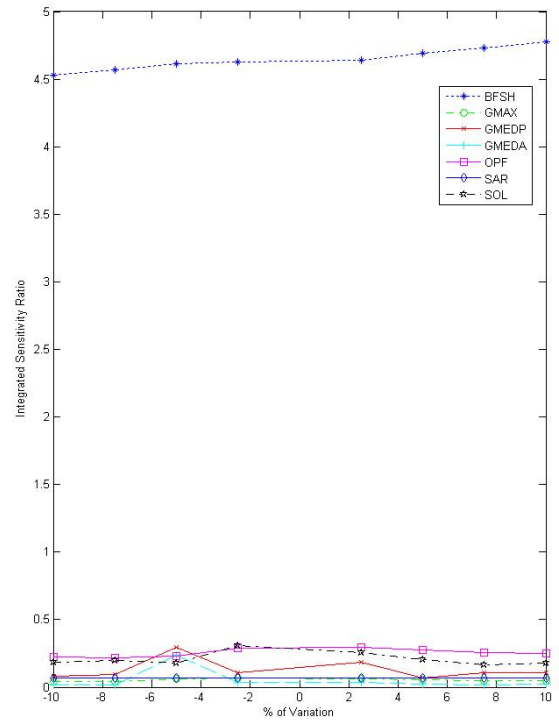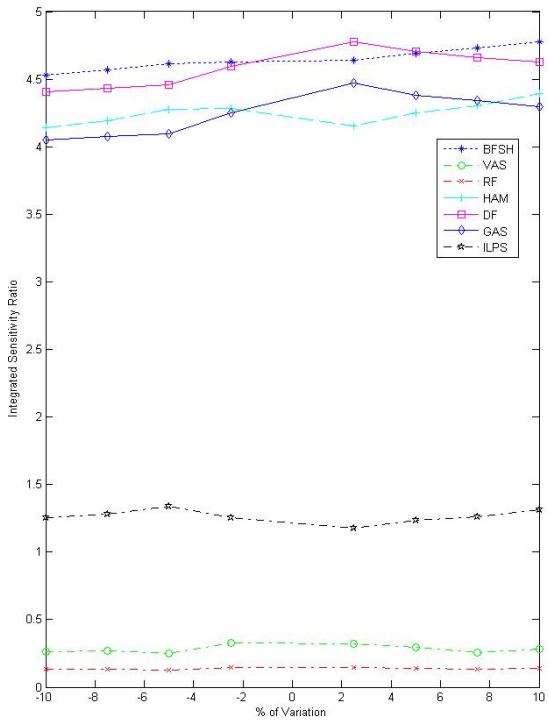
Figure 80: Sensitivity of relevance for BFSH to optimal muscle force.
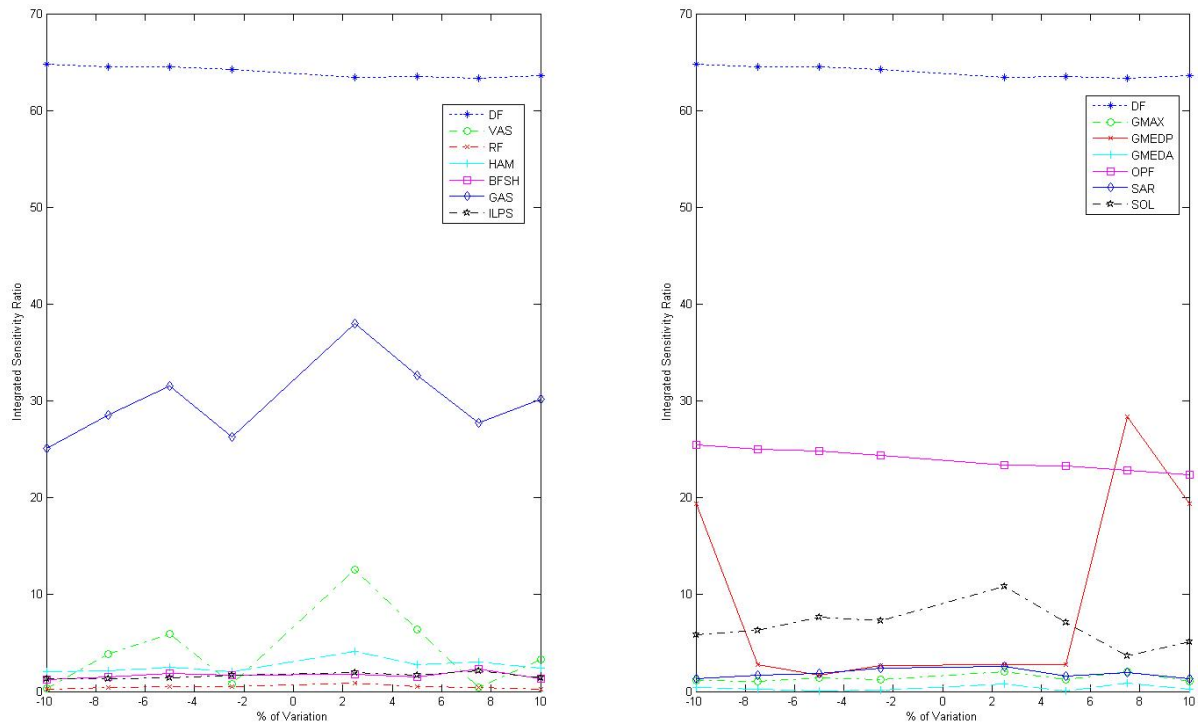
Figure 81: Sensitivity for DF to optimal muscle force.
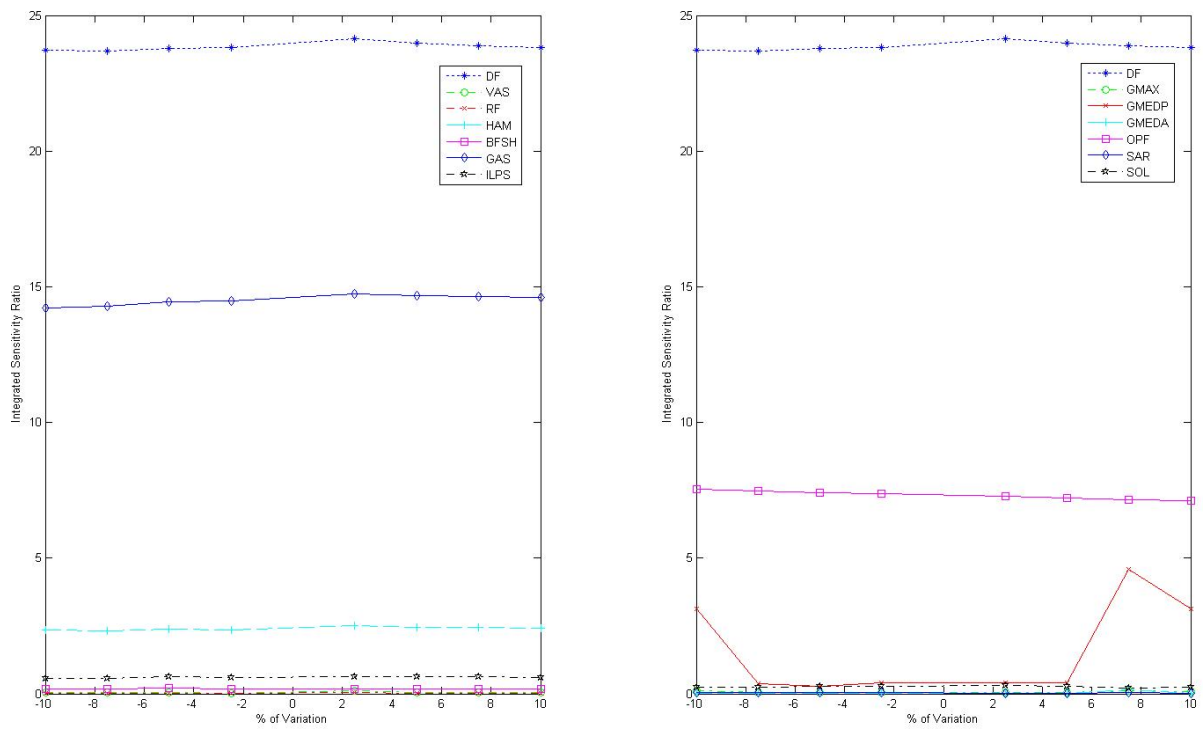
Figure 82: Sensitivity of relevance for DF to optimal muscle force.
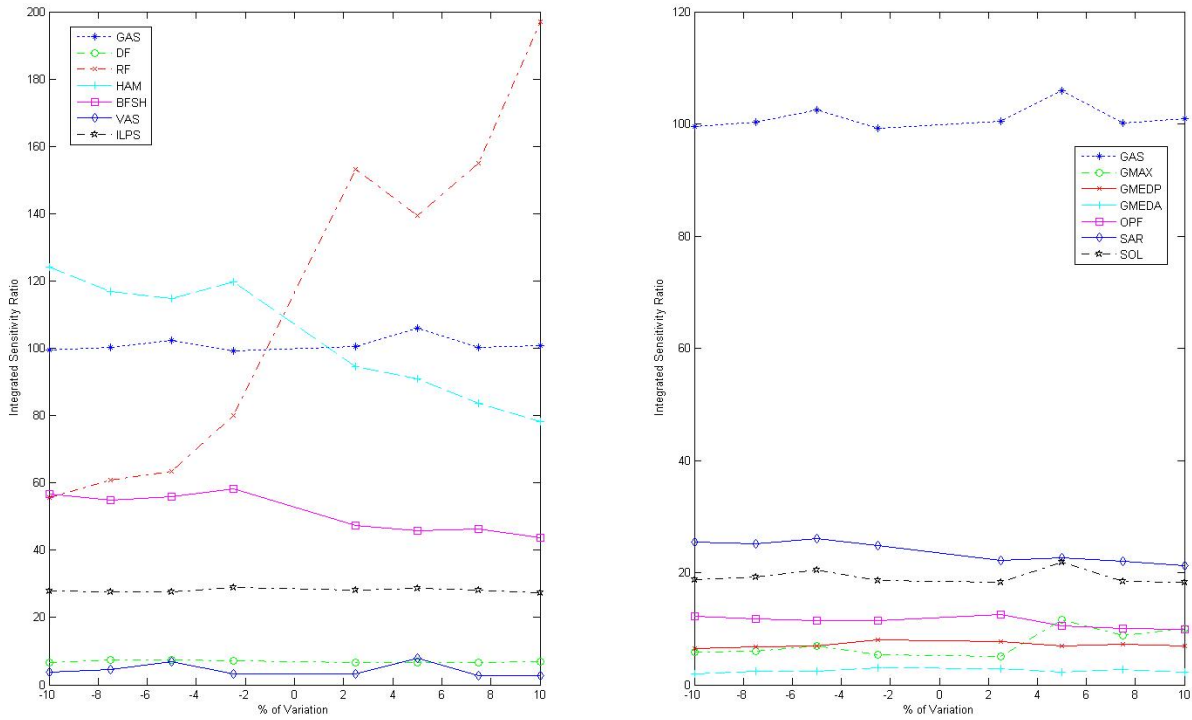
Figure 83: Sensitivity for GAS to optimal muscle force.
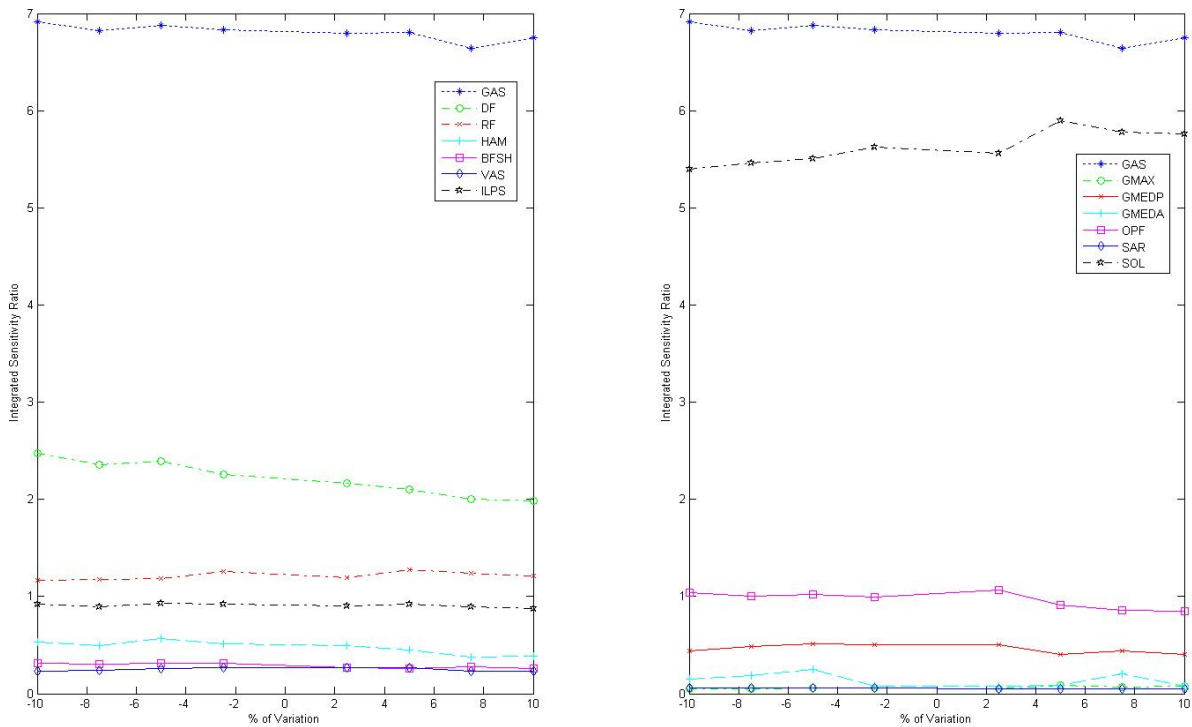
Figure 84: Sensitivity of relevance for GAS to optimal muscle force.
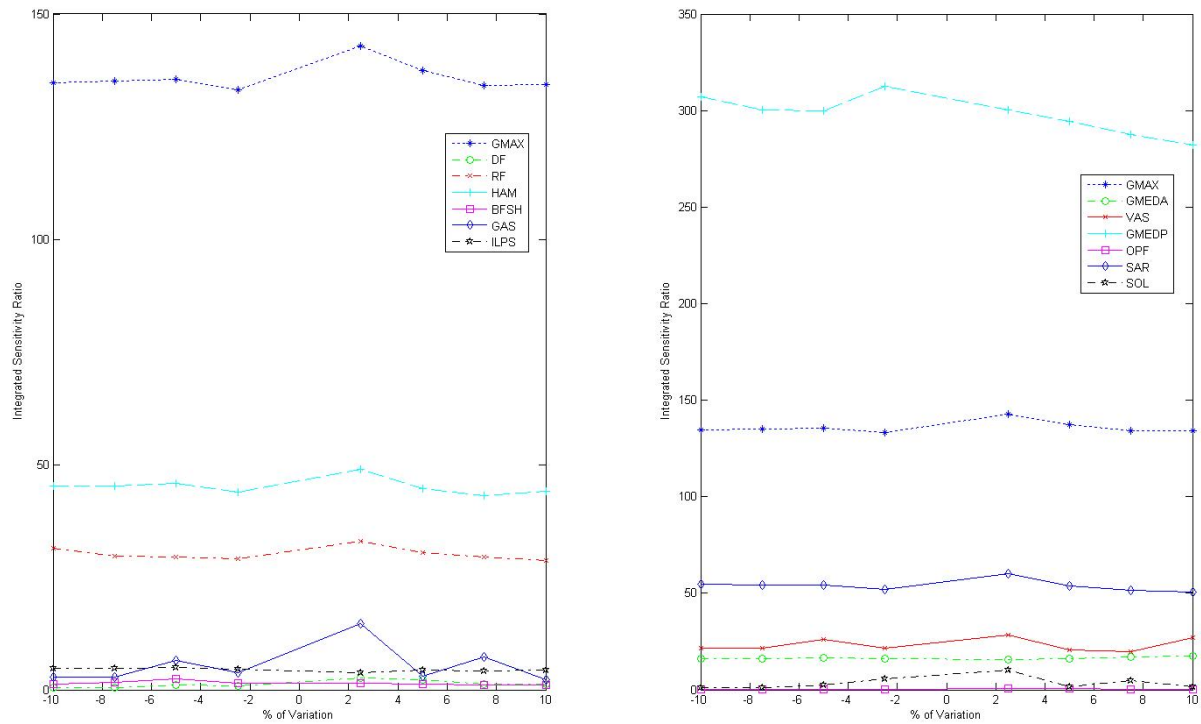
Figure 85: Sensitivity for GMAXL to optimal muscle force.
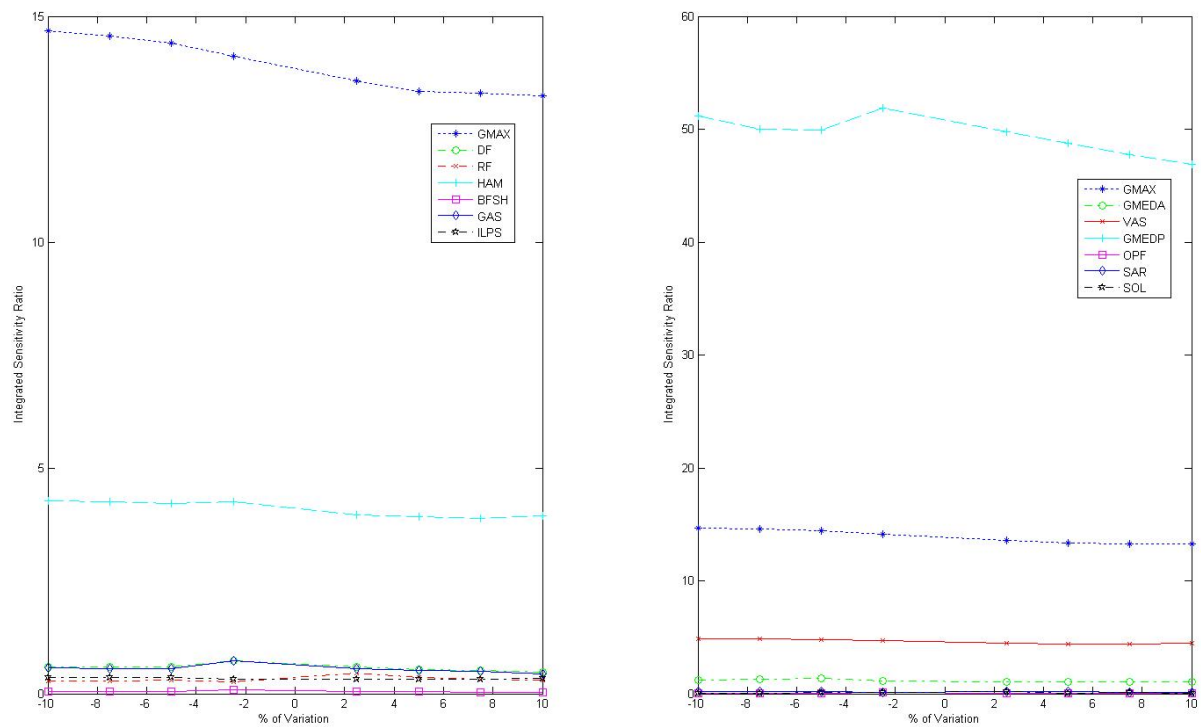
Figure 86: Sensitivity of relevance for GMAXM to optimal muscle force.
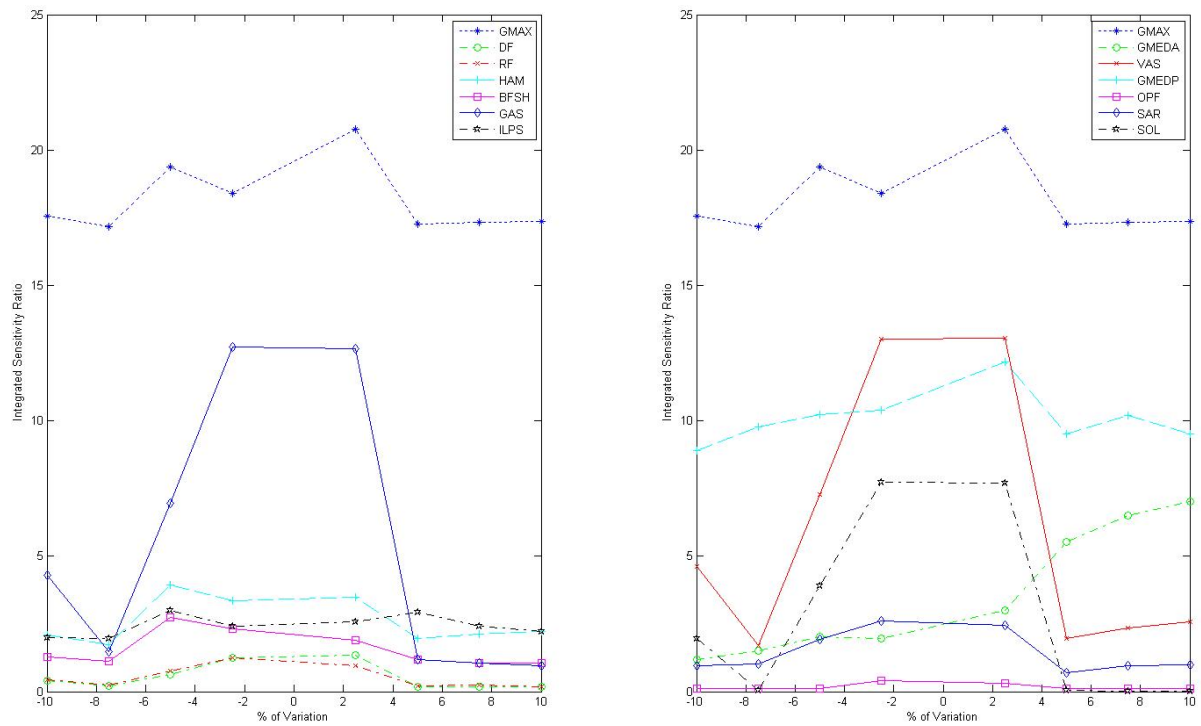
Figure 87: Sensitivity for GMAXM to optimal muscle force.
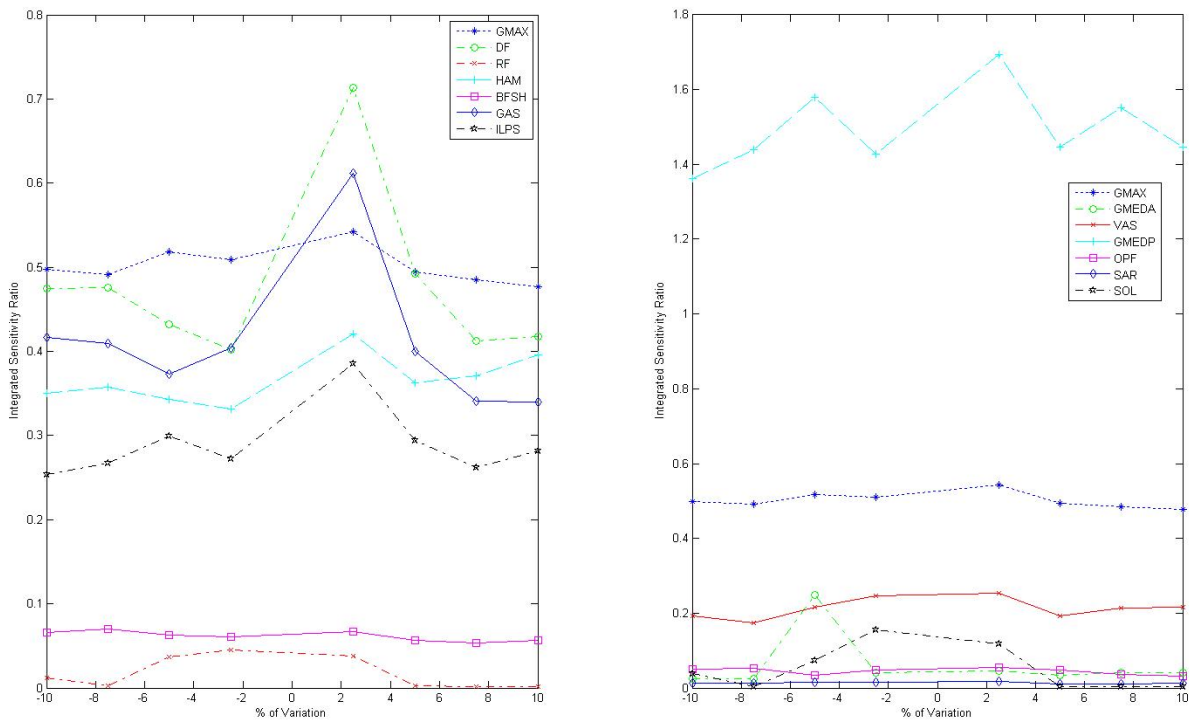
Figure 88: Sensitivity of relevance for GMAXM to optimal muscle force.

124
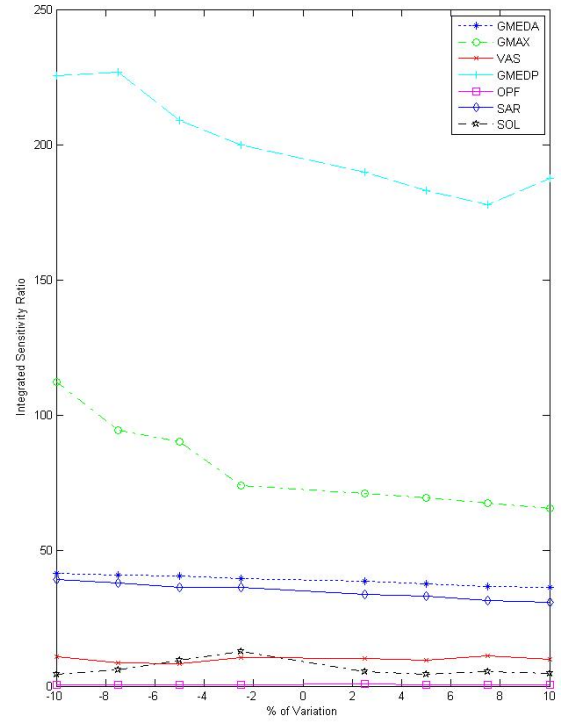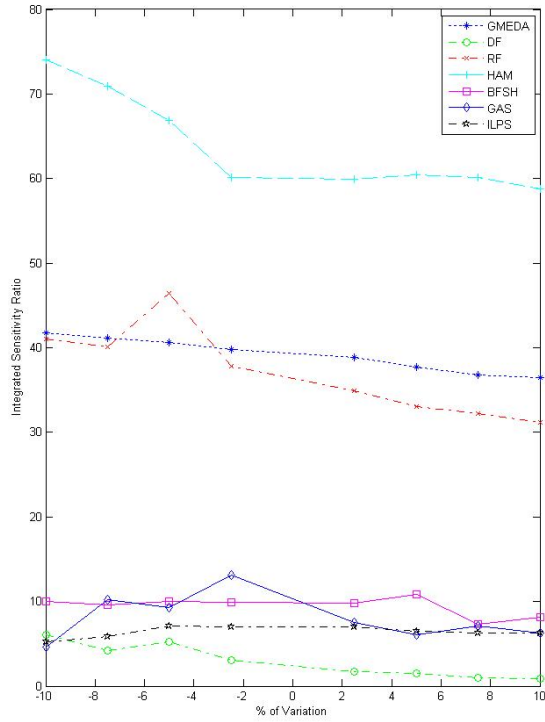
Figure 89: Sensitivity for GMEDA to optimal muscle force.
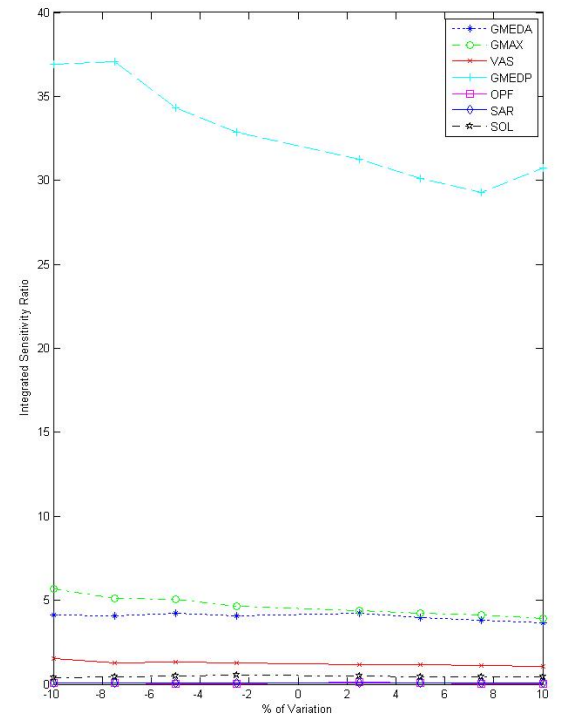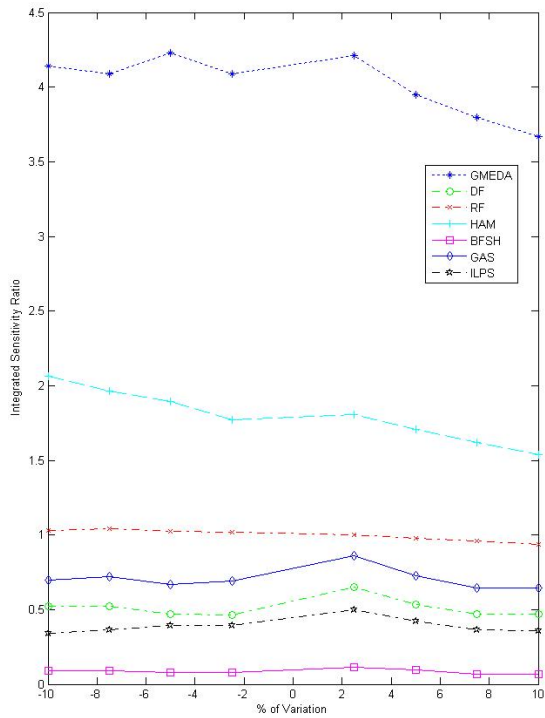
Figure 90: Sensitivity of relevance for GMEDA to optimal muscle force.
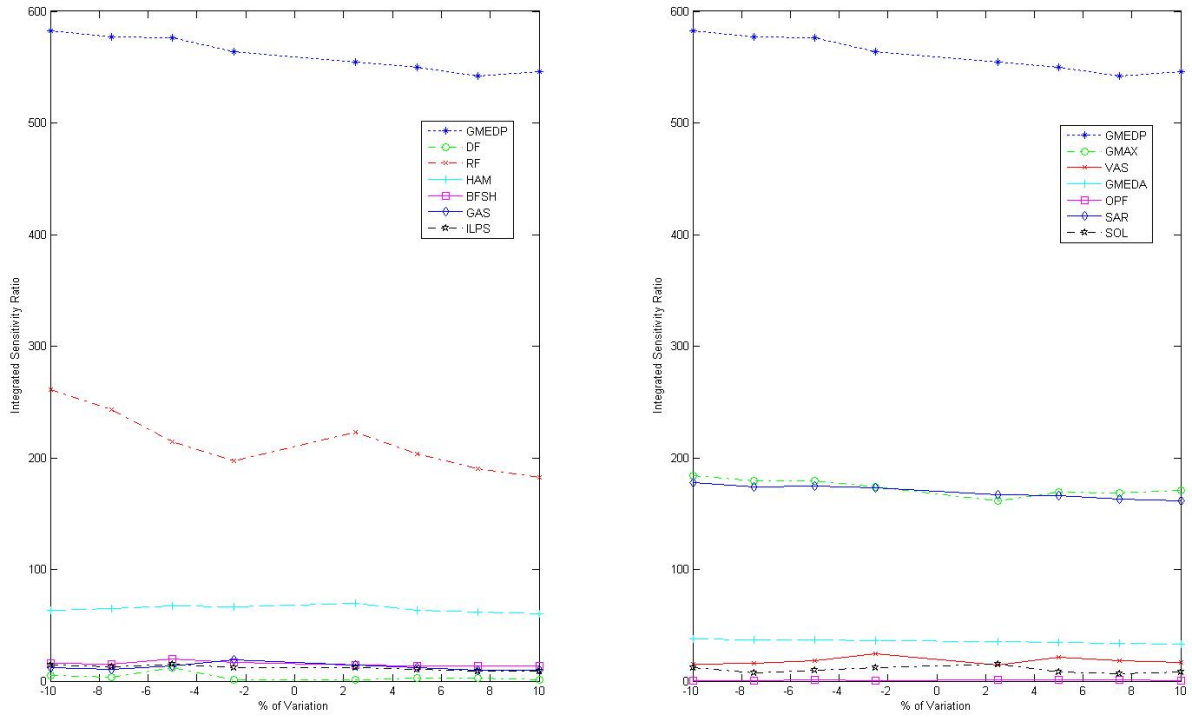
Figure 91: Sensitivity for GMEDP to optimal muscle force.
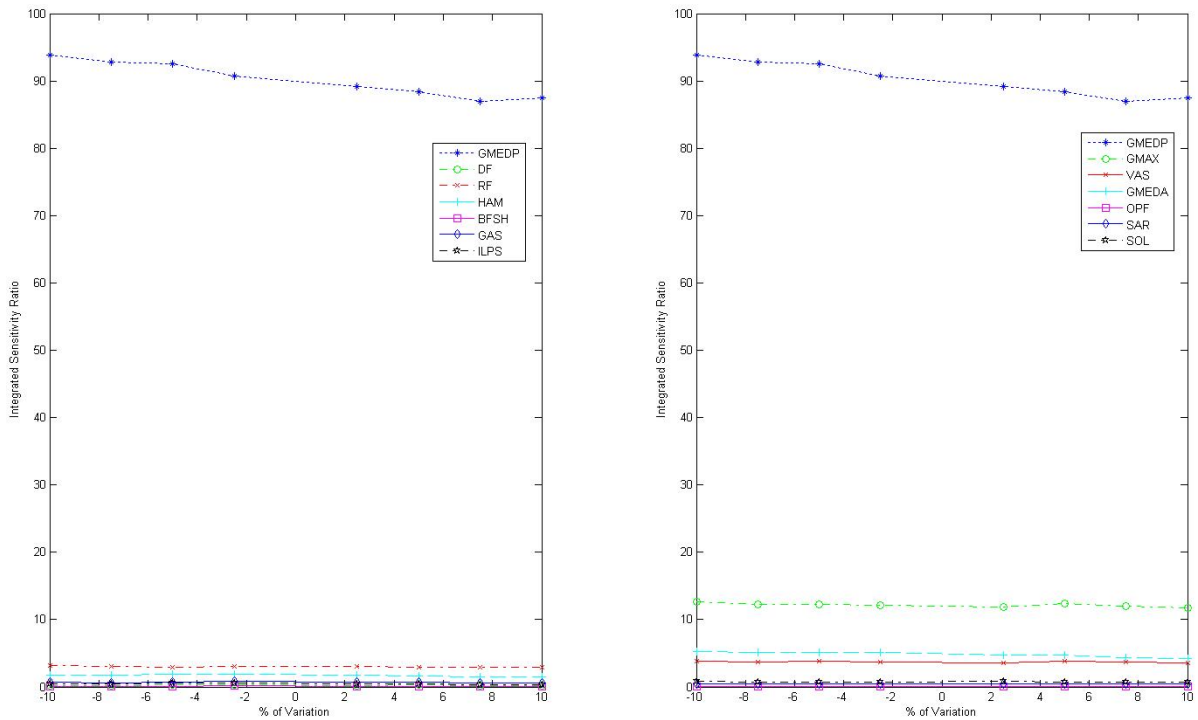
Figure 92: Sensitivity of relevance for GMEDP to optimal muscle force.
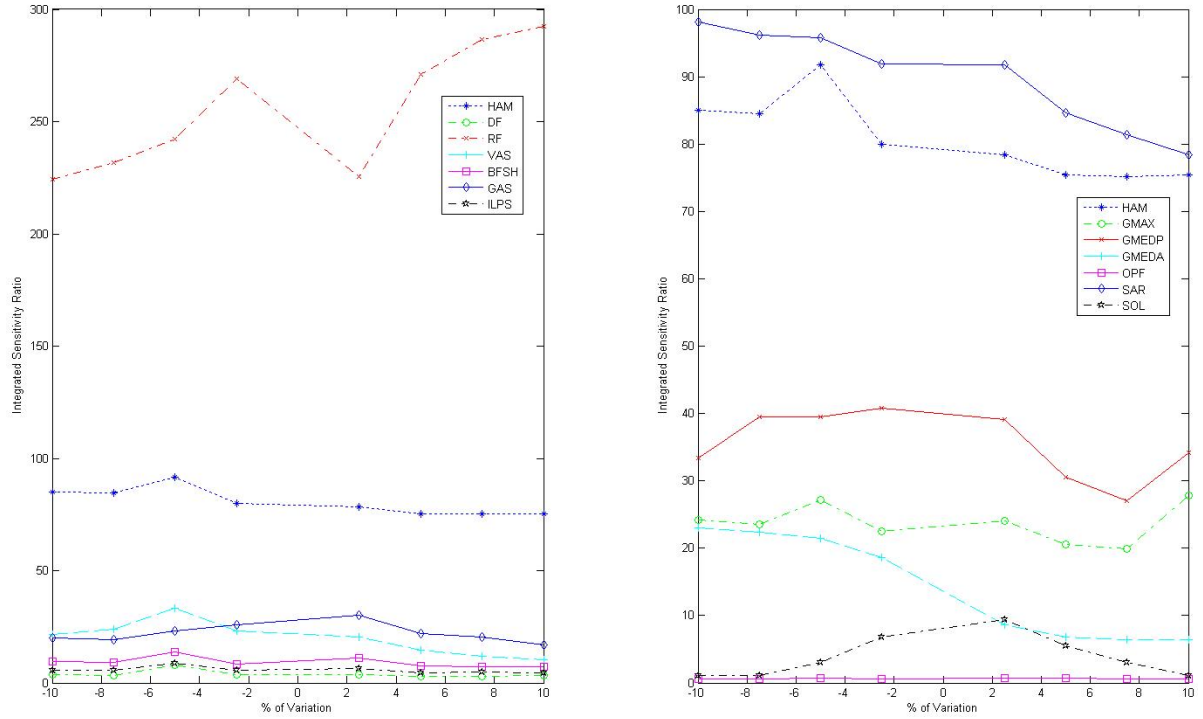
Figure 93: Sensitivity of relevance for HAM to optimal muscle force.
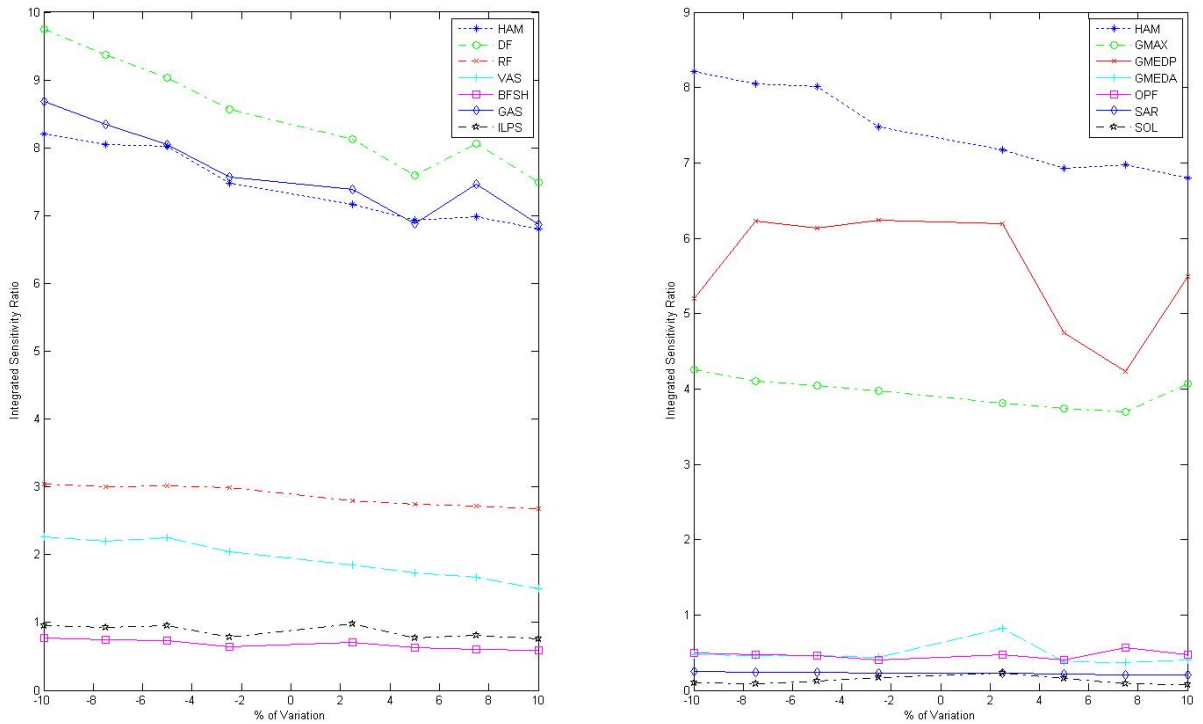
Figure 94: Sensitivity of relevance for HAM to optimal muscle force.
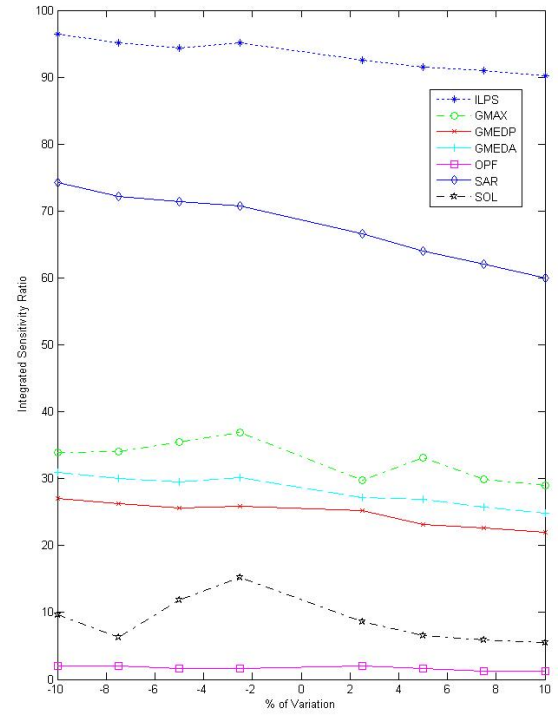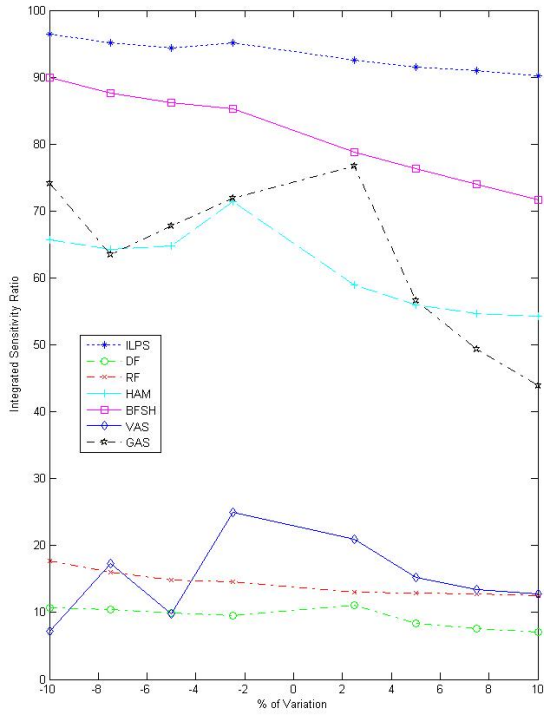
Figure 95: Sensitivity for ILPSO to optimal muscle force.
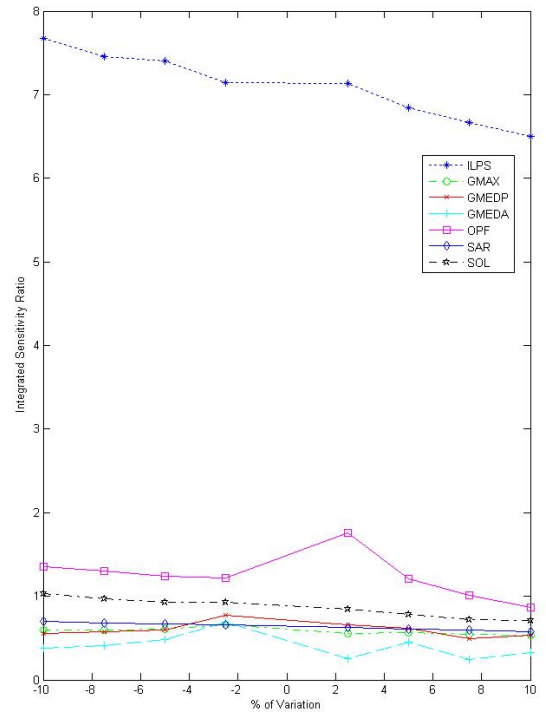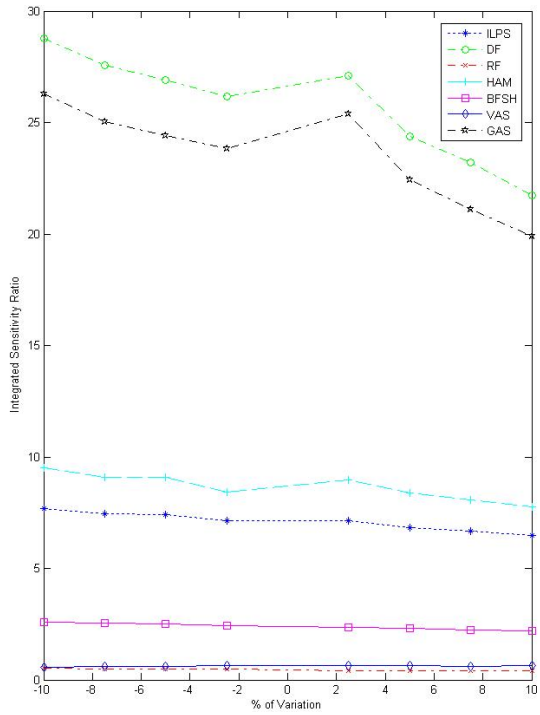
Figure 96: Sensitivity of relevance for ILPSO to optimal muscle force.
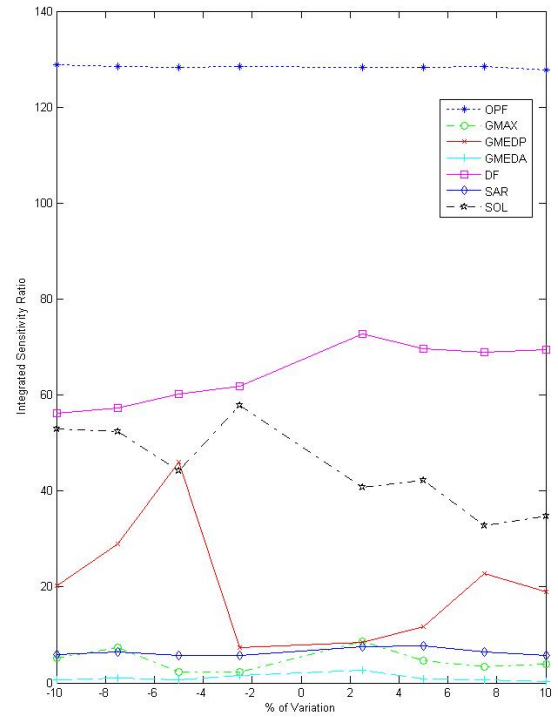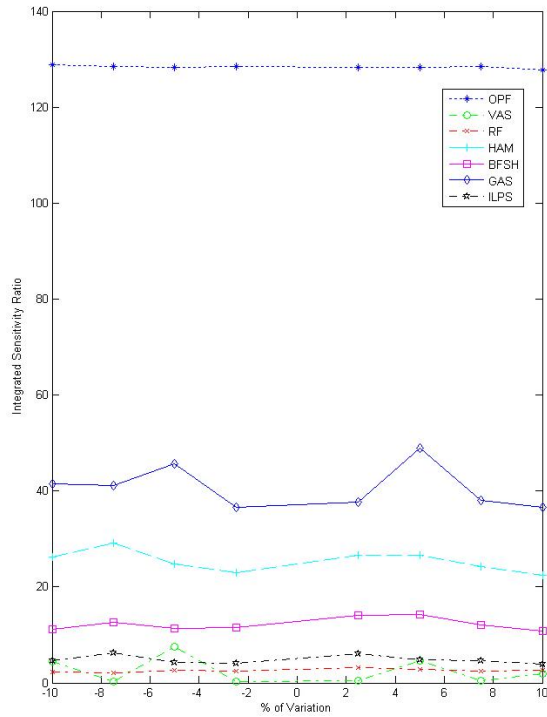
Figure 97: Sensitivity for OPF to optimal muscle force.
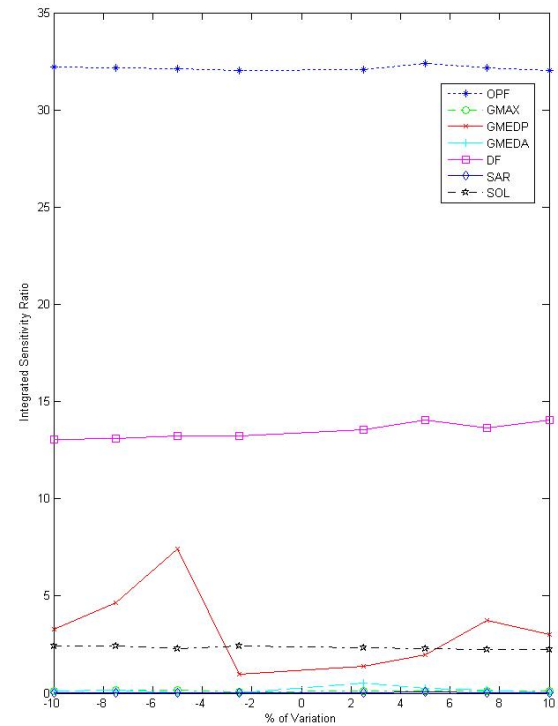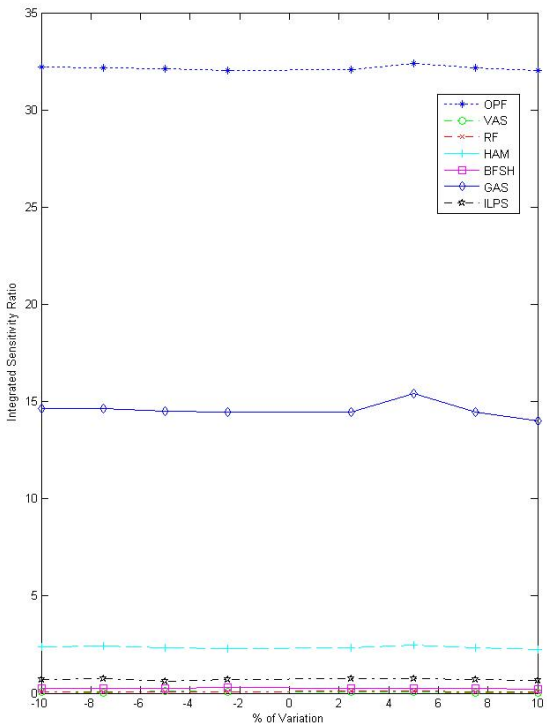
Figure 98: Sensitivity of relevance for OPF to optimal muscle force.

129
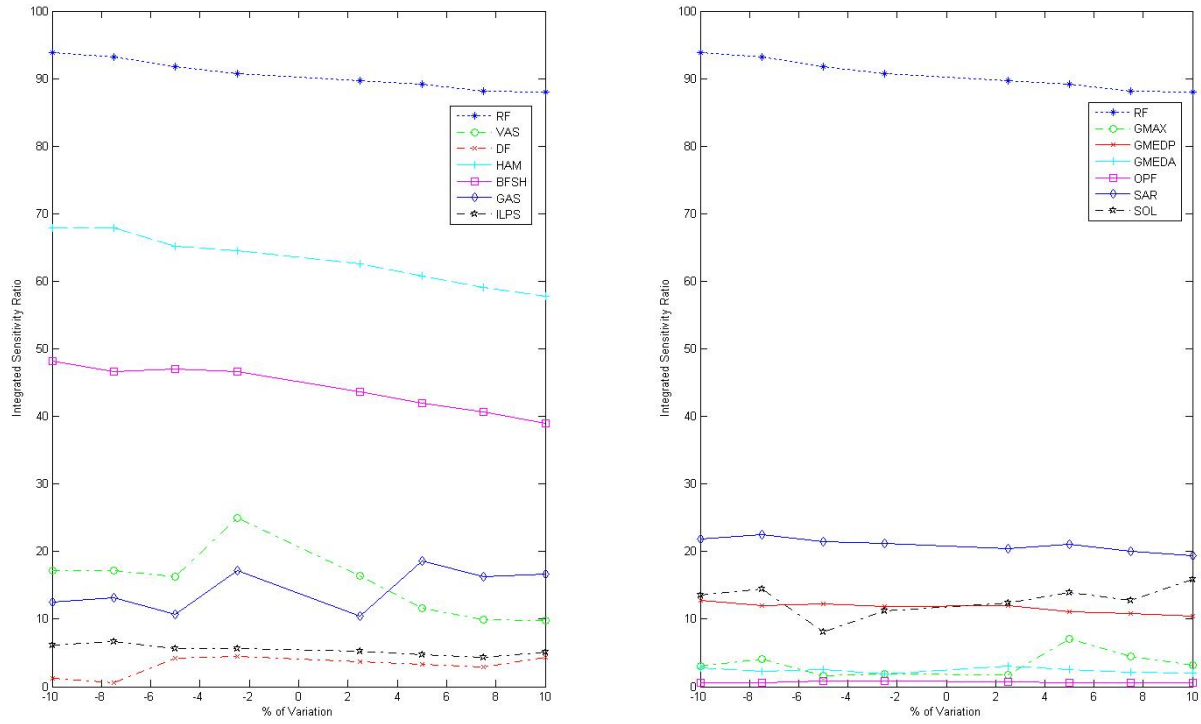
Figure 99: Sensitivity for RF to optimal muscle force.
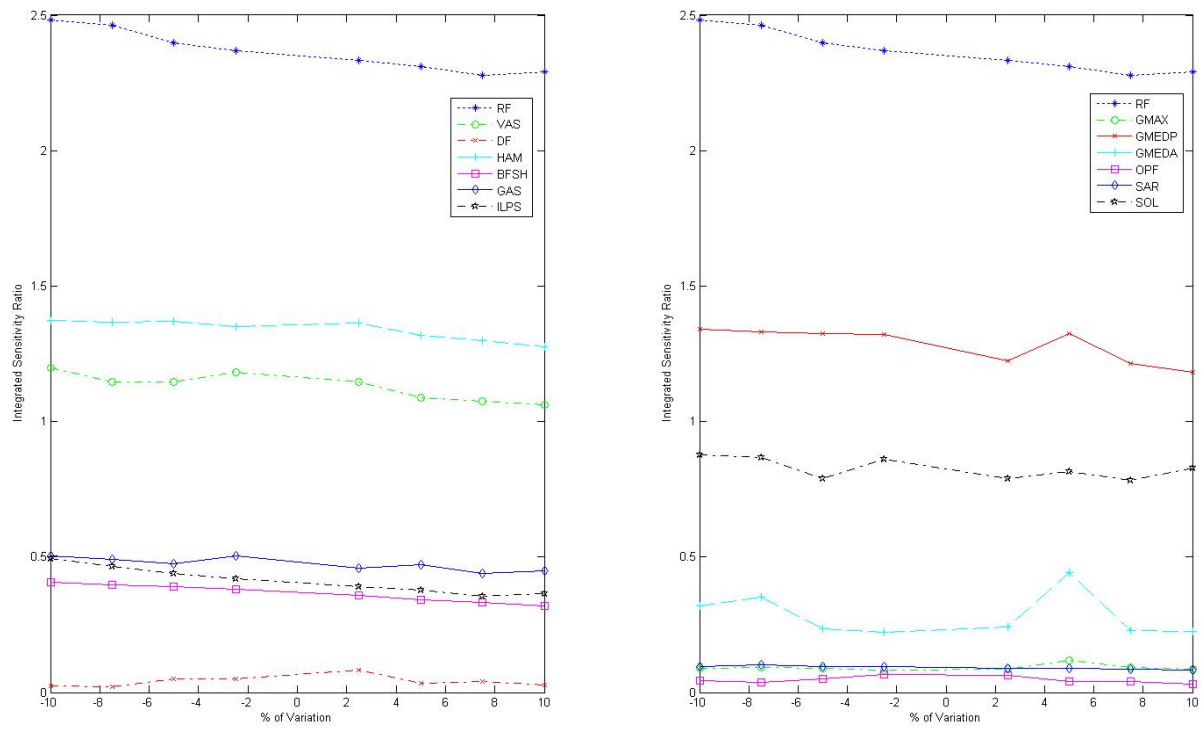
Figure 100: Sensitivity of relevance for RF to optimal muscle force.
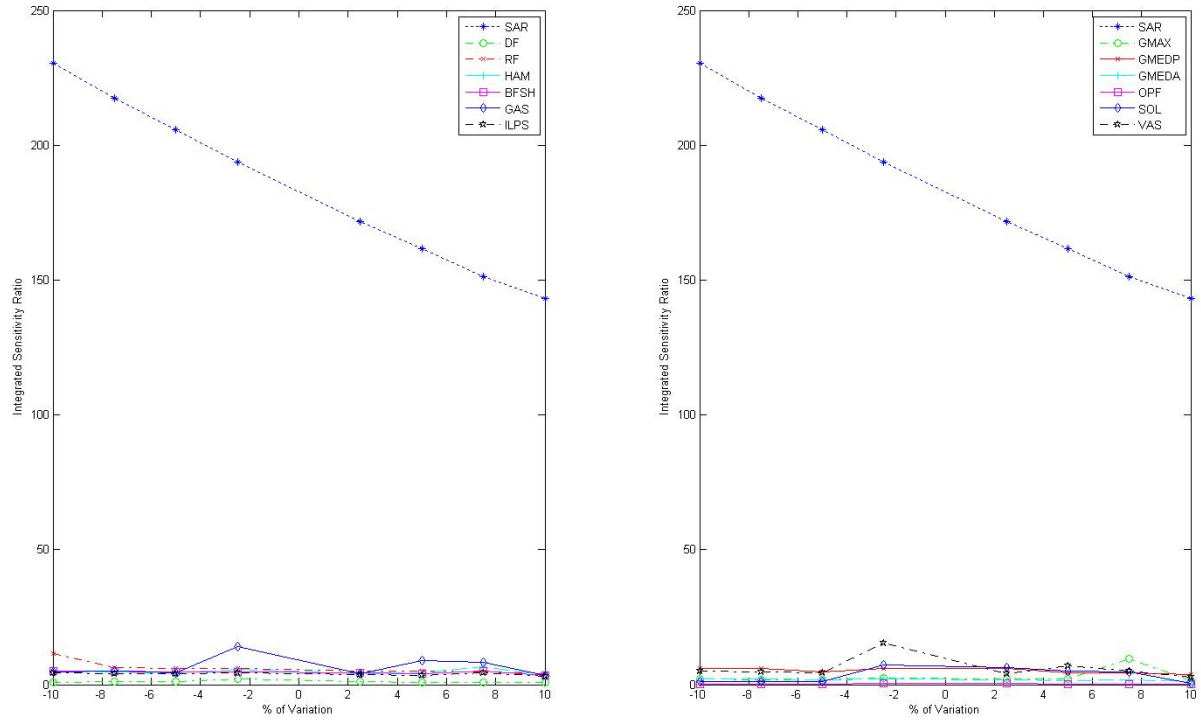
Figure 101: Sensitivity for SAR to optimal muscle force.
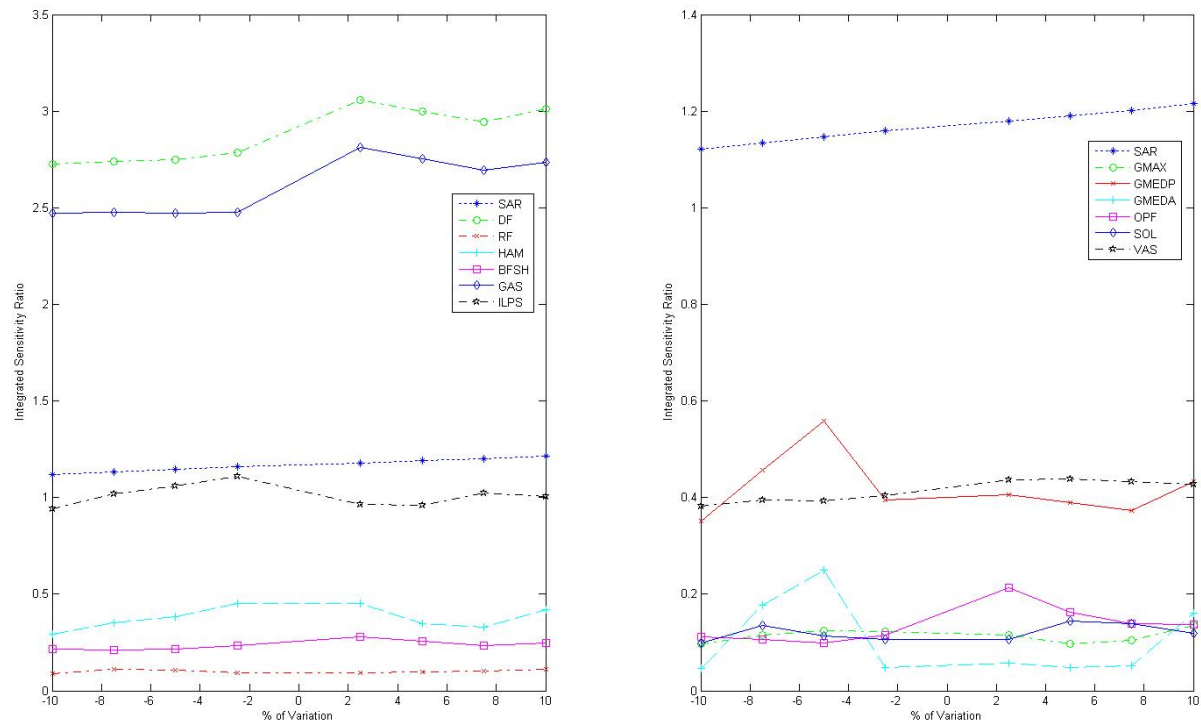
Figure 102: Sensitivity of relevance for SAR to optimal muscle force.
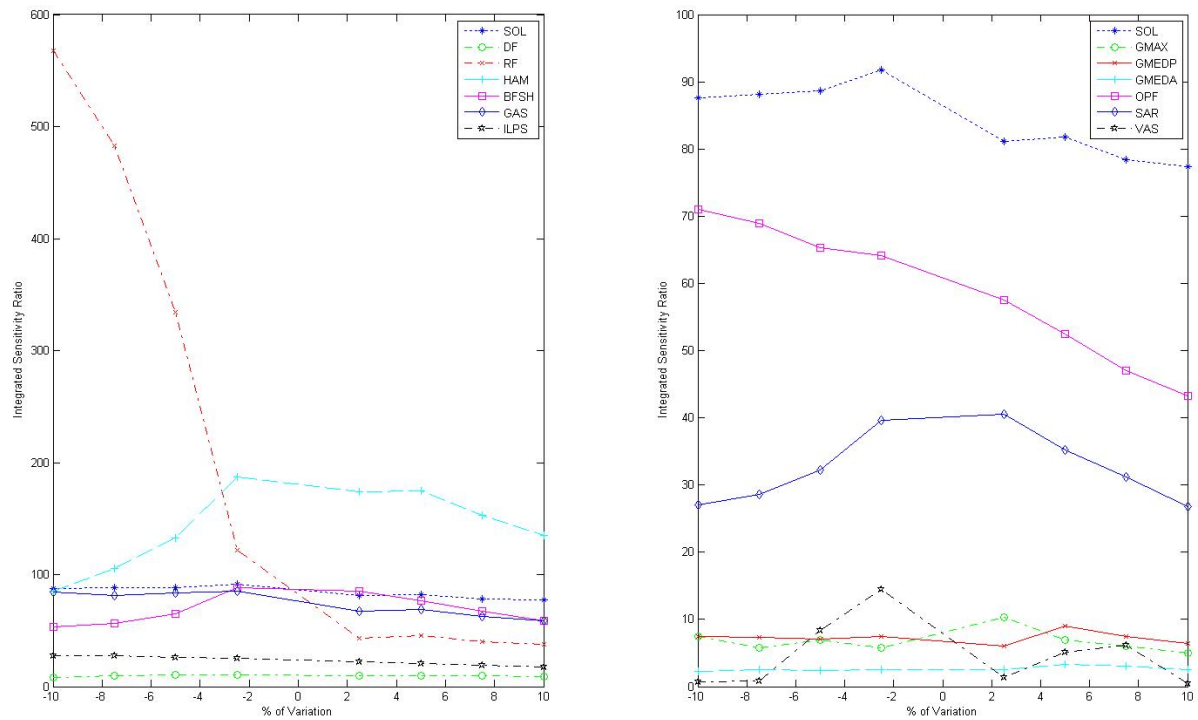
Figure 103: Sensitivity for SOL to optimal muscle force.
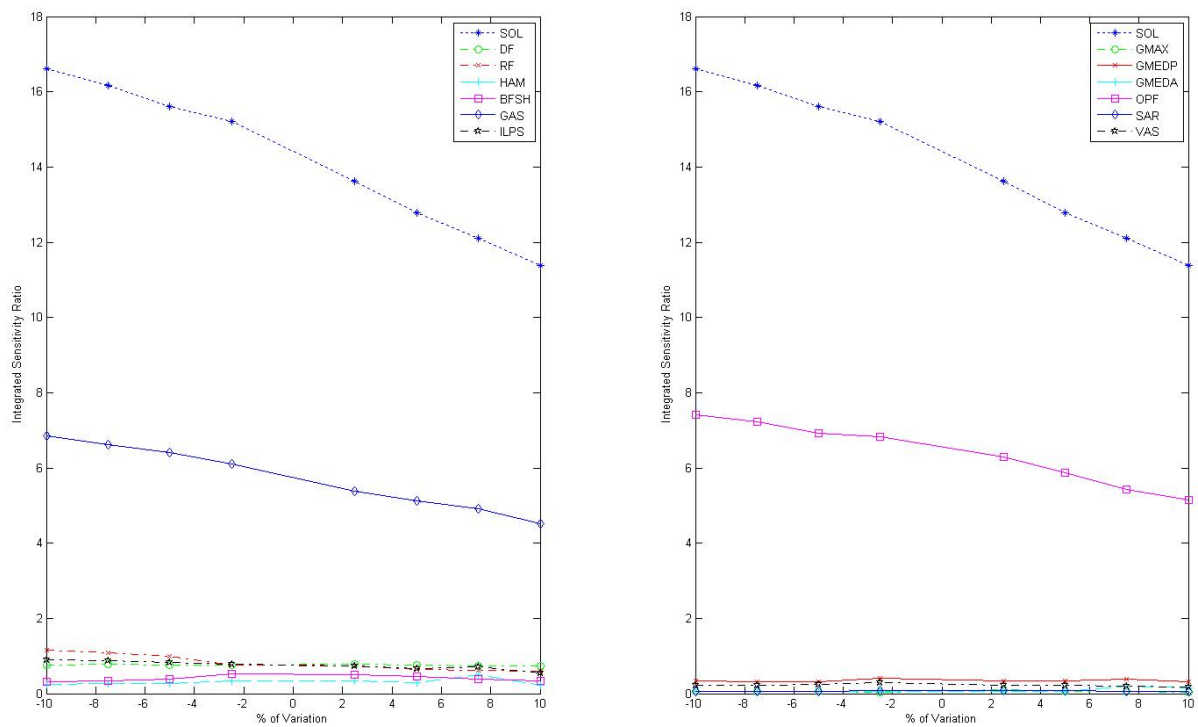
Figure 104: Sensitivity of relevance for SOL to optimal muscle force.

132
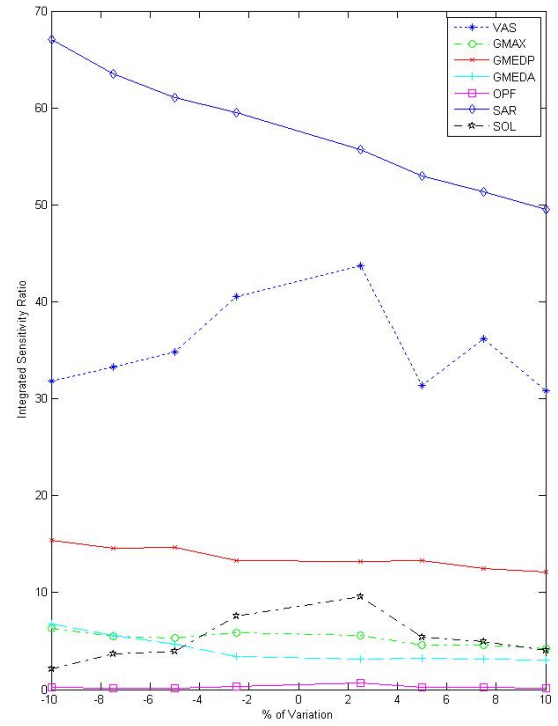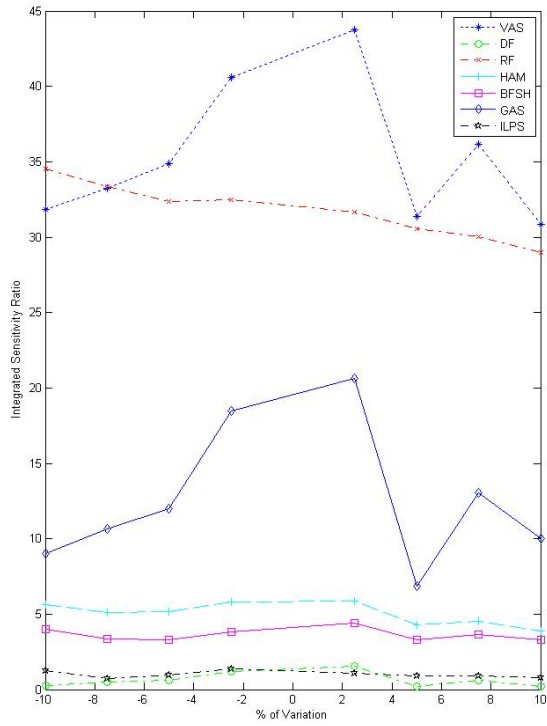
Figure 105: Sensitivity for VAS to optimal muscle force.
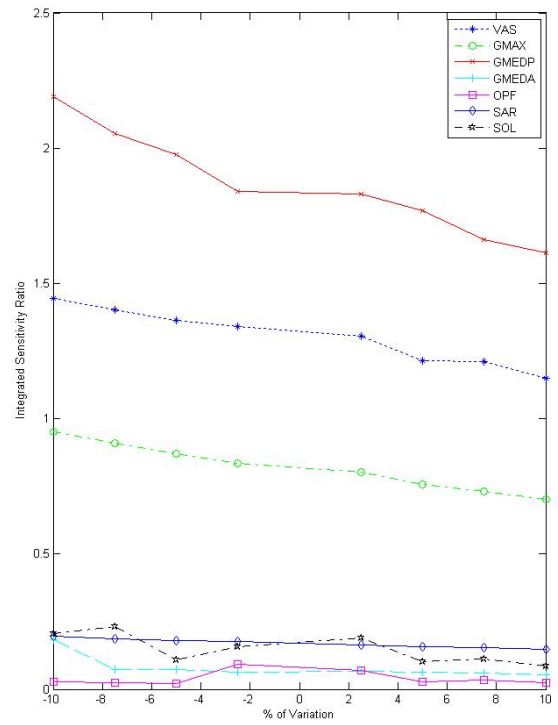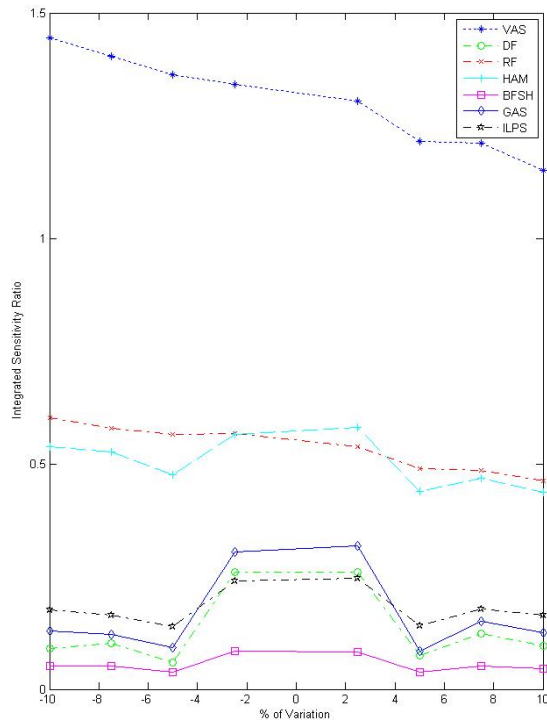
Figure 106: Sensitivity of relevance for VAS to optimal muscle force.
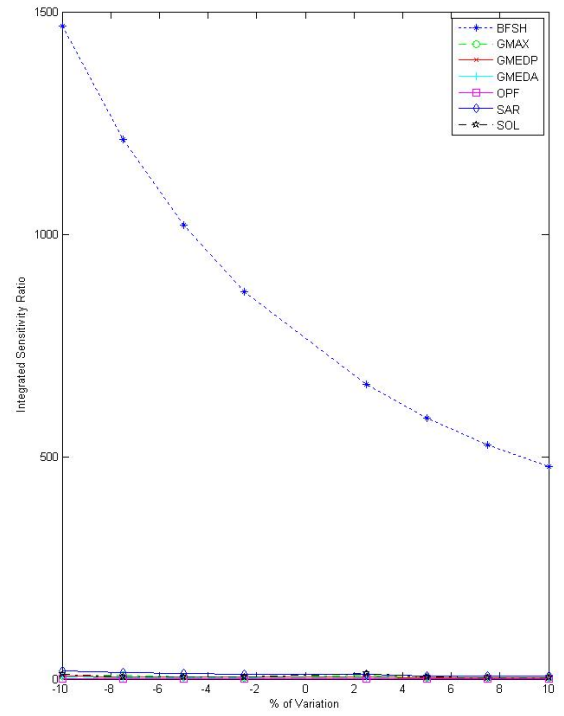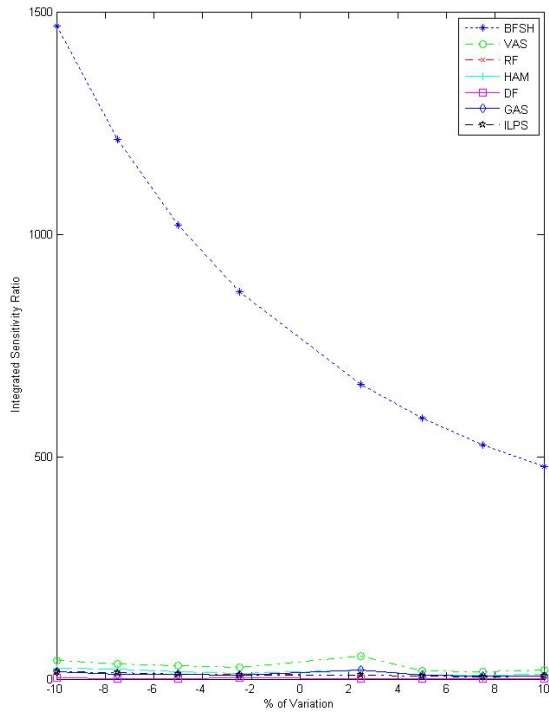
Figure 107: Sensitivity for BFSH to resting fiber length.
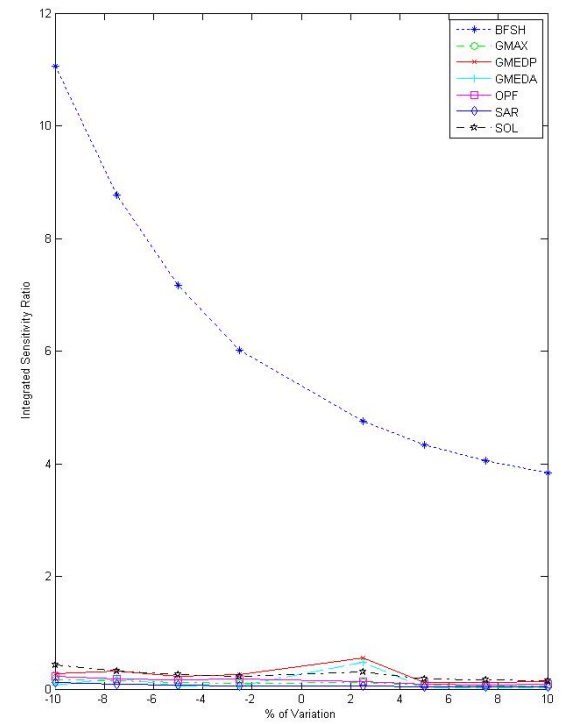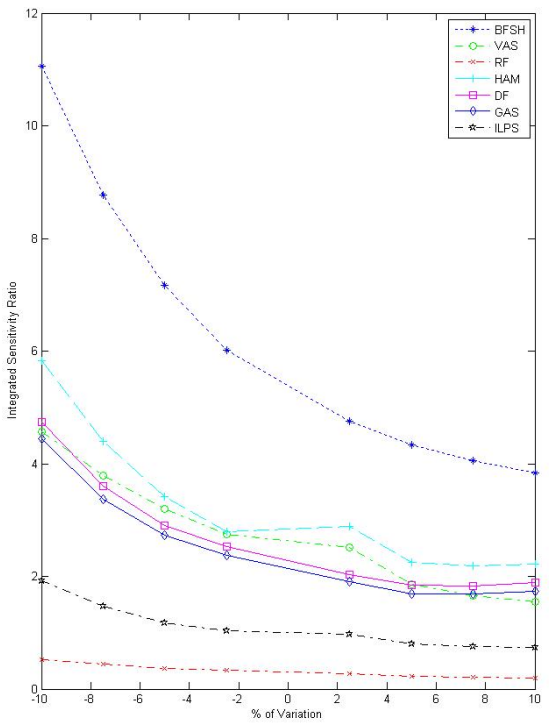
Figure 108: Sensitivity of relevance for BFSH to resting fiber length.
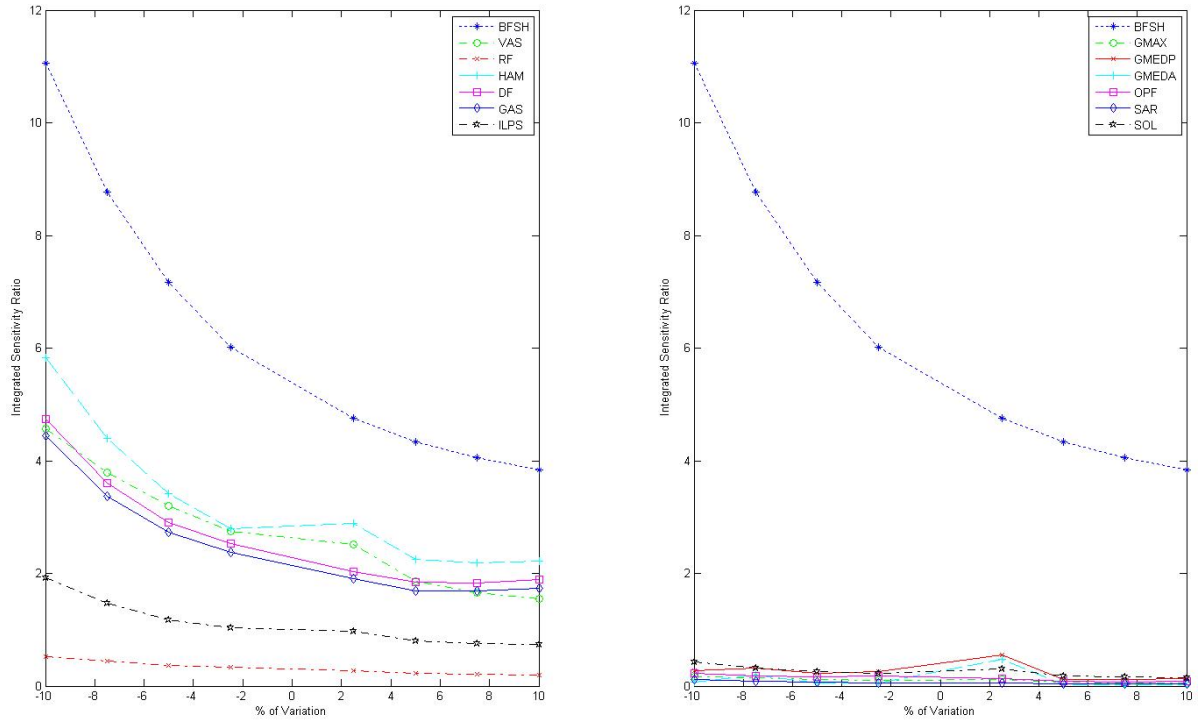
Figure 109: Sensitivity for DF to resting fiber length.
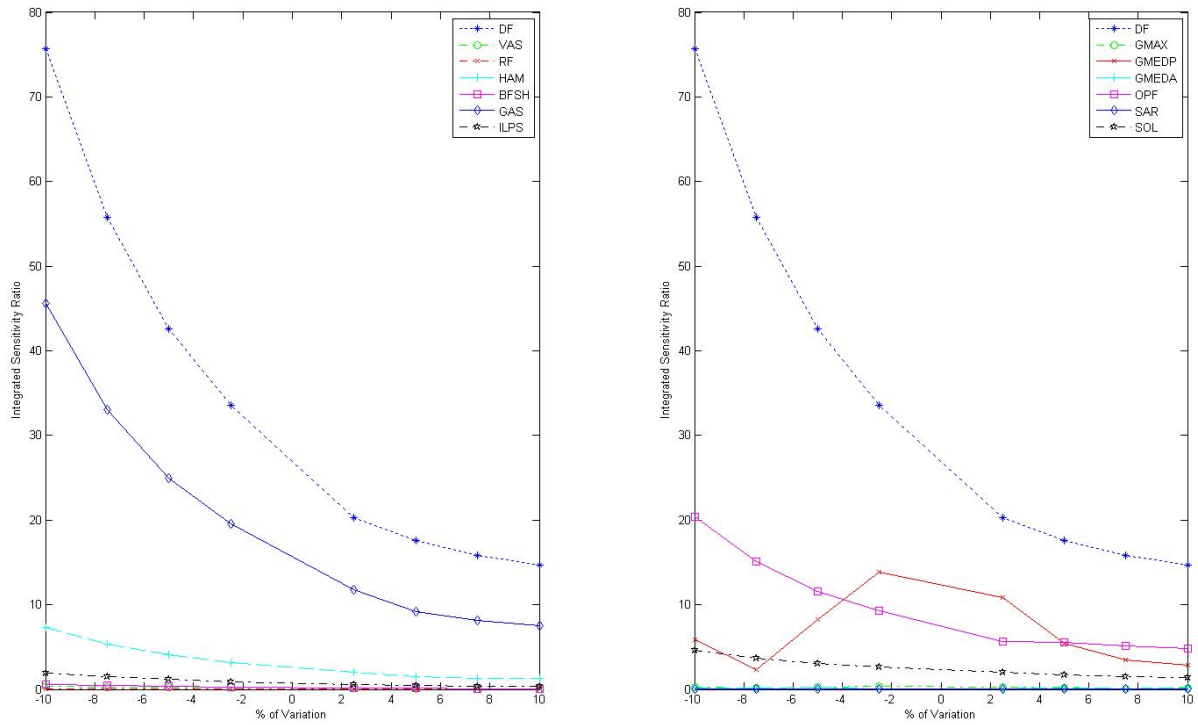
Figure 110: Sensitivity of relevance for DF to resting fiber length.

135
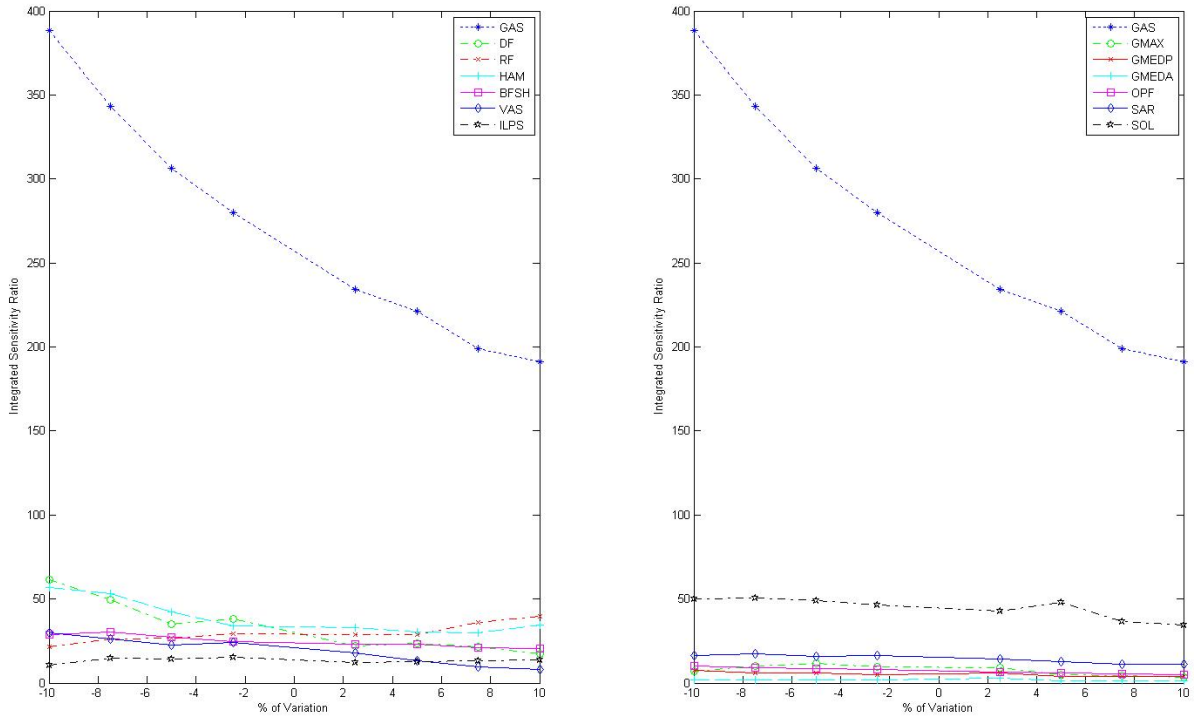
Figure 111: Sensitivity for GAS to resting fiber length.
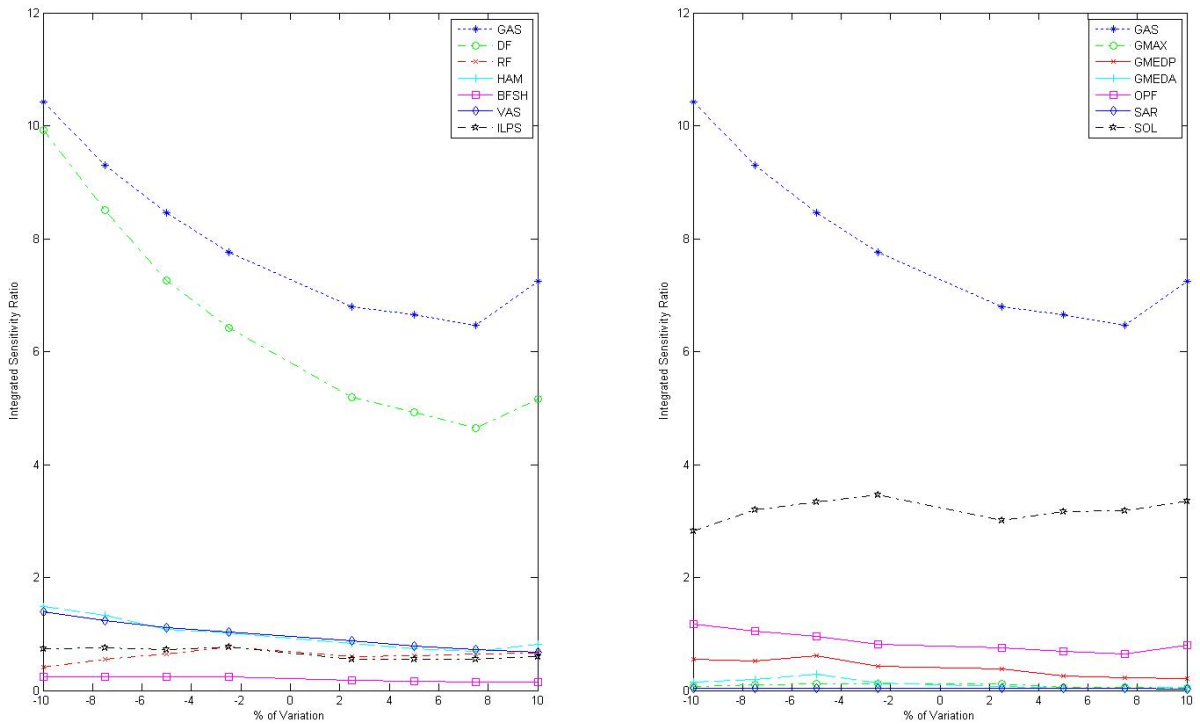
Figure 112: Sensitivity of relevance for GAS to resting fiber length.

136
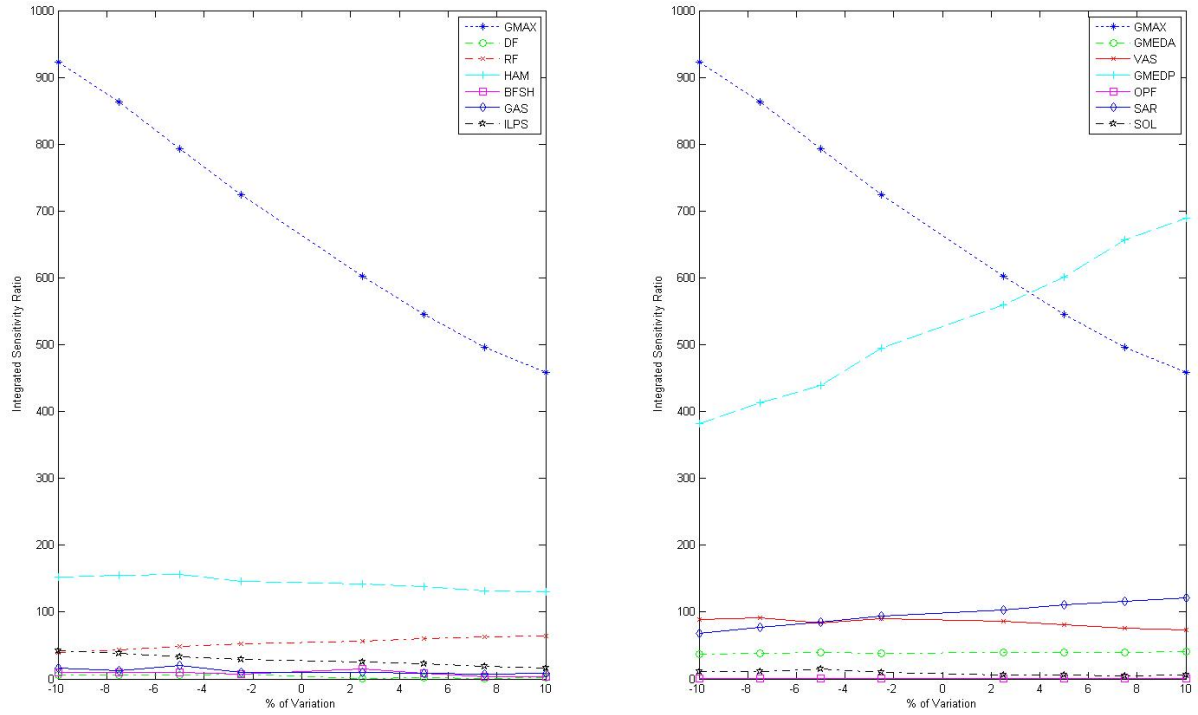
Figure 113: Sensitivity for GMAXL to resting fiber length.
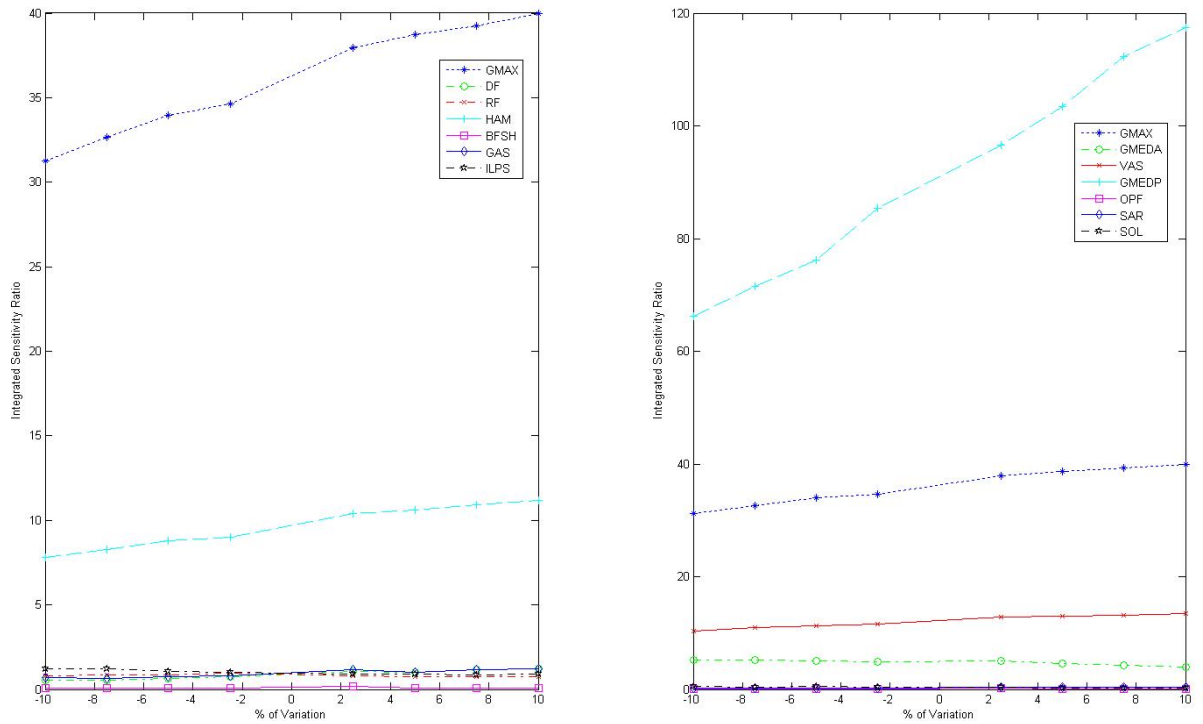
Figure 114: Sensitivity of relevance for GMAXL to resting fiber length.
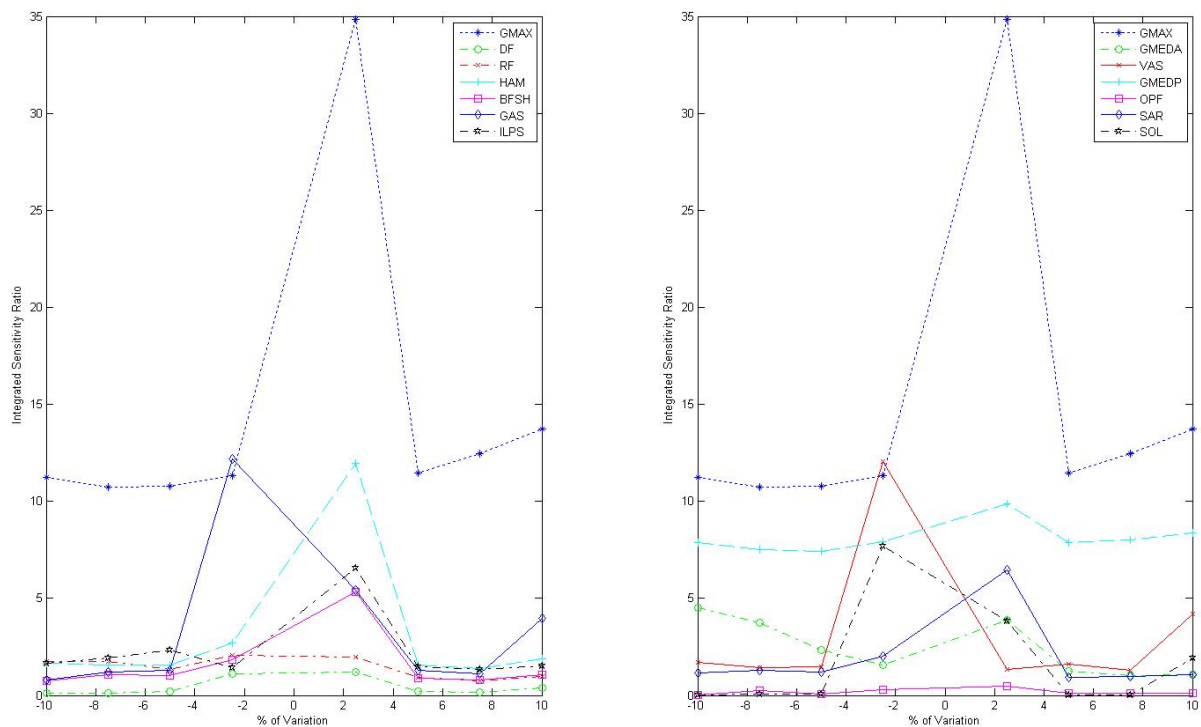
Figure 115: Sensitivity for GMAXM to resting fiber length.
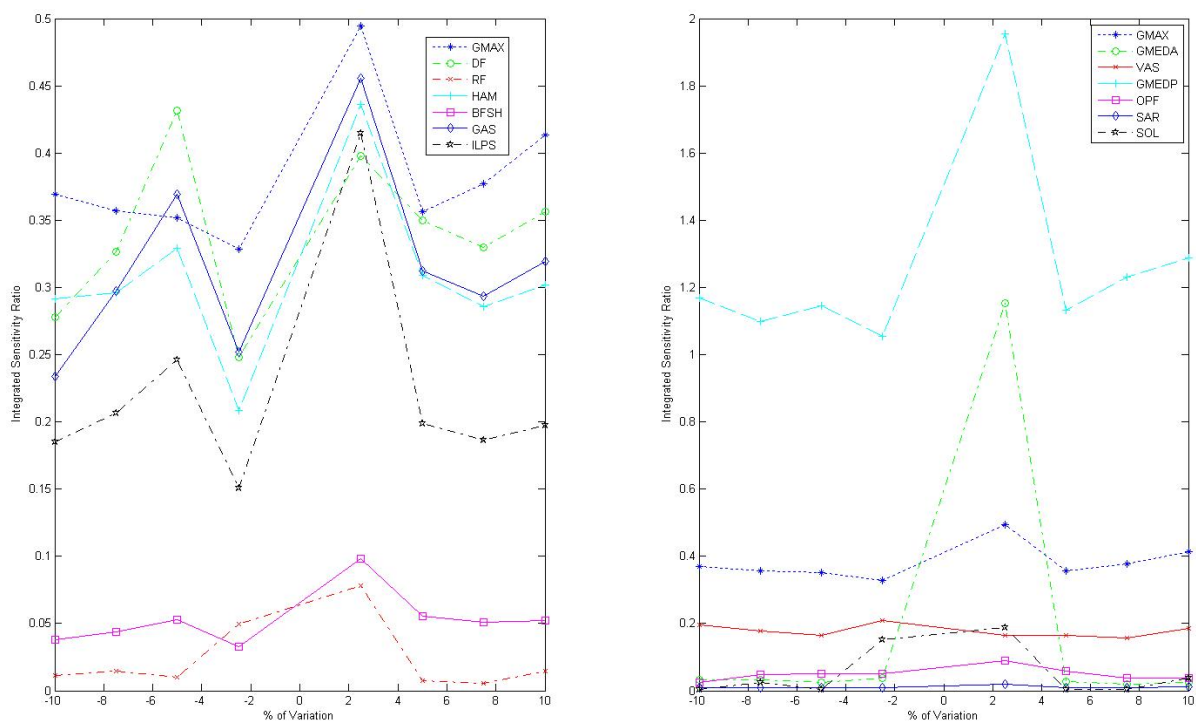
Figure 116: Sensitivity of relevance for GMAXM to resting fiber length.
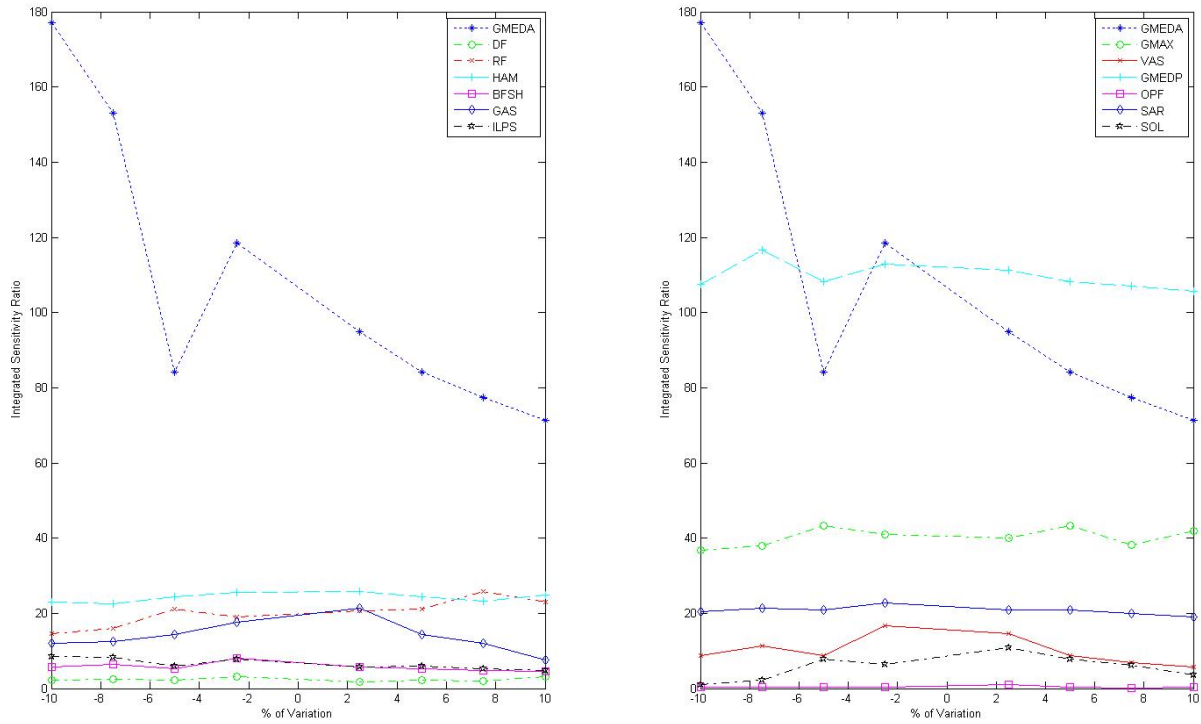
Figure 117: Sensitivity for GMEDA to resting fiber length.
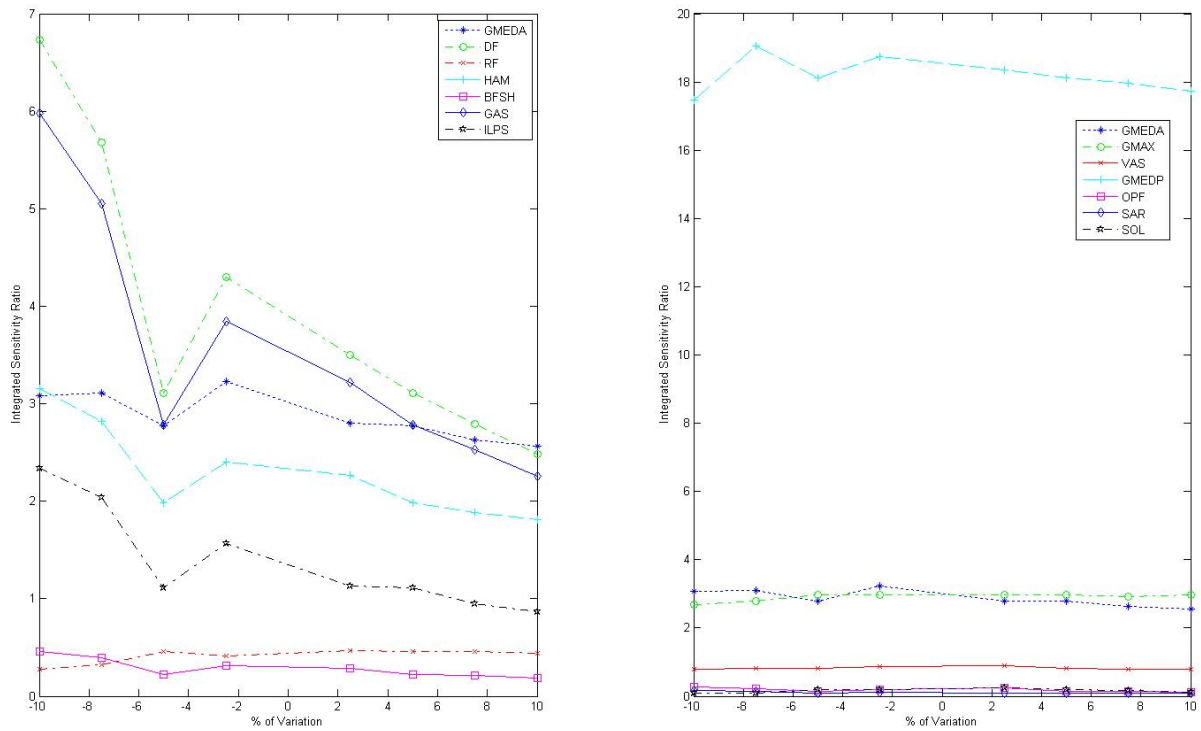
Figure 118: Sensitivity of relevance for GMEDA to resting fiber length.
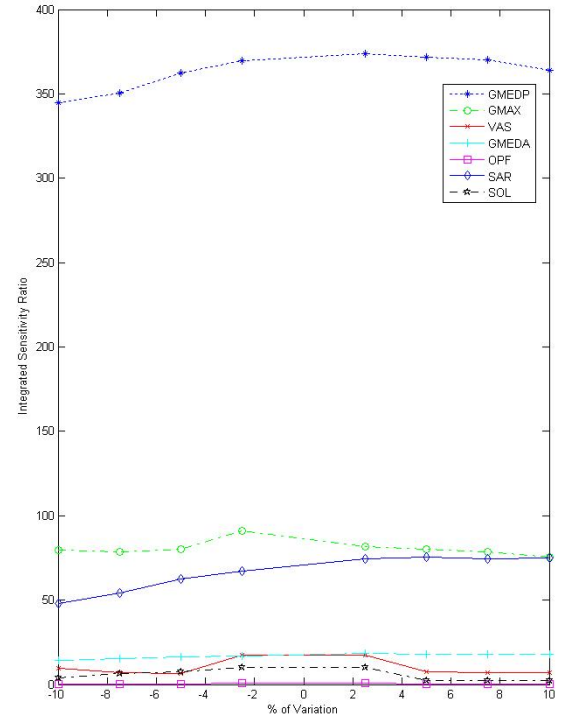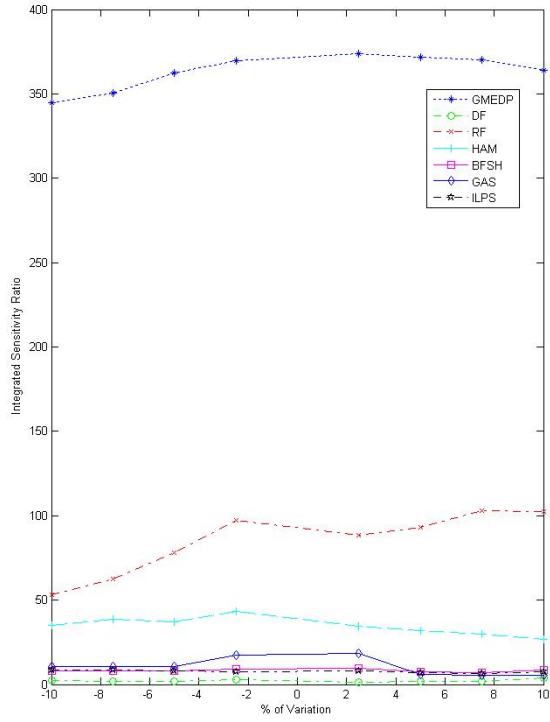
Figure 119: Sensitivity for GMEDP to resting fiber length.
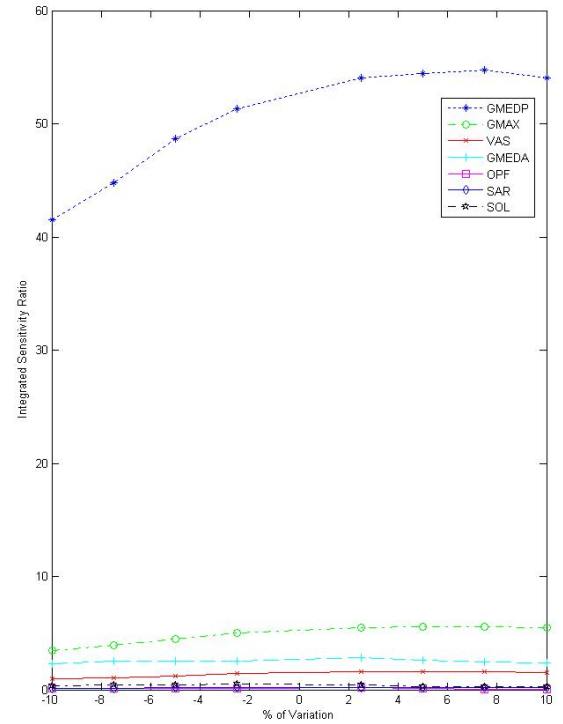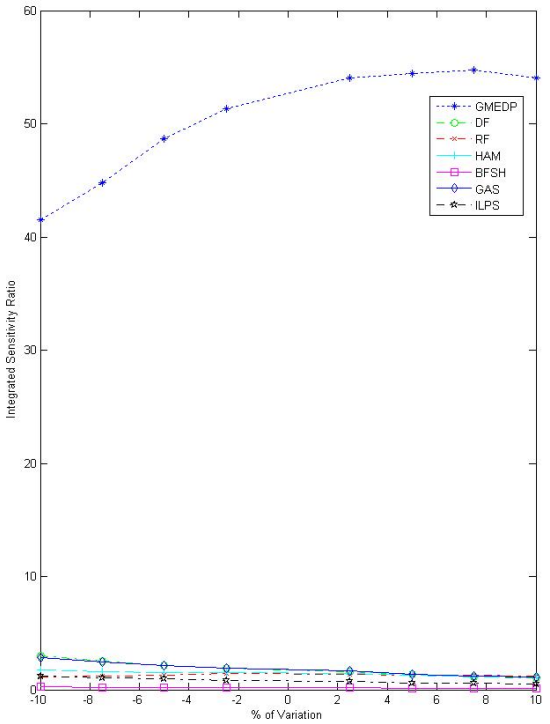
Figure 120: Sensitivity of relevance for GMEDP to resting fiber length.
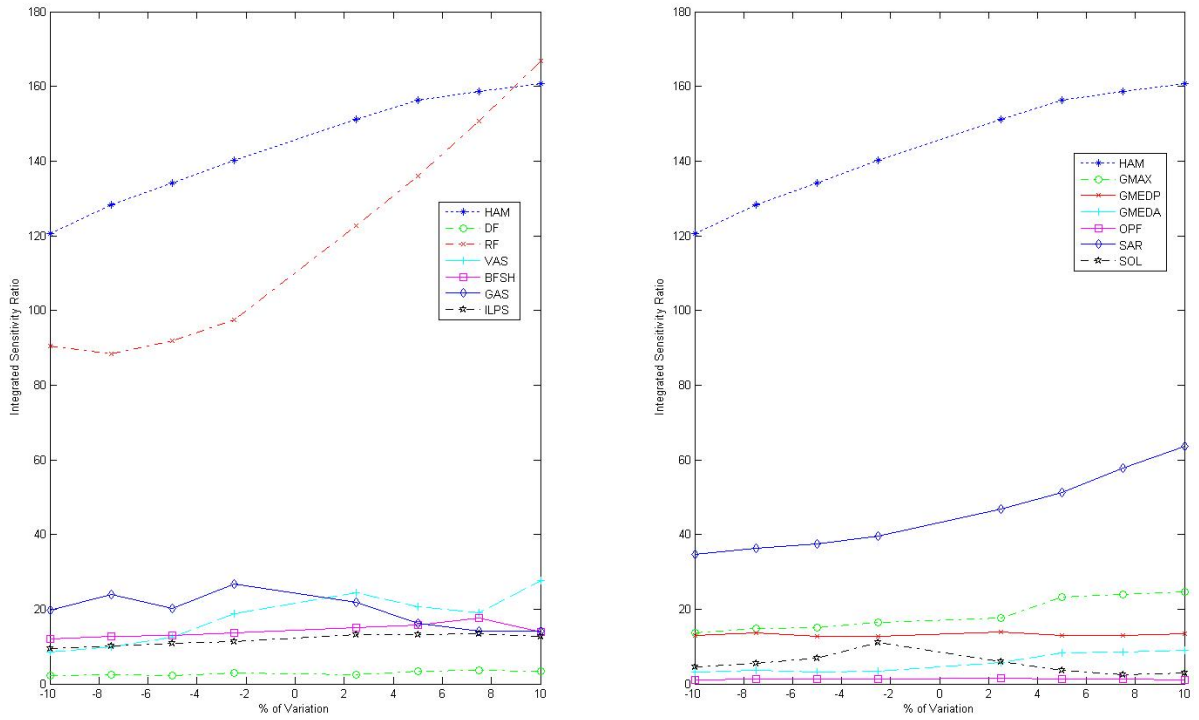
Figure 121: Sensitivity for HAM to resting fiber length.
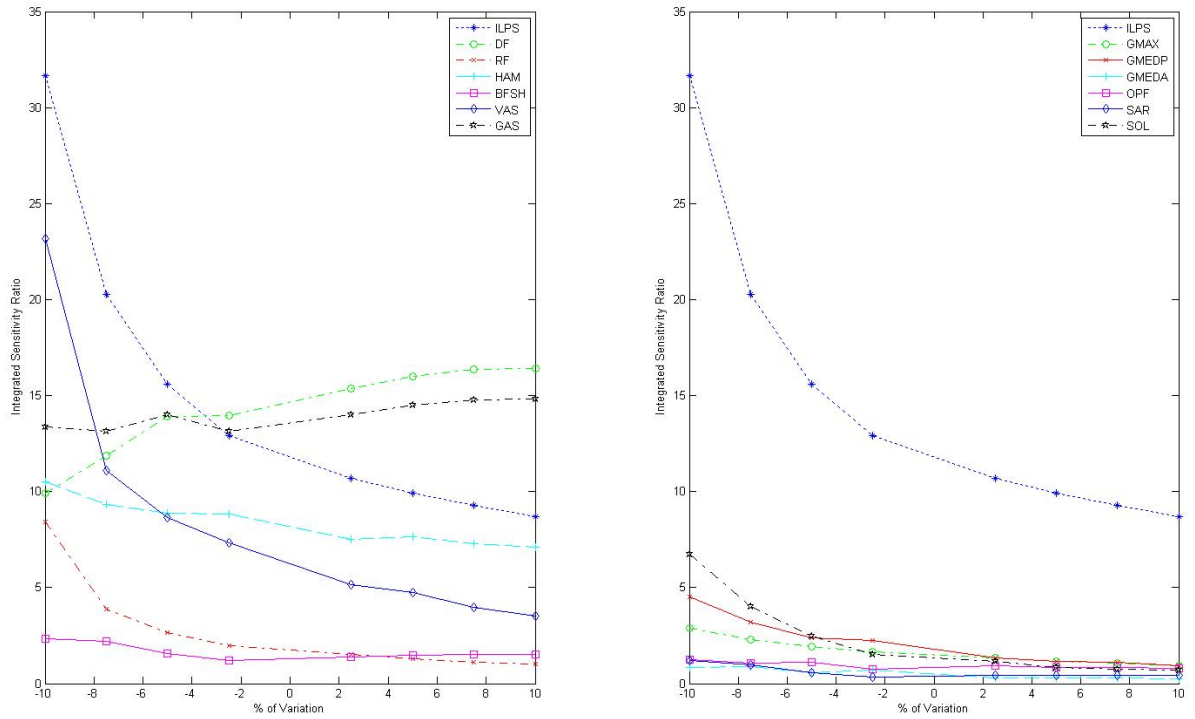
Figure 122: Sensitivity of relevance for HAM to resting fiber length.
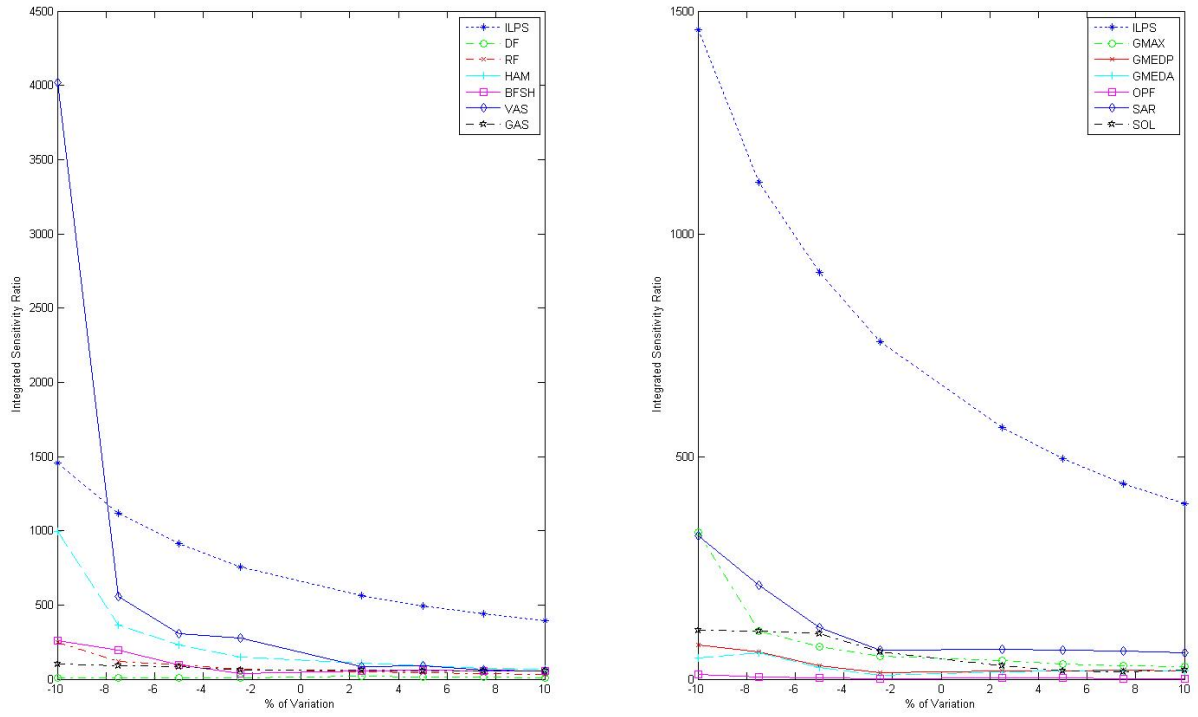
Figure 123: Sensitivity for ILPSO to resting fiber length.
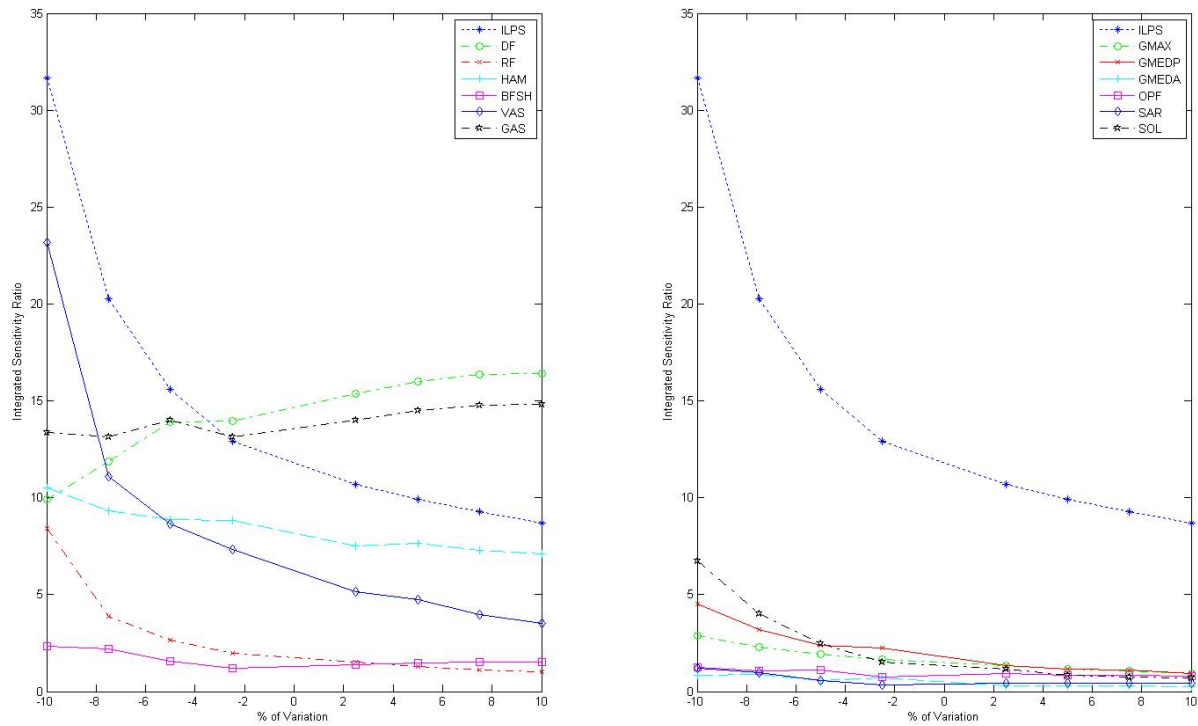
Figure 124: Sensitivity of relevance for ILPSO to resting fiber length.
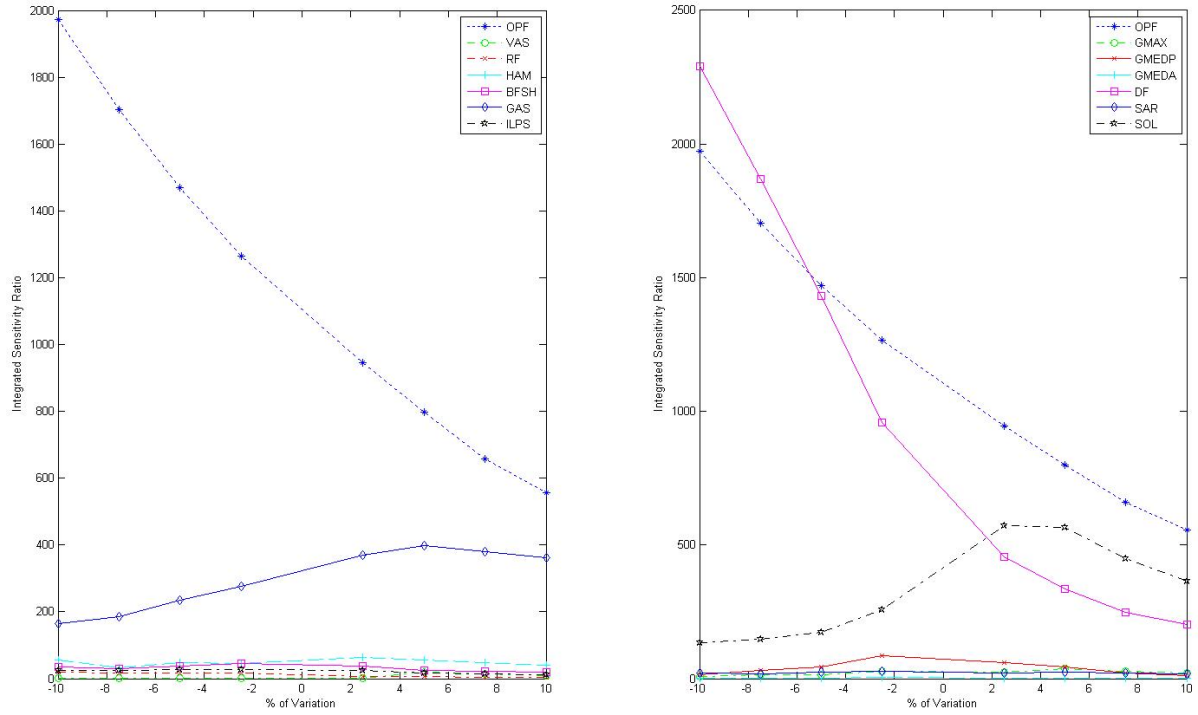
Figure 125: Sensitivity for OPF to resting fiber length.
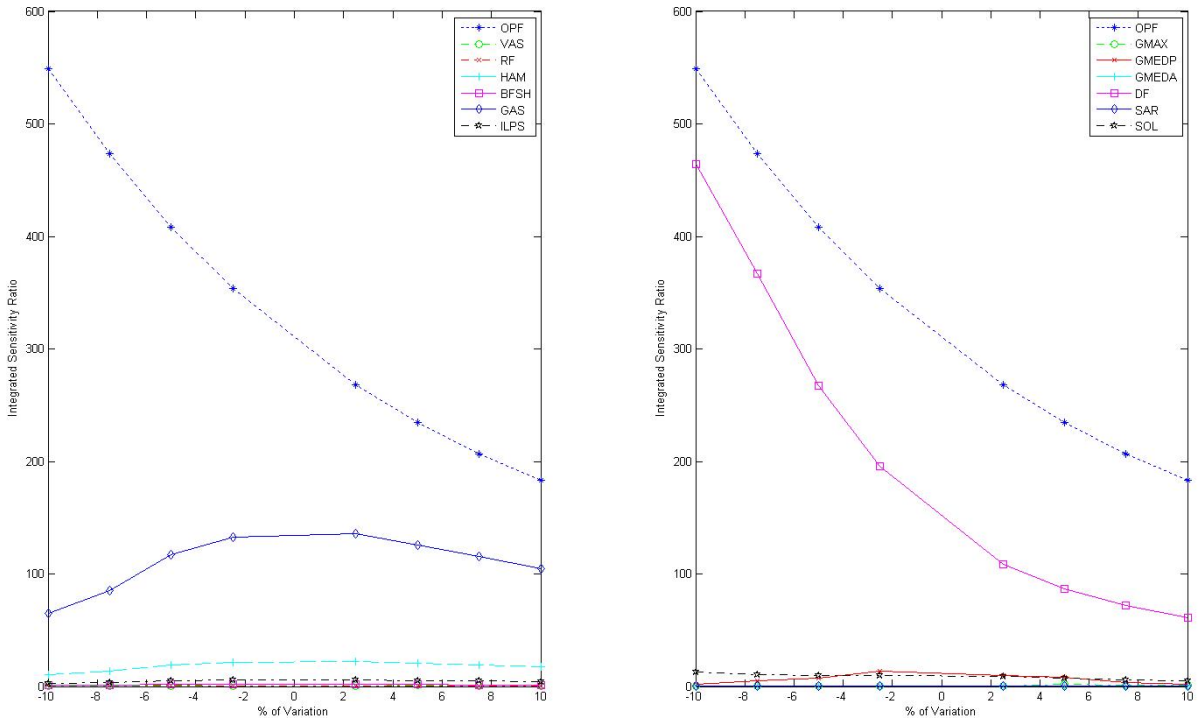
Figure 126: Sensitivity of relevance for OPF to resting fiber length.
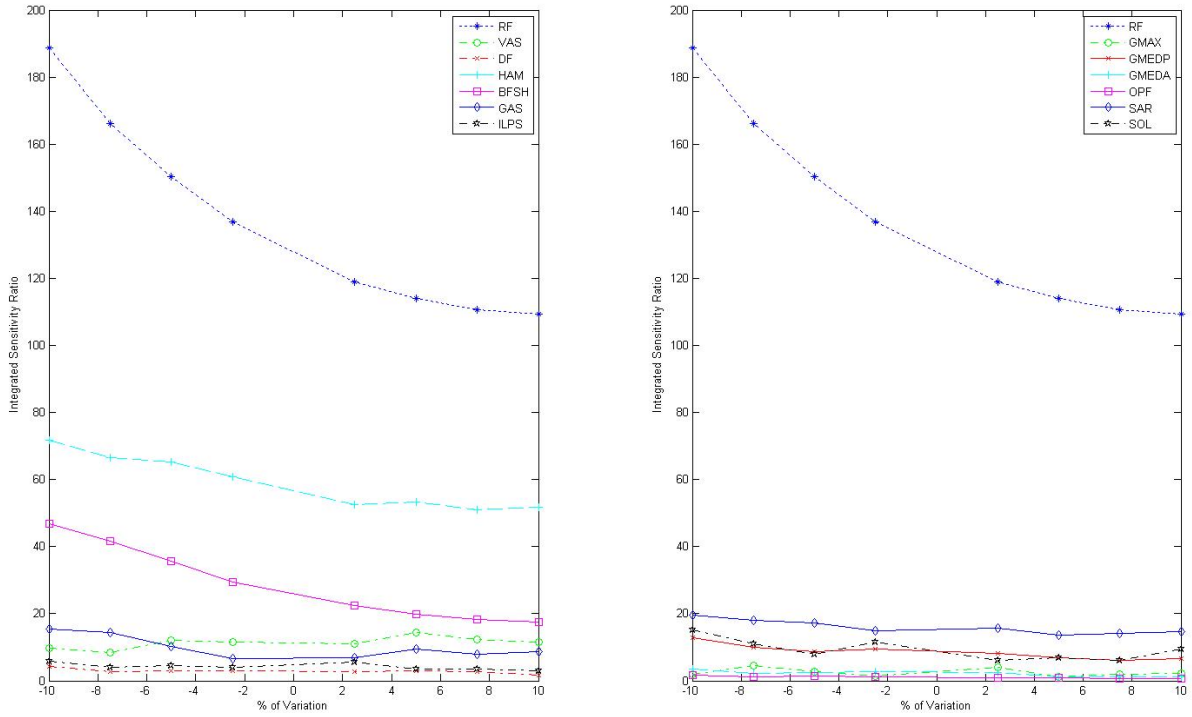
Figure 127: Sensitivity for OPF to resting fiber length.
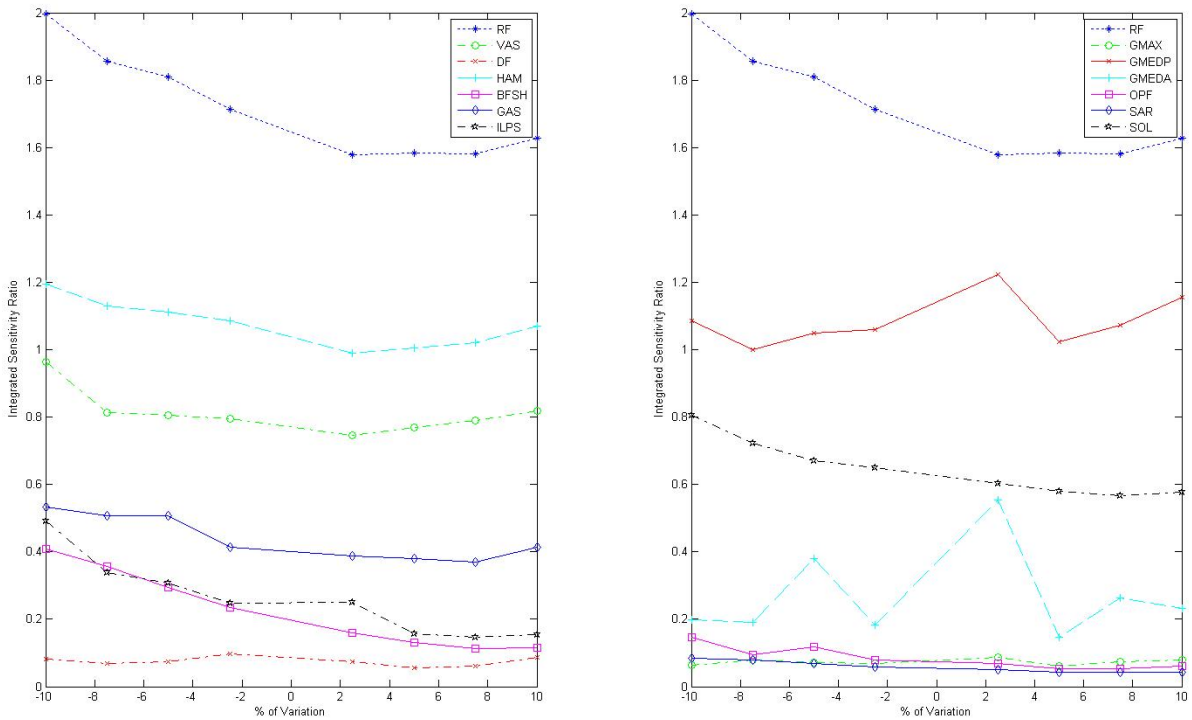
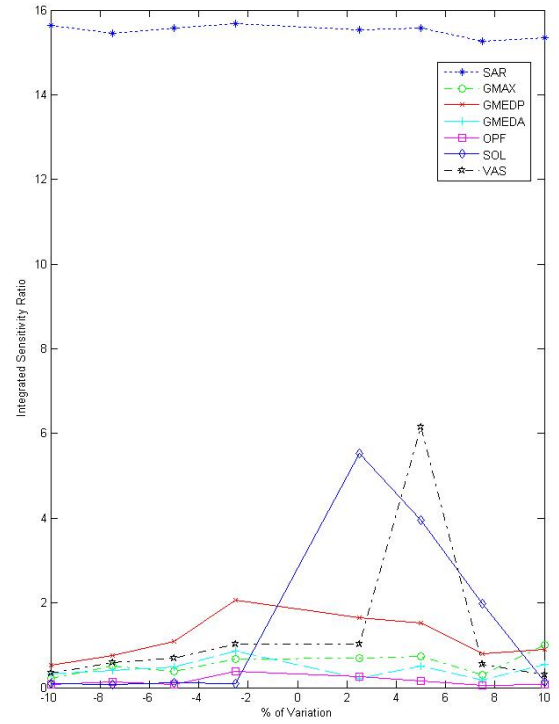Figure 128: Sensitivity of relevance for RF to resting fiber length.

144
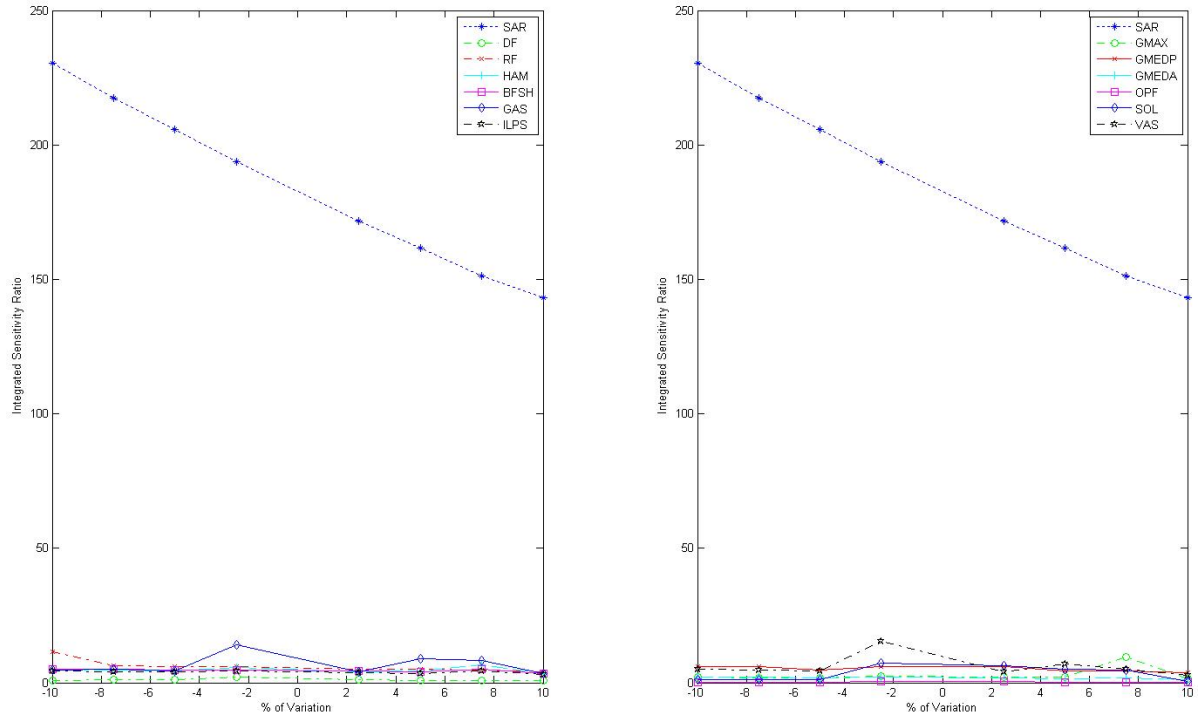
Figure 129: Sensitivity for SAR to resting fiber length.
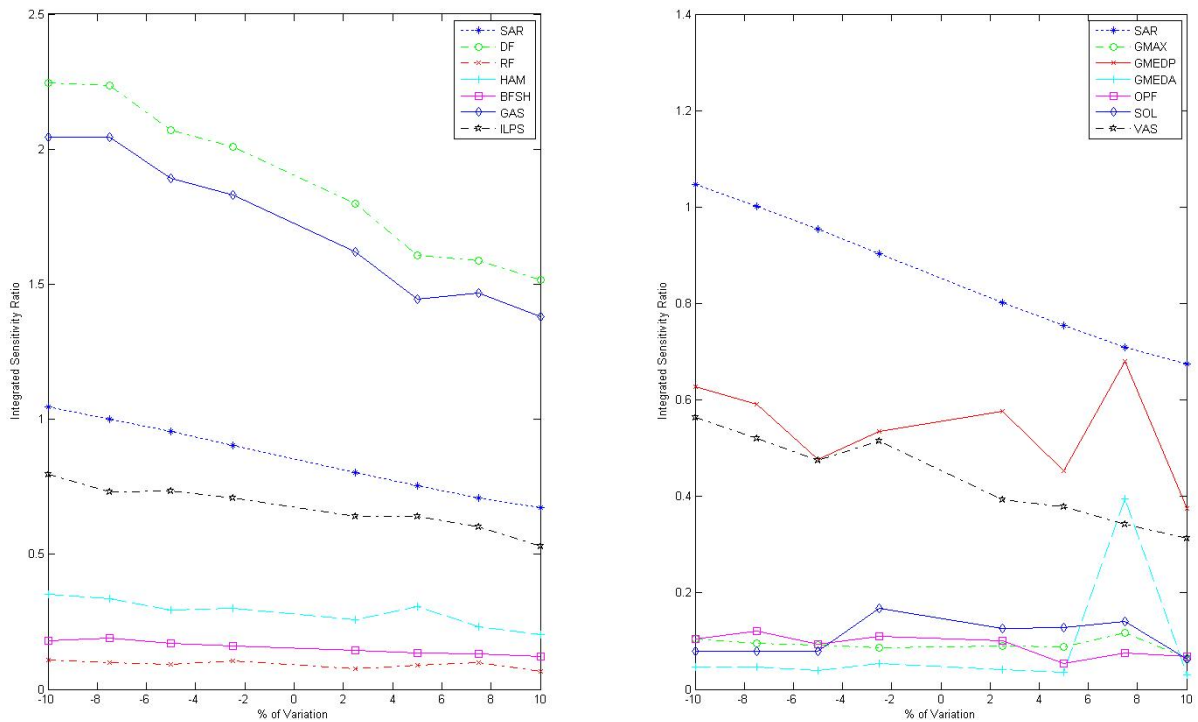
Figure 130: Sensitivity of relevance for SAR to resting fiber length.
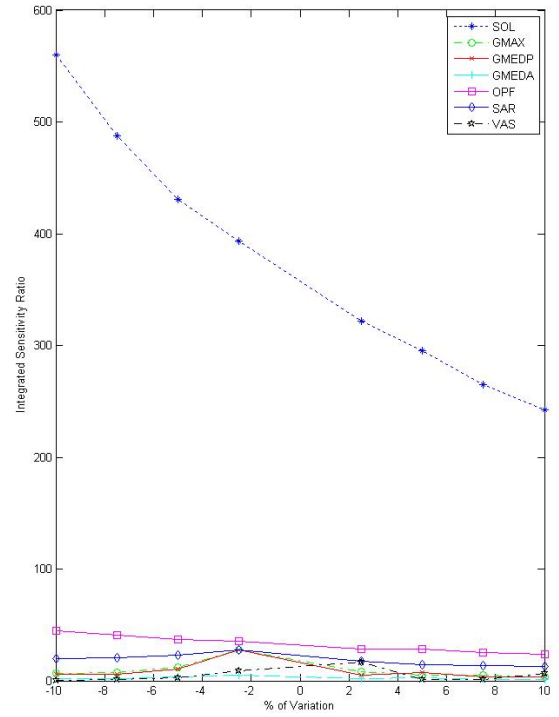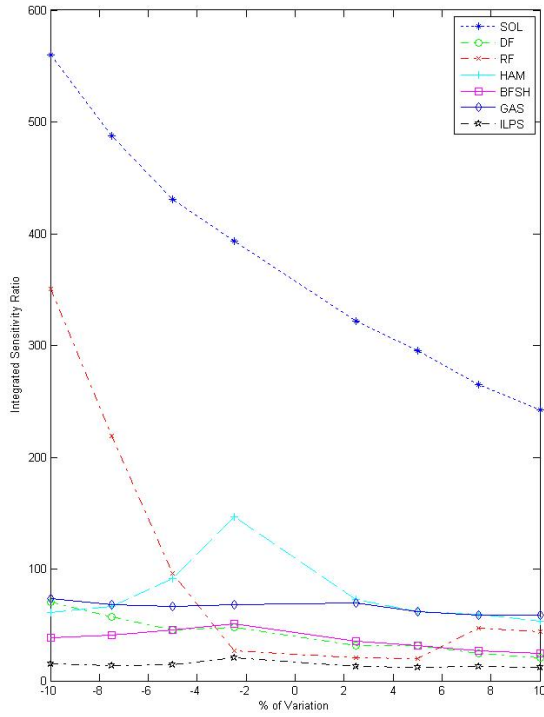
Figure 131: Sensitivity for SOL to resting fiber length.
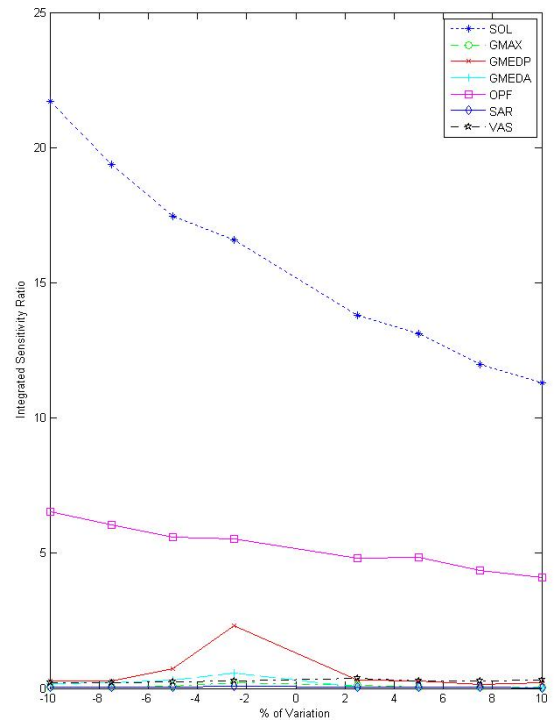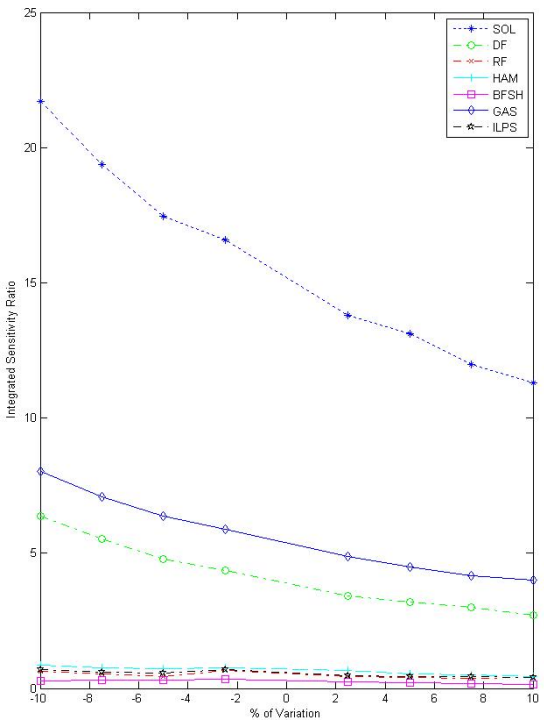
Figure 132: Sensitivity of relevance for SOL to resting fiber length.
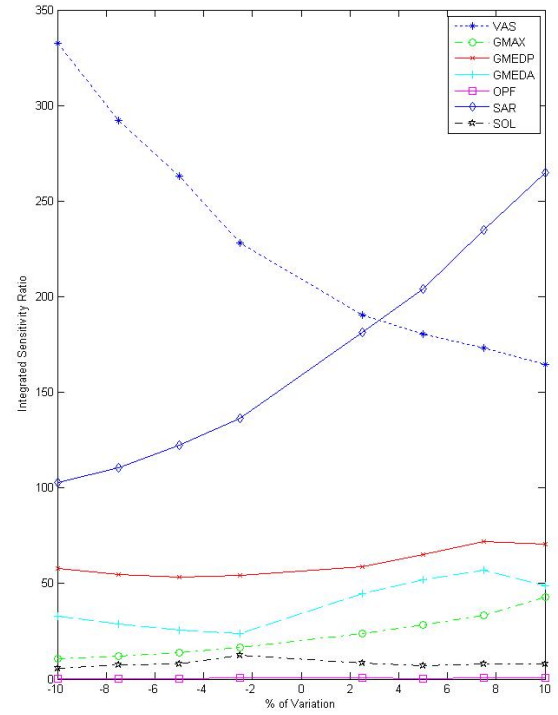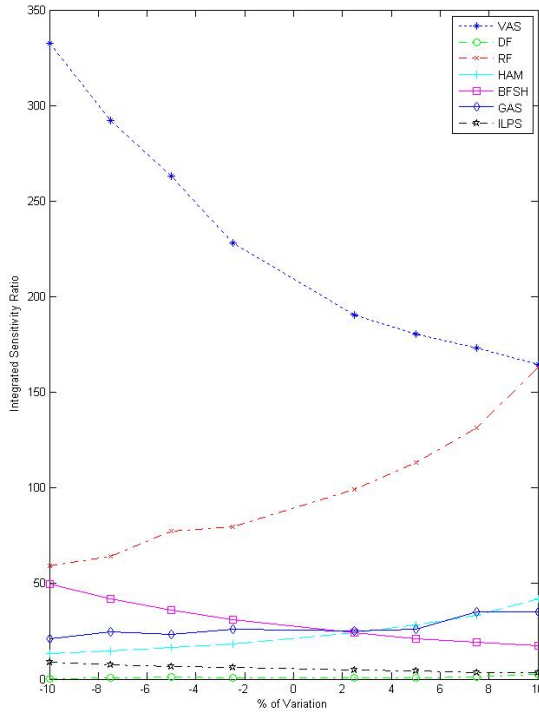
Figure 133: Sensitivity for VAS to resting fiber length.
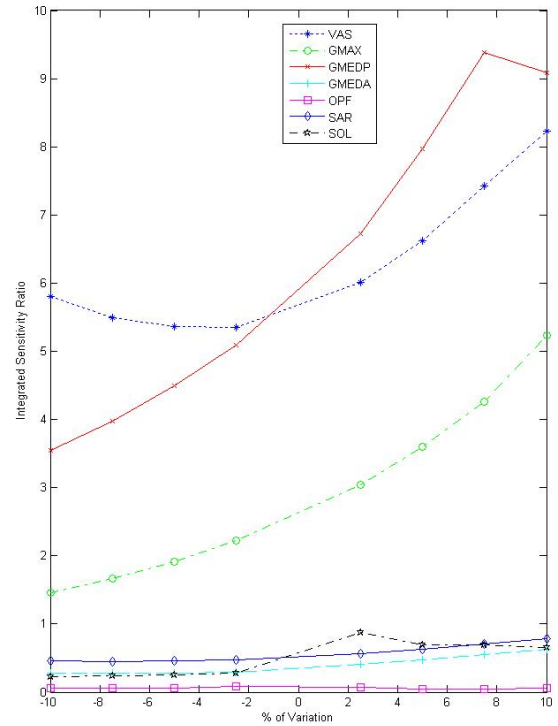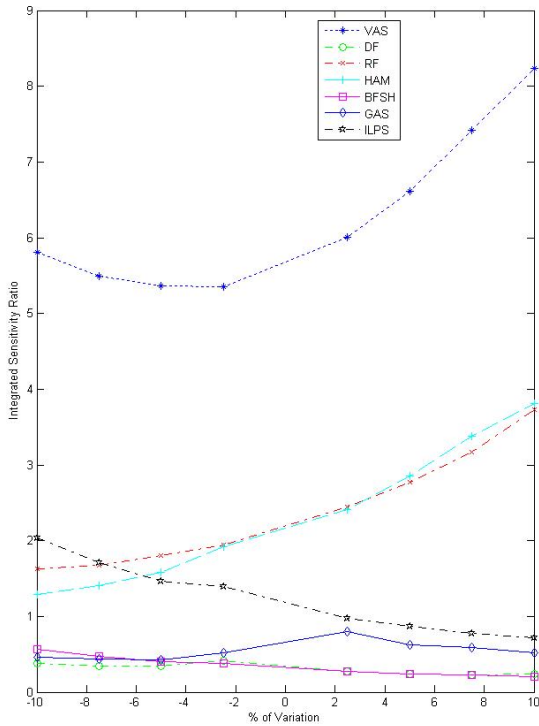
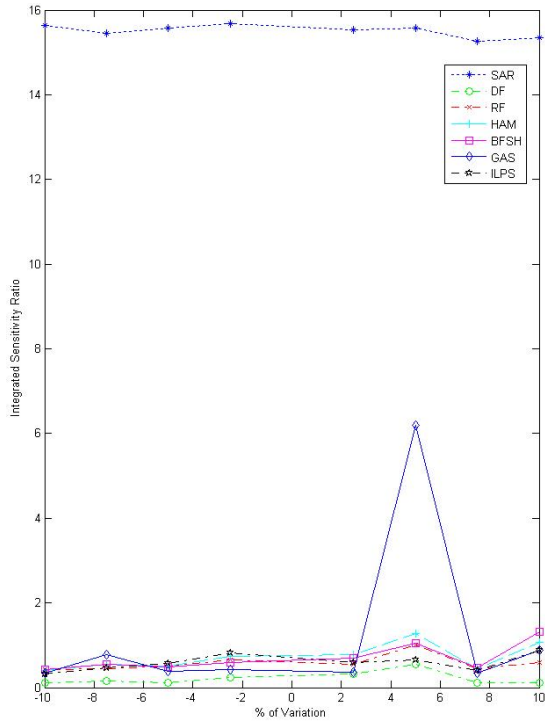Figure 134: Sensitivity of relevance for VAS to resting fiber length.

147
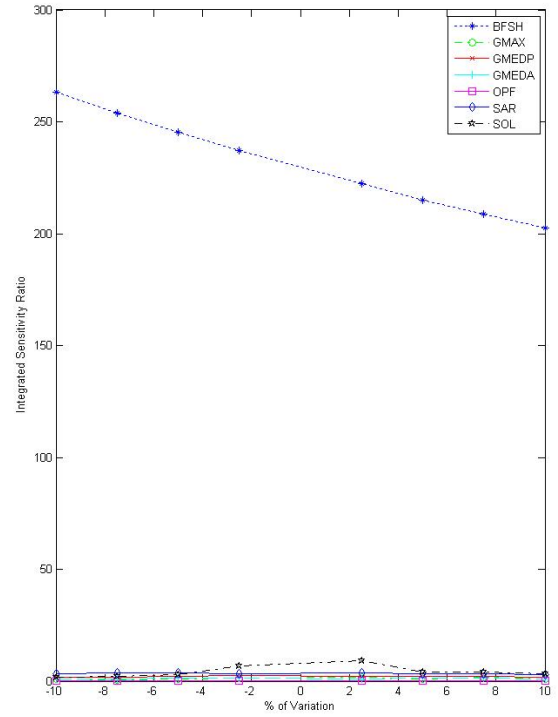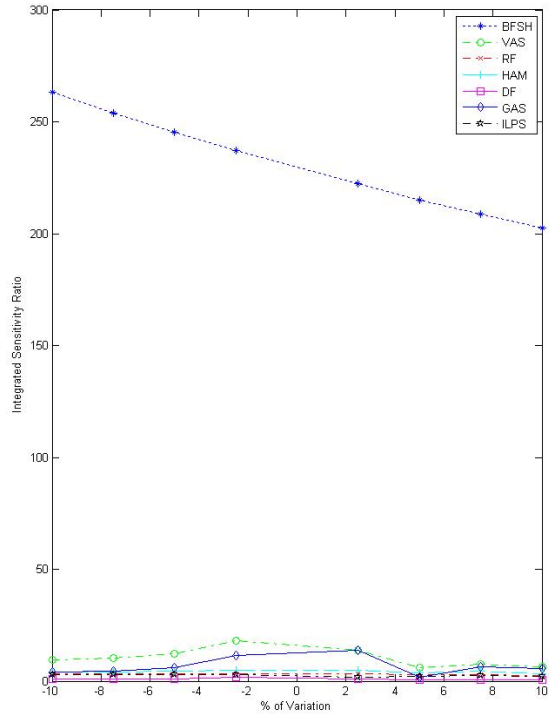
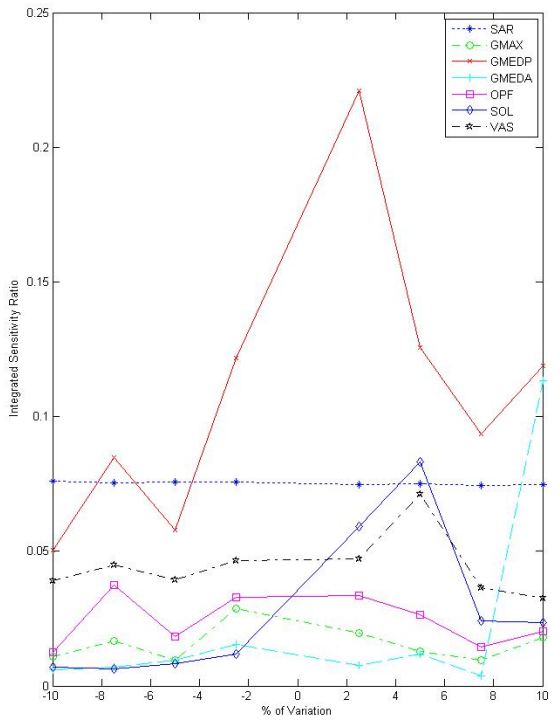Figure 135: Sensitivity for BFSH to tendon slack length.
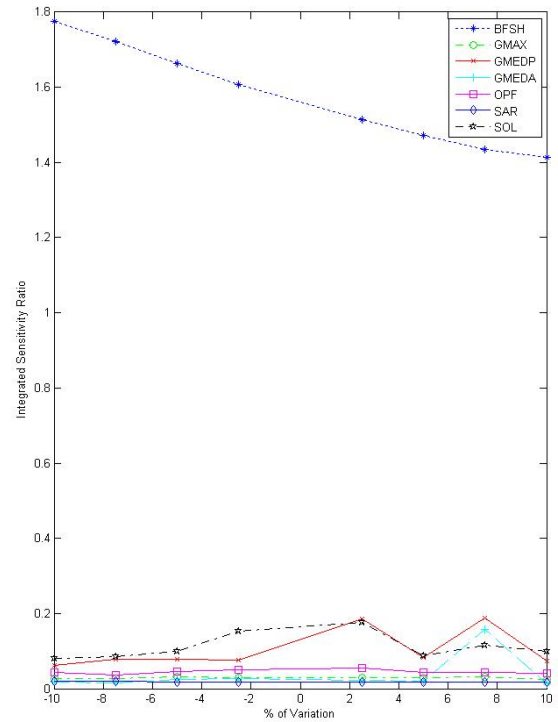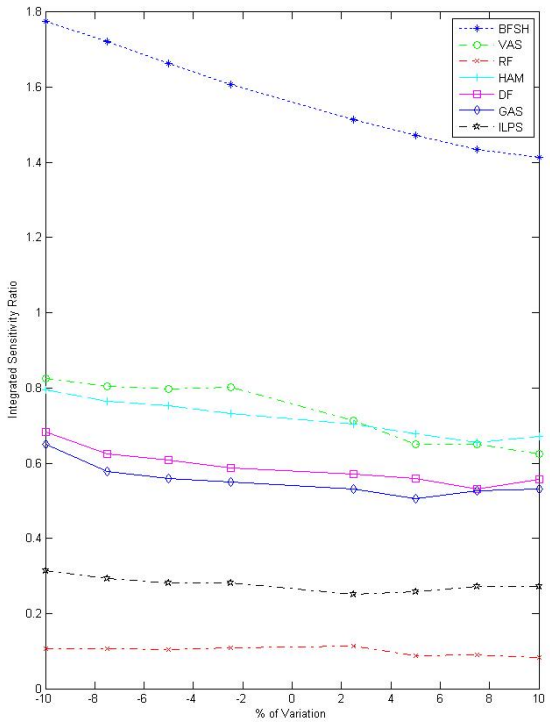
Figure 136: Sensitivity of relevance for BFSH to tendon slack length.

148
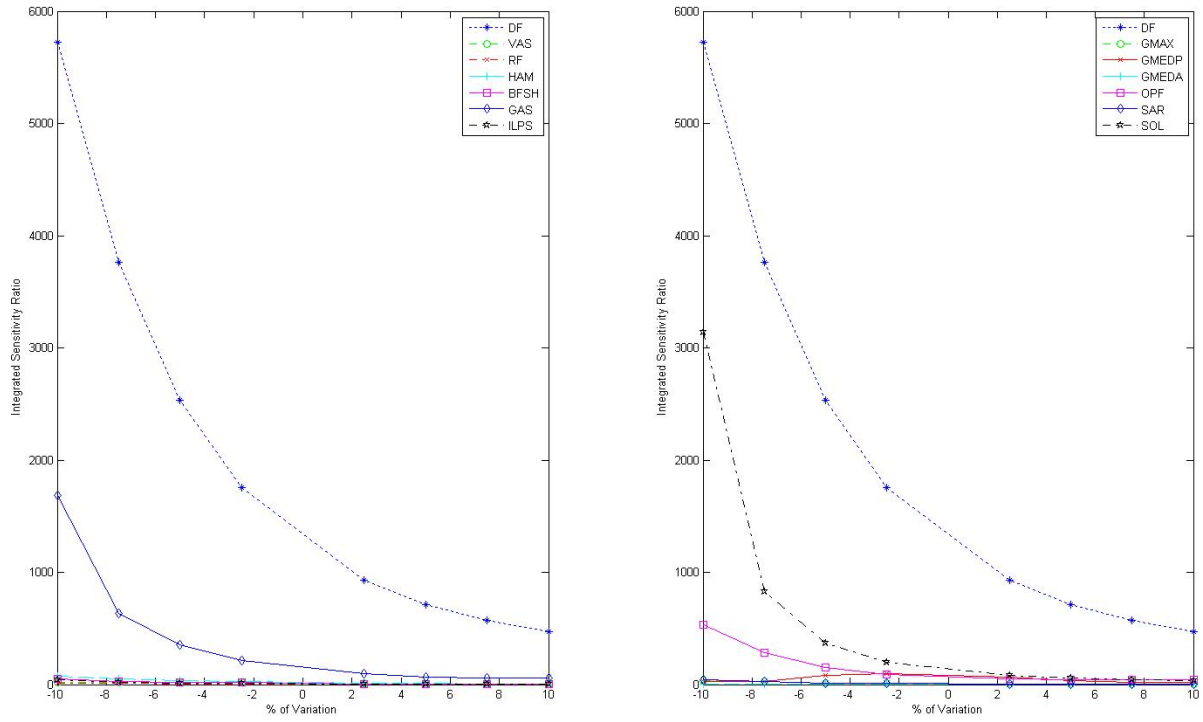
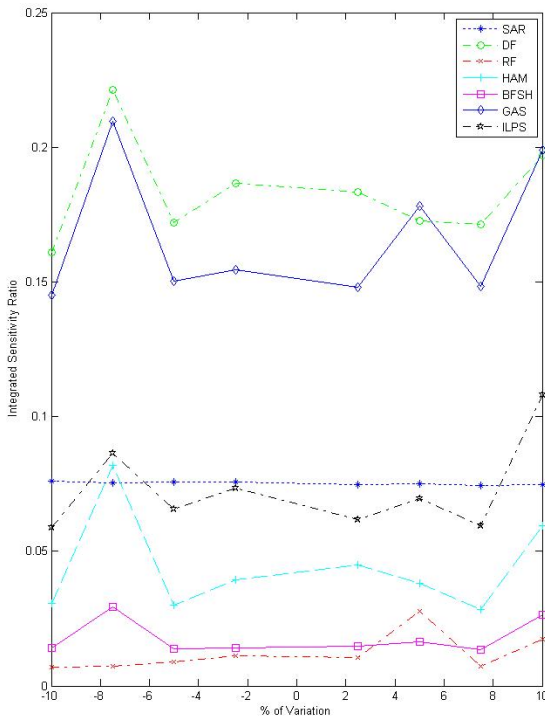Figure 137: Sensitivity for DF to tendon slack length.
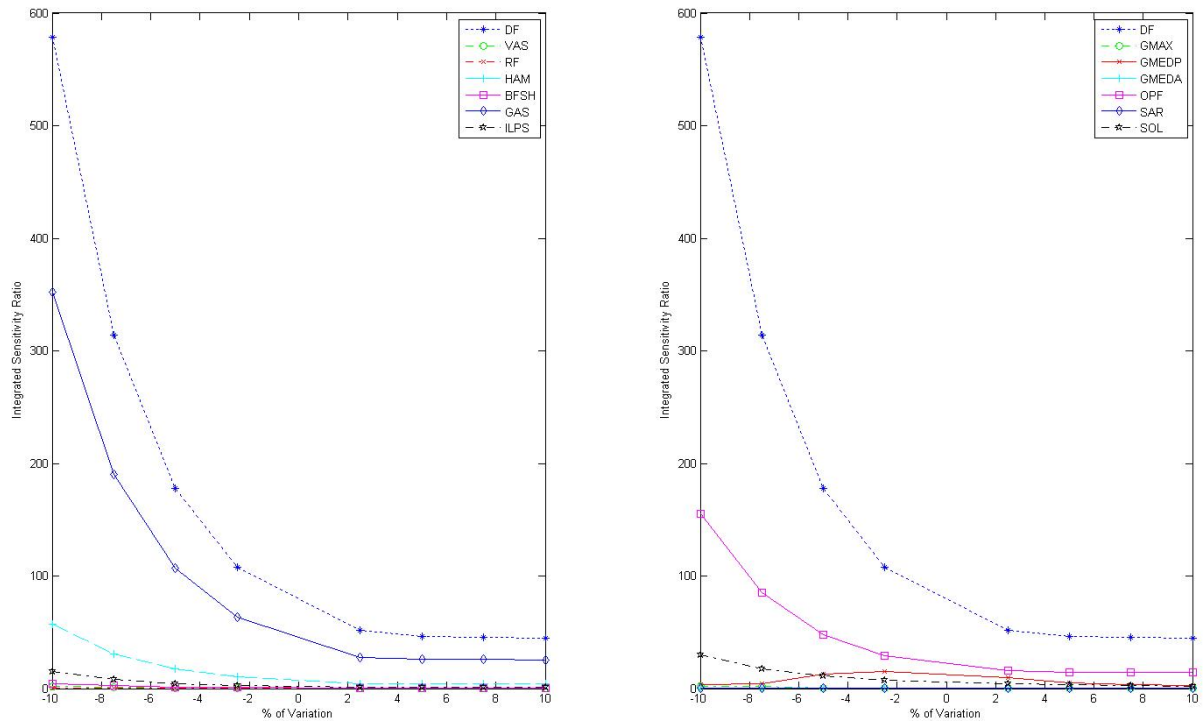
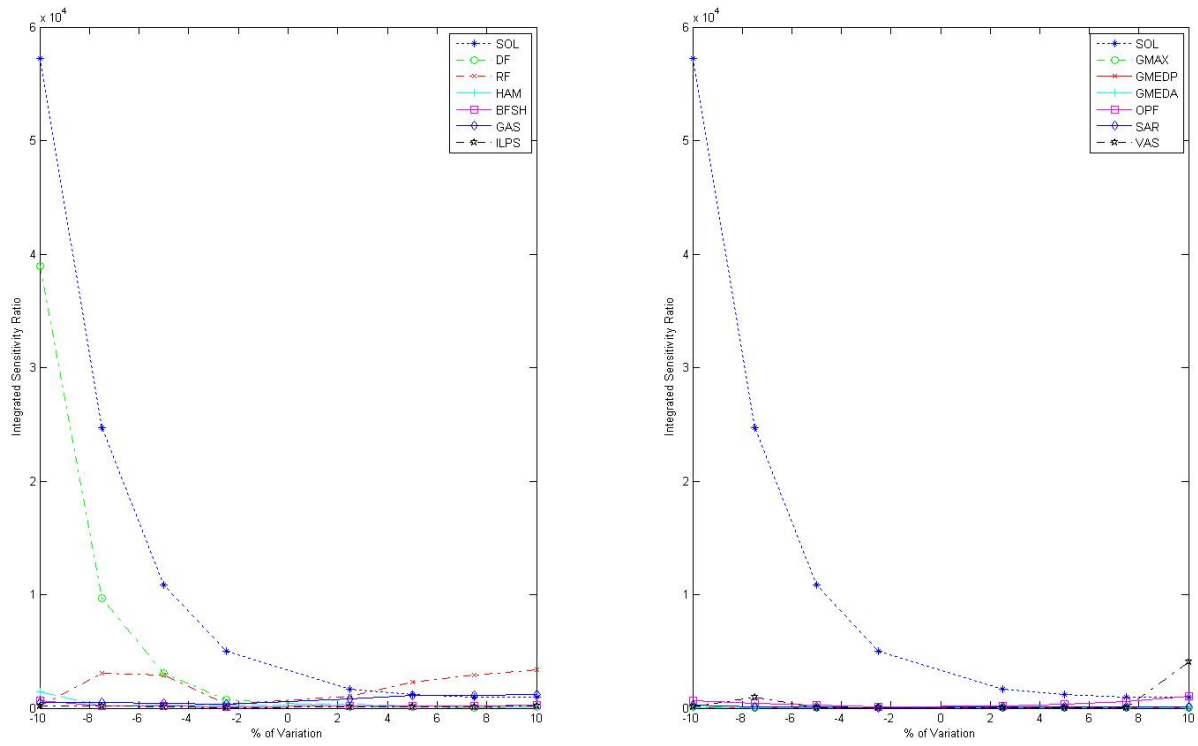Figure 138: Sensitivity of relevance for DF to tendon slack length.

149
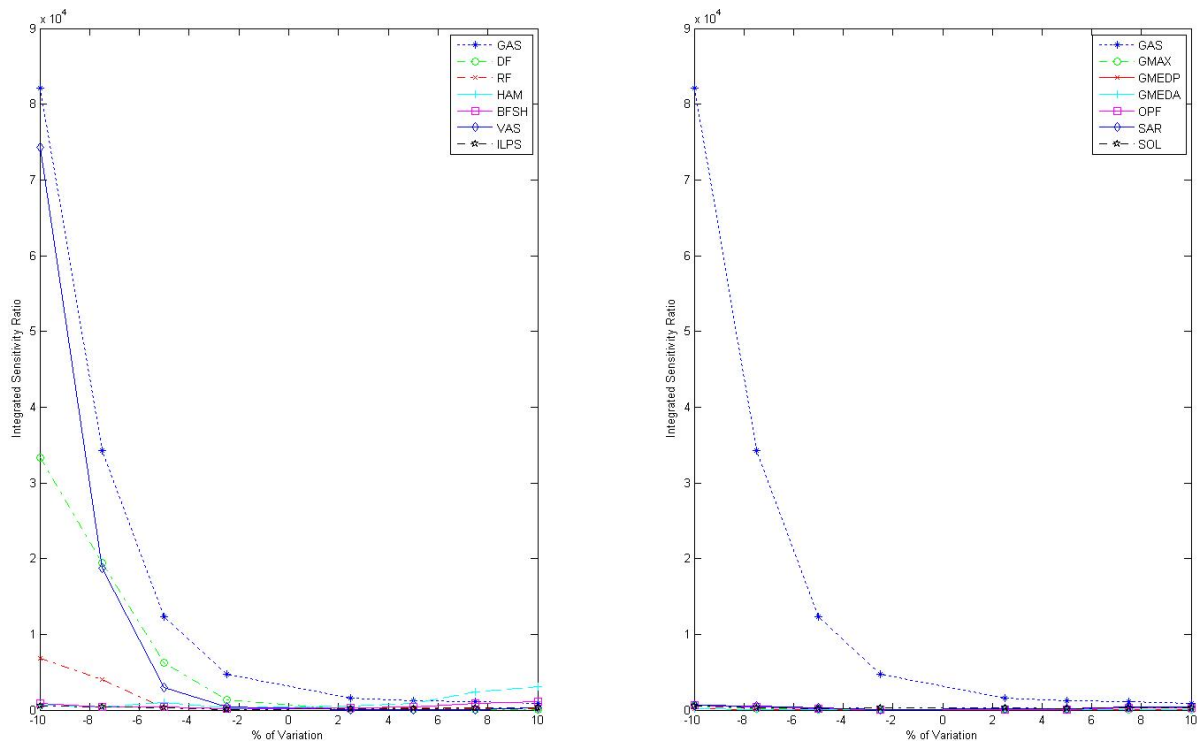
Figure 139: Sensitivity for GAS to tendon slack length.
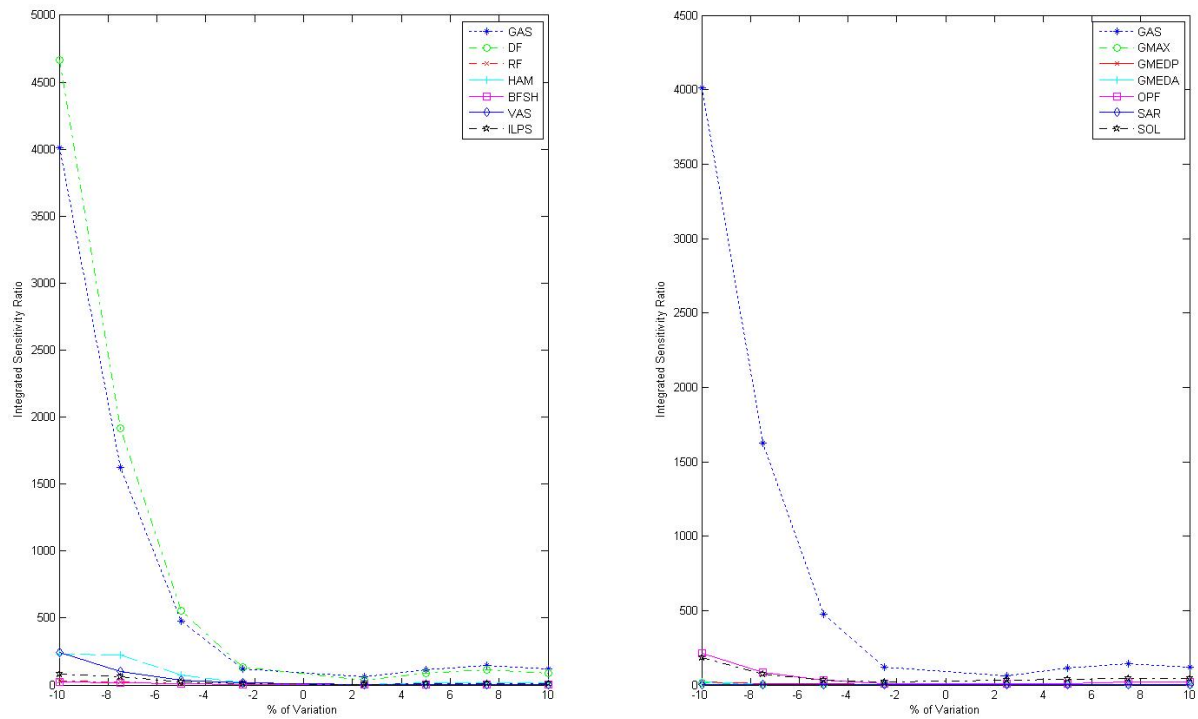
Figure 140: Sensitivity of relevance for GAS to tendon slack length.

150
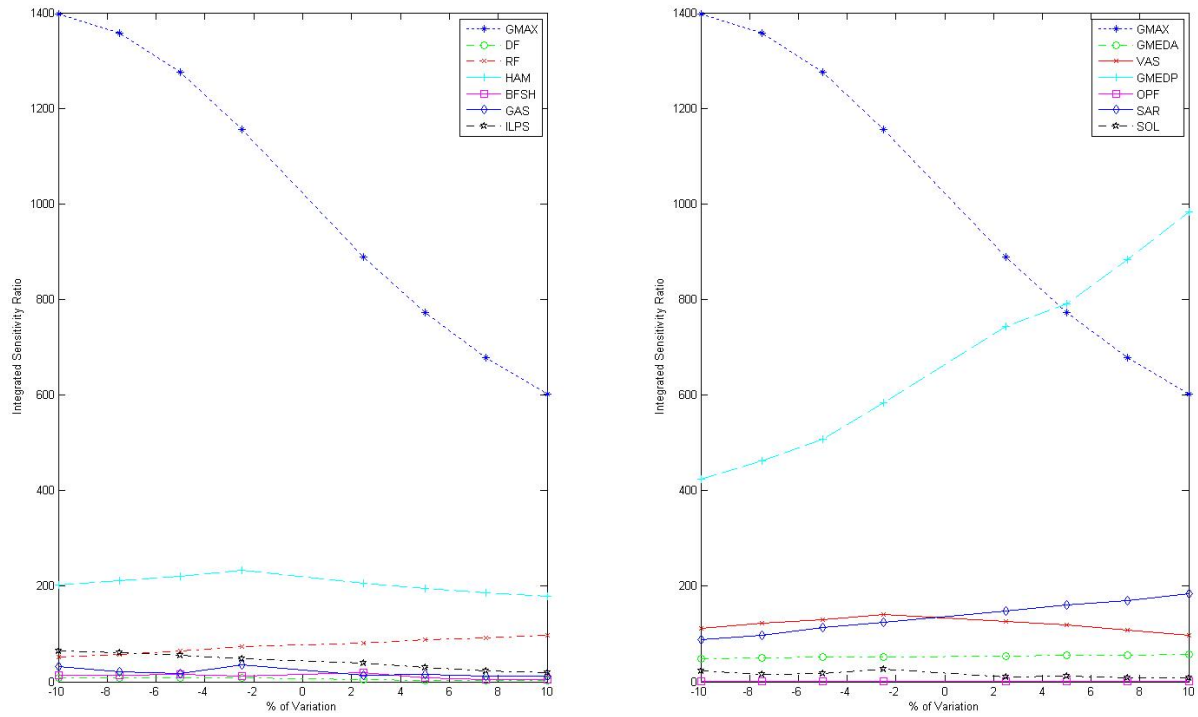
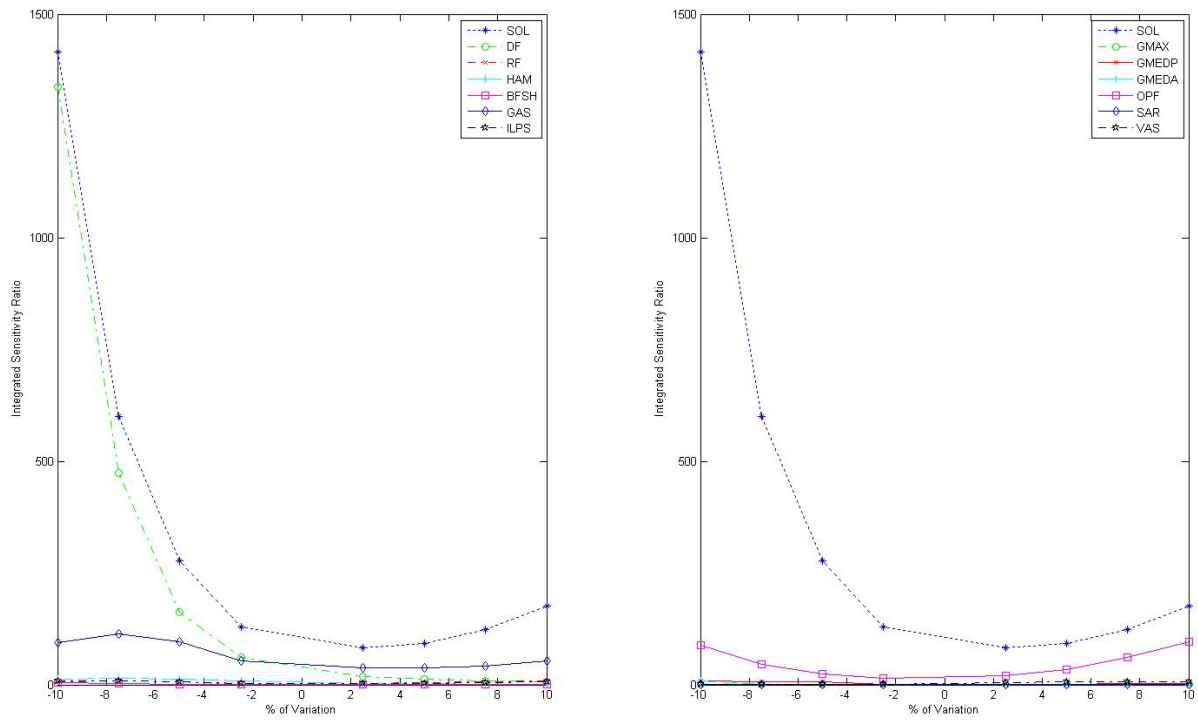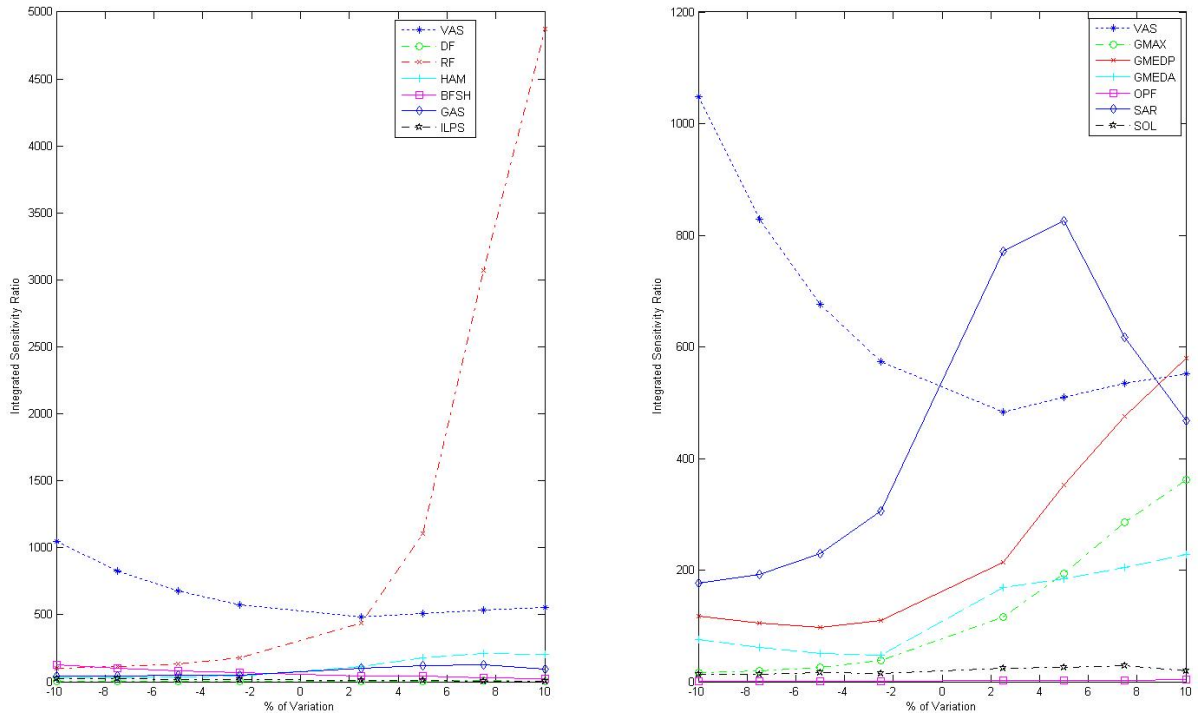Figure 141: Sensitivity for GMAXL to tendon slack length.
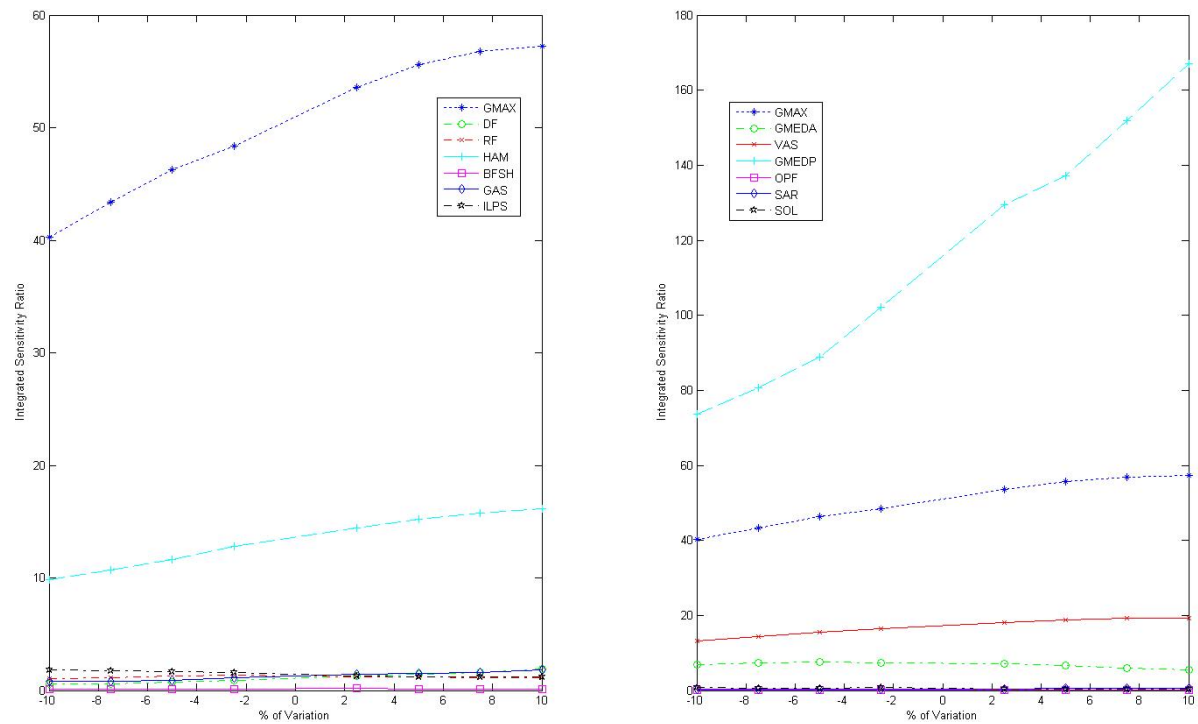
Figure 142: Sensitivity of relevance for GMAXL to tendon slack length.
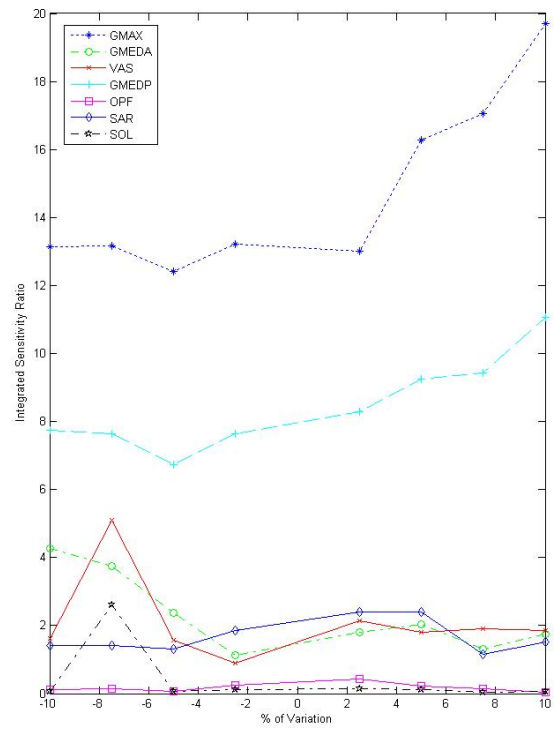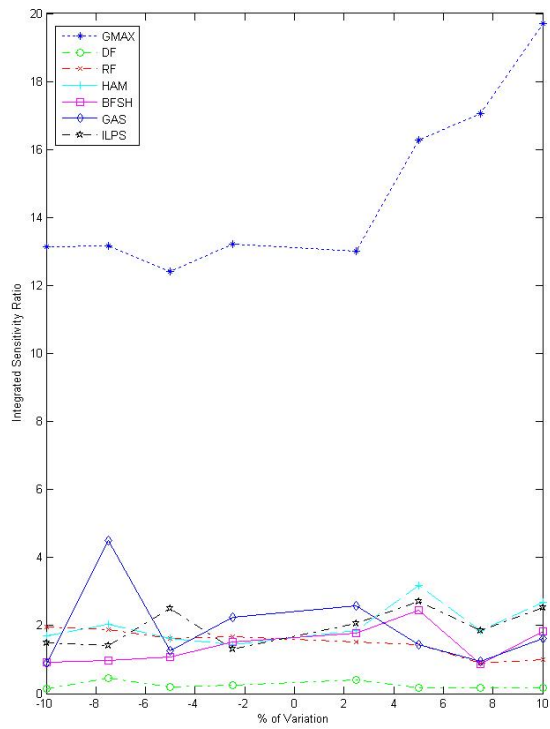
Figure 143: Sensitivity for GMAXM to tendon slack length.
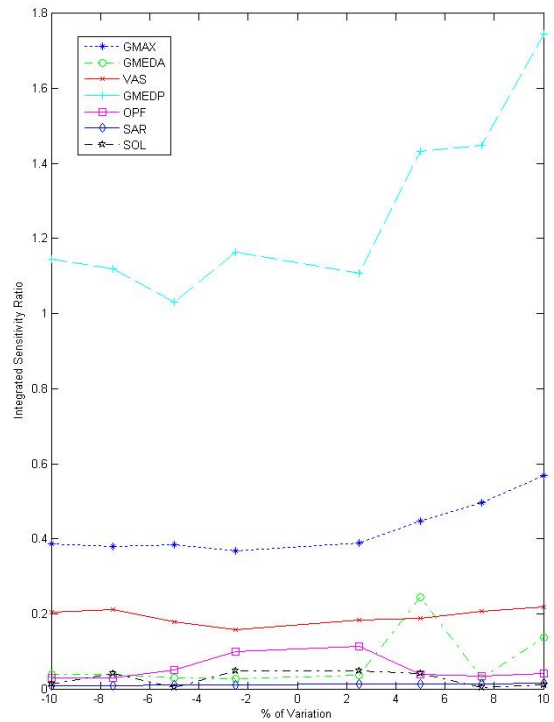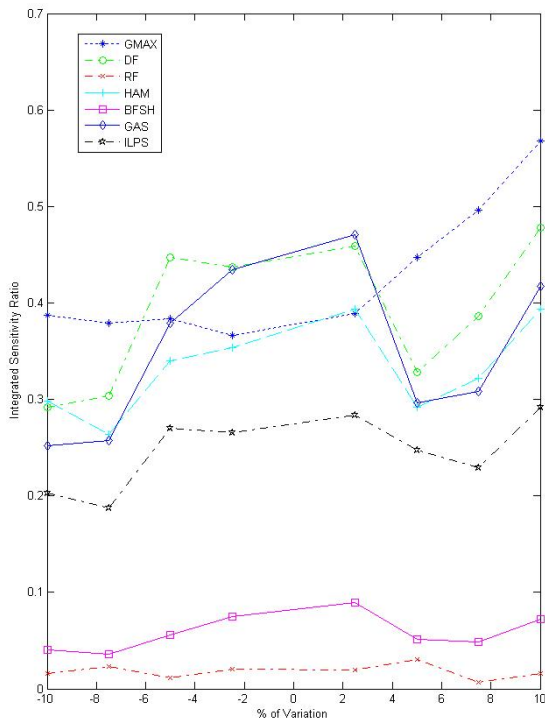
Figure 144: Sensitivity of relevance for GMAXM to tendon slack length.
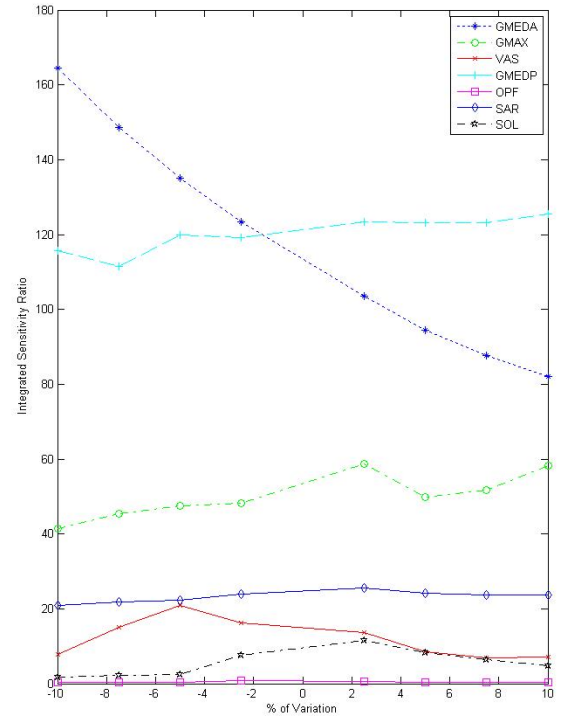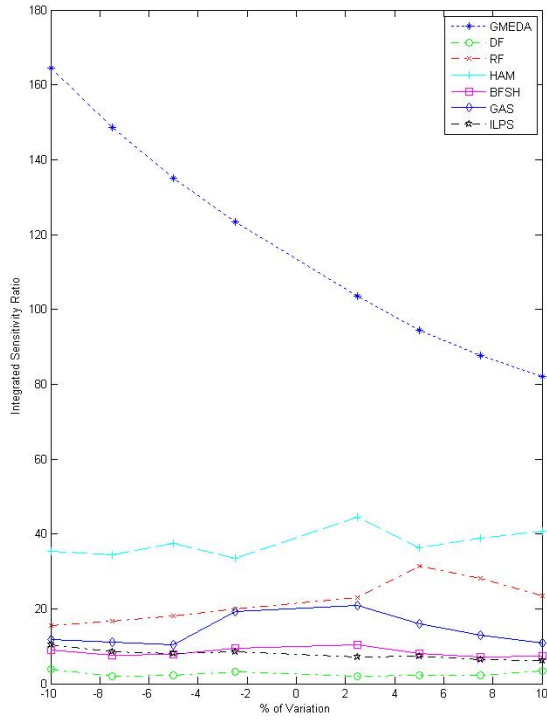
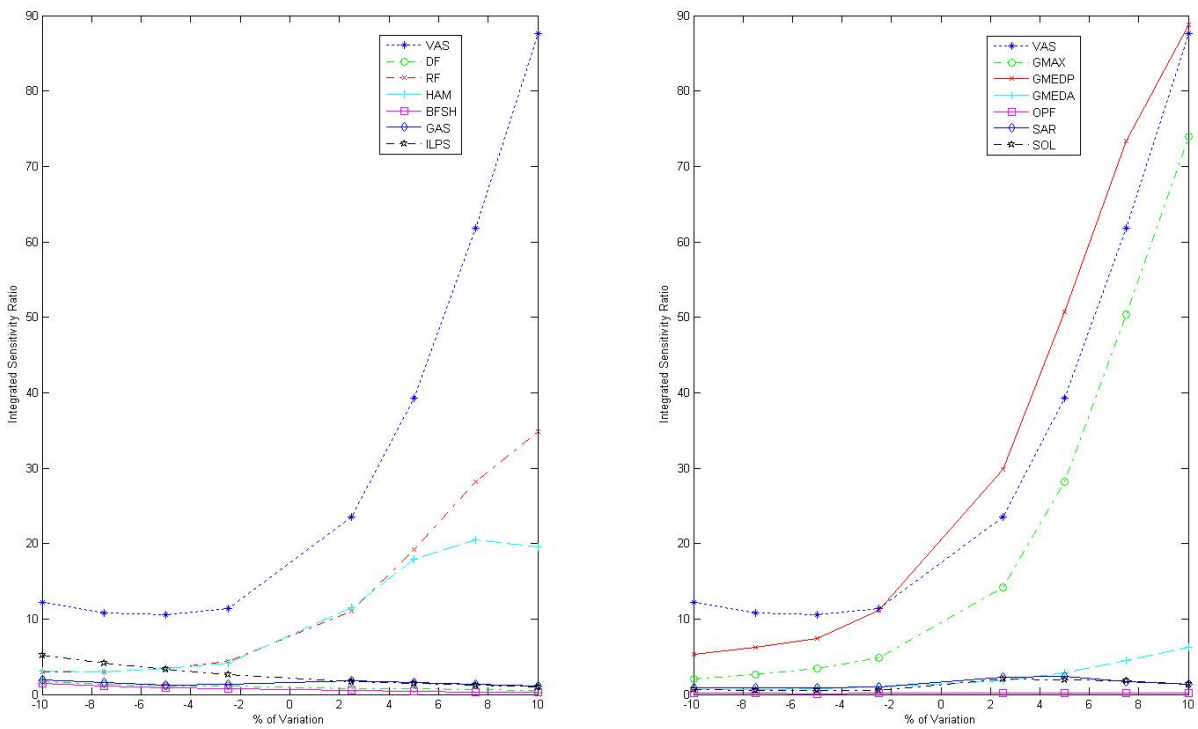Figure 145: Sensitivity for GMEDA to tendon slack length.
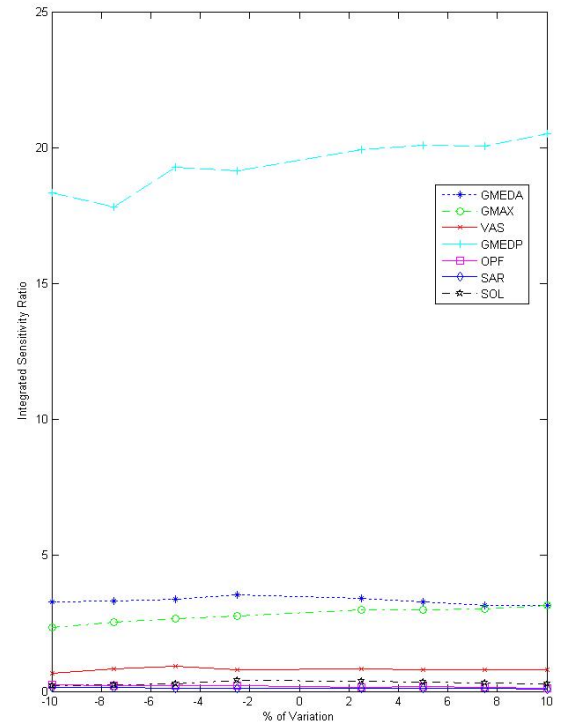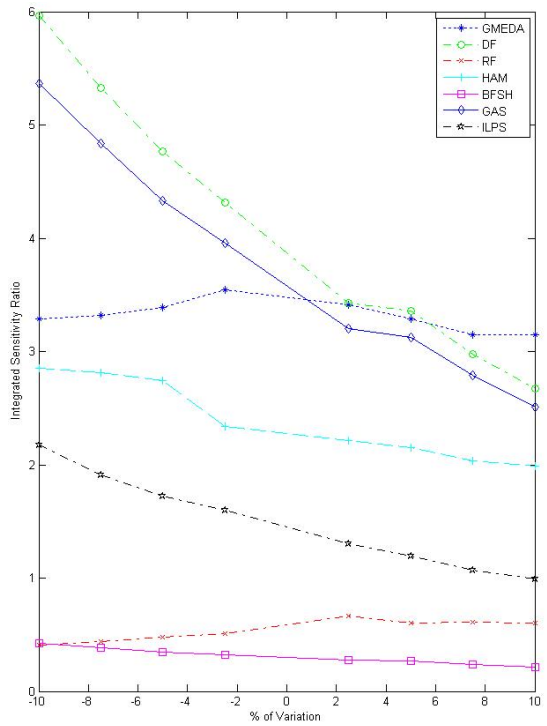
Figure 146: Sensitivity of relevance for GMEDA to tendon slack length.

153
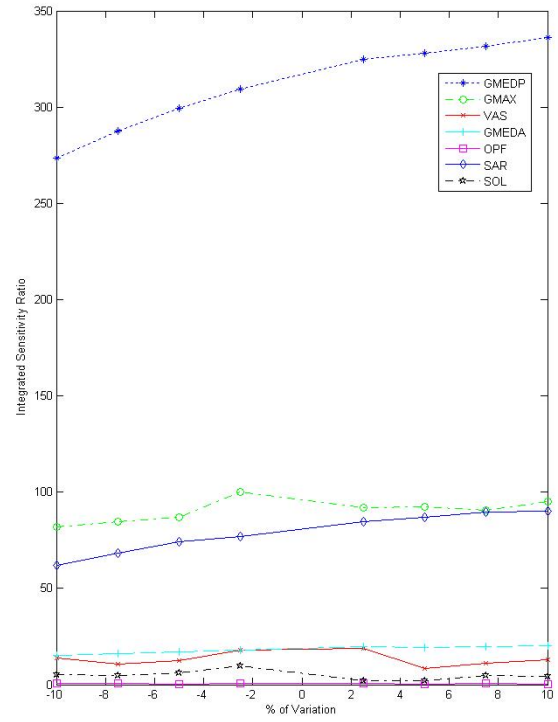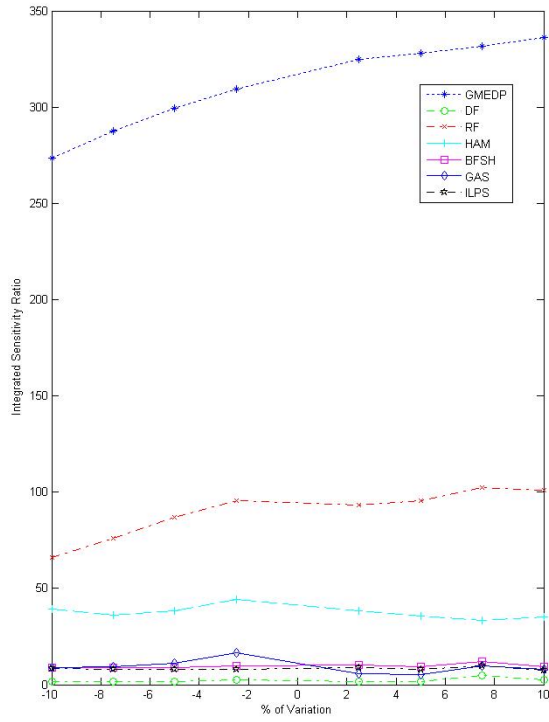
Figure 147: Sensitivity for GMEDP to tendon slack length.
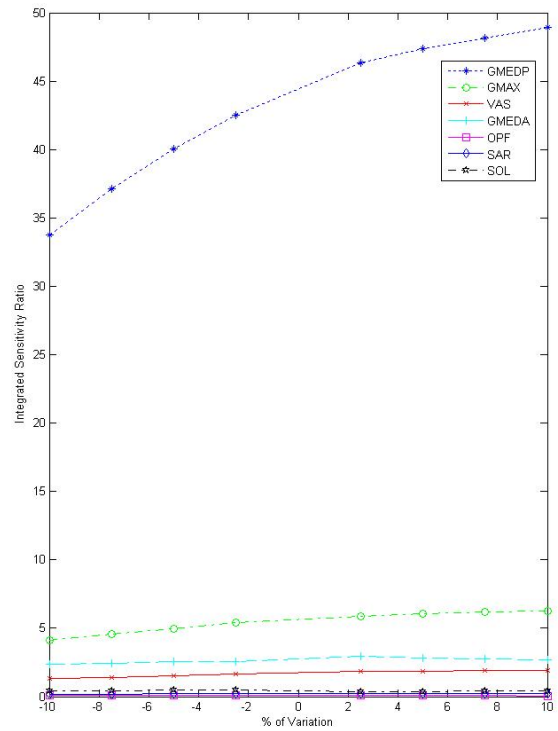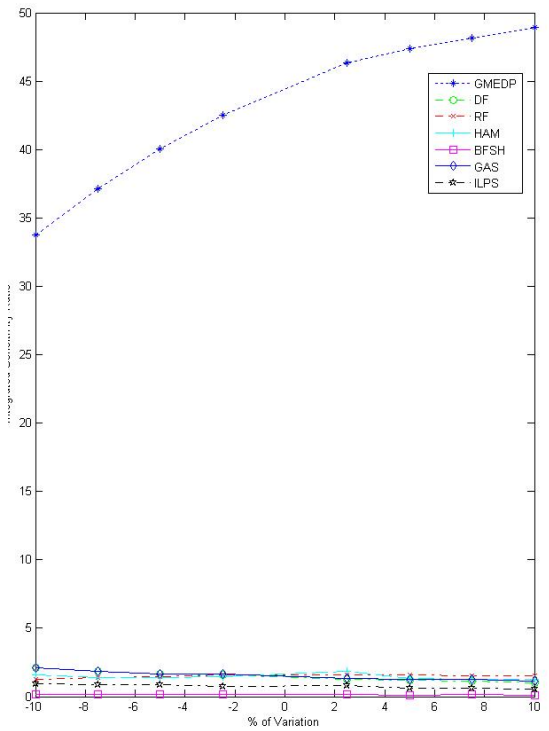
Figure 148: Sensitivity of relevance for GMEDP to tendon slack length.
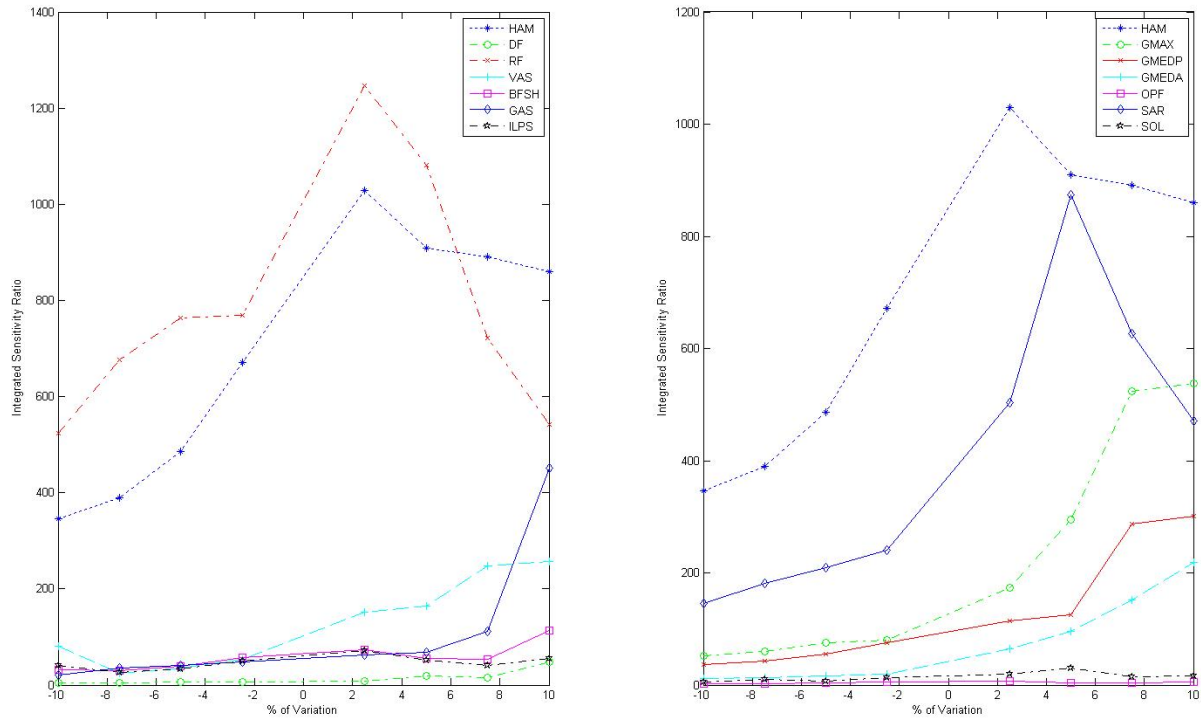
Figure 149: Sensitivity for HAM to tendon slack length.
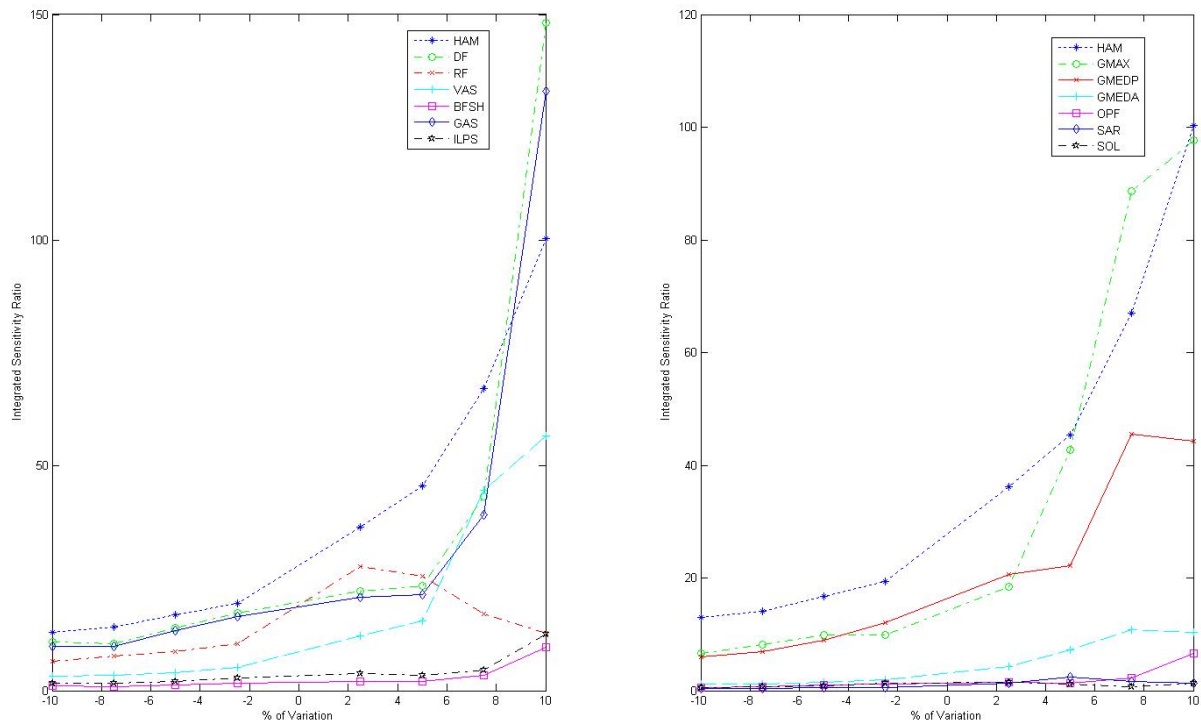
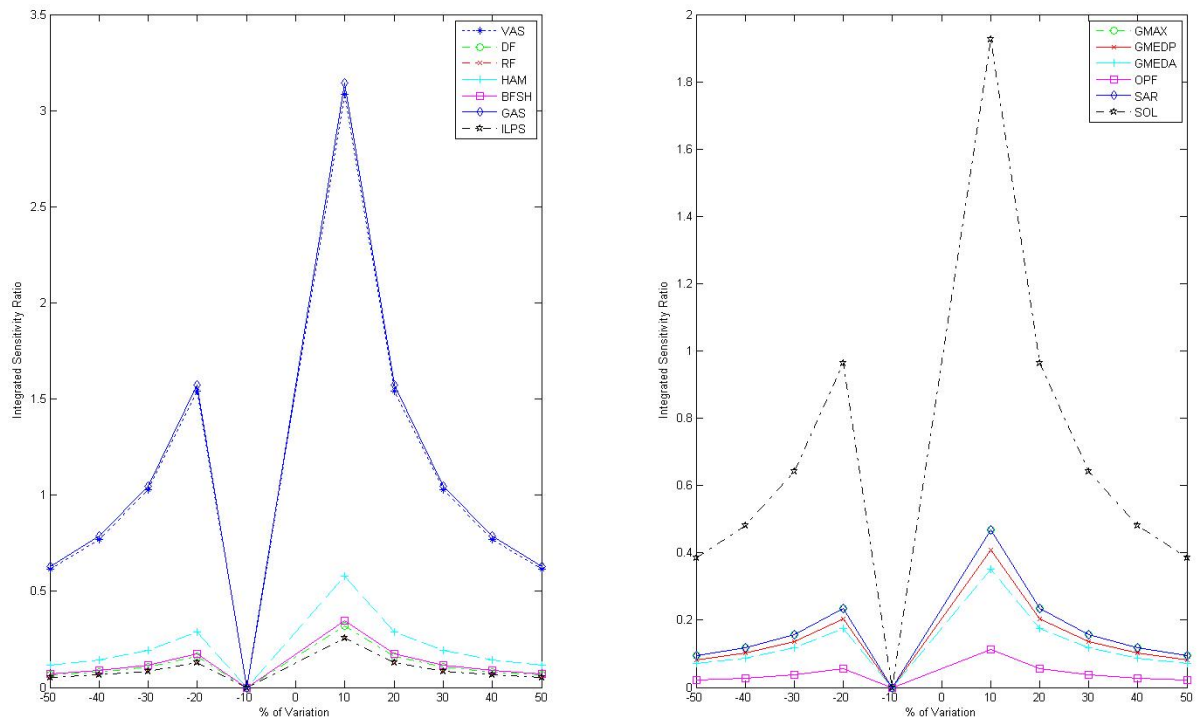Figure 150: Sensitivity of relevance for HAM to tendon slack length.
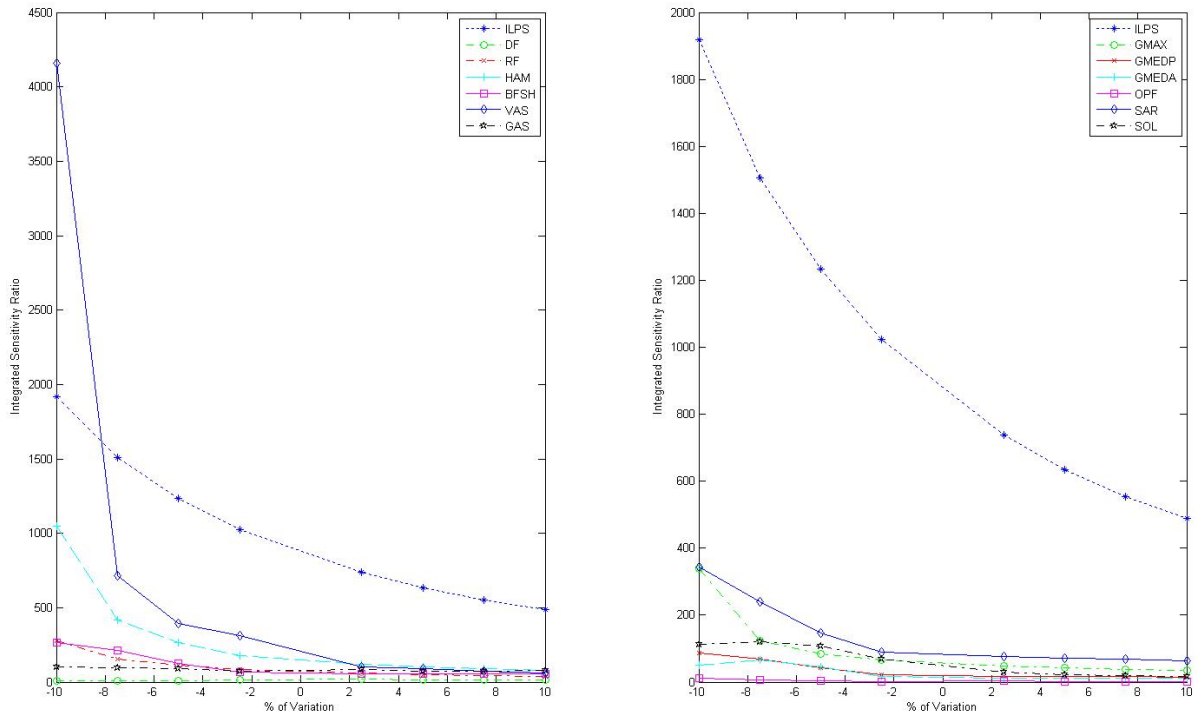
Figure 151: Sensitivity for ILPSO to tendon slack length.
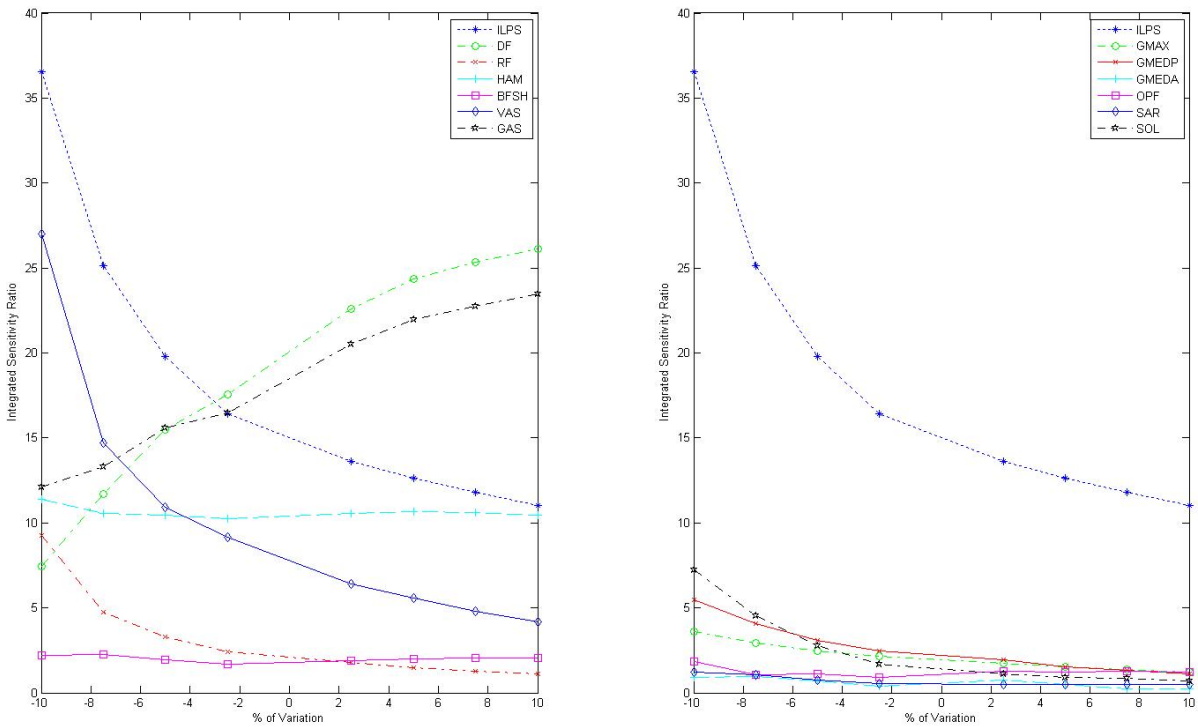

Figure 152: Sensitivity for of relevance ILPSO to tendon slack length.
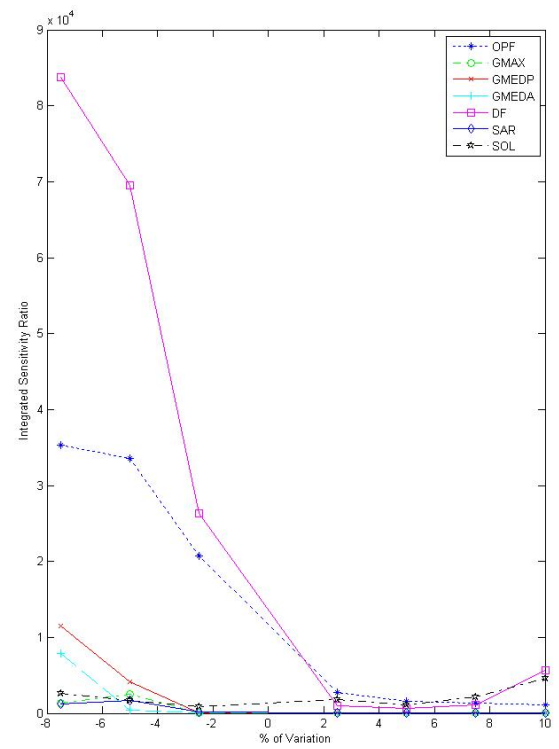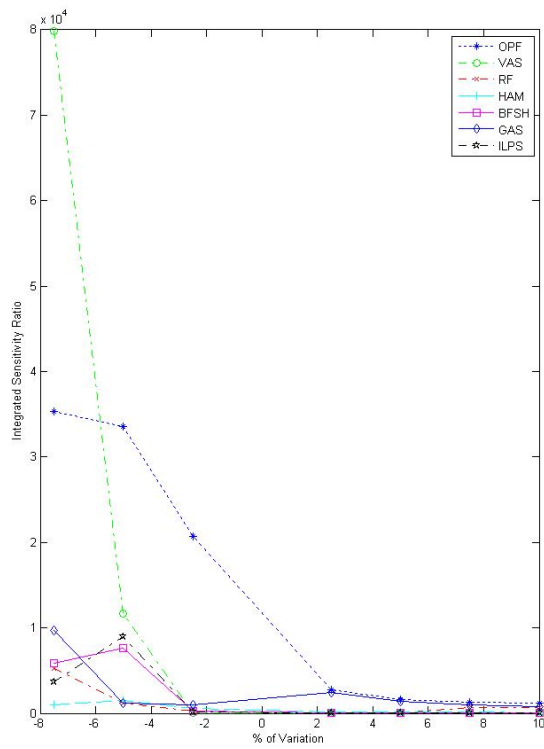
Figure 153: Sensitivity for OPF to tendon slack length.
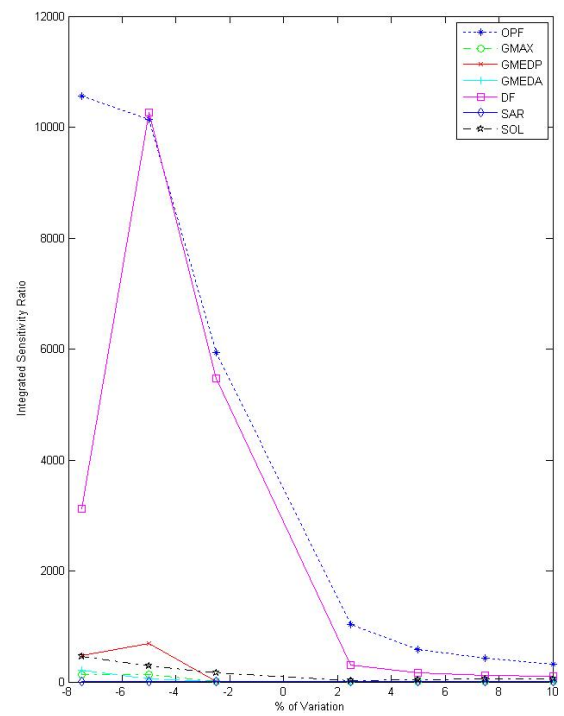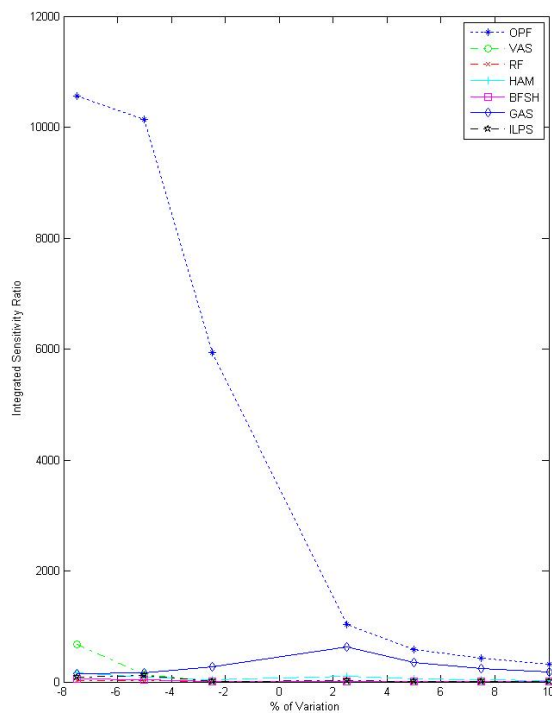
Figure 154: Sensitivity of relevance for OPF to tendon slack length.
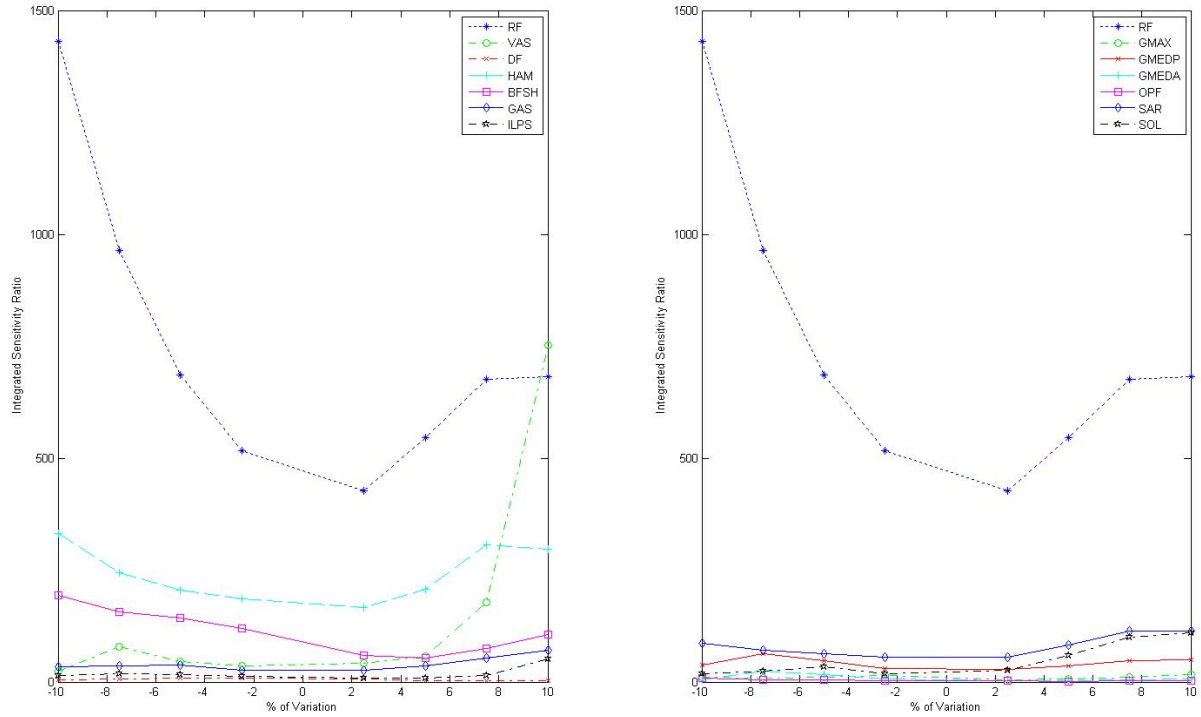
Figure 155: Sensitivity for RF to tendon slack length.
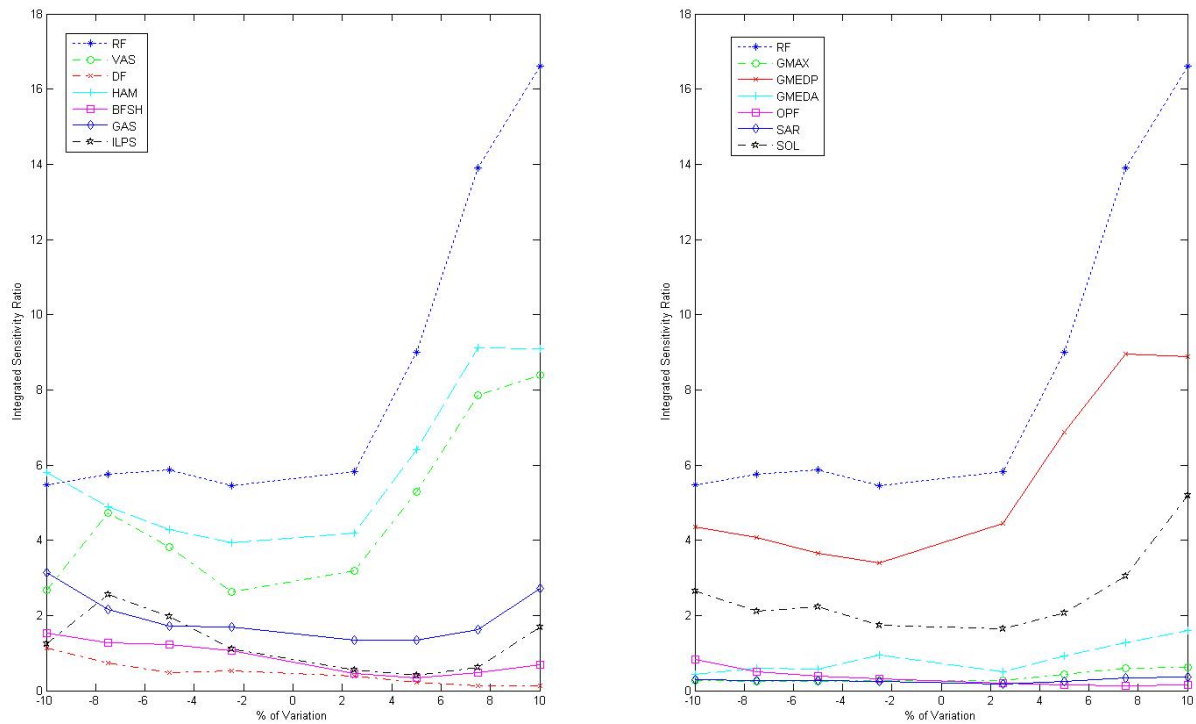
Figure 156: Sensitivity of relevance for RF to tendon slack length.

Figure 157: Sensitivity for SAR to tendon slack length.

Figure 158: Sensitivity of relevance for SAR to tendon slack length.

Figure 159: Sensitivity for SOL to tendon slack length.

Figure 160: Sensitivity of relevance for SOL to tendon slack length.

Figure 161: Sensitivity for VAS to tendon slack length.

Figure 162: Sensitivity of relevance for VAS to tendon slack length.

Figure 163: Sensitivity to deactivation time
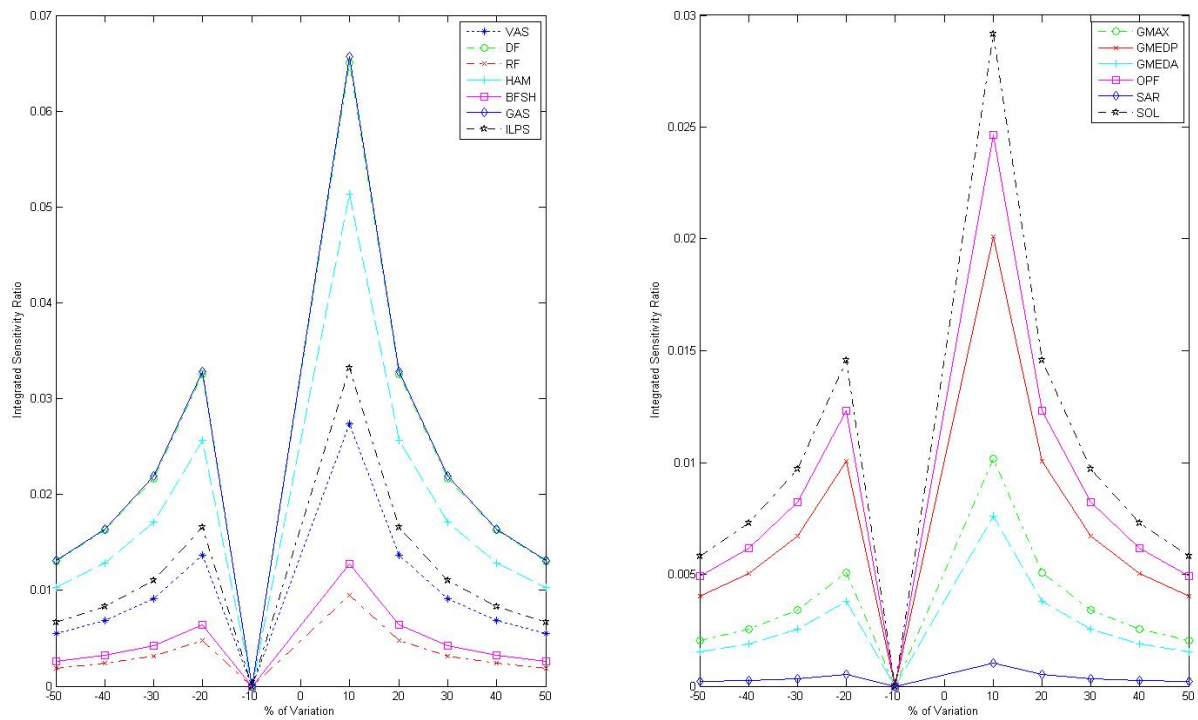
Figure 164: Sensitivity of relevance to actiavation time
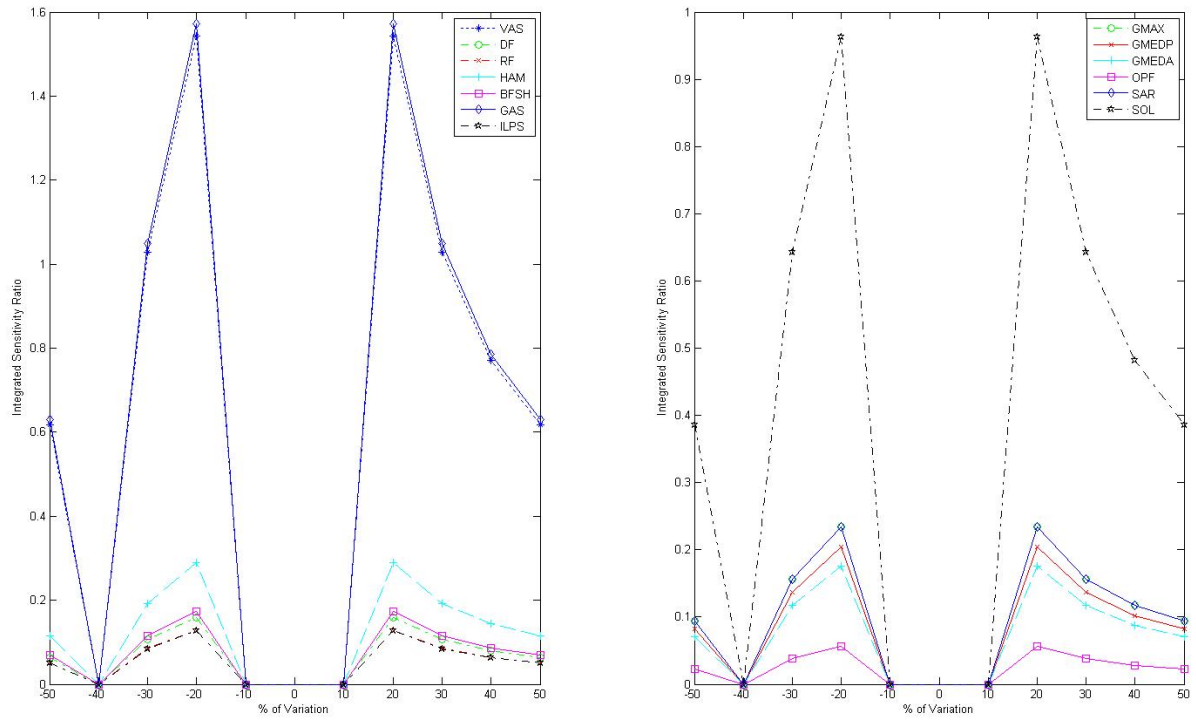
Figure 165: Sensitivity to deactiavation time
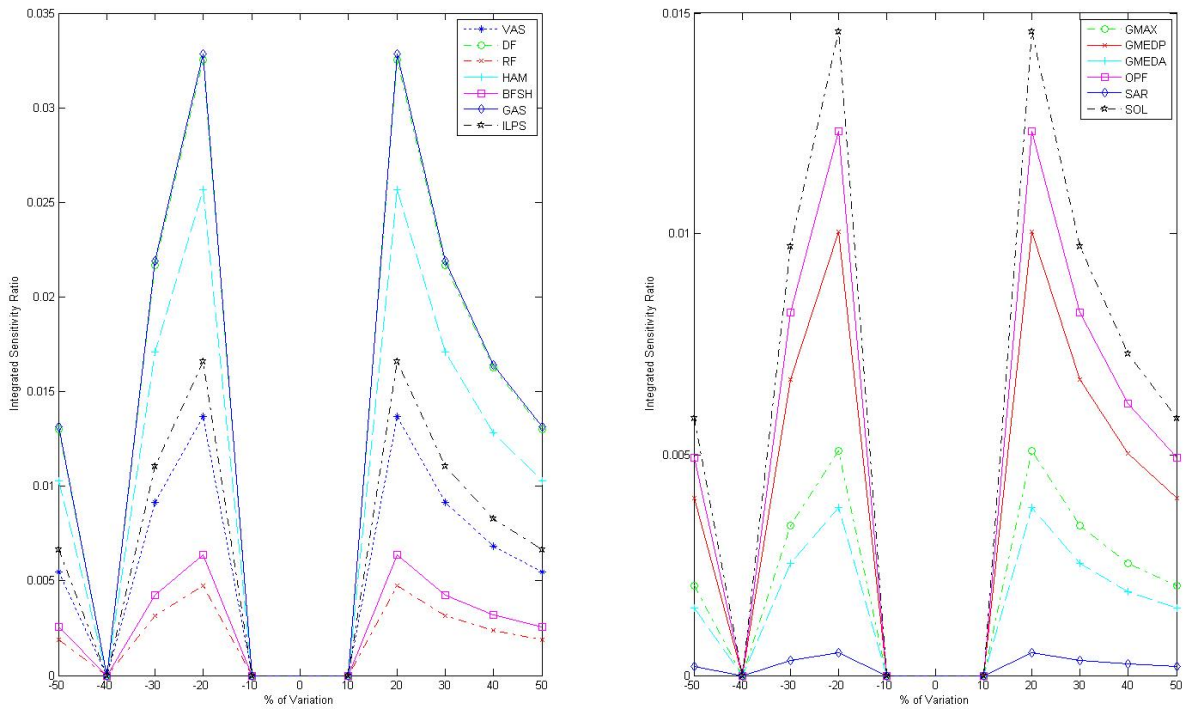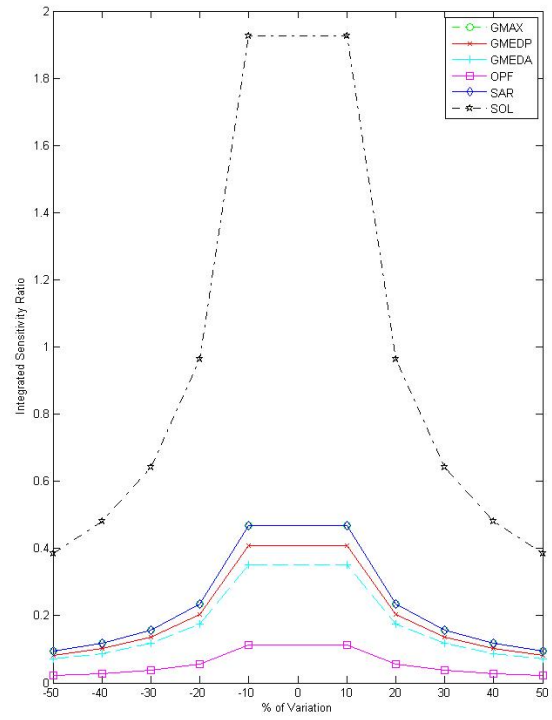

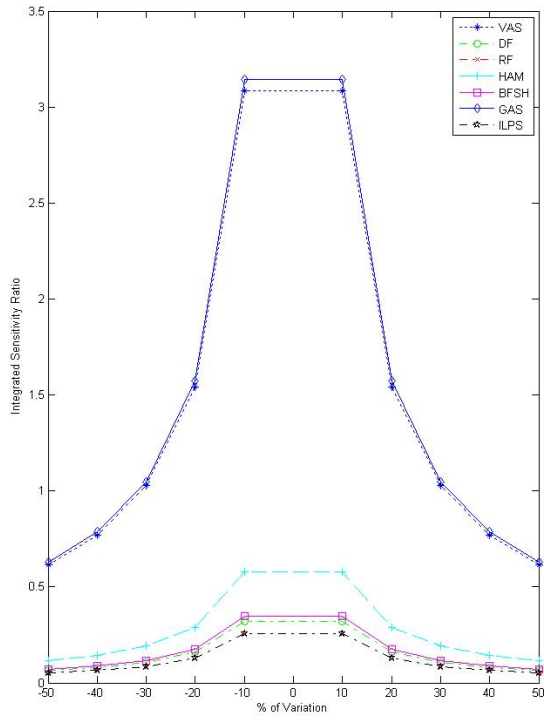
Figure 166: Sensitivity of relevance to deactiavation time

163

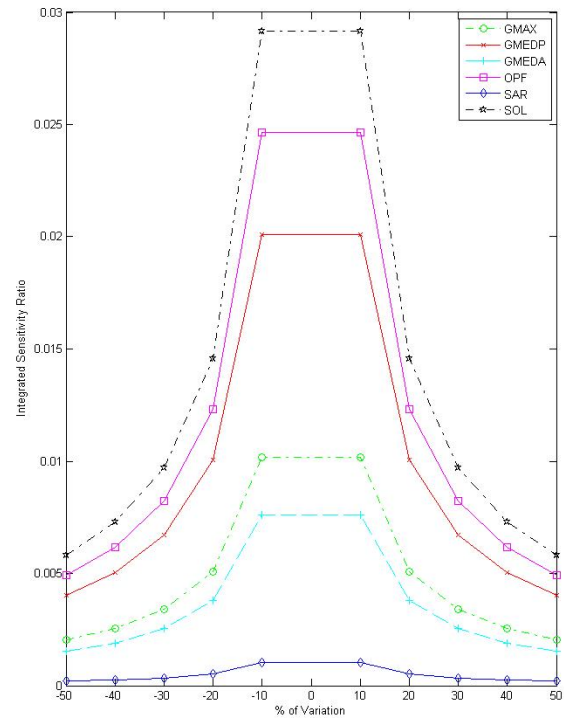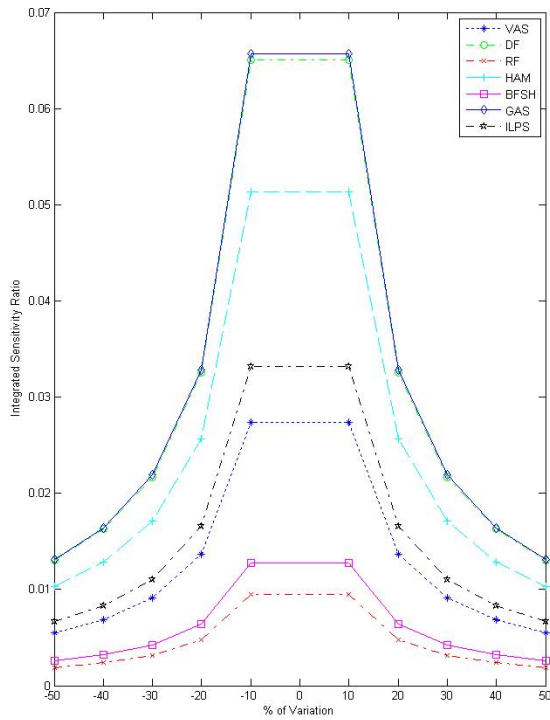Figure 167: Sensitivity to maximum shortening velocity

Figure 168: Sensitivity of relevance to maximum shortening velocity